



## City Research Online

### City, University of London Institutional Repository

---

**Citation:** Mamouei, M. H. (2017). Energy efficient adaptive cruise control: Towards benchmarking energy efficiency in the control of partially and fully automated vehicles. (Unpublished Doctoral thesis, City, University of London)

This is the accepted version of the paper.

This version of the publication may differ from the final published version.

---

**Permanent repository link:** <https://openaccess.city.ac.uk/id/eprint/19154/>

**Link to published version:**

**Copyright:** City Research Online aims to make research outputs of City, University of London available to a wider audience. Copyright and Moral Rights remain with the author(s) and/or copyright holders. URLs from City Research Online may be freely distributed and linked to.

**Reuse:** Copies of full items can be used for personal research or study, educational, or not-for-profit purposes without prior permission or charge. Provided that the authors, title and full bibliographic details are credited, a hyperlink and/or URL is given for the original metadata page and the content is not changed in any way.

**Energy Efficient Adaptive Cruise Control:  
Towards Benchmarking Energy Efficiency in the  
Control of Partially and Fully Automated Vehicles**

by

**Mohammad Hossein Mamouei**

**(B.Sc., M.Sc. EE&E)**

A thesis submitted in the fulfilment of the requirements for the degree of

**Doctor of Philosophy**

in

**Systems and Modelling**

**Department of Electrical & Electronic Engineering**

**City, University of London**



**Sep 2017**

**To my beloved parents Azimeh Bahaedini and Morteza Mamouei.**

## **Acknowledgements**

Firstly, I would like to thank Dr. Ioannis Kaparias for his continuous professional and social support throughout my PhD. He provided me with the freedom to be creative and dive into new research questions, and gave me directions when I needed them the most. Dr. Kaparias provided me with exciting opportunities at City, University of London and elsewhere, and supported me to undertake other roles in order to advance my skills and gain more experiences. I would also like to thank Prof. George Halikias. His insights significantly contributed to a number of my publications.

For the past four years I was given the opportunity to pursue my passion in research. This would not have been possible without the help of Prof. Panos Liatsis. I am very thankful to him for making this journey possible.

Towards the end of my PhD, I had the opportunity to join Transport Systems Catapult for a few months. There, I met amazing people who were generous to share their knowledge and expertise. They significantly contributed to the validation work using the PTV VISSIM micro-simulation software. I would like to thank Dr. Fabio Galatioto, Dr. Patrizia Franco, Ecaterina McCormick and Dr. Vittoria Parisi for their help and insights.

Last but not least, my deepest gratitude and much love goes to my Maman and Baba, Azimeh Bahaedini and Morteza Mamouei, my sisters, Farzaneh and Sara, and my beloved nephew and niece, Mohammad Reza and Sonia. You have always given me more support and love than I could have asked for. I am indebted, forever grateful, and so lucky to have you all!

I hereby declare that no portion of the work produced in this document has been submitted to any other University.

London, \_\_\_\_\_

---

(Mohammad Hossein Mamouei)

## **Abstract**

Fully automated vehicles are expected to have a significant share of the road network traffic in the near future. Several commercial vehicles with full-range adaptive cruise control systems or semi-autonomous functionalities are already available in the market. This provides a unique opportunity to improve the acceleration behaviour of vehicles, and thereby, improve network's efficiency in terms of important performance indicators such as fuel consumption and traffic throughput. However, automated driving systems usually adopt a highly conservative driving strategy to ensure safety and fuel efficiency for individual vehicles. The collective impacts of such strategies on the network level can lead to the deterioration of traffic flow and to an increase in fuel/energy consumption. Much of the existing research in this area either target driving conditions where there are no additional complexities caused by interaction between vehicles, or make simplistic assumptions about the dynamics of driving behaviour and its relationship with fuel consumption in order to formulate a feasibly solvable optimisation problem.

The reduction of the question of fuel efficiency to optimisation scenarios where only a pair of vehicles are considered and little attention is paid to the surrounding traffic, leads to a user-optimal driving strategy at best, however addressing environmental concerns and a more efficient use of fossil fuels in road transport networks necessitates a system-optimal approach. A system-optimal approach means the scope of the problem must be broadened so that a) the complex relationship between individual driving styles and the dynamical features of traffic flow are incorporated within the optimisation framework and b) the long-term impacts of driving strategies on network's performance are modelled within optimisation scenarios. The challenge here is to model driving behaviour and traffic flow with sufficient accuracy and devise

an optimisation framework that is computationally efficient enough to cope with the complexity of the problem.

In this study, the use of car-following models and limiting the search space for optimal strategies to the parameter space of car-following models is proposed. This framework enables performing much more comprehensive optimisations and conducting more extensive tests on the collective impacts of fuel-economy driving strategies. The results obtained in this study show that formulating the optimisation in a short-sighted way where merely individual vehicles are considered and no attention is paid to the collective impacts of a fuel-economy driving strategy, can lead to significant increase in fuel consumption for the whole network while delivering marginal benefits for the target vehicle. This study establishes a complex relationship between traffic flow and fuel consumption on the link level, where the former cannot be achieved without addressing the latter correctly in the optimisation process.

In addition to the main research question discussed above, the present thesis proposes a new method for the analysis of car-following models. The conventional method in the analysis of car-following models relies on the cumulative error between real data and modelled data in order to benchmark car-following models. Although the cumulative error is indeed an informative measure of performance, it leaves many questions regarding the capacity of models for replicating driving behaviour unanswered. Here the use of dynamic system identification is investigated as a way to provide a more in-depth analysis of the strengths and weaknesses of car-following models in reproducing realistic driving behaviour. Subsequently, the proposed method is applied to compare a number of car-following models. Although the application of this method for the comparison of car-following models presents some challenges that require further research, the results are very promising.

# Table of Contents

Acknowledgements.....	I
Abstract .....	III
1. Introduction .....	1
1.1 Context and motivation .....	1
1.1.1 Safety.....	4
1.1.2 Environmental effects .....	4
1.1.3 Traffic efficiency .....	5
1.1.4 Automated driving .....	6
1.2 Aim and objectives .....	7
1.3 Structure of the thesis.....	11
2. Literature review .....	13
2.1 Background on traffic modelling.....	13
2.1.1 Fundamental diagram and congestion.....	14
2.1.2 Phase-diagram and different types of congested traffic .....	19
2.1.3 Traffic modelling.....	23
2.2 Car-following models .....	28
2.2.1 Car-following regime .....	28
2.2.2 Gipps' general acceleration model.....	32
2.2.3 Benekohal's model .....	35
2.2.4 Ahmed's model .....	37
2.2.5 Intelligent Driver Model .....	44
2.3 Adaptive cruise control methodologies .....	46
2.3.1 Fuzzy logic.....	49

2.3.2	Adaptive cruise control as an optimal control problem.....	52
2.3.3	Concluding remarks.....	57
2.4	Energy-efficiency and fuel consumption.....	60
2.4.1	Fuel consumption models.....	60
2.4.2	Fuel efficient driving strategies.....	63
2.5	Summary.....	68
3.	Using car-following for automated vehicle control.....	70
3.1	Criteria of importance.....	71
3.1.1	Safety.....	71
3.1.2	Stability.....	72
3.1.3	Traffic flow.....	84
3.1.4	Practical implementation aspects.....	85
3.1.5	Environmental impacts.....	88
3.1.6	Summary.....	88
3.2	Sensitivity Analysis.....	92
3.2.1	Local sensitivity analysis.....	93
3.2.2	Global sensitivity analysis.....	97
3.2.3	Summary.....	103
3.3	A new approach to the comparison of car-following models.....	105
3.3.1	Car-following models.....	106
3.3.2	Calibration of car-following models.....	109
3.3.3	Dynamic system identification using Particle Filtering.....	111
3.3.4	Sensitivity analysis.....	117
3.3.5	Results.....	120
3.3.6	Conclusion and future work.....	131
4.	Energy Efficient Driving.....	135

4.1	Methodology.....	136
4.1.1	Optimisation framework.....	136
4.1.2	Microscopically formulated optimisation.....	138
4.1.3	Macroscopically formulated optimisation.....	140
4.1.4	Sensitivity Analysis.....	142
4.1.5	Fuel consumption.....	143
4.2	Dataset.....	145
4.3	Results.....	150
4.3.1	Microscopically formulated optimisation.....	150
4.3.2	Macroscopically formulated optimisation.....	156
4.3.3	Impacts on traffic flow.....	161
4.3.4	Stability features.....	164
4.4	Conclusion and summary.....	166
5.	Validation in an urban network.....	170
5.1	Simulation setup.....	171
5.2	Simulation results.....	173
5.3	Conclusion.....	177
6.	Conclusion and Future work.....	178
6.1	Summary of work.....	178
6.2	Contributions and future work.....	180
6.2.1	A new method for the comparison of car-following models.....	180
6.2.2	A quantitative approach to behavioural analysis of drivers.....	182
6.2.3	Fuel efficiency: system-optimal vs. user-optimal.....	183
6.3	Concluding remarks.....	184
	References.....	186

Appendix – A quantitative approach to behavioural analysis of drivers in motorways using particle filtering ..... 205

## List of Figures

Figure 1. A depiction of the fundamental diagram derived from a car-following model, namely the IDM (a) Coefficient $\delta$ determines how fast cars accelerate to their desired speed (b) Coefficients $T$ and $v_0$ represent safe headway and desired velocity respectively. Finally, $s_0$ and $L$ are the standstill bumper to bumper spacing between vehicles and vehicle lengths. Only one parameter is varied at a time and the rest of the parameters are default parameters given in [26].	15
Figure 2. Three-phase diagram [30].	17
Figure 3. Relation between the mean distance between centres of narrow jams and the average vehicle speeds between jams in the pinch region.	18
Figure 4. Spatio-temporal representation of an MLC [32].	20
Figure 5. a) Stationary PLC b) Oscillatory PLC [26].	21
Figure 6. HCT [32].	22
Figure 7. STG and OCT [32].	22
Figure 8. Phase diagram of an open system simulated with a car-following model, the intelligent driving model [26].	23
Figure 9. Speed-time plots for seven successive vehicles using Gipps' model with following parameters: $a_n = 2\text{ms}^{-2}$ , $b_n = -3\text{ms}^{-2}$ , $v_n = 30\text{ms}$ and $\tau = 23\text{sec}$ when a) $b = -3.5\text{ms}^{-2}$ b) $b = -2.5\text{ms}^{-2}$ [38].	34
Figure 10. The impact of the relative speed on drivers' acceleration decisions [47, p. 50].	41
Figure 11. A depiction of the fundamental diagram derived from a car-following model, namely the IDM (a) Coefficient $\delta$ determines how fast cars accelerate to their desired speed (b) Coefficients $T$ and $v_0$ represent safe headway and desired velocity respectively. Finally, $s_0$ and $L$ are the standstill bumper to bumper spacing between vehicles and vehicle lengths. Only one parameter is varied at a time and the rest of the parameters are default parameters given in [26].	46
Figure 12. Optimisation of a single speed profile [125].	65

Figure 13. A schematic representation of Porsche InnoDrive ACC a) the upper and lower limits on the optimisation space due to different environmental factors b) the optimal path representing the optimal velocity plan within a road section [127]. .....	66
Figure 14. Fundamental diagram: relationship between density and flow a,b) empirical observations [142, 143] c) two-phase fundamental diagram derived from IDM model with specified critical densities [32]. .....	76
Figure 15. Response of the immediate following vehicle to a perturbation in the speed of the lead vehicle when its speed drops to by 2 ms and immediately restores to the equilibrium speed of 20 ms after 2 secs. The response is simulated using IDM model with default parameters.....	79
Figure 16. a) Response of the platoon of 18 vehicles to a perturbation in the speed of lead vehicle when its speed drops to by 2 ms and immediately restores to the equilibrium speed of 10 ms after 2 secs. The response is simulated using the IDM model with default parameters except for $a = 0.5 \text{ ms}^2$ , $b = 3 \text{ ms}^2$ b) trajectories of all vehicles other than the second and last in line are eliminated.....	80
Figure 17. Formation of a cluster after the introduction of a small disturbance in the velocity of one of the vehicles. The default parameters for the IDM where chosen. Other simulation parameters used are; number of vehicles=38, length of the road=1793 m, equilibrium velocity and density prior to the introduction of the disturbance were 22.3 m/s and 21.2 cars/km respectively.....	81
Figure 18. The spacing plots for the test scenario above. In the plot on the left-hand side, fluctuations for a short period are magnified for a better illustration of details.....	81
Figure 19. a,b) Propagation of the traffic jam in the upstream direction of a highway [24]......	82
Figure 20. The direction of propagation of disturbances in a) convectively downstream (string) instability b) absolute string instability c) convectively upstream (string) instability where $c +$ and $c -$ are the velocities of the moving congestion fronts [71]......	82
Figure 21. 2D visualisation of the local sensitivity of fuel consumption to different model parameters of the IDM car-following model. The results are derived from simulations where the subject vehicle is driving according to the IDM car-following model. The trajectory of the leading vehicle is obtained from the Naples dataset 25B, particularly vehicle with ID 234. ....	96

Figure 22. Scatter plots representing the fuel consumption of a vehicle that is driving according to the IDM car-following model. The trajectory of the lead vehicle is obtained from the Naples dataset 25B, particularly, vehicle with ID 234.....	98
Figure 23. Total sensitivity indices for the effects of the IDM model parameters on fuel consumption in a simulation scenario where the vehicle with ID 234 from the Naples dataset 25B is the leading vehicle. ....	103
Figure 24. The visualisation of the three stages of importance sampling, resampling, and sampling (prediction) in PF, figure from [178].....	116
Figure 25. Total sensitivity indices of the IDM car-following model w.r.t. the calibration error in a simulation scenario where the trajectory of the lead vehicle is that of the vehicle with ID 362 from the NGSIM-I80. ....	119
Figure 26. a) Trajectory of the lead vehicle selected from the NGSIM I-80 dataset, Lane 2 b,c,d) trajectories, velocities, and accelerations of the lead vehicle and the modelled follower in dashed red line and blue solid line respectively. ....	121
Figure 27. The result of the estimation of the parameter $T$ . The blue shadow denotes the distribution of particles at each time instance while the red curve is the selected particle. ....	122
Figure 28. The comparison of the actual data with the simulated data when the dynamic estimates of the parameter $T$ , given by particle filtering, is used.....	124
Figure 29. The trajectories of the five vehicles selected for comparison. ....	126
Figure 30. The comparison of real trajectories with the simulated ones for the vehicle ID 362 when the dynamic estimates of the parameter $T$ , produced by PF, is used for the IDM car-following model.....	127
Figure 31. Dynamic parameter estimates for the for the vehicle ID 362 and the car-following models: a) IDM-VDT b) EIDM c) IDM d) GHR-Ozaki.....	127
Figure 32. The application of a simple moving average filter, with the averaging time widow of 10 s, to the dynamic estimates of the parameter $T$ for the IDM and a) vehicle with ID 368 b) vehicle with ID 378. ....	128
Figure 33. The comparison of the trends of the parameter $T$ with the velocities and spacing for the IDM car-following model and NGSIM Naples dataset 25B. ....	129
Figure 34. Histograms of the values of the tracked parameter for the vehicle ID 362 and car-following models a)IDM-VDT b)EIDM c)IDM d)GHR.....	130

Figure 35. Schematic representation of the microscopic optimisation scenario. ....	140
Figure 36. Schematic representation of the macroscopic optimisation scenario. ....	141
Figure 37. The comparison of fuel consumption prediction between VT-micro and the new model. a, b) Fuel consumption for the whole envelope of velocities and accelerations using VT-micro and the new model respectively. c) Instantaneous fuel consumptions for the FTP drive cycle. ....	144
Figure 38. The spatio-temporal velocity of the traffic in lanes 1-6 in the NGSIM-I80 dataset. ....	145
Figure 39. Trajectories of a) the platoon of vehicles with IDs 441, 452, 453, and 467 and b) the platoon of vehicles with IDs 362 , 368 , 378, 381. ....	146
Figure 40. Vehicles that remain within the lane for the whole period of observation are denoted with red. ....	147
Figure 41. Data collection sites for the Naples dataset (figure from [158]). ....	148
Figure 42. Velocity and spacing measures of the first to fourth vehicles in the platoon in three Naples dataset, a,b) 25B, c,d)25C, and e,f) 30B.....	149
Figure 43. a) position, b) velocity, c) acceleration and d) spacing values produces using the optimal parameters compared to the real ones for the vehicles with IDs 441-467. ....	152
Figure 44. Comparison of the spatiotemporal velocities of the modelled scenario with the real data. The trajectory of the lead vehicle is $Tl = 441$ . ....	153
Figure 45. Two-hour-long simulation with the inflow of 1333 vehhr and with the microscopic optimal parameters. a) $Tl=441$ b) $Tl=362$ . ....	155
Figure 46. Spatio-temporal diagram when the macroscopic optimal parameters are used. The inflow rate is 1333 vehh , and the trajectories of the lead vehicle are a) $Tl = 441$ b) $Tl= 362$ . ....	159
Figure 47. The comparison of the simulation results for different sets of model parameters when the trajectory of the lead vehicle from Naples 30C dataset is used. Macroscopic optimal parameters are used for diagrams on the left-hand-side and microscopic optimal parameters are used for diagrams on the right-hand-side. ....	162
Figure 48. Comparison of flow-density diagrams for the micro and macro optimal parameters. Macroscopic optimal parameters are used for the diagrams on the left-hand-side and microscopic optimal parameters are used for the graphs on the right-hand-side. ...	164
Figure 49. Response to a disturbance for the default set of model parameters when the circumference of the road is 500 meters. ....	164

Figure 50. Fluctuations in velocities of the platoon when road length is equal to 10 km, 600 vehicles are used along with following parameters a) $a = 5, b = 0.5, T = 0.5$ b) $a = 0.5, b = 5, T = 0.5$ c) $a = 0.5, b = 5, T = 2$ d) $a = 5, b = 0.5, T = 2$ . The velocities of the first 20 vehicles are shown here. ....	166
Figure 51. Milton Keynes city centre.....	171
Figure 52. A representative sample of the inflow levels from 6 input section.....	173
Figure 53. Grafton Street. ....	174
Figure 54. Average fuel consumption in a) the whole network b) Grafton Street. ....	174
Figure 55. Total Emissions in the network and Grafton Street.....	175
Figure 56. The comparison of the network performance measurements between the proposed driving strategy and base case.....	176

## List of Tables

Table 1. The six levels of driving automation defined by SAE International [5].	3
Table 2. The criteria of importance in the automation of driving	91
Table 3. IDM default model parameters	95
Table 4. Lower and upper boundaries used	98
Table 5. Lower and upper boundaries used and total sensitivity indices	103
Table 6. Calibration results for the IDM car-following model using trajectory data	110
Table 7. The lower and upper boundaries used in this study	118
Table 8. The comparison of the total sensitivity indices obtained in this study with the ones reported in [170]	120
Table 9. The means and standard deviations of the dynamic parameter estimates	131
Table 10. Total sensitivity indices for the effects of the IDM model parameters on fuel consumption in the microscopically formulated simulation scenario	143
Table 11. The optimal parameters obtained for a platoon of three vehicles when the trajectory set 441-467 is used for the lead vehicle	151
Table 12. Optimisation parameters for the macroscopically formulated optimisation	157
Table 13. The macroscopic optimal parameters obtained for different trajectory sets from the NGSIM Naples dataset and different inflow rates when $t = 60$ min	158
Table 14. Results obtained for the microscopic and macroscopic optimisation frameworks	160
Table 15. The comparison of the traffic throughput and average fuel consumptions when the micro and macro optimal parameters are used	162

## Nomenclature

### Abbreviations

ACC	Adaptive cruise control
ADAS	Advanced driver assistance systems
ADP	Adaptive dynamic programming
AI	Artificial intelligence
ANOVA-HDMR	Analysis of variance with high dimensional model representation
AV	Autonomous vehicles
CACC	Cooperative adaptive cruise control
CAS	Collision avoidance system
CCD	Charged couple device
CH <sub>4</sub>	Methane
CO/CO <sub>2</sub>	Carbon monoxide/dioxide
CWS	Collision warning system
DP	Dynamic programming
EIDM	Extended IDM
EKF	Extended Kalman filter
FTP	Federal test procedure
GHG	Green house gases
GHR	Gazis-Herman-Rothery
GKT	Gas kinematic-based traffic
GM	General Motors
HCT	Homogenous congested traffic
HDM	Human driver model
IDM	Intelligent driver model
IDM-VDT	IDM with variance-driven time headway
IDMM	IDM with memory
ITS	Intelligent transport systems
KF	Kalman filter
ktoe	Kilo tonnes of oil equivalent
LDWS	Lane departure warning system
LKA	Lane keeping assist
LMM	Lagrange multiplier method
LQ	Linear quadratic
MLC	Moving localised cluster
mtoe	Million tonnes of oil equivalent
MoP	Measure of performance
MSE	Mean square error
NN	Neural networks
NO <sub>x</sub>	Nitrogen oxides
O <sub>3</sub>	Ozone
OAT	One-at-a-time
OCT	Oscillatory congested traffic

PBIL	Population based incremental learning
PF	Particle filtering
PID	Proportional-integral-derivative
PLC	Pinned localised cluster
PLC	Pinned localised cluster
PM	Particulate matter
RD	Relative deviation
RL	Reinforcement learning
SADP	Supervised adaptive dynamic programming
TD	Temporal difference
TfL	Transport for London
TSG	Triggered stop-and-go
VDIFF	Velocity difference model
VOC	Volatile organic compounds

## **1. Introduction**

### **1.1 Context and motivation**

Traffic network is a sophisticated multi-dimensional network. Billions of trips are made within global cities on a daily basis. Transport for London's report (TfL) in 2015 estimated that the average number of trips in, to or from London on a single day in 2014 was 26.6 million. Private cars constituted 37% of the total trips [1, 2, 3].

Transportation demands and the number of car owners continue to increase globally. Although London road traffic volumes have remained stable during recent years, and even experienced a reduction between 2000 and 2014, the UK's aggregate national figures show an increase in road traffic during the same period [4].

London's achievement in controlling its traffic demands is due to policies that encourage a shift in transportation modes from private cars to public transport and other modes such as cycling. The outcome of such policies has been a trend in reduction of road traffic volumes that has been continuing since the early 1990s.

Between 2000 and 2007, public transport's share in journey stages rose from 33% to 40% while the share of private motorised transport fell from 44% to 38% [2]. A similar trend continued between 2008 and 2015. In 2015, public transport accounted for 45% of journey stages, whereas private transport's share fell to 32%. Supporting public transport, laying down restrictions such as the congestion charge introduced in 2003, and encouraging the use of other modes of transport such as cycling, are some of the important measures taken that have contributed to the decrease in mode share of private cars and consequently the decrease in road traffic in London [1].

However, it is clear that cars are going to remain a significant entity of road transport. Technological advancements in the design of cars, along with innovation in areas such as car sharing and car clubs, make this mode of transport an attractive choice. New technologies such as fully automated driving are expected to make private cars a convenient option for those who currently cannot, or prefer not to, use this mode of transport; namely those with physical limitations or those who would rather use their journey times to do things other than driving. Therefore, improving the established motorised ground transport system in terms of environmental effects, energy consumption, safety, and efficient usage of roadways, remains a critical issue within the transport sector. The significant demands for car ownership, the considerable share of the road transport sector in fuel consumption, and the social and financial costs caused by inefficiencies in the road transport network indicate a need for further improvements in this field.

The present study focuses on the acceleration behaviour in the car-following regime of driving and investigates how driving automation can contribute to a more efficient road network in terms of fuel consumption and traffic flow. Since this study revolves around the acceleration behaviour in the car-following regime, the findings presented here are applicable to a wide range of automation levels. Six levels of automation are defined by the Society of Automotive Engineers (SAE International), Table 1 summarises the levels of driving automation.

Table 1. The six levels of driving automation defined by SAE International [5].

SAE Level	Name	Narrative Definition	Execution of Steering and Acceleration/Deceleration	Monitoring of Driving Environment	Fallback Performance of Dynamic Driving Task	System Capability (Driving Modes)
<b>Human driver monitors the driving environment</b>						
0	<b>No Automation</b>	The full-time performance by the human driver of all aspects of the dynamic driving task, even when enhanced by warning or intervention systems	Human driver	Human driver	Human driver	n/a
1	<b>Driver Assistance</b>	The driving mode-specific execution by a driver assistance system of either steering or acceleration/deceleration using information about the driving environment and with the expectation that the human driver perform all remaining aspects of the dynamic driving task	Human driver and system	Human driver	Human driver	Some driving modes
2	<b>Partial automation</b>	The driving mode-specific execution by one or more driver assistance systems of both steering and acceleration/deceleration using information about the driving environment and with the expectation that the human driver perform all remaining aspects of the dynamic driving task	<b>System</b>	Human driver	Human driver	Some driving modes
<b>Automated driving system monitors the driving environment</b>						
3	<b>Conditional Automation</b>	The driving mode-specific performance by an automated driving system of all aspects of the dynamic driving task with the expectation that the human driver will respond appropriately to a request to intervene	System	<b>System</b>	Human driver	Some driving modes
4	<b>High Automation</b>	The driving mode-specific performance by an automated driving system of all aspects of the dynamic driving task, even if a human driver does not respond appropriately to a request to intervene	System	System	<b>System</b>	Some driving modes
5	<b>Full Automation</b>	The full-time performance by an automated driving system of all aspects of the dynamic driving task under all roadway and environmental conditions that can be managed by a human driver	System	System	System	<b>All driving modes</b>

In the following sections, the issues outlined above are explored in more detail. This chapter is then concluded by highlighting the contributions that can be made to the road transport network by extending the applications of Intelligent Transport Systems (ITS) and automated control to the area of driving.

### **1.1.1 Safety**

Annual road fatalities in the EU are reported as high as 26,000 in 2016. This is about the size of a medium town. Moreover, almost four times as many people as this sustained permanently disabling injuries (such as damage to the brain or spinal cord) due to road accidents, and eight times as many people were seriously injured [6, 7]. Such high numbers, where even one is a tragedy, point to the necessity of serious considerations.

Interestingly, the EU has made great progress in reducing road fatalities. In particular, in the past two decades the number of fatalities has reduced by about 60%, from 64,000 in 1995 to 26,000 in 2016. This has been due to the implementation of various policies and regulations targeting a variety of areas such as road infrastructure, emergency services, law enforcements, training, and safety features in the automotive industry. However, in spite of the fact that remarkable improvements have been brought about due in part to the introduction of such policies, there seems to be a natural limit to the extent to which such policies alone can be effective. From 1991 to 2013 (except for one instance of 1995-1996), each year saw a significant reduction in annual road fatalities. Since 2013, however, this number has remained static. One could argue that further reductions in the number of road fatalities and injuries may require us to consider disruptive technologies, particularly since about 95% of these accidents are linked to driving errors and 22% of them are caused by lack of alertness in drivers [8]. Both advisory systems and driving automation can make a significant contribution to the reduction of road accidents.

### **1.1.2 Environmental effects**

Between 1990 and 2011 energy consumption by all different sectors fell remarkably in the UK. Energy consumption in industry fell by one third (12.8 million tonnes of oil equivalent (mtoe)), in the domestic sector it fell by 5% (1.9 mtoe), and in the services sector by 4% (0.7 mtoe). However, the transport sector saw an increase in energy

consumption of 11% (5.4 mtoe) in the same period. The transport sector is responsible for 36% of total energy consumption in the UK, as reported in 2012 [9]. Road transport accounts for 74% (39,468 ktoe) of total energy consumption by the transport sector in the UK, and this figure is relatively consistent with what was reported for EU-28 countries in 2012, when the share of road transport was almost 72% of the total energy consumed by the transport sector (352 mtoe) [10, 11]. This has a significant environmental consequence as almost all energy in the transport sector is provided by fossil fuels. For example, in 2012 94% of energy consumption in the transport sector in the EU was provided by petroleum products. The use of electricity and renewable energies in this sector is gaining significant attention and popularity, but the share is not yet comparable to that of petroleum products. Of the 68.7 mtoe rise in overall energy consumption by road transport between 1990 and 2006 in the EU, only 8% was made up by renewable and other fuels, while 92% was provided by increased consumption of oil fuels [10]. This figure implies worrisome ecological consequences associated with emissions of carbon dioxide ( $CO_2$ ), other Green House Gases (GHG) (namely, methane ( $CH_4$ ), Nitrous Oxide ( $NO_2$ )), and fluorocarbons, along with emissions of heavy metals and polycyclic aromatic hydrocarbons, particulate matter ( $PM_{10}$ ) and ozone ( $O_3$ ) precursors. These emissions are a cause for concern due to their negative effects on global warming and the health of humans, animals and soil [10, p. 167]. Therefore, reducing these emissions is among the most important challenges that the world cities face. For instance, London's outdoor air quality (particularly in inner London) has been continuously breaching national and EU health-based air quality objectives [12]. The aim of the present study is to reduce fuel consumption in automated cars by means of modifying their acceleration behaviour, a direct result of this is less emissions.

### **1.1.3 Traffic efficiency**

Traffic congestion and traffic jams occur as a result of traffic breakdown and capacity drop when the number of vehicles in a roadway (traffic density) exceeds a critical

value. This phenomenon causes considerable economic, social, and environmental costs in a lot of major cities around the globe [13]. One study suggests that the combined annual cost of traffic congestion in Europe and the US is about \$195 billion [14]. The same study predicts that this cost will soar to \$293 billion in 2030. In the UK the combined annual cost of traffic congestion was estimated to be \$20.5 billion in 2013 and is expected to rise to \$33.4 billion in 2030. Londoners alone are estimated to face a drain of more than \$200 billion on their economy from 2013 to 2030.

Such studies calculate costs based on a number of direct and indirect factors such as the value of fuel, time wastage in traffic which could otherwise be spent on productive activities at work, and increased cost of freighting that is passed on to households. However, it may be even more challenging and important to assess the social, psychological, and health costs resulting from traffic jams and congestion.

These staggering costs, along with the increasing demand for motorised ground transport, indicate the crucial importance of utilising all means possible for a more efficient traffic flow.

#### **1.1.4 Automated driving**

The introduction above points out some of the challenges arising from modern transportation needs. Technological developments can make a great deal of contribution to these issues. The advances in mathematical sciences, telecommunications, and mechanical and electrical engineering can merge and bring about new horizons in transportation.

Subjects such as dynamic traffic signal control [15, 16], dynamic route choice and traffic assignment [17, 18, 19], cooperative traffic management [20], Advanced Driver Assistance Systems (ADAS), and Adaptive Cruise Control (ACC) systems [21, 22, 23] are active areas of research. They attract researchers and scientists from a wide range of

disciplines, including telecommunications, Artificial Intelligence (AI), control, and modelling, all aiming to tackle the aforementioned problems.

Technological advances in sensory devices and computational power leading to affordable automated decision making, may enable technologies to tackle the existing challenges in road transport. In particular, ACCs and Autonomous Vehicles (AVs) are potentially capable of making remarkable contributions to all the challenges discussed above. Autonomous Vehicles perform all aspects of driving tasks without the need for driver intervention. In spite of the remarkable achievements of many companies in testing AVs, the successful commercialisation of these systems requires further progress in technological and legislative issues. The ACCs, however, have become commercially available since about two decades ago. These systems, of course, offer much more limited functionalities compared to AVs and require constant driver engagement. Nevertheless, they can potentially make a positive impact on transport networks through functionalities such as adjusting vehicles' speeds and spacing relative to preceding vehicles and exerting partial control over the acceleration behaviour of vehicles in certain driving conditions.

In addition to the safety and fuel savings that can be provided by these systems, numerous studies have investigated how the use of automated control can increase the efficiency of roadway usage and improve traffic flow. Moreover, the significant number of manufactured cars which now offer ACC, a form of partial automation, is an indicator of a remarkable potential for making contributions to road transport challenges through this platform.

## **1.2 Aim and objectives**

Some of the main challenges that transport networks face were explored in section 1.1. It was observed that policies and regulations can make a significant contribution towards a better transport network, for example in the cases of road accident reduction in Europe and traffic management in London. However, it was also argued

that such policies are likely to have intrinsic limitations, and further improvements may not be possible without exploiting the significant technological advances that have been rapidly introduced in the past decades.

A wide range of innovations and inventions such as more efficient control methods for traffic signals and dynamic route choice methods that exploit real-time data, alongside significant advances in computer science and artificial intelligence, have made transport an exciting area where emerging technologies and established technologies can merge in order to bring about remarkable improvements.

One of the more sought-after technologies that has received a lot of attention is automated driving. Partially automated vehicles with functionalities such as Adaptive Cruise Control (ACC) are commercially available and these systems are becoming an important feature of modern cars. Moreover, fully automated vehicles are expected to become a reality in the near future. Therefore, it is necessary to accurately examine the impacts and possible improvements that such systems can bring about in transport networks.

Automation of driving is, of course, a broad term which encompasses a wide range of topics from machine vision, to decision making in complex conditions such as interaction with pedestrians and cyclists. In this study, the focus is on the longitudinal control of vehicles, that is how cars adjust their brake and throttle in different circumstances. The longitudinal control of vehicles can be further categorised into two areas; 1) the car-following regime in which the control is mainly a response to the actions of the lead vehicle(s), and 2) the free-flow regime in which cars are free to accelerate to their desired speed. The goal of this study is to build upon previous studies in this field and tackle the challenging question of fuel efficiency in the car-following regime of driving. Chapter 2 explores these concepts in more detail and provides an overview of different subjects related to the control and modelling of driving.

Transport networks are complex systems consisting of several, sometimes conflicting, criteria. Therefore any improvement proposed needs to address resulting implications on other criteria. A thorough understanding of the important criteria for a practical and efficient transport network is necessary to avoid propositions that, despite introducing improvements in one aspect, result in poor performances in other aspects. For example, a driving strategy that achieves fuel savings but degrades the capacity usage of roadways or safety is not desirable. The present study seeks to adopt a comprehensive approach to the question of fuel efficiency that appreciates the intrinsic sophistication and multi-objective nature of the motorised ground transport network. Safety, stability and the acceptance of these systems, along with other important considerations such as their impact on traffic flow and fuel consumption, have been studied in numerous studies and these subjects are still open areas of research. Chapter 3 provides a comprehensive overview of these important requirements.

The introductory material provided in chapters 2 and 3 highlights a gap in the literature that is worth noting. This gap relates to finding a methodological framework for optimisation that is suitable for application to the car-following regime of driving, while having the potential to incorporate other important criteria such traffic safety, flow efficiency, and stability.

In chapters 2 and 3, a number of studies related to the control of vehicles and fuel efficiency are explored. Most of these studies use methods such as velocity optimisation given the initial and terminal state; dynamic programming-based algorithms are often used to find the optimal velocity values at different time steps. However, due to the complexities that arise from interaction with other vehicles, these studies mainly consider interaction-free scenarios such as approaching a traffic signal or driving in an empty roadway. In such studies, knowledge or prediction about what lies ahead in terms of the topography of the roadway or the state of traffic signals is used to formulate energy efficiency as an optimal control problem. The interaction

between vehicles in the car-following regime eliminates this predictability and therefore, poses a challenge. Thus, the methods used in these studies are not suitable for the car-following regime of driving.

Another group of studies that aim to address energy efficiency in the car-following regime of driving as an optimisation problem, make somewhat simplified assumptions about the dynamics of driving or its relationship with fuel-consumption. For instance, the complex, nonlinear relationship between velocity, acceleration, and fuel consumption may be reduced to an attempt to minimise accelerations. Some studies make the assumption that fuel efficiency is obtained by maintaining stable and large headways. This approach is based on the intuition that large headways provide sufficient time periods for the vehicle in order to smoothly react to the lead vehicle's movements, and this reduces fuel consumption. In spite of such simplifications, fuel-economy driving remains a complex nonlinear problem which requires computationally expensive, real-time, nonlinear optimisation methods. Such optimisations cannot be easily implemented in large-scale simulations with thousands of equipped vehicles. This results in a shortcoming in terms of the evaluation of their collective impacts on stability, traffic flow, and fuel consumption.

This introduction indicates the need for a new framework that meets the following criteria.

1. It must address the issue of computational complexity that is observed in the existing control methods in the car-following regime, where the unpredictability of the behaviour of the lead vehicle poses a challenge.
2. It must have the potential to incorporate and address important collective features such as stability and traffic flow in the optimisation process.

The aim and objectives of the present research are summarised below;

**Aim:** development of a control method for the acceleration behaviour in the car-following regime of driving that is efficient with respect to fuel consumption and traffic flow.

**Objectives:**

1. Carrying out a comprehensive literature review in order to identify an optimisation framework that can appropriately incorporate the microscopic details of driving while allowing for macroscopic, flow-related, characteristics of traffic to be addressed.
2. Carrying out a comprehensive literature review in order to identify different requirements for the longitudinal control of vehicles.
3. Identification of a suitable car-following model.
4. Development of a simplified fuel consumption model to be used within the optimisation process without adding a significant computational burden to it.
5. Identification of the most influential model parameters on fuel consumption.
6. Development of an optimisation framework that can deliver fuel-efficiency without deteriorating traffic flow. This is done through simulation-based optimisation. The simulations involve the modelling of traffic flow in sufficiently long stretches of roadways and for long durations of time in order to enable a good assessment of the long-term impacts of different driving strategies.
7. Validation of the optimal control method through comparison with real data and implementation in the micro-simulation software PTV VISSIM.

### **1.3 Structure of the thesis**

In chapter 1 the context and motivation of the present study was described and the aim and objectives of this research were set out. Chapter 2 provides a comprehensive review on different background subjects, such as traffic modelling, methodological approaches for the development of automated control, and energy efficiency. Chapter 3 deals with the question of what constitutes a good control model and provides a review of different requirements for an efficient control. This chapter is concluded

with the selection of a suitable car-following model and identification of the parameters that have the highest influence on fuel consumption. In chapter 4, the proposed framework for the optimisation of fuel consumption is presented and two distinct formulations of the problem are considered;

1. A microscopically-formulated problem where the movement of the vehicle with respect to its immediate leader is the subject of optimisation. This formulation is similar to numerous studies in the literature.
2. A macroscopically-formulated problem that captures the long-term impacts of driving strategies.

The results are validated using a real dataset and a discussion on the results concludes chapter 4. In chapter 5, the validation of the findings is carried out in an urban network using the micro-simulation software PTV VISSIM. Finally, chapter 6 concludes this thesis by highlighting the conclusions, contributions and future directions of research.

## **2. Literature review**

This chapter provides an overview of some of the fundamental concepts in traffic modelling, development of automated driving, and energy efficiency. In section 2.1, traffic flow theory and microscopic and macroscopic approaches to simulation are briefly discussed. In section 2.2, an overview of car-following models which constitute an important entity of micro-simulation is given. Some of the methodologies used in the development of automated control for the task of driving are explored in section 2.3. Energy-efficiency and fuel consumption are discussed in section 2.4, and finally, section 2.5 concludes this chapter by identifying a gap in the literature.

### **2.1 Background on traffic modelling**

Congested traffic giving rise to capacity breakdown is typically caused by bottlenecks (e.g. uphill gradient, lane closing, on/off-ramps, etc.) [24]. In [25], about 400 congestion patterns on a German freeway were investigated and no evidence of a traffic breakdown without a bottleneck was found. The bottleneck usually stimulates a traffic breakdown upstream of it with a stationary downstream front at the location of

the bottleneck. Capacity breakdown can be associated with a drop of about 20% in capacity [26], and hence it is important to take all measures possible to avoid capacity breakdown, or manage capacity breakdown once it occurs.

Since automated control systems introduce changes in driving dynamics, it is necessary to analyse how these changes affect traffic flow. The applicability of a control module, therefore, may be restricted to particular scenarios where it does not cause negative impacts. For instance, in [27], different traffic conditions are identified and a longitudinal control module is selected accordingly.

Since ACCs are expected to function in a wide range of traffic conditions, it is necessary to accurately identify and analyse different factors that give rise to congested traffic. This analysis could establish a foundation on the basis of which mechanisms for congestion avoidance or delaying capacity breakdown could be suggested. It is therefore necessary to provide an insight into the fundamentals of traffic flow theory before proceeding to the formulation of problem. In this section important concepts such as the fundamental diagram, traffic bottlenecks, the formation of traffic jams, phase diagrams and different types of congested traffic are explored.

### **2.1.1 Fundamental diagram and congestion**

The simplest and most conventional depiction of collective traffic characteristics is done by the well-known fundamental diagram which sets up a two-phase relation between density and flow for stable equilibrium traffic. The two phases are free flow, where vehicles can freely move with their desired speed, and congested flow, in which the movement of vehicles is constrained due to the surrounding traffic. Important parameters of the fundamental diagram such as maximum traffic flow,  $Q_{max}$ , and maximum free-flow density,  $\rho_{FF_{max}}$ , can be associated to drivers' attitudes (e.g. conservative or aggressive driving), characteristics of roadway (e.g. design, quality, and gradient), and environmental factors (e.g. weather conditions). It has been suggested that traffic velocity,  $V$ , which is a function of traffic density,  $\rho$ , and consequently traffic

flow,  $Q$ , are determined by drivers' collective perception of safe distance and risk readiness, and environmental factors such as road condition and speed limits are other contributory factors that need to be considered [28].

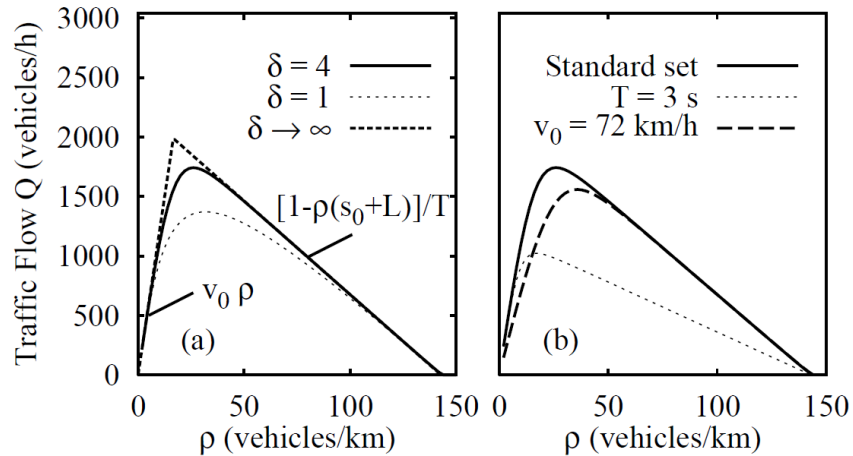


Figure 1. A depiction of the fundamental diagram derived from a car-following model, namely the IDM (a) Coefficient  $\delta$  determines how fast cars accelerate to their desired speed (b) Coefficients  $T$  and  $v_0$  represent safe headway and desired velocity respectively. Finally,  $s_0$  and  $L$  are the standstill bumper to bumper spacing between vehicles and vehicle lengths. Only one parameter is varied at a time and the rest of the parameters are default parameters given in [26].

Another extension of this theory is Kerner's three-phase diagram which can successfully explain some of the observed phenomena in empirical data. This new understanding of the behaviour of traffic flow could entail new principles for the control of traffic flow [29]. Therein, a congestion region is assumed whereas in the two-phase fundamental diagram congested traffic is denoted by a line, that is the right branch of the curve. Moreover, using the three-phase diagram a more in-depth understanding of the formation of congested traffic can be provided.

1. The local transition from free flow to synchronised flow usually takes place due to a bottleneck. A bottleneck refers to a drop in the capacity of the roadway due to phenomena such as lane blockage or traffic flow merging from an on-ramp.

The downstream boundary of the synchronised flow usually remains fixed at the bottleneck while the upstream boundary propagates in the upstream direction.

2. Several moving and growing narrow jams occur in the upstream direction of the bottleneck and inside the region with synchronised flow patterns. This would happen in a region of motorway where the state of the synchronised traffic can be described by a point above the characteristic line  $J$  in the flow-density plane.

The line  $J$  is a characteristic line in the flow-density diagram that represents the steadily propagation of the downstream front of a wide moving jam. The slope of the characteristic line  $J$  represents the mean velocity of the downstream jam front. The two ends (coordinates) of this line are the pair  $(\rho_{min}, q_{out})$  on the top-left end and  $(\rho_{max}, 0)$  on the bottom-right end, where  $\rho_{min}$  and  $q_{out}$  are the density and flow rate of the outflow of the wide moving jam if this outflow is in the form of free flow. The coordinates at the bottom-right end of line  $J$  are related to traffic variables within a jam, that is the maximum density and the minimum flow which is assumed to be equal to zero.

The formation of narrow moving jams inside the region with synchronised flow is referred to as the pinch effect. This is linked to the spatial compression, otherwise known as self-compression, of synchronised flow where the average speed and density are respectively lower and higher compared to the synchronised flow in the surrounding neighbourhood. Therein, in spite of the low speed and high density, traffic flow can increase. The region where the pinch effect takes place in is called the pinch region.

The downstream boundary of the pinch region is usually in the vicinity of the location on the motorway where the synchronised flow is maintained (usually bottleneck) and the upstream boundary is where narrow jams are transformed to wide jams.

3. Several narrow jams occur in close proximity to each other and move with a speed more negative than the downstream front of wide jams, i.e. between  $1.1v_g$  to  $1.3v_g$  [30], where  $v_g$  is the velocity of the downstream front of the wide jam. Some of these narrow jams grow as they propagate in the upstream direction and are consequently transformed into wide moving jams. The remaining narrow jams near the wide jam either catch up with the wide jam and merge or dissipate. Only a narrow jam far

enough from the wide jam downstream front (2.5-5km which is much larger than the mean distance between narrow jams) can continue to grow and form another wide jam. Once a sequence of wide jams is formed, no narrow jam occurs in between wide jams, even if the outflow of the wide jam upstream of another wide jam is synchronised flow.

4. Free or synchronised flow can be formed in the downstream front of a wide jam. In the latter case, the flow rate of the traffic stream that is being discharged out of the jam,  $q_{out}^{syn}$ , and the vehicle density in the outflow stream,  $\rho_{out}^{syn}$ , are usually respectively lower and higher than the former case. Moreover these values,  $q_{out}^{syn}$  and  $\rho_{out}^{syn}$ , can change significantly over time [30].

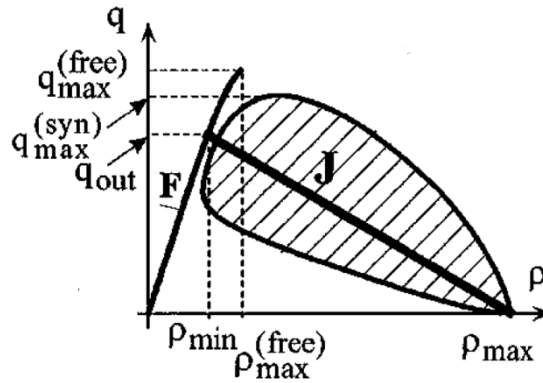


Figure 2. Three-phase diagram [30].

5. Motorway capacity depends on the phase that traffic is in and the related maximum capacity usually satisfies the following equation;

$$\frac{q_{max}^{free}}{q_{out}} \approx 1.5 \quad , \quad q_{out} < q_{max}^{syn} \lesssim q_{max}^{free} \quad (2.1)$$

where  $q_{out}$ ,  $q_{max}^{syn}$  and  $q_{max}^{free}$  are wide jam downstream outflow, maximum synchronised traffic flow, and maximum free flow respectively.

6. Metastable states of free flow range from  $p_{min}$  to  $p_{max}^{free}$

7. The line J separates homogenous states of both free flow and synchronised flow into two regions. In states below the line J no jam can occur. This can be explained in the following way. By drawing a characteristic line from any state below line J to

$(\rho_{max}, 0)$  the velocity of the upstream front of a wide jam can be derived as the slope of the characteristic line. Since this slope would have a less negative value than that of the upstream front,  $v_g$ , this would suggest that the width of the jam would gradually decrease. On the other hand, for states above the line  $J$  the same analysis suggests the width would increase. Therefore, the states above the line  $J$  are metastable and fluctuations with amplitudes exceeding a critical value can result in formation of wide jams. The further the states are above the line  $J$  in the metastable region, the higher the probability of exciting a wide jam with smaller fluctuation [30].

8. The velocity of the downstream front of the wide jam,  $v_g$ , is independent of the state of flow that is formed in the outflow of jam (in the upstream of the jam downstream front) and is given by:

$$v_g = -\frac{1}{\rho_{max}\tau_{del}}, \quad (2.2)$$

where  $\tau_{del}$  is the average time delay between two successive vehicles escaping traffic jam after one another and  $\frac{1}{\rho_{max}}$  is the average distance between vehicles including an average length of vehicles.

9. The mean distance between centres of emerging narrow jams,  $R_{narrow}$ , increases with vehicle speed in the pinch region.

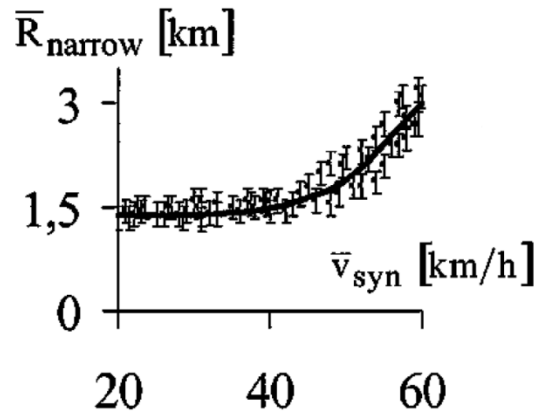


Figure 3. Relation between the mean distance between centres of narrow jams and the average vehicle speeds between jams in the pinch region.

10. The frequency of wide jams increases as the density in synchronised flow increases

Furthermore, the concept of over-acceleration and speed adaptation play an important role in Kerner's theory. Over-acceleration is defined as accelerating in spite of preceding vehicles' slower speeds. This can be interpreted as overtaking in a multi-lane road. Speed adaptation refers to slowing down and speed adjustment to the lead vehicle. The probability of each can be related to the speed as well as the regime of driving. For instance, given the same speeds, one would expect higher probabilities of over-acceleration in free-flow traffic compared to traffic with synchronised flow [29].

Local disturbances can be suppressed if over-acceleration is stronger than speed adaptation. However, if the opposite holds transition from free flow to synchronised flow may occur. Moreover, the existence of a region of synchronised flow in the flow-density plane, as opposed to a line, can be justified by the following explanation.

For gaps below a certain value,  $g_{safe}$ , drivers will decelerate to avoid collision. For gaps greater than another threshold,  $G$ , drivers will accelerate. Within the range between,  $g_{safe} < g < G$ , drivers adapt their speed to the lead vehicle without paying attention to the precise "desired gap".

### **2.1.2 Phase-diagram and different types of congested traffic**

The mechanisms resulting in congestion and traffic breakdown as explained by the three-phase traffic theory were discussed in subsection 2.1.1. In this subsection, different types of traffic congestion are discussed.

The state of traffic can be classified into four types namely, free flow, moving localised cluster, pinned localised cluster, and extended congested traffic that may occur in different patterns. The emergence of a particular traffic pattern depends on two important factors; the volume of inflow into the freeway section, and the "bottleneck strength" which characterises an inhomogeneity in the roadway capacity [31] [26] [27].

For a given set of inflow,  $Q_{in}$ , and bottleneck strength,  $\delta Q$ , one or more of the following patterns may occur due to a perturbation in the downstream traffic;

- Free flow: This regime occurs in low traffic densities where interaction between vehicles is not the main influential factor in defining longitudinal behaviour of drivers and, therefore, drivers have a relative freedom to drive with their desired velocity. For a region characterised by the pair  $(Q_{in}, \delta Q)$ , with relatively low inflow and low bottleneck strength, initial perturbations will dissipate and free-flow will persist.
- Moving Localised Cluster (MLC): The perturbation triggers a localised cluster that moves through the inhomogeneity and neither dissipates nor triggers new breakdowns.

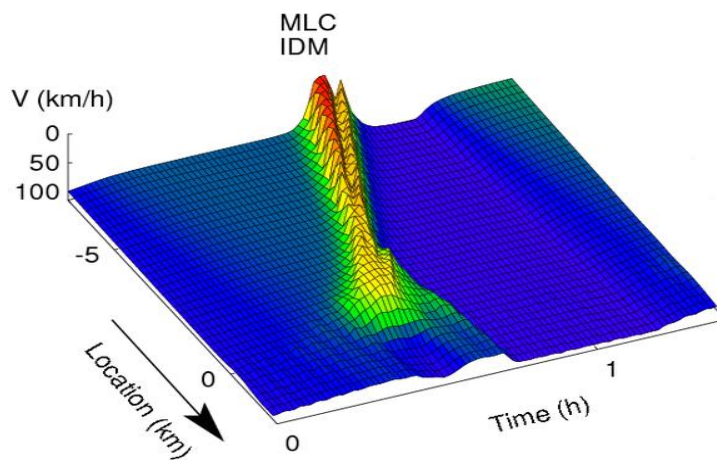


Figure 4. Spatio-temporal representation of an MLC [32].

- Pinned Localised Cluster (PLC): A traffic breakdown will be triggered that remains localised near the inhomogeneity. This could be stationary or oscillatory.

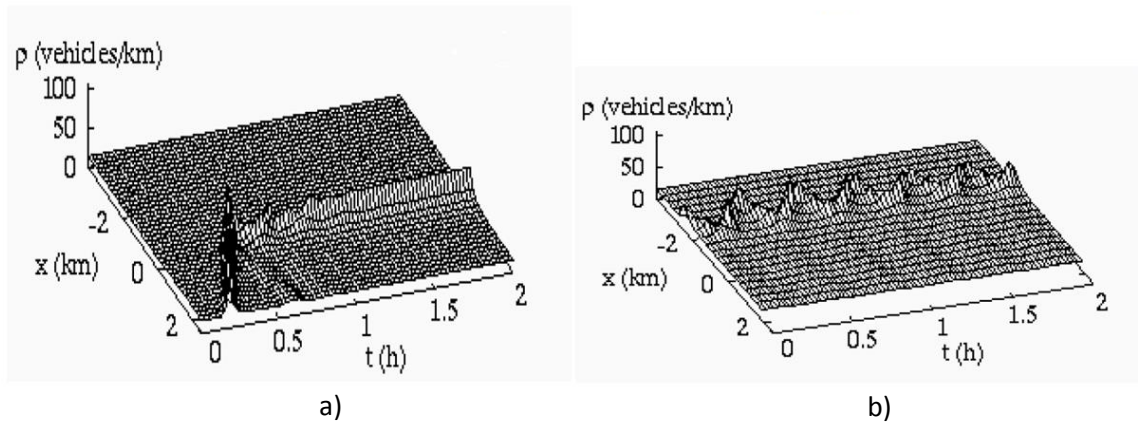


Figure 5. a) Stationary PLC b) Oscillatory PLC [26].

- Extended congested traffic (CT): The downstream end of congestion is fixed at the bottleneck and the upstream end of congestion propagates in the upstream direction. Such congested traffic can be either homogenous (HCT), oscillatory (OCT), or consist of triggered stop-and-go waves (TSG). TSG can be distinguished from OCT by the existence of a permanently congested state at the bottleneck in OCT, whereas in TSG each wave triggers a new isolated cluster as it crosses the inhomogeneity. Additionally, a signature characteristic of an OCT is the existence of congested traffic between the waves whereas in TSG free traffic can emerge between the clusters. Finally, another characteristic that can be attributed to OCT, compared to HCT, is that the exact regions of free-flow and congested flow cannot be separated for the former in empirical data.

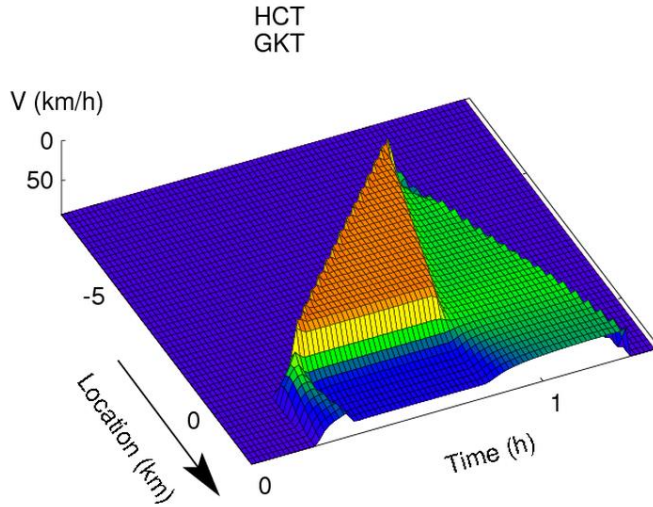


Figure 6. HCT [32].

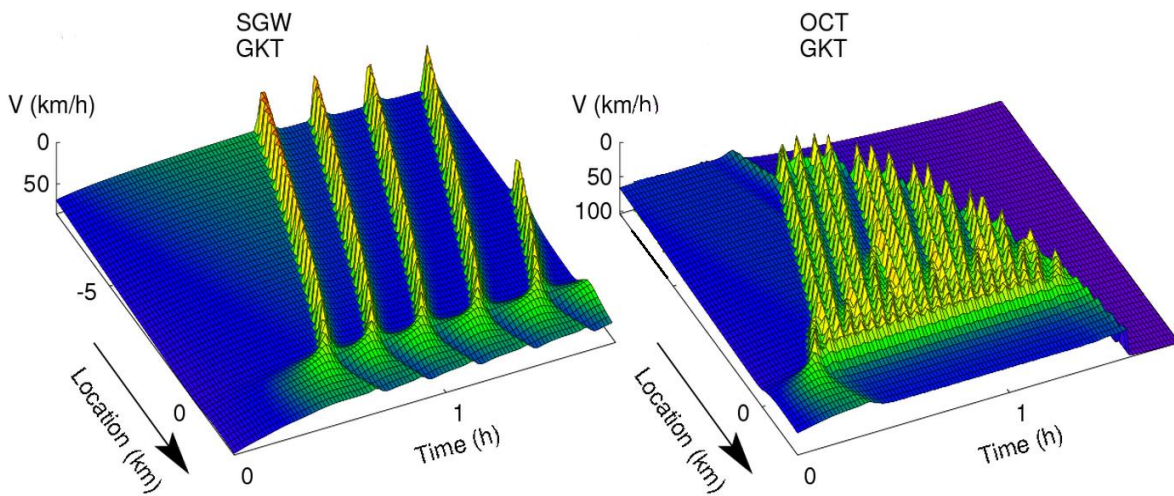


Figure 7. STG and OCT [32].

Since the same patterns are reported for identical bottlenecks and control parameters (density in the closed-system and inflow in the open system) one can qualitatively represent the relation of these patterns with the bottleneck strength and the inflow by means of a phase diagram. It is worth mentioning that for an accurate identification of the different congestion patterns, the hysteresis effect needs to be taken into account

[33]. This adds to the complexity of visualisation of the relationship between bottleneck strength, inflow (or density in the closed system), and different congested traffic patterns since for different histories different phase diagrams may be derived.

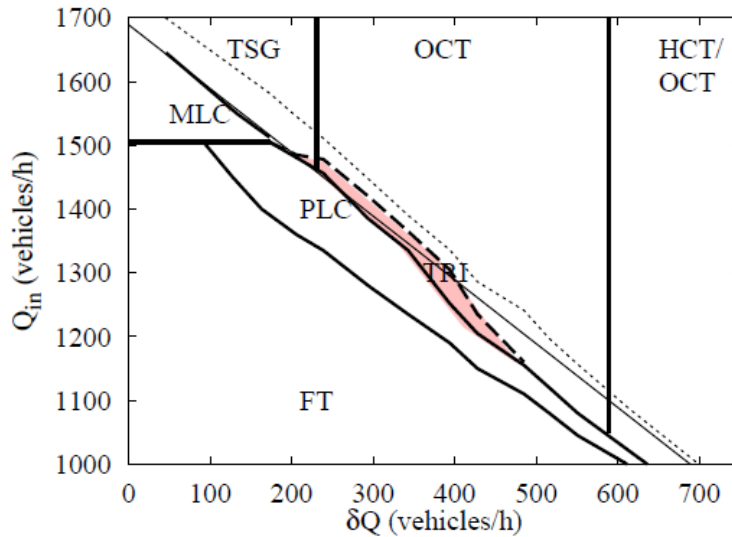


Figure 8. Phase diagram of an open system simulated with a car-following model, the intelligent driving model [26].

### 2.1.3 Traffic modelling

Transport networks play a crucial role in modern society. With the growth of urban populations around the world in the past century and the increasing number of cities with populations of millions, it is crucial to address the question of effective movement of people. The costs incurred on countries around the world as a result of inefficiencies in transport networks include a significant variety of economic, environmental, health-related, and social costs. This subject was touched on in chapter one. Providing efficient transport networks is, therefore, an important challenge faced globally. However, this cannot be achieved without an accurate and in-depth understanding of transport networks. Transport modelling addresses this need. It provides a platform for more educated planning for future demands, be it preparing for an international event at a major city, addressing increasing travel demands of a city with a growing population, planning and designing new roadway infrastructure, investigating new

solutions in urban design such as dedicated cycle lanes and shared spaces, or understanding the implications of new technologies such as autonomous vehicles and connected vehicles.

Three distinguishable approaches to roadway traffic simulation are macroscopic, mesoscopic, and microscopic models. Macroscopic models view traffic as a whole and ignore interactions between individual vehicles. They provide a description of the collective vehicle dynamics in terms of the spatial vehicle density,  $\rho(x,t)$ , and the average velocity,  $V(x,t)$ , as a function of roadway location and time [34, 35]. Microscopic traffic models, on the other hand, provide a more detailed account of individual vehicles' movements and their interactions with one another. A comparison of the approaches can be found in [36]. Mesoscopic simulation models fall in between the two; meaning the flow of vehicles is broken down into groups of neighbouring vehicles where all the vehicles within a group are considered homogenous. There is a number of commercial software based on the three aforementioned approaches; SUMO, MATSim, CORSIM, and Quadstone Paramics for micro-simulation, PTV Vissum for macro-simulation, PTV Vissim for microscopic and mesoscopic simulation, and AIMSUN for an integrated micro-meso-macro simulation to name a few.

The importance of micro-simulation in the analysis of new technologies and transport planning has significantly increased in the past decade. New technologies can potentially change transport networks as we know them and micro-simulation plays an important role in the assessment of the impacts of these technologies. The great potential of micro-simulation traffic is the reproduction of subtle characteristics and more detailed behaviours of individual drivers which are simply ignored or averaged out in macro-simulation models.

Nowadays, with increased computational power, more and more complex micro-simulation models can be implemented and used for the simulation and study of different aspects of transport networks such as network design, transport planning,

and the investigation of new solutions and technologies. As a result, this field has emerged as a crucial entity in the evaluation of traffic policies and technological developments within the transport sector. Automated driving is one of the areas where micro-simulation has a lot to offer. Micro-simulation with its potential to capture and analyse subtle traffic-related phenomena can play an important role in the investigation of different issues arising from ACCs and the validation of different proposals relating to their application. Moreover, acceleration models and lane-changing models that are fundamental aspects of micro-simulation can be considered as a foundation on which ACCs and autonomous vehicles can be built. For instance, the question of “what are the required explanatory variables in order to plausibly model driving behaviour?” that is highly relevant to micro-simulation, can also be directly linked to the sensory requirements of ACCs. The control and decision making processes [37] are some of the other subjects widely investigated within modelling driving behaviour that can lay down the basis for the development of automated driving.

In order to derive a microscopic model of driving behaviour one needs to address the question of the variables that motivate drivers’ actions. However, the trade-off between simplicity and accuracy plays an important role in this issue. For instance, consider the process of lane. In a congested road where sufficient gaps in order to allow a lane-changing manoeuvre to be performed may not always be available, and in a scenario where a car from the most right lane needs to go to the most left lane in order to enter an off-ramp, forced merging and courtesy yielding plays a critical role. One can even go as far as to discuss the impacts of drivers’ attitudes and personalities in such a process. While such complex models could be potentially developed,

1. They may not necessarily lead to a more accurate reproduction of the reality. The problem of calibration and over-fitting will be discussed in chapter 3.
2. They may require immense computational resources, making large-scale simulations excessively time consuming.

Acceleration models or car-following models could be categorised based on their complexity and their methodology. For instance, the Intelligent Driver Model (IDM) [26], Gipps' model [38], and Herman's model [37] provide relatively simple equations with only a few model parameters in order to describe the driving behaviour, while the Wiedemann model [39, 40] and the model used in the MITSIMLab simulation software [41, 42] have more complex structures and a larger number of model parameters [26]. Another way of categorising microscopic models could be based on the methodological approaches from which they are derived. Such classification can be found in [43] where car-following models are classified into models based on stimulus-sensitivity (Heman's model), safety distance or collision avoidance models (Gipps' model), linear models, psychophysical or action point models (Wiedemann model), and fuzzy logic based models.

Besides acceleration models and car-following models, another important subject that defines the movement of vehicles in the operational level of driving is lane-changing. Lane-changing manoeuvres consist of two important entities. Firstly, lane-changing as a decision-making process where a driver decides that he or she should change lane. The modelling of this decision-making process includes a description of it as a procedure, with a certain structure and a number of parameters. Secondly, gap acceptance models which pertain to the possibility of lane-changing in terms of safety considerations and the desirability of lane-changing. Gap acceptance models can be thought of as a criterion through which the admissibility or desirability of performing lane-changing manoeuvres is evaluated. This evaluation stage is an important step within the hierarchy of the lane-changing decision-making process. Gap acceptance models are sometimes explicitly based on underlying car-following models and appear as constraints on its parameters such as braking imposed on the subject vehicle and/or its follower [44, 45]. A significant body of conventional studies in this area are dedicated to modelling drivers' gap acceptance as a distribution that represents drivers' perception of critical gaps. The following are important issues arising in this framework.

1. The capability of a model to project drivers' inconsistencies and inhomogeneities. In this context, inconsistency refers to variations in gap acceptance that is observed in a given driver in similar situations, while inhomogeneity refers to inter-driver variations in gap acceptance. For instance, a conservative driver may on average recognise 10 seconds of time gap as acceptable while merging onto a motorway from an on-ramp, whereas for an aggressive driver this value in average could be much less.
2. The capability of a model to capture variations in the perception of the critical gap in different situations. In other words, a model should be able to produce different gap acceptance behaviour in different traffic situations, such as lane-changing in congested traffic, merging onto a motorway, merging to the major leg in a stop-controlled T-intersection from the minor leg, and etc.

Two types of lane-changing are widely accepted and addressed by researchers in transportation [44, 46, 47, 48, 45]:

1. Discretionary lane-changing: This refers to lane-changing manoeuvres that are performed by drivers in order to improve their driving condition. For instance, longer headways in an adjacent lane could motivate a lane-changing manoeuvre. However, performing the lane-changing would still be subject to satisfying some criteria such as availability and safety.
2. Mandatory lane-changing: This type of lane-changing may be motivated by the strategic level of driving such as route choices or may be the result of lane blockage or lane drops.

A more-detailed survey on this subject can be found in [47, pp. 38-43].

In section 2.2, car-following models are described in more details and some of the car-following models mentioned in this section are described. More comprehensive reviews on car-following models and other related topics can be found in [43, 49, 37, 50] and references therein.

## 2.2 Car-following models

An important step in describing the longitudinal behaviour of vehicles is the choice of different parameters that affect the driving behaviour. These parameters could be different attributes such as what driver perceive as a safe headway, their desired speed, their relative speed to the leading vehicle, and the speed of the subject car, to name a few. A car-following model describes the relationship between such parameters, some of which are variables and some constants, and drivers' actions in different driving conditions. The drivers' actions or the output variable of a car-following model is typically given in the form of acceleration or velocity. Since the driving behaviour in the free-flow regime and in the car-following regime are expected to be different, sometimes different models are used for the two regimes. It is important to bear in mind that each of the aforementioned regimes of driving, the car-following regime and the free-flow regime, consists of a wide range of possible scenarios. For instance, a driver is expected to decelerate when the spacing between its car and leading vehicle is perceived to be low. This braking happens even when the relative speed to the leading vehicle is zero. A driver is also expected to brake when the leading vehicle has a lower velocity. Another example of common driving behaviour is a tendency to accelerate to a certain speed whenever possible. These are only a few examples of the common phenomena that car-following models should be able to reproduce. What follows provides a brief review of some of the well-known micro-scale car behaviour models. Additional requirements and considerations in micro-scale modelling of drivers' behaviours are also discussed.

### 2.2.1 Car-following regime

This regime of driving has been studied since 1950s with the pioneering works of Herman [51], Gazis [52], Chandler [53], Pipes [54], Kometani and Sasaki [55] . A wide class of conventional car-following models can be formulated as in [47, 26, 37]:

$$a_n(t) = stimulus(t - \tau) \times sensitivity(t - \tau), \quad (2.3)$$

where  $a_n(t)$  is the acceleration of the  $n^{th}$  vehicle within a platoon of  $n$  vehicles at time  $t$ ,  $\tau$  denotes driver's reaction time, stimulus is usually the relative speed to the leading vehicle, and sensitivity is a function of spacing, the subject vehicle's speed and other model-specific parameters. The model developed by Gazis et al. (1961) [52] known as the General Motors (GM) Nonlinear Model, or the Gazis-Herman-Rothery model, is one of the most popular and well-studied models of this type. This model is as follows,

$$a_n(t) = \alpha \frac{V_n(t)^\beta}{\Delta X_n(t - \tau_n)^\gamma} \Delta V_n^{front}(t - \tau_n), \quad (2.4)$$

where,

- $V_n(t)$  is the speed of the subject vehicle,
- $\Delta X_n(t - \tau_n)$  denotes the net bumper-to-bumper spacing,

$$\Delta X_n = X_{n-1} - X_n - l_n, \quad (2.5)$$

lagged by a reaction time,  $\tau_n$ . The parameters  $X_n$  and  $X_{n-1}$  are the positions of the front bumpers of the subject vehicle and the preceding vehicle respectively,  $l_n$  is the length of the vehicle  $n$  [26]. The fraction in the equation with the velocity as its numerator and the spacing as its denominator represents the sensitivity parameter in equation (2.3).

- $\Delta V_n^{front}(t - \tau)$  is the perceived relative speed to the leading vehicle given by,

$$\Delta V_n^{front}(t - \tau) = V_{n-1}^{front}(t - \tau_n) - V_n(t - \tau_n), \quad (2.6)$$

and represents the stimulus, and

- $\alpha, \beta$  and  $\gamma$ , are model parameters.

Several empirical and theoretical studies on the estimation of the model's parameters, extension of the model, and incorporation of other influential parameters into the

model are addressed in [47]. Some of the most relevant results are briefly summarised below.

- In 1968, Bexelius [56] suggested extending the influence of leading vehicles from merely immediate leader to more vehicles in front. This can be mathematically formulated as

$$a_n(t) = \sum_{i=1}^N \lambda_i (V_n^i(t - \tau_n) - V_n(t - \tau_n)) \quad (2.7)$$

where  $\lambda_i$  is the sensitivity associated with the influence of  $i^{th}$  leading vehicle,  $V_n^i$  denotes its speed, and  $N$  is the number of leading vehicles that their influence are taken into account.

- A typical reaction time of about 1.5 seconds was reported in [57, 58] .
- Preferred headway values ranging from 1.1 to 1.9 seconds with a mean of 1.47 seconds were reported by Aycin and Benekohal in 1998 [59].
- In 1968, Leutzbach [60] pointed out different sensitivities in deceleration and acceleration decisions, that is to say different reaction behaviours were observed for negative relative speeds and positive relative speeds. This supported the motivation of having two distinct sets of estimated parameters for deceleration and acceleration, an approach that was also pursued by others like Ozaki in 1993 [61], Subramanian in 1996 [62], and Yang in 1997 [46].
- In 1993, Ozaki [61] also pointed out that the reaction time,  $\tau_n$ , is influenced by other factors such as the spacing and the leader's acceleration.
- A spacing threshold was used by some of the researchers (Subramanian in 1996 [62] and Yang in 1997 [46]) in order to identify the regime of driving (car-following or free flow), while Aycin and Benekohal [59] suggested a headway-based threshold. This was supported by the following observations a) equal spacing will result in identical driving regimes regardless of the subject vehicle's speed and its relative speed to the lead vehicle and b) studies have shown that drivers tend to maintain headways independent of speeds in a steady-state car-following regime [59, 47, pp. 48-49]

- In the free flow regime the main objective is to achieve the desired speed. Mathematical equations are usually obtained based on simple laws of motion while taking into account constraints such as maximum acceptable acceleration, safe gap, and comfortable and minimum decelerations [46, 62, 38].
- One of the noteworthy and more recent works on the calibration of the GHR model is [63] where multiple data sources are used.

In [26], some of the issues arising as a result of formulation of car-following behaviour as denoted by equation (2.4) are pointed out.

1. Since the acceleration depends on a leading vehicle, this model is not applicable to very low densities. In the case of no leading vehicles ( $\Delta X \rightarrow \infty$ ), a driver is expected to accelerate to a desired speed, whereas in this model the acceleration is either not determined or is equal to zero.
2. Moreover, in high densities the model produces somewhat unrealistic behaviour, since the gap,  $\Delta X_n(t - \tau_n)$ , does not necessarily relax to an equilibrium value. Even small gaps do not lead to a brake if  $\Delta V_n^{front}$  is equal to zero, while this is necessary in order to maintain a safe distance to the lead vehicle.

The Newell model [64] and the Gipps' model [38] addressed these issues [64, 47]. The Gipps' model is described in details in section 2.2.1. The Newell model is a collision-free model that incorporates a mechanism for accelerating to a desired velocity,  $v_d$ , in low densities. Additionally, a safe headway parameter,  $T$ , characterises the car-following behaviour in the equilibrium traffic.

$$V(t + \tau) = v_d \left( 1 - e^{-\frac{s(t) - s_0}{v_d T}} \right) \quad (2.8)$$

However, the model still fails to produce realistic driving dynamics. In particular, positive or negative deviations of the velocity from the equilibrium velocity produce similar decelerations. Moreover, in some scenarios accelerations with an unrealistically high magnitude of  $\frac{v_d}{\tau}$  may be produced. For instance, for a car with the speed of

$V = 0 \frac{m}{s}$ , in the presence of no leading vehicles ( $s \rightarrow \infty$ ), and assuming the values of  $\tau = 1 \text{ s}$  and  $v_d = 30 \frac{m}{s}$ , an acceleration of  $30 \frac{m}{s^2}$  is obtained [26].

### 2.2.2 Gipps' general acceleration model

Gipps was the first to propose a general acceleration model capable of describing cars' behaviours in both free flow and car-following regimes [47, p. 34]. The Gipps' model can also be classified as a collision-free model. In the derivation of the Gipp's model firstly an inequality was obtained that represents the following facts;

1. the driver's desired speed set the upper bound for vehicle's speed, and
2. free acceleration is initially an increasing function of vehicle's speed, due to the high engine torque. As the vehicle approaches its desired speed acceleration smoothly drops to the value of zero.

In order to find a mathematical relationship encompassing the previous criteria, an envelope was fitted to the plot of instantaneous speeds and accelerations that was obtained from a single vehicle. As a result, the following inequality

(2.9) was obtained:

$$V_n(t + \tau) \leq V_{n(t)} + 2.5a_{n\_max}\tau \left(1 - \frac{V_n(t)}{v_d}\right) \left(0.025 + \frac{V_n(t)}{v_d}\right)^{\frac{1}{2}}, \quad (2.9)$$

where  $a_{n\_max}$ ,  $\tau$ , and  $v_d$  are maximum desired acceleration, apparent reaction time, and desired speed in free flow, respectively.

The second constraint arises from safety considerations. If vehicle  $n - 1$  (the vehicle followed by vehicle  $n$ ) is incited to brake with the maximum desired braking,  $b_{n-1} \leq 0$ , at time  $t$  and come to rest, taking into account the natural reaction time,  $\tau$ , and an additional safety margin  $\theta$ , vehicle  $n$  has to come to rest behind vehicle  $n - 1$  without violating the safe distance in standstill. This led to the inequality [38]:

$$\begin{aligned}
X_{n-1}(t) - \frac{V_{n-1}(t)^2}{2b_{n-1}} - s_{n-1} & \quad (2.10) \\
& \geq X_n(t) + [V_n(t) + V_n(t + \tau)] \frac{\tau}{2} + V_n(t + \tau)\theta - \frac{V_n(t + \tau)^2}{2b_n}
\end{aligned}$$

where  $s_{n-1}$  represents the effective size of the vehicle  $n - 1$ , denoting the physical length as well as the distance margin that will be kept even in standstill. It is worth mentioning that the parameter  $\theta$  introduces some kind of anticipative behaviour into the model as addressed by Treiber [26]. Without this parameter, the vehicle would drive with its desired speed until it reaches the point where it has to brake with the maximum desired deceleration.

Rearrangement of the aforementioned constraints leads to Gipps' model:

$$\begin{aligned}
V_n(t + \tau) = \min\{ & V_n(t) + 2.5a_n\tau \left(1 - \frac{V_n(t)}{v_d}\right) \left(0.025 + \frac{V_n(t)}{v_d}\right)^{\frac{1}{2}}, & (2.11) \\
b_n\tau + \sqrt{ & b_n^2\tau^2 - b_n[2(X_{n-1}(t) - s_{n-1} - X_n(t) - V_n(t)\tau - \frac{V_{n-1}(t)^2}{\hat{b}})]} & \}
\end{aligned}$$

where  $\hat{b}$  is an estimation of the lead vehicle's braking magnitude  $b_{n-1}$ . Finally, in this equation  $\theta$  was replaced by  $\frac{\tau}{2}$  as a sensible value.

The validation of the model was carried out for a set of selected parameters by the evaluation of a) the macroscopic features of the model, i.e. the speed-flow diagram, that were obtained through simulations, and b) examining the braking behaviour of a platoon of seven vehicles in the car-following regime. The conclusions made are as follows.

1. The flow-speed curve is relatively insensitive to changes in the values of  $a_{n\_max}$ ,  $b_n$  and  $s_n$ , but varies with changes in  $v_d$ ,  $\tau$  and  $\hat{b}$ . In particular, the mean and the standard deviation of the distribution of desired speeds affect the position and the shape of the upper arm of the speed-flow curve. The parameters  $\tau$  and  $\hat{b}$ , on the other hand, determine the maximum flow. This is justified by the fact that the behaviour of

vehicles is typically governed by their leaders and they do not have the freedom to accelerate to their desired speeds, therefore the speed-flow diagram is insensitive to  $a_{n\_max}$ . The same logic can be applied to the parameter  $b_n$ , since the following vehicles in a platoon do not reach the maximum braking value unless they have underestimated the braking willingness of their leaders. Finally,  $s_n$  is usually much smaller than the actual gap in between the vehicles, therefore even errors in the estimation of it would affect neither the collective characteristic, e.g. the speed-flow diagram, nor the individual behaviour except in nearly stationary conditions.

2. The parameter  $\hat{b}$  also determines the response of the following vehicles to disturbances. This parameter defines whether the disturbances that are passed on to the following vehicles are damped or amplified. If the estimation of the preceding vehicle's  $b$  value, i.e.  $\hat{b}$ , is greater than the actual  $b$ , that is to say that the follower overestimates the leader's braking tendency (conservative driving), disturbances are damped. Alternatively, if the leading vehicle's braking tendency,  $b$ , is underestimated, then disturbances are amplified. This is illustrated in Figure 9.

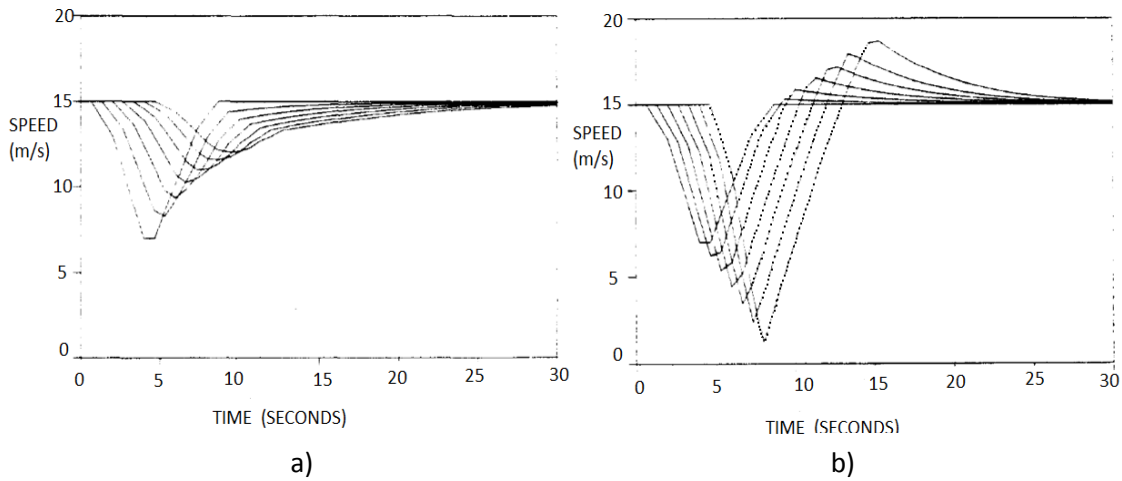


Figure 9. Speed-time plots for seven successive vehicles using Gipps' model with following parameters:  $\mathbf{a_n = 2 \frac{m}{s^2}}$ ,  $\mathbf{b_n = -3 \frac{m}{s^2}}$ ,  $\mathbf{v_n = 30 \frac{m}{s}}$  and  $\mathbf{\tau = \frac{2}{3} sec}$  when a)  $\hat{\mathbf{b}} = -3.5 \frac{m}{s^2}$  b)  $\hat{\mathbf{b}} = -2.5 \frac{m}{s^2}$  [38].

For more details the reader is referred to [38].

Gipps proposes the following decision-making procedure for lane-changing manoeuvres [44].

1. Choosing a target lane according to drivers' paths or with the expectation of improving the driving experience (mandatory and discretionary lane-changing).
2. Evaluating the feasibility of performing the lane-changing by taking into account the drivers' sense of urgency. For instance, more intense braking may be acceptable for a driver that is getting closer to its turn or a lane blockage. In such a scenario, forcing a lane-changing manoeuvre and imposing relatively high decelerations on the following vehicles might become more likely. This step relies on the underlying car-following model.
3. Performing the lane-change manoeuvre with respect while meeting a safety criterion.

Gipps's proposed procedure covers many aspects of lane-changing in urban traffic. This model uses a multi-layered decision tree in order to assess the priorities and criteria before initiating the lane-changing manoeuvre. More details on this subject can be found in [44]. However, as pointed out in [47], such prioritised decision-making process overlooks the variety in drivers in terms of handling conflicting goals. Yang's model [65], implemented in the software MITSIMLab, incorporates variety in drivers' decision-making upon encountering conflicting goals by adopting a stochastic framework.

### **2.2.3 Benekohal's model**

Benekohal [66] [67] adopts a somewhat different approach in modelling drivers' acceleration behaviour. In this model, a number of driving conditions are identified and different acceleration models are developed accordingly. An overview of these conditions sheds light on the complexity of modelling driving behaviour. These conditions are as follows.

1. Vehicles are merely constrained by their physical dynamics, as opposed to constraints imposed by the traffic flow, to accelerate to their desired speeds. In order to model the driving behaviour under this condition, a table was constructed from the data related to maximum accelerations for different speed ranges [68]. The accelerations are then selected according to different speed ranges.

2. Vehicles are deviated from their desired speed as a result of a disturbance. In this case, they accelerate/decelerate in order to reach that speed again. A courtesy factor is assigned to account for the percentage of vehicles that respect speed limits when they are below their desired speed.

3. For the specific situation where a following vehicle comes to rest and begins to move again, accelerations of  $2 \frac{ft}{s^2}$  ( $\cong 0.61 \frac{m}{s^2}$ ) for passenger cars and  $1 \frac{ft}{s^2}$  ( $\cong 0.3 \frac{m}{s^2}$ ) for trucks were assumed in the first time instance of movement, and thereafter acceleration is governed by the car-following algorithm. The vehicle will not start to move immediately after its leader has moved but will have a “start-up” delay. Twenty percent of vehicles which are considered faster (with a short surprise reaction time of 0.68 sec) wait for 1 sec before moving while others will experience start-up delays of up to 2 secs.

4. The maximum acceleration that satisfies the spacing constraint can be calculated using equation below,

$$x_l - \left( x_f + v_f \Delta t + \frac{1}{2} a_f \Delta t^2 \right) \geq s_l, \quad (2.12)$$

where  $\Delta t$  is the time period between successive reassessments, and  $s_l$  represents the effective length. Similar to the Gipps’ model, the parameter  $s_l$  does not merely denote the length of the vehicle, but includes the safe spacing between the pair of vehicles as well. Herein, the safe spacing parameter changes with traffic density. For near standstill conditions a 5 to 7-foot (1.5 to 2.13 meters) buffer space is assumed.

5. The maximum acceleration that satisfies the non-collision constraint in the following regime is calculated using the following inequality,

$$x_l - \left( x_f + v_f \Delta t + \frac{1}{2} a_f \Delta t^2 \right) - s_l \geq \min \left\{ \begin{array}{l} (v_f + a_f \Delta t) \tau \\ (v_f + a_f \Delta t) \tau + \frac{(v_f + a_f \Delta t)^2}{2b_{f,max}} - \frac{v_l^2}{2b_{l,max}} \end{array} \right. , \quad (2.13)$$

where the following constraint for collision-free driving is applied,

$$(v_f + a_f \Delta t) \tau + \frac{(v_f + a_f \Delta t)^2}{2b_{f,max}} - \frac{v_l^2}{2b_{l,max}} \geq 0 . \quad (2.14)$$

The acceleration for each vehicle is selected according to equation

(2.13) in each time step .For deceleration, an additional comfortable deceleration is considered. This value is selected from a table with different speed ranges. Finally, the deceleration is selected by comparing the values obtained in mode 2, mode 5 as given by equation

(2.13), and the comfortable deceleration obtained from the table.

$$a_f = \begin{cases} a_{comf} & \text{if } a_2 < a_{comf} < \min(a_4, a_5) \\ a_2 & \text{if } a_{comf} < a_2 < \min(a_4, a_5) \\ a_5 & \text{otherwise .} \end{cases} \quad (2.15)$$

#### 2.2.4 Ahmed's model

In [47], a detailed study of modelling and model estimation based on remarkable prior works is provided. Therefore, a review of this work can shed light on some important issues in modelling and model estimation.

The main contributions of Ahmed's work in modelling are stated as follows [47].

1. Ahmed's probabilistic lane-changing model was a significant improvement over conventional deterministic rule-based lane-changing models.
2. In this model, the stimulus (Equation (2.3)) is a nonlinear function of the relative speed to the leading vehicle, whereas in most known models prior to this, a linear relationship was assumed.
3. Traffic conditions ahead of the driver are taken into account. This was consistent with Ozaki's observations in 1993 [61].
4. A headway threshold determines the regime of driving. This threshold is given as a distribution and according to its value the style of driving may differ in terms aggressiveness or conservativeness.
5. A reaction time is integrated within the model.
6. Forced merging and courtesy yielding is addressed in the model.

#### **2.2.4.1 The acceleration Model**

Ahmed's acceleration model is an extension of Subramanian's work in 1996 [62]. The model distinguishes the car-following and free flow regimes based on a headway threshold, as opposed to a spacing-based threshold.

$$h_n(t) = \frac{\Delta X_n(t)}{V_n(t)} , \quad (2.16)$$

In Equation (2.16), the parameter  $h_n$  is the headway for vehicle  $n$ ,  $\Delta X_n$  is the spacing between the two vehicles, and  $V_n$  is the speed of the subject vehicle.

The use of headway over spacing was justified on the basis that a) some of the previous works in this area recommended the use of headway, and b) in high speeds, the behaviour of drivers is expected to be more conservative and therefore more responsive to their leading vehicles.

#### **2.2.4.2 The headway threshold distribution**

As mentioned earlier, the headway threshold specifies the regime of driving. This parameter defines whether the driver's acceleration is a response to its leading vehicle, or is according to his objective of attaining his desired speed. However, this

behaviour is expected to vary among different drivers, e.g. conservative drivers and aggressive drivers. Moreover, although drivers do not always choose exact values for this purpose, and inconsistencies are expected from a given driver, one expects a correlation between such values for a specific driver. These characteristics give rise to following truncated normally distributed  $h_n^*$  with truncation on both sides,

$$f(h_n^*) = \begin{cases} \frac{\frac{1}{\sigma_h} \phi\left(\frac{h_n^* - \mu_h}{\sigma_h}\right)}{\Phi\left(\frac{h_{max}^* - \mu_h}{\sigma_h}\right) - \Phi\left(\frac{h_{min}^* - \mu_h}{\sigma_h}\right)} & \text{if } h_{min}^* < h^* < h_{max}^* \\ 0 & \text{otherwise,} \end{cases} \quad (2.17)$$

where,

- $\phi(\cdot)$  is the probability density function of a standard normal random variable,
- $\Phi(\cdot)$  is the cumulative distribution function of a standard normal random variable,
- $\mu_h, \sigma_h$  are the mean and standard deviation of the untruncated distribution,
- $h_{min}^*, h_{max}^*$  are minimum and maximum values of  $h_n^*$ .

Hence, the probability of the vehicle  $n$  being in the car-following regime is given by,

$$P(h_n(t) < h_n^*) = \begin{cases} 1 & h_n(t) < h_{min}^* \\ 1 - \frac{\Phi\left(\frac{h_n(t) - \mu_h}{\sigma_h}\right) - \Phi\left(\frac{h_{min}^* - \mu_h}{\sigma_h}\right)}{\Phi\left(\frac{h_{max}^* - \mu_h}{\sigma_h}\right) - \Phi\left(\frac{h_{min}^* - \mu_h}{\sigma_h}\right)} & h_{min}^* < h_n(t) < h_{max}^* \\ 0 & h_n(t) > h_{max}^* \end{cases} \quad (2.18)$$

### 2.2.4.3 The reaction time

In order to accurately model drivers' reaction times, one may suggest many explanatory variables that lie along a broad spectrum of attributes; the driver's age, mental condition, visibility, environmental factors like weather condition, roadway geometry, traffic condition, and finally vehicle's characteristics and speed [47]. Ahmed uses the following generic framework used by Subramanian [62] to deal with this issue.

All the aforementioned explanatory variables are considered to form a vector,  $X_n^\tau$ . This vector is then multiplied by a vector of model parameters,  $\beta^\tau$ , in order to linearly weight the explanatory variables and derive a single measure. This measure can then be related to the mean value of observations. Subramanian [62] suggests a truncated lognormal distribution for this purpose, giving rise to following model,

$$f(\tau_n) = \begin{cases} \frac{1}{\Phi\left(\frac{\ln(\tau_{max})-\mu_\tau}{\sigma_\tau}\right)\tau_n\sigma_\tau\sqrt{2\pi}} e^{-\frac{1}{2}\left(\frac{\ln(\tau_n)-\mu_\tau}{\sigma_\tau}\right)^2} & \text{if } 0 < \tau_n \leq \tau_{max} \\ 0 & \text{otherwise,} \end{cases} \quad (2.19)$$

where,

- $\tau_n$  is the reaction time of driver  $n$ ,
- $\mu_n$  is equal to  $X_n^\tau\beta^\tau$  and is the mean of the distribution of  $\ln(\tau_n)$ ,
- $\sigma_\tau$  is the standard deviation of the distribution of  $\ln(\tau_n)$ , and
- $\tau_{max}$  is the upper bound of the distribution of  $\tau_n$ .

### **The car-following regime**

In the car-following regime, the stimulus-sensitivity generic formulation based on the GM model is used. However, the following extensions are made; 1. a nonlinear function of relative speed is used as the stimulus, and 2. traffic conditions are taken into account. These extensions are discussed below.

1. Stimulus is a nonlinear function of relative speed.

In the GM model, Equation (2.4), the impact of the relative speed is modelled linearly. This corresponds to the simplistic stimulus depicted in Figure 10.a), while in Ahmed's model the following assumptions have given rise to the stimulus depicted in Figure 10b).

- Perception of low relative speeds is difficult, hence drivers avoid large acceleration rates in this area

- In intermediate relative speeds, high acceleration rates are adapted to keep up with the leader
- In high relative speeds, drivers' motivation for high acceleration rates are suppressed by mechanical constraints, resulting in decreasing acceleration rates

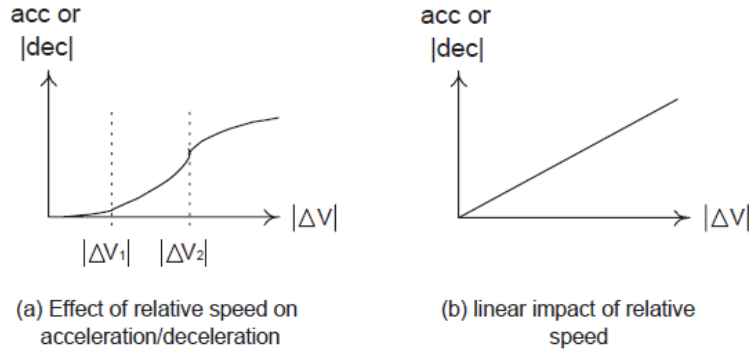


Figure 10. The impact of the relative speed on drivers' acceleration decisions [47, p. 50].

This is mathematically formulated by Equation (2.20),

$$f[\Delta V_n(t - \tau_n)] = \Delta V_{1n}(t - \tau_n)^{\lambda_1^g} + \Delta V_{2n}(t - \tau_n)^{\lambda_2^g} + \Delta V_{3n}(t - \tau_n)^{\lambda_3^g}, \quad (2.20)$$

where,

- $\Delta V_{1n}(t - \tau_n) = \min(|\Delta V_n(t - \tau_n)|, |\Delta V_1|)$ ,
- $|\cdot| = \text{absolute value}$ ,
- $\Delta V_{2n}(t - \tau_n) = \max(0, \min(|\Delta V_n(t - \tau_n)| - |\Delta V_1|, |\Delta V_2| - |\Delta V_1|))$ , and
- $\Delta V_{3n}(t - \tau_n) = \max(0, |\Delta V_n(t - \tau_n)| - |\Delta V_2|)$ .

The terms  $|\Delta V_1|$  and  $|\Delta V_2|$  represent the thresholds depicted in Figure 10. The power exponent  $\lambda$  defines the acceleration rate for the aforementioned phases. The superscript  $g$  denotes the acceleration mode which could either be acceleration or deceleration, so that as mentioned earlier, different parameter sets can be used for acceleration and deceleration processes. In order to apply what was previously discussed with regard to the properties of the acceleration response below and above  $\Delta V_1$  and above  $\Delta V_2$ , the thresholds  $\lambda_1^g$  and  $\lambda_2^g$  must be greater than one. This

corresponds to increasing acceleration rates. The parameter  $\lambda_3^g$  must be less than one, corresponding to decreasing acceleration rates until reaching a maximum acceleration value. Furthermore, due to the insignificant effect of stimulus below  $\Delta V_1$ ,  $\lambda_1^g$  needs to be less than  $\lambda_2^g$ .

2. Traffic condition ahead of the driver is taken into account.

Most of the car-following models do not incorporate the traffic condition into the model explicitly. Nevertheless, the influence of traffic condition is implicitly addressed through the flow-density relationship and its impacts on other model parameters, e.g. the safe headway in the IDM model [26, pp. 6-7]. While this may be sufficient for modelling purposes and macro-scale properties of the homogenous traffic may be reproduced through such approaches, a more accurate modelling of the micro-scale driving dynamics may be necessary for the investigation of the impacts of new technologies such as Adaptive Cruise Control (ACC) systems or autonomous vehicles, especially if such models are intended to be the basis for the control of vehicles. The driving dynamics in congested traffic are likely to be different from those in uncongested traffic and it is appropriate to reflect this in the model.

Ahmed delineates the impact of traffic condition by extending the sensitivity term in the GM according to Equation (2.21),

$$s[X_n^{cf,g}(t - \xi\tau_n)] = \alpha^g \frac{V_n(t - \xi\tau_n)^{\beta^g}}{\Delta X_n(t - \xi\tau_n)^{\gamma^g}} k_n(t - \xi\tau_n)^{\rho^g}. \quad (2.21)$$

where,

- $s[\bullet]$  is the the sensitivity term,
- $X_n^{cf,g}(t - \xi\tau_n)$  is the vector of explanatory variables for the vehicle  $n$  in the car-following regime ( $cf$ ), given the acceleration mode specified by  $g$  (acc/dec), and as perceived at time  $(t - \xi\tau_n)$ ,
- $\tau_n$  is the reaction time,

- $\xi \in [0,1]$  is a parameter denoting a sensitivity lag,
- $k_n(t - \xi\tau_n)$  is the perceived traffic condition ahead of the driver and in the form of traffic density, and
- $\alpha^g, \beta^g, \gamma^g, \rho^g$  are model parameters.

In addition to the density term added to the original GM model and the superscript  $g$  that allows different model parameters in acceleration and deceleration modes, the parameter  $\xi$  is introduced. This parameter represents a relaxation of the sensitivity lag in the GM model and generalises the GM model in this aspect. In particular, in the GM model the perception of spacing and relative speed are lagged by a reaction time,  $\tau_n$ , and  $\xi = 1$ , whereas for the perception of own speed,  $\xi$  is zero. Furthermore, in the specific case where  $\xi = 1$  the stimulus and the sensitivity are lagged by the same amount, while for values smaller than 1 the sensitivity can be updated within the response time to the stimulus.

The addition of a random term that accounts for omitted variables and the stochastic nature of driving finalises the model yielding,

$$a_n^{cf,g}(t) = \alpha^g \frac{V_n(t-\xi\tau_n)^{\beta^g}}{\Delta X_n(t-\xi\tau_n)^{\gamma^g}} k_n(t - \xi\tau_n)^{\rho^g} f[\Delta V_n(t - \tau_n)] + \epsilon_n^{cf,g}(t), \quad (2.22)$$

where,  $\epsilon_n^{cf,g}(t)$  is a normally distributed random variable with the mean of 0,

$$\epsilon_n^{cf,g}(t) \sim N(0, \sigma_{\epsilon^{cf,g}}^2), \quad (2.23)$$

and is assumed to be independent for a given driver at different times as well as for different drivers,

$$cov\left(\epsilon_n^{cf,g}(t), \epsilon_{n'}^{cf,g'}(t')\right) = \begin{cases} \sigma_{\epsilon^{cf,g}}^2 & \text{if } g = g', t = t', n = n' \\ 0 & \text{otherwise} \end{cases}. \quad (2.24)$$

The expected correlation for a driver's acceleration decisions is modelled by the reaction time and the headway threshold distributions as discussed earlier.

### **Free flow regime**

In free flow regime, the objective is to attain the driver's desired speed. This is modelled by using the difference between the current speed and the desired speed, lagged by a time delay, as stimulus. A constant sensitivity is associated with the stimulus.

$$a_n^{ff}(t) = \lambda^{ff}[V^*(t - \tau_n) - V(t - \tau_n)] + \epsilon_n^{ff}(t), \quad (2.25)$$

where  $\lambda^{ff}$  is the constant sensitivity and  $V^*(t - \tau_n)$  is the desired speed,

$$V^*(t - \tau_n) = \beta^{DS} X_n^{DS}(t - \tau_n). \quad (2.26)$$

Moreover, a normally distributed random term,  $\epsilon_n^{ff}(t)$ , is added to the equation in order to account for the anticipated inconsistency in drivers' acceleration behaviour.

### 2.2.5 Intelligent Driver Model

The Intelligent Driver Model (IDM) [26] is a continuous, deterministic model with important merits. In this model both the car-following and free flow regimes are modelled by a single equation. This means a smooth and differentiable transition occurs between the two driving regimes which is consistent with the intuition. This also provides a significant simplicity in various aspects such as the implementation and the calibration of the model. The IDM has a small number of parameters with intuitive meanings. This facilitates the calibration and behavioural analysis of the model. Moreover, the model has a good performance in terms of modelling microscopic behaviour and subtle macroscopic phenomena. For instance, different types of congested traffic states such as triggered stop-and-go waves, oscillatory congested traffic, and homogenous congested traffic can be modelled with the IDM while the model parameters remain within sensible ranges. Furthermore, the IDM is a collision-free model and it has been tested on a real car, with some improvements, as the basis of an ACC [69, 70]. Last but not least, the availability of numerous analytical and empirical studies on different aspects of the model facilitates further investigations. For instance, the stability [71], calibration [63, 72, 73, 74, 75, 76], collective

characteristics [26], time-related parameters of driving and how they influence stability [77], are some of the aspects of this model that have been addressed in the literature.

The model is given by,

$$\begin{aligned} \dot{v}_n &= a_n \left[ 1 - \left( \frac{v_n}{v_n^d} \right)^\delta - \left( \frac{s^*(v_n, \Delta v_n)}{s_n} \right)^2 \right], \\ s^*(v, \Delta v) &= s_n^0 + s_n^1 \sqrt{\frac{v}{v_n^d}} + T_n v + \frac{v \Delta v}{2\sqrt{a_n b_n}}, \end{aligned} \quad (2.27)$$

where,  $a_n$  is maximum acceleration,  $v^d$  is desired speed,  $\delta$  is free acceleration exponent,  $s^0$  and  $s^1$  determine jam distances in fully stopped traffic and in high densities respectively,  $T$  is safe headway,  $b_n$  is comfortable deceleration, and they are all model parameters. Input variables are relative speed,  $\Delta v = v_n - v_{n-1}$ , speed of the subject vehicle,  $v_n$ , speed of the preceding vehicle,  $v_{n-1}$ , and spacing,  $s_n$ . Finally, the output variable,  $\dot{v}_n$ , determines the acceleration of the subject vehicle.

This function produces four distinguished driving behaviours according to different driving modes:

- Equilibrium traffic ( $\Delta v, \dot{v} = 0$ ) where the collective behaviour and the corresponding fundamental diagram can be derived.
- Acceleration to desired speed where the term  $a_n \left[ 1 - \left( \frac{v_n}{v_n^d} \right)^\delta \right]$  dominates.
- Braking as a reaction to high approaching rate where the term  $\frac{(v \Delta v)^2}{4b_n s^2}$  dominates.
- Braking in response to small gaps where the term  $-a \frac{(s_0 + vT)^2}{s^2}$  dominates.

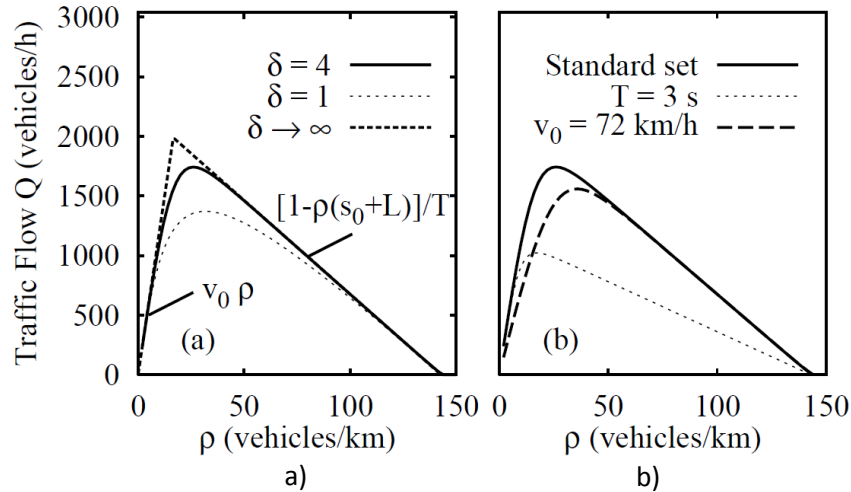


Figure 11. A depiction of the fundamental diagram derived from a car-following model, namely the IDM (a) Coefficient  $\delta$  determines how fast cars accelerate to their desired speed (b) Coefficients  $T$  and  $v_0$  represent safe headway and desired velocity respectively. Finally,  $s_0$  and  $L$  are the standstill bumper to bumper spacing between vehicles and vehicle lengths. Only one parameter is varied at a time and the rest of the parameters are default parameters given in [26].

In Figure 11,  $\delta$  is the acceleration component that specifies the acceleration behaviour when a driver is accelerating to its desired speed. This component becomes especially important in the free flow regime when the spacing parameter,  $s$ , has large values. In this model, when the parameter  $\delta$  tends to infinity, acceleration will happen with a constant value of  $a$ , whereas  $\delta = 1$  corresponds to an exponential relaxation to the desired speed with the relaxation time of  $\tau = \frac{v_d}{a}$ .

### 2.3 Adaptive cruise control methodologies

As of today, adaptive Cruise Control systems are entering their third decade of commercial use. The idea of enforcing control upon throttle for improving drivers' comfort and achieving steadier speeds and thereby reducing fuel consumption was introduced around the 1950s by Ralph Teetor. This invention found its way into manufacturing and commercial use for the very first time only a couple of years later in 1958 [78], coining the term cruise control. However, with regard to the technology used and the functionality, Adaptive Cruise Control (ACC) can be distinguished with the introduction of the system developed by Mitsubishi in 1995 [79]. Mitsubishi's "Preview

Distance Control” used laser radar to measure spacing and produced audible and visual alarms as unsafe conditions were detected. Additionally, the system encompassed multiple cutting edge Advanced Driver Assistant Systems (ADAS), with features such as Lane Departure Warning System (LDWS) and rear side view system producing warning alarms when the vehicle was strayed from its lane, and when there were vehicles approaching from the rear side, known as drivers’ blind spot. The two systems, namely LDWS and rear side monitoring, used Charged Couple Device (CCD) video camera and image processing algorithms for detection of line marking and approaching vehicles. Audible alarm, vibration of the steering wheel and a corrective steering torque were used for the LDWS. Audible and visual alarms were used as cautionary means in the case of detecting approaching cars or motorbikes in the driver’s blind spots [80]. These systems have been developing ever since and currently numerous varieties with remarkable features are available including Collision Avoidance Systems (CAS), Collision Warning Systems (CWS), and Lane Keeping Assist (LKA) systems.

ACCs are capable of bringing about significant changes to traditional ground transportation. Automation of the function of driving, which is carried out by humans, is the revolutionary core of ACC systems. As in many other fields, automation of driving is intended to improve motorised ground transport in terms of efficiency, safety, and comfort. Moreover, driving behaviours that are caused by bad habits or limitations in human perception and decision-making give rise to inefficiencies with respect to fuel consumption and emissions, utilisation of roadway capacity, and safety.

The operational level of driving consists of the two functions - lane-changing, and longitudinal control. Advisory systems inform the driver about the best course of action or produce warnings in critical situations in order to increase the driver’s awareness. Intervening systems, on the other hand, enforce certain actions such as emergency braking or producing steering torque in order to maintain a safe distance or keep vehicles in the middle of the lane.

The remarkable advances in computational power and sensory capabilities over the past decade have enabled researchers and car manufacturers to take the concept of automation of driving beyond advisory and intervening systems. Autonomous vehicles and full automation of driving builds upon the previous achievements of ACCs and ADAS and may be seen as the natural evolution of this technology.

The progress in the commercialisation of autonomous vehicles, the technological inheritor of the ACCs, has been exponential. Numerous companies and projects have successfully tested their working prototypes. A brief summary of some of these achievements and milestones follows.

- VisLab launched the VisLab Intercontinental Autonomous Challenge (VIAC) where a fleet of four autonomous vehicles were used in a journey from Italy to China, facing all possible kinds of difficulties [81, 82].
- Mercedes-Benz demonstrated 100 km of fully autonomous driving in urban areas and motorways in 2013 [83].
- Nissan demonstrated a series of autonomous driving in motorways and urban roads in 2013 [84].
- Google announced 300,000 miles of accident free autonomous driving in August 2012, 700,000 miles in 2014 [85, 86], and 2 million miles in October 2016 [87].
- Many companies including, Google, Tesla, BMW and Intel, Daimler and Bosch, General Motors, Volvo & Uber, Nissan and Ford, have made announcements about testing fleets of autonomous vehicles in 2017 [88, 89, 90].

However, due to the fierce commercial competition in this area important details remain confidential and researchers cannot get but a glimpse of the methodological details, technological advances, and the current state of research from the general announcements made by the companies that work on this technology.

Partially and fully automated driving aim at providing different degrees of enhanced safety, comfort, and efficiency compared to human drivers. The control theory,

optimisation, and modelling play a crucial role in achieving the objectives of maximised safety, robust acceleration behaviour, maximised comfort, optimal utilisation of the traffic capacity, and efficient use of the source of energy.

The transport network is a complex system with opposing objectives such as safety and traffic throughput. An efficient automated transport network must meet a wide range of complex micro-scale and macro-scale requirements such as drivers' comfort and string stability. These difficulties, along with modelling complexities, render the application of multi-objective optimisation challenging. However, an understanding of different optimisation approaches, their applications, advantages, and limitations facilitates the selection of a method that is fit for purpose. This section provides a review of some of the optimisation methods that have been put forward by researchers in the field of automation of driving. Herein, different aspects of these methods, namely their potentials, limitations and main areas of applications, are briefly discussed.

### **2.3.1 Fuzzy logic**

The fuzzy logic, as known and recognised today, was developed and proposed by Zadeh in 1965 [91]. Even though the notion of fuzzy sets, as an abstract idea, existed prior to Zadeh, he was one of the key pioneers in the development of the mathematical framework for fuzzy sets and their operations. This was a necessary step for the validation of the concept and bringing the notion of fuzzy sets to the realm of scientific applications and engineering. Prior to Zadeh, the necessity of such conceptual development in mathematics was understood and expressed by mathematicians and philosophers such as Bertrand Russell, Wittgenstein, and Max Black. Moreover, mathematicians such as Jan Lukasiewicz, H. Weyl, Kaplan, and Schott had taken the initial steps in the formulation of this concept, even though the concept was referred to by different terms, namely consistency and vagueness. For a detailed conceptual and historical review on the subject, the reader is referred to [91, 92].

The revolutionary contribution of fuzzy logic is based on the existence of a continuum of grades of membership for an object in different sets. This is in contrast with the crisp and binary essence of the classical set theory where an object is either a member of a given set or not, where a statement is either true or false. In this subsection, the fundamentals of fuzzy logic are explored and its application in modelling and control of transport systems is briefly discussed. More details on the subject can be found in [93].

Assuming a space of points or objects,  $X$ , with a generic element  $x \in X$ , a fuzzy set,  $A$ , associated with an attribute can be defined and characterised by a membership function  $f_A(x)$ . This membership function maps the elements of  $X$  to their grade of membership in  $A$ . These memberships are normalised to take values in the interval of  $[0,1]$ . This can be seen as a generalisation of the classical sets since the special cases of  $f_A(x) = 1$  and  $f_A(x) = 0$  correspond to the classical notion of either belonging or not belonging to a set, respectively.

For instance, consider the problem of Adaptive Cruise Control system. One can simplify the model of behaviour or control to the following descriptive form, “drivers accelerate when the relative distance to the preceding vehicle is sufficiently large and decelerate when the opposite is perceived”. This statement describes different actions for different conditions or states. A crisp and binary interpretation of this statement, based on the classical set theory, yields states with either “high” or “low” relative distances. Instances of such mathematical formulations were seen in section 2.2, where based on a criterion a car was assessed to be either in the free flow regime or in the car-following regime.

A fuzzy-based interpretation of this statement would suggest that the “relative distance to the preceding vehicle” can be considered as a continuous space of quantitative values,  $X$ , and the adjectives of “sufficiently large” and “small” are attributes that should be considered as fuzzy sets,  $A$  and  $B$  respectively. Given this interpretation, each element of  $X$ , i.e.  $x$ , may have different degrees of memberships

of the attributes  $A$  and  $B$ . For instance, the spacing of 5 m could be 90% small and 10% large, while the spacing of 100 m could be 80% large and 20% small. The levels of memberships are defined by the corresponding membership functions  $f_A(x)$  and  $f_B(x)$ . It is clear that the fuzzy-based perspective better models the perception of humans. This logic can also be the basis of a robust control algorithm that provides a smooth transition between different states and is more compatible with human driving. Additionally, since this approach is very closely related to the human perception of various attributes and the way in which we exert control to maximise desired outcomes, fuzzy logic provides a good framework to integrate the experts' knowledge base in the automation process. For this purpose, once the input values consisting of  $X$ ,  $A$ , and  $f_A(x)$ , are established, fuzzy rules can be used to form the rule base and implement the control. The fuzzy rules are defined using logical operators. For instance, the control of vehicles in the car-following regime can be implemented using the following rule:

**If the spacing is *small* and the approaching speed is *high*, then  $a = -b_{max}$  ,**

where  $b_{max}$  is the maximum deceleration. In this fuzzy rule, a situation that is perceived as dangerous by drivers (human knowledge base) and the corresponding action, i.e. intense braking, is implemented by a fuzzy rule. The action of braking with the maximum deceleration will only be performed if the spacing is 100% "small" and the approaching speed is 100% "high", i.e. the membership of the value of spacing in the set of "Small Spacing" is  $f_{X_{Small\_Spacing}}(x_0) = 1$  and  $f_{X_{high\_Approaching\_Speed}}(x_0) = 1$ . In this example, the rule base is incomplete because all of the different possibilities have not been covered and, for example, it has not been defined what the acceleration should be if the spacing is large and the approaching speed is small.

One of the first attempts in the application of fuzzy logic to car-following models was carried out by Kikuchi and Chakroborty [94, 95] where the Gazis-Herman-Rothery

(GHR) [52] model was fuzzified. The motivation for this study was to deal with multiple shortcomings of the GHR model in reproducing,

- a natural, approximate car-following behaviour,
- an asymmetric response to stimuli,
- the closing-in and shying-away phenomenon, and
- the phenomenon of drifting around the steady-state spacing that is observed in the empirical evidence.

The fuzzy logic based model proposed by Kikuchi and Chakroborty successfully reproduced these features and, as a result, produced a more realistic car-following behaviour. Similar works were conducted in fuzzifying the MISSION model [96] and other models as addressed by [43]. The micro-simulation model, FLOWSIM, uses fuzzy logic for both its longitudinal control and lane-changing models [97]. One of the important stages in the application of fuzzy logic is the calibration of the membership functions. The calibration of the aforementioned simulation models is addressed in [98, 99, 95].

Some other interesting applications of this method in ADAS are car parking [100], control of a model car based on an expert's driving actions [101], and the investigation of the trajectory stabilisation features of a nonlinear car model approximated from the Takagi-Sugeno fuzzy model [21].

### **2.3.2 Adaptive cruise control as an optimal control problem**

A different approach in developing ACCs is the optimal control theory and Dynamic Programming. Optimal control theory and Dynamic Programming (DP), in essence, seek the sequence of actions that result in the maximised cumulated reward (or minimised cumulated penalty) over the course of time. Richard Bellman and Lev Pontryagin developed the mathematical formulation of this concept and thereby not only introduced a useful tool in dealing with various problems in finance and economy,

engineering, and control, but also laid down the foundation for numerous methods in Artificial Intelligence such as Reinforcement Learning (RL).

A dynamic programming problem in its general form, can be formulated as [102]:

$$J(t, x; u) = \int_t^\tau L(s, x(s), u(s)) ds + \Psi(\tau, x(\tau)) \quad , \quad (2.28)$$

where

- $\tau$  is the smaller of  $t_1$  and the exit time of  $(s, x(s))$  from  $\bar{Q} = [t_0, t_1] \times \bar{O}$ , where  $t_1$  is the upper bound of the time interval  $[t_0, t_1]$  within which control takes place
- $O$  is the state space ( $x(s) \in \bar{O}$ ) and  $O, \bar{O}$ , and  $\partial O$  are interior, closure, and boundaries of the set  $O \subset \mathbb{R}^n$
- $\bar{Q}$  is a closed cylindrical region of dimension  $\mathbb{R}^{n+1}$ .
- $L(s, x(s), u(s))$  is the so-called running cost,
- $x(\cdot)$  is the state of the system  $x(s) \in O$  with either of the following definitions of the state space,  $O$ :

(i)  $O = \mathbb{R}^n$ ,

(ii)  $\partial O$  is a compact manifold of class  $C^2$ .

- $C^k(O)$  represents all the  $k$ -times continuously differentiable functions on  $O$ ,
- $u(\cdot)$  is the control input from the control space  $u(s) \in U$  where  $U(t, x) \subset \mathbb{R}^m$ ,
- $\Psi(\tau, x(\tau))$  is the so-called terminal cost, and

The optimisation is also subject to the natural evolution of the system. In other words, the dynamics of the systems impose a constraint in the optimisation problem. This constraint is sometimes referred to as the equation of motion, given in the form of:

$$\frac{dx}{dt} = F(x(t), u(t), t) \quad . \quad (2.29)$$

The objective of the control is to find the optimal control  $u^*$  that minimises the cost function  $J(t, x; u)$ .

$$V(t, x) = J(t, x; u^*) = \min_{u \in U} \int_t^\tau L(s, x(s), u(s)) ds + \Psi(\tau, x(\tau)) \quad (2.30)$$

s. t  $\frac{dx}{dt} = F(x(t), u(t), t),$

where  $V(t, x)$  is the so-called value function.

Due to the difficulties associated with defining the terminal cost, which represents the optimal cumulative cost from the terminal time  $\tau$  up to infinity, in many problems a plausible alternative would be discounting the running cost in time and cumulating it (integration in time) up to infinity rather than considering a terminal time  $\tau$ . By doing so, the difficulty associated with the assignment of terminal cost can be resolved. Furthermore, the discount factor eases the process of defining the running cost, since the value function need not be bounded. For an autonomous system, the discounted cost infinite time horizon problem can be written in the form of:

$$V(x) = J(x; u^*) = \min_{u \in U} \int_t^\infty e^{-\eta s} L(s, x(s), u(s)) ds \quad (2.31)$$

s. t  $\frac{dx}{dt} = F(x(t), u(t)),$

where,  $\eta$  is the discount factor with a value within the range of  $[0, \infty)$ . The special case of  $\eta = 0$  is equivalent of not discounting at all since in this case future costs, for  $s \in [t, \infty)$ , and the current cost will be weighted with the same weight of 1. Large, non-zero values of  $\eta$  would result in giving smaller weights to future rewards, which is known as a short-sighted optimisation. For a more detailed review of applications and solving methods the reader is referred to [103, 104].

Solving a dynamic programming problem in closed-form becomes difficult as the complexity of the system exceeds that of systems with linear dynamics and quadratic cost functions (LQ). Moreover, stochastic systems whose dynamic equations are

defined via transition probability functions introduce additional layers of complexity. Approximate, numerical methods provide a good solution for dealing with such complex systems. For instance, Q-learning and its numerous algorithms that are proposed for different types of problems are a form of reinforcement learning that deal with such systems. In what follows, a review of some of the applications of these methods in ADAS and ACC is provided.

Wang [105] formulated the problem of ACC as an optimal control problem, an approach that can also be seen in earlier works [106]. Therein, the multi-criteria nature of the traffic network is modelled with a simple weighted sum function that represents the running cost for safety, desirability, and comfort. This is shown in the top branch of Equation (2.32). In this model, the intrinsic differences between the car-following and free flow regimes have been modelled by defining two different running cost functions for each regime. In the free flow regime, the term that represents the cost for safety has vanished. This is due to the fact that safety is only defined in relation to other vehicles and avoiding short gaps. Additionally, the desired speed in the car-following regime is considered as a function of the headway, whereas in the free flow regime it could be a preset desirable speed. The two regimes are distinguished by the gap threshold  $s_f$ .

$$L(X = [v, v_d, s], U = u_n) \tag{2.32}$$

$$= \begin{cases} c_1 e^{\frac{s_0}{s}} \Delta v_n^2 + c_2 (v_d(s) - v_n)^2 + \frac{1}{2} u_n^2 & \text{if } s \leq s_f = v_0 t_d + s_0 \\ c_3 (v_0 - v_n)^2 + \frac{1}{2} u_n^2 & \text{if } s > s_f = v_0 t_d + s_0 \end{cases},$$

where  $L$  is the running cost function,  $v_0, t_d, s_0$  are user-defined free speed, user-defined desired time gap, and distance between two vehicles at standstill, respectively.

The optimal acceleration model that minimises the cost in each regime is then found as a function of own speed, relative speed, and spacing.

Moriarty and Langley propose a distributed cooperative lane selection method based on the principles of RL and supervised learning [22]. Therein, the objective of lane selection is defined as increasing traffic throughput and reducing the average deviation from desired speeds among drivers. The objective of increasing traffic throughput is achieved by minimising the number of lane changes since this could reduce the number of shockwaves that are initiated as a result of unnecessary lane changes. These objectives are reflected in the performance function given by,

$$P(C) = \frac{\sum_{t=1}^T \sum_{i=1}^N (v_{it} - v_{it}^d)^2}{TN} + \frac{4 \times 60 \sum_{i=1}^N L_i}{TN}, \quad (2.33)$$

where  $L_i$ ,  $T$ , and  $N$  are the number of lane-changes per second, time horizon, and number of vehicles, respectively, and  $P(C)$  is the performance measure for a set of cars,  $C$ .

Solving the optimisation problem is carried out by a multi-level learning approach based on the principles of RL and supervised learning by making use of Neural Networks (NN). It was shown that the learnt strategy successfully outperforms the two “selfish” and “polite” lane-changing behaviours that were used as benchmarks. Therein, selfish driving represents the self-interest-maximising behaviour that can be related to frequent lane changes at the cost of others and traffic throughput, whereas polite driving means obeying the following rule “slower traffic yield to the right”.

The subject of lane-changing was also investigated in [23] with a similar approach and formulation. In this study, the performance of two algorithms, the Distributed Q-learning (DQL) and Approximate Piecewise Policy Iteration (APPIA), in finding the optimal policy was evaluated. However, both methods illustrated inferior performance compared to the hand-crafted “selfish drone” strategy.

In [107], Adaptive Dynamic Programming (ADP), a method combining Neural Networks and RL to deal with continuous time nonlinear DP problems, was combined with supervised learning to overcome training time deficiencies of the former. The resulting

method, Supervised ADP (SADP), was then applied to the problem of ACC and produced promising results.

In [108], Cooperative ACC (CACC) was considered where both the longitudinal control and lane-changing behaviour are coordinated between adjacent vehicles and the optimal policy is learnt using an implementation of Q-learning. Discretisation of the action and state spaces is a necessary step in the implementation of this method and this gives rise to a trade-off between computational complexity and accuracy. This trade-off is a well-known issue in this context. A precise presentation of a multi-dimensional state-space, especially in a cooperative multi-agent setup, gives rise to the “curse of dimensionality”. However, integration of Q-learning with other techniques such as NN and supervised learning, as already investigated in other works [22, 107], was shown to be a good way forward.

The applications of DP in transport systems can also be found in other areas such as route choice [109, 110] and traffic signal control [15, 16, 111]. For a more detailed review the reader is referred to [112].

### **2.3.3 Concluding remarks**

Development of a reliable fully (or partially) automated vehicle involves finding concrete solutions to numerous problems in the strategic, tactical, and operational levels of driving. For instance, the tactical level of driving concerns short-term objectives such as overtaking a slow leading vehicle and performing driving manoeuvres. This was addressed in [113], as a part of the PATH project, conducted by University of Berkeley. Therein, a distributed reasoning system was used in conjunction with Population-Based-Incremental-Learning (PBIL) in order to deliver a good performance in different scenarios. Other interesting projects that deal with different aspects of automated driving are “HAVE it” [8] and VisLab [81]. More detailed reviews on international projects and other related topics can be found in [114, 115] and their references.

Different approaches may be used to find an optimal, or an acceptable suboptimal solution, to different problems related to automated vehicles. These approaches may be relatively simple, heuristic models such as the Gipps' decision tree for lane changing, or more complex hybrid machine learning algorithms such as the integration of RL and NN [22]. Before selecting one method over another, one has to take the problem-dependant requirements and objectives into account. Therefore, an educated choice of approach requires sufficient knowledge of the problem domain and methods that are well-suited to the problem.

The optimal control theory and Dynamic Programming provide an important mathematical basis for solving optimal control problems. For systems that can be approximated by simple dynamical systems, such as Linear Quadratic (LQ) systems, a closed-form solution can be obtained. However, when the complexity of the system increases or when the stochastic features of the system become non-negligible and problems such as identification of the probability transition function arise, machine learning and numerical approaches such as Reinforcement Learning, Q-learning, Monte-Carlo methods and Temporal Difference (TD) can be used.

A number of applications of dynamic programming based algorithms, such as reinforcement learning, in the field of Intelligent Transport Systems (ITS), especially ACCs, were investigated. It was seen that these approaches can provide promising solutions to challenging problems in a wide range of subjects, such as cooperative driving, longitudinal control, lane-changing and tactical reasoning. However, one needs to be aware of the limitations of this approach and formulate the problem accordingly. The curse of dimensionality arises as a result of large state-action spaces. This means that an exponential increase in the number of possible courses of actions/states leads to a problem that cannot be solved within the required time frame. The modelling of complex systems, where a wide range of possibilities may occur at any given time and a wide range of actions may be considered accordingly, is highly susceptible to this issue. For instance, the problem of coordinating vehicles' lane-changing and

acceleration decisions as a collaborative, multi-agent, DP problem is likely to lead to unaffordable computational complexities. However, it was seen in the literature that promising results can be obtained by using complementary methods such as supervised learning, NN, distributed algorithms, and limiting the state-action spaces to manageable sizes.

Supervised learning methods alone may not be capable of finding efficient longitudinal control or lane-changing behaviour since producing a training set that would prepare the inference backbone, e.g. NN, to converge to the optimal solution across a wide range of scenarios and different driving conditions could be quite challenging. However, as seen in the literature, this method can be used in conjunction with RL to speed up the learning process.

In addition to the curse of dimensionality, another factor that may limit the application of DP based, machine learning methods in a stochastic environment is that DP based methods rely on evaluation of different strategies by examining them a number of times. In a stochastic setting, the rule of “large number of experiments” must be satisfied before meaningful solutions can be obtained. For instance, RL approaches require learning from experience. In a safety critical task such as driving, the process of learning cannot take place in real experiments. The alternative is a simulated environment. This gives rise to two fundamental issues. Firstly, derivation of a general policy for automated driving needs an accurate modelling of environmental factors, including complex features such as different driving styles and the impact of weather conditions and roadway-related features on driving, to name a few. This is clearly a challenging task. Secondly, developing a precise simulation of environment requires more processing times for each trial.

To conclude, although RL may be suitable for finding solutions, it is unable to do so efficiently in time-critical situations, such as real-time decision-making for longitudinal control and lane-changing. The application of the method is particularly challenging in

the presence of unpredictable agents such as pedestrians or other drivers. Therefore, while RL may not be a good choice as the sole method in the automation of driving, it can still play an important role in conjunction with other supervised learning approaches or heuristic methods, to deal with specific tasks such manoeuvring in a scenario of complex road curvatures and in the absence of complex interactions with other vehicles, or for lane-keeping assist [22, 104, 23, 15, 16, 112, 116, 117, 118].

## **2.4 Energy-efficiency and fuel consumption**

Since the aim of this research is to address the question of fuel-efficiency in automated driving, modelling fuel consumption plays an important role in the framework of this research. In this section, some of the subjects related to fuel consumption models are explored.

### **2.4.1 Fuel consumption models**

Emission and fuel consumption models play a key role in the evaluation of the environmental impacts of different transportation policies. This includes a wide range of subjects from vehicle-related technologies and driving strategies to roadway design and assessment of new policies. Depending on the area of study and the required level of accuracy, macroscopic or microscopic models may be used. In the former case, detailed microscopic behaviour of individual cars is not considered and the input variables are usually collective variables such as average speeds and densities. In the microscopic case the driving parameters of individual vehicles are used. The choice of parameters depends on the subject of study and may be categorised into travel-related, weather-related, vehicle-related, roadway-related, traffic-related, and driver-related factors [119].

Macroscopic models may be used to approximate the aggregate level of energy consumption in a link. These models are useful for planning and route choice applications, but cannot capture the delicate dynamics of individual vehicles in sufficient detail necessary for the analysis of microscopic driving strategies, since for

instance, the impacts of excessive acceleration/decelerations are typically averaged out in these models. An example of this is the macroscopic model proposed in [19], Equation (2.34), which only takes the average cycle speed in a link,  $v$ , as its input variable;

$$Fuel = 39.705188 + \frac{702.856}{v} + 0.0096227v^2. \quad (2.34)$$

Microscopic models, on the other hand, aim to produce a more accurate estimation of the fuel consumption of individual vehicles. However, this could come at the cost of more model parameters, for example the model demonstrated by Equation (2.35), proposed in [120].

$$E(t) = \int_{t_0}^t \left( \frac{v(t)F(t)}{\eta_B(t)\eta_M(t)} + \frac{P(t)}{\eta_B(t)} \right) dt, \quad (2.35)$$

Where,

- $E(t)$  is the instantaneous energy consumption,
- $v(t)$  is the simulated vehicle speed and is given by Equation (2.36),

$$v(t) = \min(v_0(t), \max(v_b(t), v_u(t)e^{-0.1H(t)})), \quad (2.36)$$

where  $v_0(t)$  is vehicle's speed,  $v_u(t)$  and  $v_b(t)$  are the maximum and minimum allowable speed in the target road segment, and  $H(t)$  is the level of humidity.

- $F(t)$  is the road force given by,

$$F(t) = f_r(t)m(t)g + \frac{\rho\alpha Av^2(t)}{2} + F_a(t) + \frac{Ma(t)G^2}{r\eta_g^2}, \quad (2.37)$$

where  $f_r(t)$  is the rolling friction coefficient and is calculated from Equation (2.38),  $m(t)$  denotes the vehicle mass at time  $t$ ,  $g$  is the gravity acceleration rate ( $9.8 \text{ m/s}^2$ ), the three coefficients  $\rho$ ,  $\alpha$ , and  $A$  represent air density, air resistance coefficient, and vehicle cross area respectively, together determining the aerodynamic drag force, and  $F_a(t)$  is the linear acceleration force. The last term of the equation estimates the rotational acceleration force provided by the motor to propel the wheels of the

vehicle, where  $M$  is the moment of the inertia of the rotor of the motor,  $a(t)$  is the acceleration rate, and the remaining three parameters  $G$ ,  $r$ , and  $n_g$  represent gear ratio, tire radius, and the gear efficiency indicator respectively.

$$f_r(t) = \mu + 7 \times 10^{-6}v^2(t) \quad (2.38)$$

$$\mu = \begin{cases} [0.025, 0.037] & \text{for ordinary car tires on a} \\ & \text{concrete road with snow} \\ [0.012, 0.015] & \text{for ordinary car tires on a} \\ & \text{concrete road without snow} \end{cases}$$

- $\eta_M(t)$  and  $\eta_B(t)$  are efficiency indicators of vehicle's motor and battery respectively, and
- $P(t)$  is the power consumed by onboard devices.

For a detailed definition of the other parameters the reader is referred to [120].

The level of detail required in such a model may not be available or necessary when the subject of interest is the longitudinal control of cars. Moreover, such complex models can potentially impose an excessive computational complexity on the evaluation process for subjects where roadway friction or external environmental factors such as humidity are not the focus of study. Therefore, the level of computational complexity, type of input variables, and estimation accuracy are all key factors to take into account and depend on the area of study.

In [121], a model based on instantaneous speed and acceleration, the Virginia Tech microscopic (VT-micro) model, was proposed. This model was specifically developed for the investigation of problems relating to the operational level of driving. The data used for the derivation of the model consisted of 1305 observations of instantaneous fuel consumptions and emissions for six light-duty cars and three light-duty trucks. Numerous model structures were examined and the one demonstrated by Equation (2.39) was reported to deliver promising microscopic and aggregate estimates.

$$\ln(\text{Fuel}) = \sum_{i=0}^3 \sum_{j=0}^3 K_{i,j}^e \times x^i \times y^j \quad (2.39)$$

$$\text{Fuel}(x, y) = e^{a+bx+cx^2+dx^3+ey+fy^2+gy^3+hxy+ixy^2+jxy^3+kx^2y+lx^2y^2+mx^2y^3+nx^3y+ox^3y^2+px^3y}$$

where  $x$  is acceleration ( $a$ ),  $y$  denotes speed ( $s$ ), and  $e$  denotes whether the subject car is accelerating or decelerating as the model has different coefficients for each mode.

Some of the key advantages of this model for applications related to the operational level of driving are; a minimal number of input variables, relatively simple and differentiable model structure, and acceptable accuracy at the microscopic and macroscopic levels. This model has been used in multiple studies related to energy efficiency in the longitudinal control of vehicles [122], investigating the impacts of different driving behaviour on fuel consumption [123], and optimisation of acceleration behaviour with respect to fuel consumption while approaching signalised intersections [124] to name a few.

#### 2.4.2 Fuel efficient driving strategies

In this subsection, some of the works that focus on energy efficiency in the longitudinal control of vehicles are reviewed and the key aspects related to methodology and conclusions are highlighted.

In [122], improving acceleration behaviour with the help of an advisory system led to reductions of between 12-31% in fuel consumption. This saving was achieved during a simulated acceleration and deceleration processes in a scenario where drivers with and without the advisory system approach a signalised intersection. Therein, environmental factors, namely speed limit, spacing, distance to traffic light or other road signs, and dynamic vehicle variables, namely speed and acceleration, are were used as input variables to produce the optimal acceleration. The optimal acceleration could then be suggested to the driver via an in-car Human-Machine Interface (HMI) or

be applied directly in automated vehicles. The main application of the module was considered to be in the free flow regime since in congested traffic conditions safety considerations have the priority and the method does not explicitly address these considerations. An extension for the car-following regime was also proposed without validation. The objective of the optimisation was set to minimise the cumulative fuel consumption, given by VT-micro instantaneous fuel consumption model [119], while environmental factors such as own speed and the distance to traffic signal were taken into account as constraints. Within the time interval of interest, namely the deceleration/acceleration period, the environmental factors were combined with the discretised function of cumulative fuel consumption and the resulting function was optimised using the Lagrange Multiplier Method (LMM).

In [125], the speed trajectory that leads to energy efficiency was calculated based on the principles of DP and making use of Dijkstra algorithm. In this study discretised velocities were represented as a graph where nodes represent speed values. The acceleration rate and the choice of fuel efficient deceleration mechanisms such as coasting in neutral and fuel cut-off, was included in the action space. The graph consisted of nodes that represented discrete velocity values along the route and edges that represented the cost or utility. In order to facilitate drivers' acceptance of the longitudinal control, the utility function (the weight of edges) was not rigidly defined based on fuel consumption, but drivers' preference in the trade-off between fuel efficiency and trip time was incorporated in the utility function through equation below.

$$u_{opt}(f_{eco}, t_{eco}) = k_w w f_{eco} + (1 - w) t_{eco}, \quad (2.40)$$

where  $u_{opt}$  is the utility value,  $f_{eco}$  is the fuel consumption,  $t_{eco}$  is the trip time,  $w$  is the weighting coefficient set by the drivers for sporty or fuel efficient driving, and  $k_w$  is a normalisation parameter that automatically adjusts to the current traffic condition.

The problem was then formulated as a single-pair shortest-path problem and the optimal path was sought between the current velocity in the origin (current time) and the predicted velocity that the driver is assumed to have in the prediction horizon. In order to predict the driver’s velocity, a model that was developed in the framework of eCoMove and eSiM research projects was used. This model considers a number of factors related to the vehicle, driver, environment, and traffic and subsequently produces a prediction of the future velocities. The optimisation approach discussed above is presented in Figure 12.

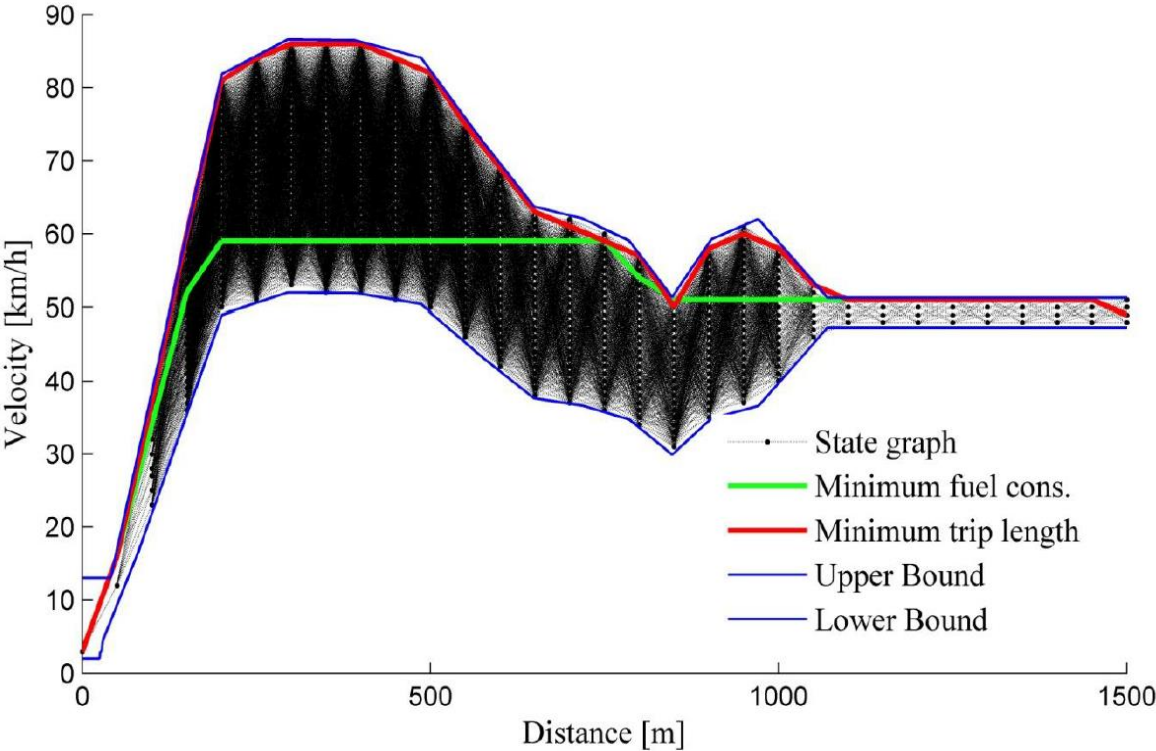


Figure 12. Optimisation of a single speed profile [125].

In [126], a similar approach was implemented with the exception that a genetic algorithm was used for optimisation. A more commercial application of this optimisation approach can be found in Porsche’s InnoDrive ACC [127, 128] where reduction of about 10% in fuel consumption was reported. In this study the cost associated with each edge was defined by:

$$J = M + \beta_1 C_1 + \beta_2 C_2 + \dots, \quad (2.41)$$

where  $M$  represents fuel consumption,  $C_i$  represents different cost elements accounting for comfort, the difference between maximum allowable speed and the calculated one, etc., and  $\beta_i$  is a weighting factor for each cost element.

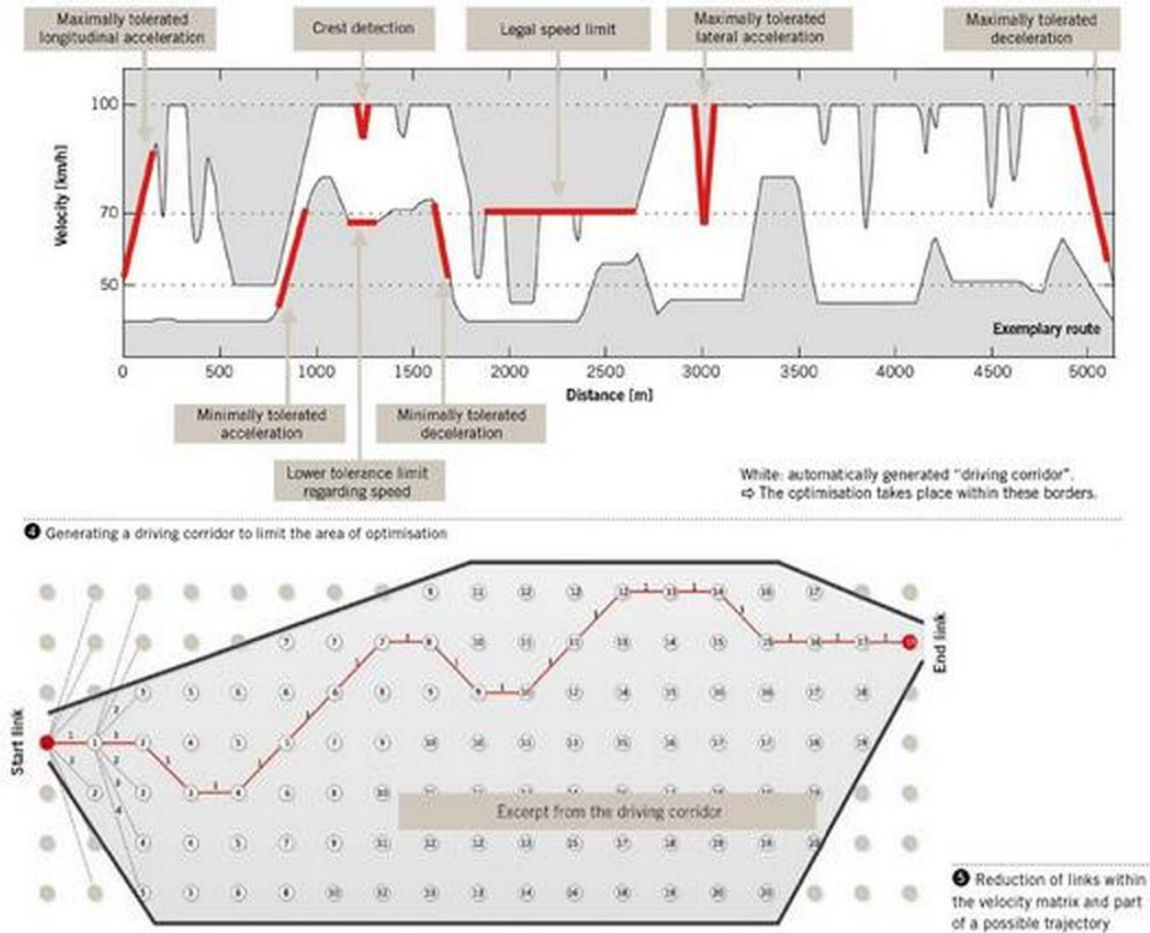


Figure 13. A schematic representation of Porsche InnoDrive ACC a) the upper and lower limits on the optimisation space due to different environmental factors b) the optimal path representing the optimal velocity plan within a road section [127].

In [129] a fuel-optimal control algorithm was proposed for trucks. The control algorithm was based on the optimisation of fuel consumption and gear-shifting according to the topography of the roadway. In this study the problem was formulated as a Dynamic Programming optimisation. In [130] a Proportional-Integral-Derivative

(PID) controller was designed for the car-following regime of driving. The method delivered fuel-economy driving by avoiding unnecessary accelerations and decelerations. The objective of the controller was set to track the velocity of the preceding vehicle while maintaining a specified range of gaps. In [131], a model predictive control algorithm was proposed in order to improve the vehicle's tracking capability in the car-following regime while delivering fuel-efficiency. The reduction in fuel consumption was obtained by the minimisation of accelerations while tracking the leading vehicle's speed. The system was then tested in urban and motorway driving scenarios and fuel savings of 8.8% and 2% were obtained in each scenario respectively.

The use of advanced technologies has also been widely investigated in the literature in order to achieve fuel efficiency. For example, in [132] the potential of technologies such as hybrid electric powertrains and telematics for the provision of traffic-related information was considered, and in [133] pulse and gliding was shown to provide significant savings in fuel consumption.

The body of research that concerns driving behaviour can be categorised into two groups. One group seeks to optimise fuel consumption for simple scenarios where there are no additional complexities caused by interactions between vehicles. In this case, information about roadways' topography or positions of traffic signals are used in the formulation of the optimisation problem; solving the optimisation yields the optimal velocity profile. The second group targets the car-following regime of driving. In these studies often simplistic assumptions are made about the relationship between fuel consumption and acceleration or the dynamics of driving. Moreover, due to the complexity associated with the car-following regime these works narrow down the optimisation framework to a single pair of vehicles and overlook the potential negative impacts of the proposed control strategies on the traffic flow and fuel consumption of the network.

The studies that have been reviewed so far mainly aim at individual vehicles and ways to reduce their fuel consumption irrespective of the complex, mutual relationship between traffic flow and individual driving behaviour. In [134], the negative impact of congestion on fuel consumption was studied based on a trajectory dataset obtained from a 640-meter long US motorway, namely the NGSIM I-80 dataset [135]. The NGSIM I-80 dataset is an open source trajectory data that is collected from an interstate motorway in the San Francisco Bay area, CA. An enhanced version of the dataset has been made available to the public through the MULTITUDE project [136]. In [134], it was reported that congestion could lead to an increase of about 80% in fuel consumption along with about four times longer travel times. This finding makes it clear that there is a significant potential for reducing fuel consumption for the whole network by pursuing traffic management policies that efficiently use the roadway capacity and, therefore, avoid or delay traffic congestions. Such policies could consider the potential of connected, automated vehicles in the provision of more efficient driving behaviours.

## **2.5 Summary**

In this chapter a brief review of the control approaches related to automated driving was given. Three fundamental approaches to modelling and control of driving behaviour were discussed, namely fuzzy logic, optimal control theory, and car-following models. It is worth mentioning that although car-following models were primarily developed for modelling purposes, instances of them being used as the foundation of a control algorithm were addressed in this chapter. Fuzzy logic allows a relatively simple way of integrating experts' knowledge in the control process. However, this method has not been widely used for longitudinal control. To the best of the author's knowledge most of the fuzzy logic-based controllers that are proposed in the literature lack a thorough discussion on stability, and collective properties. One of the main reasons for this could be the sophistication of validation in terms of the strict microscopic and macroscopic requirements which are necessary for a valid control strategy. Looking at longitudinal control as an optimal control problem mostly results

in the same issue. Solutions based on machine learning methods, namely RL and NN, cannot be systematically analysed or validated with respect to collective behaviour and stability requirements. Furthermore, for these methods to work, sometimes the problem is oversimplified or constrained to very specific driving scenarios.

On the contrary, modelling car-following behaviour has been a vast and active body of research for some decades. Simple models that are intended to describe the microscopic and macroscopic features of traffic have been widely studied and developed. As a result, a good understanding of different aspects of these models, namely collective behaviour and stability characteristics, is established. Therefore, it is no surprise to see the use of such models in practical applications. In section 2.2, a review of some of the well-known car-following models was provided. The car-following models have been mostly developed in order to passively explain and model existing driving-related and traffic flow-related features, and little focus has been given to utilising these models as active control methods for partially and fully automated vehicles. These models largely came into existence out of a need to understand and predict traffic-related phenomena and plan for transport networks. Therefore, a large number of these models do not necessarily meet safety requirements, nor do they produce completely realistic driving behaviour when individual drivers are considered. Therefore, before evaluating these models as the basis of control for automated driving, it is necessary to have a comprehensive look at the requirements of a safe and efficient road network. This enables us to have more tangible criteria for the evaluation of different car-following models as the basis of control. This is carried out in chapter 3.

### **3. Using car-following for automated vehicle control**

In chapter 2, different approaches relating to the control of vehicles were explored and the use of car-following models was put forward as a simple yet effective approach for the purpose of investigation of fuel-efficient driving strategies. The objective of this chapter is to provide a comprehensive account of different requirements in the automation of vehicles. This review will enable the author to select a car-following model that better meets the requirements of importance. Additionally, these requirements will contribute to the formulation of the optimisation framework that is discussed in chapter 4. The chapter is concluded by the choice of the car-following model that is going to be used in this study.

A longitudinal control model must meet numerous criteria before being considered for implementation. Some of these criteria are essential, for example safety and platoon stability, while others are desirable improvements that can be achieved with automated control, for example energy efficiency. These criteria are of great

importance in the design and implementation of control methods since they can be used as benchmarks in the evaluation and development of different models. However, to the best of the author's knowledge, no research work has addressed these criteria in a united way while highlighting methodological approaches for evaluation of these criteria. As a result of this lack of standardisation of requirements, many existing models are forced to rely on assumptions which may have not been validated, and could lead to undesired outcomes.

An extensive literature review was conducted in order to identify important model requirements, and to identify methods used for testing models against these requirements. Section 3.1 highlights these criteria and therefore, fills the aforementioned gap in the literature. Section 3.2 provides a detailed description of sensitivity analysis, an important step in the optimisation framework used within this study as well as in the evaluation of car-following models. Section 3.3 addresses some of the shortcomings of the existing studies in the comparison of car-following models. A new method for the comparison of car-following models is proposed in this section. This method demonstrates a much more robust performance compared to the existing comparison criterion. Finally, this chapter is concluded by a description of the car-following model that will be used in this study and a short summary.

### **3.1 Criteria of importance**

#### **3.1.1 Safety**

The subject of safety is imperative in the automation of vehicles. Advanced technologies such as ADAS and autonomous vehicles are intended to improve the safety of driving and, if possible, avoid human errors that lead to dangerous situations. This may be achieved by relying on advanced sensory and communication capabilities and prioritising safety in automated decision-making processes. Safety is also critical for the acceptance of these technologies [137]. However, ensuring safety is by no means trivial and numerous other criteria discussed in this chapter are closely tied

with this criterion. In this section some of the considerations with respect to safety and assuring safe control are discussed.

One approach to ensuring safety in control models is to assign exponentially increasing decelerations as spacing is closing. This approach is used in multiple car-following models such as the GM family of models [47, 52] and the IDM [26], and ACC models derived from the principles of optimal control and dynamic programming [105, 108]. In car-following models, this is typically done explicitly with an inverse relationship between the spacing and the magnitude of deceleration while in control models that are based on optimal control an exponentially increasing penalty is usually associated with closing gaps in the objective function.

Another approach in order to guarantee safety is to always ensure a safe spacing relative to the preceding vehicle to avoid collisions even in unexpected emergency braking situations. This can be seen in models proposed by Gipps and Benekohal [66, 38]. Such models are categorised as collision avoidance models. Some implementations of collision avoidance models in simulation-related projects and software products are mentioned in [43].

A control model must always be able to safely manage critical traffic conditions. The following scenarios have been addressed in the literature [138, 107].

- Emergency braking: the lead vehicle performs a sudden stop manoeuvre.
- Cut-in situation: a vehicle cuts in between a platoon of vehicles from an adjacent lane.

Platoon stability is another criterion of importance that is closely related to safety. This will be discussed in subsection 3.1.2.

### **3.1.2 Stability**

Two distinct features of car-following models which are of critical importance may be addressed under the subject of stability. Although both features can be distinguished by their definition and implications on traffic flow, they are bounded by the concept of stability of dynamical systems. These two features are platoon stability and string stability, where the former pertains to how disturbances are dealt with within a platoon and the latter relates to the response of a long string of vehicles to disturbances. In particular, platoon stability assures that deviation of the velocity of the leading vehicle will not be escalated into intense fluctuations in the velocity of the following vehicle. String stability, on the other hand, investigates the response of a long platoon of vehicles to an initial disturbance in the velocity of the leading vehicle. The initial disturbance would typically be passed along to the following vehicles, however it is important that the resulting disturbances are not significantly magnified and do not lead to traffic breakdowns and safety critical situations. After a brief discussion on the stability of dynamical systems, platoon stability and string stability will be discussed in more details in subsections 3.1.2.1 and 3.1.2.2 respectively.

In this section the focus is on autonomous (time-invariant) systems given by:

$$\dot{x} = \frac{dx}{dt} = f(x(t)), \quad (3.1)$$

where  $x \in X \subset \mathbb{R}^n$  is state space and  $f: X \rightarrow \mathbb{R}^n$  is the nonlinear equation of the system. It is worth mentioning that in a wide group of car-following models the function  $f$  maps the state space, usually consisting of speed, relative speed, and spacing, into a single control variable, typically acceleration or velocity. Equilibrium points of the system depicted by Equation

(3.1) may be obtained by setting the time derivative of the state equal to 0,

$$\dot{x}|_{x=x_e} = f(x_e) = 0. \quad (3.2)$$

The theory of linear stability can now be applied to analyse the behaviour of the system in reaction to small perturbation around equilibrium points [139, 24, 71].

A small perturbation around the equilibrium point can be introduced using,

$$\tilde{x} = x_e + \delta x . \quad (3.3)$$

Due to the assumption that the deviation is of a small magnitude, linearisation around the equilibrium point can be carried out, Equation (3.4), to investigate the response of the system. This essentially results in a constraint on the magnitude of the deviation for the analysis to remain valid.

$$f(\tilde{x}) = f(x_e) + \nabla f|_{x_e} \cdot \delta x \quad (3.4)$$

Since the first term on the right-hand side equals zero, Equation (3.4) can be reduced to,

$$f(\tilde{x}) = \nabla f|_{x_e} \cdot \delta x , \quad (3.5)$$

where  $\nabla f|_{x_e}$  is the Jacobean of  $f$  at the equilibrium point  $x_e$  and local stability of the system at this point can be evaluated using its eigenvalues. If all of the eigenvalues have negative real parts then by Lyapunov's first theory the system represented by linearisation of the dynamical system is globally asymptotic stable (in fact exponentially stable) and the corresponding nonlinear system is locally stable within a neighbourhood called the domain of attraction.

Even linear stability is somewhat overlooked among the transportation community, and especially within micro-simulation community [71], hence an extensive review of the concepts and methods developed in the area of stability analysis of dynamical systems and investigating possible applications of them in car-following models will be beneficial. For instance, the concept of domain of attraction may provide a way for quantitative evaluation of the magnitude of deviations for which the system remains stable.

This brief overview of linear stability is concluded by highlighting some of the limitations of linear stability analysis. Subsequently, the application of this method to platoon stability and string stability follows.

- As mentioned earlier, neglecting nonlinear terms in the linearisation process limits the validity of the linear stability analysis to deviations with very small magnitudes.
- Even finding an estimate of the neighbourhood for the equilibrium point for which the system remains stable, the so-called domain of attraction, becomes significantly challenging when the system takes more complicated nonlinear forms. The second theory of Lyapunov provides a way of dealing with this problem, however, finding Lyapunov functions for different types of state equations (dynamical systems) is not a straightforward task [140, 141]. In general, methods for estimating the region of attraction are categorised into Lyapunov and non-Lyapunov methods.
- “Large perturbation” and its implications on the system is beyond the realm of this analysis.

### 3.1.2.1 Platoon stability

Platoon stability or local stability is an important criterion that is directly related to safety and therefore is a necessary part of development and validation of car-following models. Consider a finite platoon of vehicles driving in homogenous, i.e. steady state, traffic. This corresponds to the state given by:

$$\dot{v}_n = f(v_e, \Delta v_n = 0, s_e) = 0 \quad (3.6)$$

For homogenous traffic consisting of identical cars and drivers this corresponds to the situation where all the vehicles are driving at the same speed,  $v_e$ , and keep the same spacing to preceding vehicles,  $s_e$ . This is called a uniform flow. A solution that relates  $v_e$  to  $s_e$  can then be derived using Equation (3.6). This solution, given in the form of  $v_e$  as a function of  $s_e$ , is then translated into a relationship between densities and flow, or the so-called fundamental diagram. The relationship between flows and densities for homogenous traffic is a very important feature of a car-following model. From a modelling point of view, it is expected that this diagram to some extent reproduces our observations and knowledge of traffic flow. From a control point of view, the diagram gives good insight into how a control method affects the collective features of traffic

flow such as the maximum capacity. This translation is carried out by considering equations (3.7) and (3.8),

$$\rho = \frac{1}{s_e}, \quad (3.7)$$

$$Q = \rho v_e, \quad (3.8)$$

where  $\rho$  and  $Q$  are density and flow respectively.

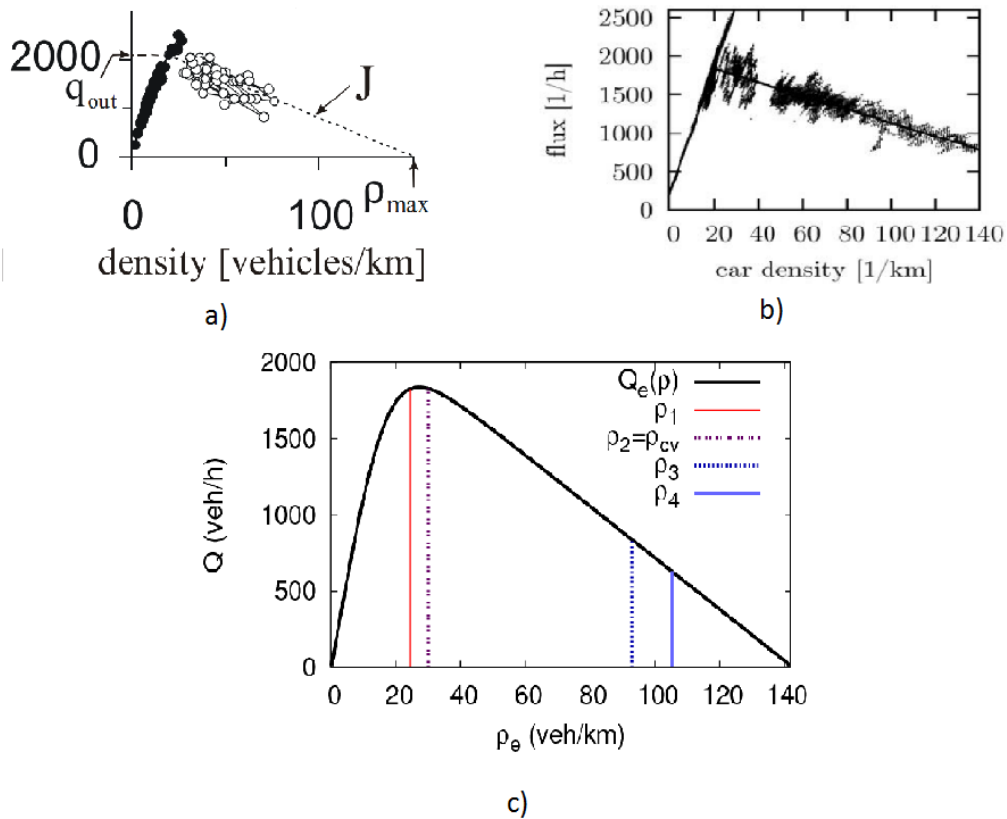


Figure 14. Fundamental diagram: relationship between density and flow a,b) empirical observations [142, 143] c) two-phase fundamental diagram derived from IDM model with specified critical densities [32].

For platoon stability a small perturbation in the speed, and consequently the spacing, of one of the leading vehicles in the platoon is considered.

$$s_n = s_e + \delta s \quad \text{and} \quad v_n = v_e + \delta v \quad (3.9)$$

This perturbation can be caused by a lane-change or an emerging vehicle from an on-ramp and it will result in deviation of the immediate follower from the equilibrium point. The following vehicles will also react to this perturbation in the same manner. The platoon stability criterion ensures that the resulting fluctuations in the speed and spacing of the following vehicle must eventually decay and the pair of follower-leader must reach an equilibrium state. If this necessary requirement is satisfied the system is said to be platoon stable.

The IDM car-following model and its merits were discussed in chapter 2. The application of platoon stability to IDM is discussed here in order to provide a better understanding of the subject. A more detailed discussion on this subject can be found in [71, 74]. The IDM is defined by Equation

(3.10).

$$\dot{v}_n = a_n \left[ 1 - \left( \frac{v_n}{v_n^d} \right)^\delta - \left( \frac{s^*(v_n, \Delta v_n)}{s_n} \right)^2 \right] \quad (3.10)$$

$$s^*(v, \Delta v) = s_n^0 + s_n^1 \sqrt{\frac{v}{v_n^d}} + T_n v + \frac{v \Delta v}{2\sqrt{a_n b_n}}$$

$$\Delta v = v_n - v_{n-1}$$

Linearisation at equilibrium point yields,

$$\delta \dot{v}_n = f_s \cdot \delta s_n - f_{\Delta v} \cdot \delta s'_n + f_v \cdot \delta v_n \quad (3.11)$$

Subtracting Equation (3.11) from that for the immediate lead vehicle yields:

$$\delta s''_n + (-f_{\Delta v} - f_v) \cdot \delta s'_n + f_s \cdot \delta s_n = -f_{\Delta v} \cdot \delta s'_{n-1} + f_s \cdot \delta s_{n-1} \quad (3.12)$$

Since a car-following model is expected to be platoon stable, as is the case in real traffic, the following conditions must be satisfied [144].

$$f_{\Delta v} < 0, f_s > 0, \text{ and } f_v < 0 \quad (3.13)$$

This intuitively means the following.

- As the spacing increases acceleration must increase. It would be more accurate to limit this statement to car-following situations as one expects that the dependency on the front vehicle should diminish when the spacing is very large.

$$f_s \rightarrow 0 \text{ for } s \rightarrow \infty$$

- As the approaching speed to the preceding vehicle becomes larger, acceleration must decrease. What was stated for spacing in terms of the diminishing impact of spacing for large values, holds true for relative speed, therefore;

$$f_{\Delta v} \rightarrow 0 \text{ for } s \rightarrow \infty.$$

- As speed increases acceleration must decrease.

Taking the right-hand side of Equation (3.12) as input perturbation,  $I(t)$ , and applying Laplace transformation yields:

$$S_n(z) = \frac{I(z)}{z^2 + (-f_{\Delta v} - f_v) \cdot z + f_s}, \quad (3.14)$$

where  $S_n(z)$  and  $I(z)$  are Laplace transformations of  $\delta s_n$  and  $I(t)$  respectively.

It can be seen that since the IDM satisfies condition (3.13), the poles of Equation (3.14) will always have negative real parts corresponding to a stable system. This can be seen in Figure 15 where the lead vehicle at a single point in time is slightly deviated from its equilibrium speed and immediately restored back to it. Following introduction of this perturbation, the spacing of the following vehicle deviates from its equilibrium point, however, platoon stability ensures that the vehicle will eventually restore to its initial condition.

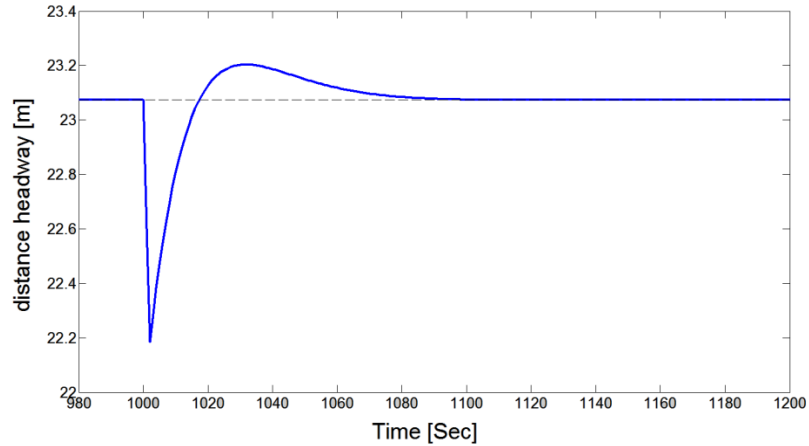


Figure 15. Response of the immediate following vehicle to a perturbation in the speed of the lead vehicle when its speed drops to by  $2 \frac{m}{s}$  and immediately restores to the equilibrium speed of  $20 \frac{m}{s}$  after 2 secs. The response is simulated using IDM model with default parameters.

### 3.1.2.2 String stability

String stability is related to the change in the characteristics of fluctuations, caused by an initial perturbation in the lead vehicle, as they are passed along to the following vehicles. Platoon stability ensures small perturbations will eventually fade away. However, if deflections from the equilibrium state grow in magnitude while moving in the upstream direction, this could lead to large enough perturbations that would trigger nonlinear effects such as stop and go waves.

Although string instability in traffic flow leading to phenomena such as stop and go waves is not desirable from a traffic management point of view, they may be required from a modelling point of view since such phenomena are frequently observed in real traffic.

Figure 16, demonstrates an example of a somewhat chaotic behaviour that can be linked to string instability for platoon of nineteen vehicles simulated using the IDM model.

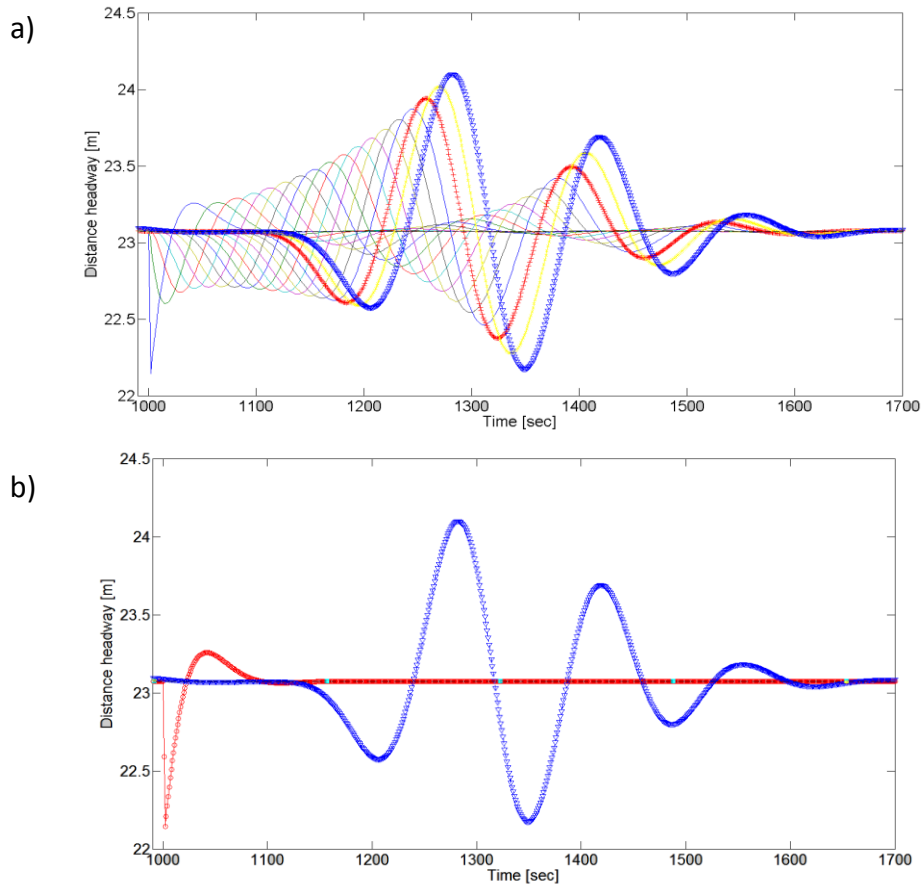


Figure 16. a) Response of the platoon of 18 vehicles to a perturbation in the speed of lead vehicle when its speed drops to by  $2 \frac{\text{m}}{\text{s}}$  and immediately restores to the equilibrium speed of  $10 \frac{\text{m}}{\text{s}}$  after 2 secs. The response is simulated using the IDM model with default parameters except for  $\mathbf{a} = 0.5 \frac{\text{m}}{\text{s}^2}$ ,  $\mathbf{b} = 3 \frac{\text{m}}{\text{s}^2}$  b) trajectories of all vehicles other than the second and last in line are eliminated.

Ring road analysis provides an effective way to investigate string stability features and the capacity drop phenomenon in a closed system. For this purpose, a simulation environment was developed to investigate the formation of stop and go waves. Figure 17 illustrates the formation of a cluster after the introduction of a small disturbance in the velocity of the leader. Here, each circle denotes a vehicle and those with spacing less than the equilibrium spacing are coloured in red. Due to the instability of the system in high densities the system does not restore to its equilibrium condition and the cluster continues to exist. The initial equilibrium condition prior to the introduction of the disturbance is shown in the plot on the left-hand side.

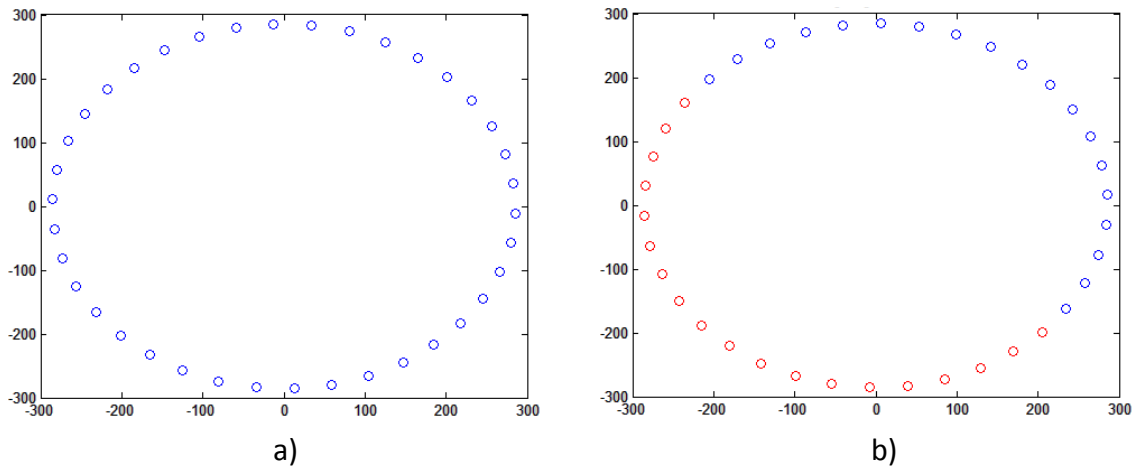


Figure 17. Formation of a cluster after the introduction of a small disturbance in the velocity of one of the vehicles. The default parameters for the IDM were chosen. Other simulation parameters used are; number of vehicles=38, length of the road=1793 m, equilibrium velocity and density prior to the introduction of the disturbance were 22.3 m/s and 21.2 cars/km respectively.

The formation of clusters and the circulation of disturbances can also be observed from the velocity, acceleration, and spacing plots. As shown in Figure 18, after the introduction of the disturbance the magnitude of fluctuations in spacing keeps increasing rather than being damped.

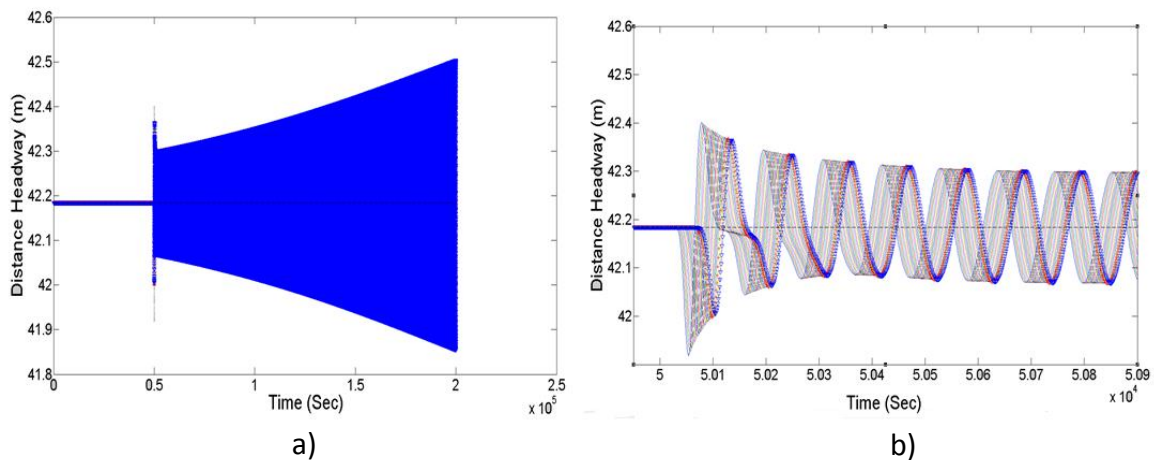


Figure 18. The spacing plots for the test scenario above. In the plot on the left-hand side, fluctuations for a short period are magnified for a better illustration of details.

More details on methodological approaches for investigation of string stability can be found in [71, 24].

### 3.1.2.3 Convective string stability

String stability can be categorised into three types based on the direction of propagation of the perturbation relative to a reference point in the road. These fluctuations may propagate in the upstream, downstream or in both directions. This is illustrated in figures below.

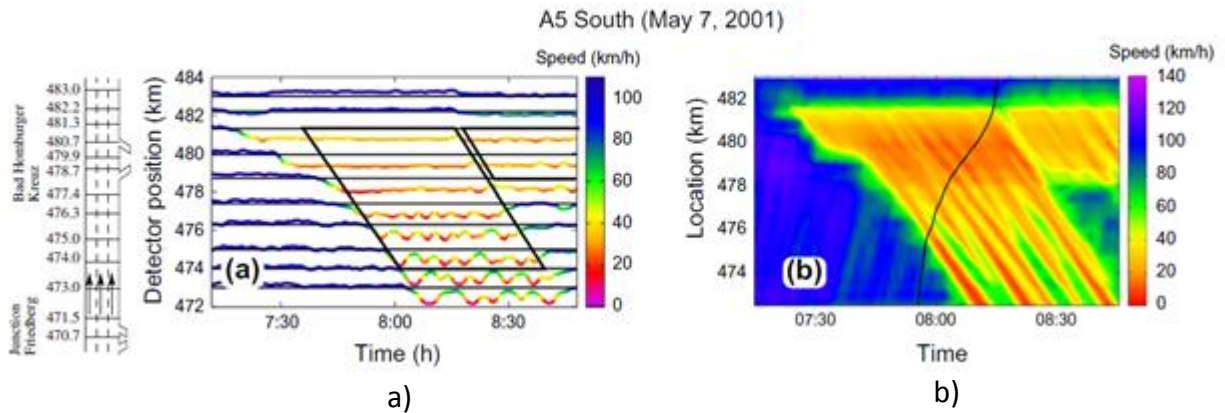


Figure 19. a,b) Propagation of the traffic jam in the upstream direction of a highway [24].

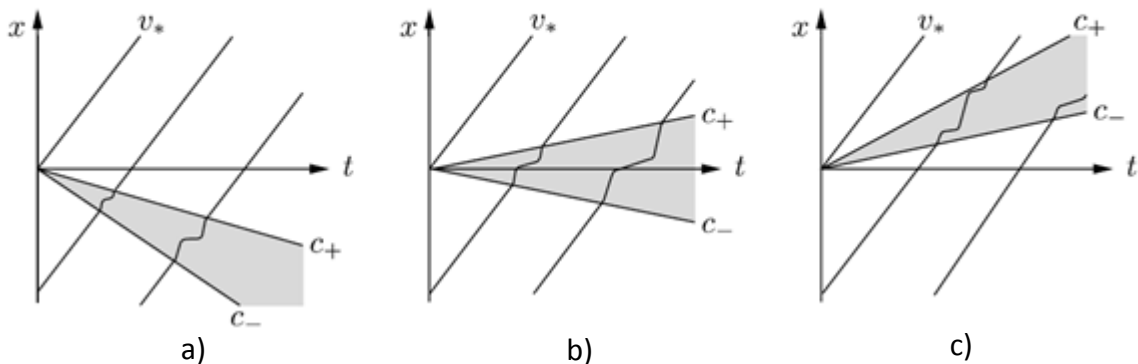


Figure 20. The direction of propagation of disturbances in a) convectively downstream (string) instability b) absolute string instability c) convectively upstream (string) instability where  $c_+$  and  $c_-$  are the velocities of the moving congestion fronts [71].

In real observations, only propagation in the upstream direction has been reported [71, 24], therefore, a similar collective behaviour is expected from car-following models. Consequently, for a given car-following model, the model parameters should

be selected from the region in the parameter space where only convectively upstream (string) instability occurs.

For mathematical frameworks for investigation of convective instability one can refer to [71, 24].

#### **3.1.2.4 Concluding remarks**

The importance of stability analysis as a tool for the investigation of car-following models and driving strategies was discussed. The definitions of platoon stability, string stability and convective stability were given and linear stability analysis, a relatively simple and useful method for the investigation of local stability of dynamical systems, was described. The works of Wilson and Ward [144, 145, 71] lay down a framework for linear stability analysis of a certain group of car-following models, although it is not applicable to all classes of car-following models and does not include reaction-time delay. Reaction-time delay has been fully studied in other studies such as [77, 146, 73] and the following findings were reported;

- There are three characteristic time constants that influence the dynamics of driving and stability of traffic flow namely; reaction time, update time, and the velocity adaptation time.
  - I. Reaction time is the time delay incorporated in the acceleration model as an explanatory variable.
  - II. Update time pertains to simulations and determines when the system is re-evaluated. This is the time step in which the accelerations and velocities of vehicles are updated.
  - III. Velocity adaptation time is the time required for adaptation to a new desired velocity.
- The first two may be considered as somewhat equivalent. In [77] it was found that the numerical update time is equivalent to about half the value of reaction time.

- Velocity adaptation time plays the main role in long-wavelength string instabilities, while large enough reaction times (or update time) chiefly influence short-wavelength, local instabilities.
- Velocity adaptation time for the IDM model is mainly influenced by the parameters of maximum acceleration,  $a$ , and the desired velocity,  $v_d$ .
- For a non-zero reaction time there is a certain range of values for  $a$  (or equivalently adaptation time) that maximises the stability and this range depends on the reaction time. Higher and lower values would result in less stability. Values above the range will result in less platoon stability as this type of instability favours agile driving, while values below the range will result in string instability as this type of instability favours sluggish driving. When the reaction time is zero, the system is always platoon stable and higher acceleration always contributes to string stability.
- The introduction of an additional explicit time delay in the IDM model as an explanatory variable does not improve the fit to the real trajectory data. This is due in part to the “anticipative intelligent braking” mechanism of the IDM [26] and the fact that drivers compensate for their reaction-delay time by anticipation which is gained from experience [73].

The author thinks that the application of the concepts and methods developed in stability analysis of dynamical systems, which is indeed a very fruitful area, remains somewhat neglected within the transport community. In particular, a very interesting subject of research would be the introduction of a new dimension to stability analysis of car-following models by taking the stability analysis from the qualitative “small perturbations” to a more quantitative level. The subject of region of attraction is well-studied in dynamical systems and the application of it to the behavioural analysis of car-following models is likely to lead to fruitful results.

### 3.1.3 Traffic flow

An ACC system can consist of different modules each applicable in a specifically defined condition. For instance, in [122] a module for energy efficient driving is proposed that can only be utilised when the vehicle is heading towards a traffic signal and there are no vehicles in front of it, or in [27] different traffic conditions are identified and a longitudinal control module is selected accordingly. However, for an ACC system which is targeted for application in congested traffic flow (where interactions with other vehicles occur frequently) it is crucial that the system is validated in terms of its impacts on traffic flow in addition to other important factors such as safety and stability. High levels of emissions and traffic instabilities may be linked to the stop-and-go phenomenon in the traffic regime, ACC can contribute to the regulation of flow and, thereby, help reduce emissions. Some of the important topics related to traffic flow and the impacts of driving strategies on traffic flow were discussed in sections 2.1 and 3.1.2.

### **3.1.4 Practical implementation aspects**

Besides safety, stability, and impacts on traffic flow, there are a wide range of practical considerations that must be taken into account in the development of automated vehicles. This section gives an overview of these requirements.

#### **3.1.4.1 Comfort**

It is important to also consider the comfort of drivers in the context of ACCs or autonomous vehicles. The feeling of discomfort has been linked to jerk and acceleration [147, 130, 148, 105], therefore appropriate values for these variables should be considered and unnecessarily high accelerations and jerks should be avoided. In terms of the methodologies used to assure comfort for drivers, one approach is to associate a cost to high accelerations, along with other factors, in the objective function that is defined to produce the optimal control policy [105, 149]. Alternatively, the values of jerk and acceleration may be constrained [148, 130].

### **3.1.4.2 Compatibility**

Fully and partially automated driving raises numerous questions and challenges regarding the compatibility of drivers with these systems. In the short term, while not all vehicles are fully automated, it is necessary that even fully automated cars produce a similar driving behaviour as humans. On the one hand, the automated systems may potentially possess some enhanced capabilities compared to drivers, such as shorter reaction times, more comprehensive perception of the surrounding environment, and execution of optimal actions. On the other hand, some studies suggest that one of the challenges for automated systems to address is a superior “anticipation” behaviour in drivers which is the result of experience and knowledge [77]. However, while due to different capabilities and characteristics one may expect completely different efficient driving styles in the extreme cases where all vehicles are driven manually or automatically, in the intermediate levels, where they coexist, automation must not result in driving styles that are unexpected to drivers. This also puts a limit on the extent to which the automated systems can be more efficient than drivers.

It has been argued that the desirability of these systems depends on the extent to which they could be customised to drivers’ driving preferences. In some studies this has been reduced to taking the driver’s desired speed into account and minimising the difference between the actual driving speed and the desired speed when possible [22, 105, 26]. However, this is likely to entail more strict requirements [150] and, therefore, further limit deviations from the existing driving norms towards more efficient driving patterns.

Other human factors such as the acceptance of these systems, degree of responsibility and mental workload required from users of partially and fully automated systems, overreliance and trust are active areas of research [151, 152].

#### **3.1.4.3 Dynamics of the vehicle**

The kinematics of vehicles and their mechanical constraints in tracking control commands is an important consideration in the realisation of automated driving. Numerous acceleration models may produce plausible driving behaviour yet the execution of the acceleration suggestions requires taking the mechanical dynamics of vehicles into account. Including even simplified models of vehicle dynamics in the derivation of control strategies, as in [138, 153], could lead to more realistic results. More details on vehicle dynamics can be found in [154, 155].

#### **3.1.4.4 Adequate reactions to different driving scenarios**

Producing an acceptable transient response to sudden changes in driving conditions is a necessity for any control strategy. The examination of the driving behaviour produced by models has traditionally been one of the ways to validate car-following models and driving strategies [138, 26, 107]. The following test scenarios are frequently used in the literature;

- Cut-in situations
- Change in the equilibrium speed
- Emergency braking and stopping
- Approaching a stationary vehicle
- Stop-and-go situation

#### **3.1.4.5 Robustness of calibration**

This criterion is specifically important for car-following models. These models have a number of model parameters that may be calibrated using specific trajectory data. The calibrated model is intended to produce a similar driving behaviour as represented by the trajectory data. Two important subjects may be raised within this context,

1. Universality of the model: To what extent the estimated parameters can reproduce driving behaviour consistent with that of real drivers in different traffic conditions and driving scenarios.

2. Relationship between model parameters and driving styles: It is expected that somewhat similar driving styles yield similar model parameters after the calibration process. For instance, ideally, calibration of a model using two different datasets from the same driver should yield similar results.

In [73], a study of these subjects, among other things, is given. Therein, the IDM model and the Velocity Difference Model (VDIFF) were compared and it was concluded that IDM achieves a better performance.

### **3.1.5 Environmental impacts**

Another important subject that is the focus of this work is fuel efficiency and reducing the footprints of ground transport networks by leveraging the potentials of automated driving. This topic was reviewed in section 2.4 and the importance of efficient driving strategies along with an effective traffic management was highlighted.

### **3.1.6 Summary**

In section 3.1, the requirements for an efficient longitudinal control system in the light of the literature were explored. In this study, the objective is to adopt a comprehensive approach to the question of fuel efficiency. Therefore, an extensive study was conducted to identify the important criteria for automated driving in the literature. The requirements were categorised into five areas, namely safety, stability, traffic flow, practical implementation aspects, and environmental impacts. In addition to providing a brief description of each requirement, methods used in the literature for testing these criteria were mentioned where possible and related references were given.

Having a comprehensive approach to the validation of control methods is very important, yet it is somewhat overlooked. The criteria such as safety and comfort are clearly crucial, but driving behaviour produced by automated vehicles can also have significant impacts on other important criteria such as traffic capacity. If and when

automated cars gain high shares of the motorised ground transport, neglecting the question of their impacts on traffic capacity could lead to unsatisfactory outcomes. For instance, the string stability properties of a platoon of ACC-equipped cars do not merely concern the platoon but also may have strong implications on the flow of the non-equipped cars. Therefore, it is necessary to identify the collective impacts of the automated driving strategies and seek to improve them or, alternatively, limit the application of automated driving to the scenarios where they do not degrade the collective performance of traffic. Table 2, at the end of this subsection, summarises the criteria discussed in this chapter.

Given the discussion provided in section 3.1 along with the analysis of different car-following models that was provided in chapter 2, the IDM car-following can be seen as a strong candidate for the evaluation of energy-efficient driving strategies. This model provides a simple deterministic structure for the longitudinal behaviour of vehicles both in free flow and car-following regimes. This simplicity becomes of great importance in computationally demanding analyses that will be carried out in this study such as the sensitivity analysis in section 3.2, the application of nonlinear, dynamic system identification methods in section 3.3, and last but not least, the optimisation that is carried out in chapter 4. The IDM has a small number of parameters with intuitive interpretations. This facilitates the calibration and behavioural analysis of the model. Moreover, the capability of the model to reproduce complex congested states and other microscopic driving features was demonstrated in section 2.1 and discussed in subsection 2.2.5. The model's collision-free structure ensures safety and the fact that it has already been tested on a real car demonstrates its reliability [66, 67]. Finally, the existence of a large number of studies on different aspects of the model from stability [71] and calibration [63, 72, 73, 74] to collective characteristics [26] facilitates further investigations.

Several modifications of the IDM model were discussed in subsection 2.2.5. After a more detailed analysis of these models in section 3.3, the model that best matches the requirements of this study will be selected.

Table 2. The criteria of importance in the automation of driving

<b>Criteria</b>	<b>Description</b>	<b>Comment</b>
<b>Safety</b>	Collision-free driving.	
<b>Stability (platoon)</b>	Pertains to damping the fluctuations around the equilibrium point caused by changes in the speed of the leading vehicle.	Linear stability analysis/ numerical methods
<b>String stability</b>	Propagation of disturbances along a long platoon of vehicles and occurrence of nonlinear effects	Linear stability analysis/ numerical methods
<b>Traffic flow</b>	Max flow, critical density, traffic flow behaviour	The fundamental diagram and phase diagram
<b>Comfort</b>	Jerky acceleration behaviour must be avoided	Constrain or penalise high accelerations
<b>Compatibility</b>	Automated vehicles must be compatible with drivers	Human factors
<b>Desirability</b>	Driving behaviour should be customised to different drivers	
<b>Dynamics of the vehicle</b>	Vehicle-related mechanical constraints in the implementation of driving strategies	The use of car models in the derivation of driving strategies
<b>Adequate reaction to different driving scenarios</b>	Testing the dynamic (transient) response of the system in different driving scenarios	Platoon stability mainly concerns asymptotic behaviour rather than transient response
<b>Robustness in calibration</b>	Pertains to how robust model parameters are in modelling a consistent driving behaviour while driving conditions change	This is important for the representation of different strategies through changing the model parameters
<b>Environmental effects</b>	Reductions in fuel consumption and emissions	The trade off with other criteria such as traffic flow

### 3.2 Sensitivity Analysis

Sensitivity analysis is an important part of many mathematical analysis methods such as calibration and optimisation. This analysis identifies the parameters with the highest level of influence to the problem and establishes the correlation between the parameters. Sensitivity analysis may be used both as a pre-optimisation measure and as a post-optimisation measure [156, 157].

The aim of this work is to explore the extent to which one can improve fuel consumption in the car-following mode of driving by finding a driving style that is not only fuel efficient but also satisfies other important criteria of the longitudinal control of vehicles namely, safety, traffic throughput, and traffic stability. This is to be achieved by exploring the parameter space of the car-following model that was selected for this study, the IDM, as the space where different driving styles can be represented.

Optimisation will be used to find the set of model parameters that result in the least fuel consumption. However, by considering the space of all the available model parameters there will not be any further model parameters, or degrees of freedom, left to be tuned for traffic throughput and stability. Some of the model parameters might have negligible impacts on fuel consumption while possibly having significant impacts on the other criteria. Therefore, it is important to identify the parameters that have the highest impact on fuel consumption and focus on them in the optimisation process. If the most influential parameters on fuel consumption turn out to be the parameters with marginal implication on traffic throughput and stability, this would mean that a fuel economy driving style can be obtained without deterioration of the traffic throughput and stability. However, if there is a significant overlap between the parameters with the most impact on fuel consumption and those which have a high impact on traffic flow and stability, then a trade-off has to be made.

Another reason for the use of sensitivity analysis before optimisation is related to computational efficiency. The inclusion of the model parameters with negligible impacts in the optimisation could result in significantly higher computation times.

It is worth mentioning that sensitivity analysis can also be used as a post-optimisation process, to investigate the robustness of optimisation with respect to small changes in the value of optimal parameters.

In what follows, some of the methods and concepts related to this subject will be briefly explored and the two fundamental approaches in sensitivity analysis, local sensitivity analysis and global sensitivity analysis, will be discussed.

In what follows, the generic model denoted by equation below is used,

$$Y = f(X_1, X_2, \dots, X_k), \quad (3.15)$$

where the variables or model parameters that are the subject of sensitivity analysis are  $X_i: i = 1, \dots, k$  and the output is denoted by  $Y$ .

### 3.2.1 Local sensitivity analysis

In this analysis, the sensitivity of output to changes in the model parameters is examined for one parameter at a time. This approach is also known as one-at-a-time (OAT) technique. This means that a single point in the  $k$ -dimensional space of parameters is considered and the impact of changes along the different dimensions are analysed one at a time. For instance, a measure of sensitivity is based on the calculation of the output variance,  $Y$ , with respect to the parameter  $X_i$ , when the rest of the parameters,  $X_{\sim i}$ , are kept constant .

$$S_i \propto V_{X_i}(Y|X_{\sim i}) \quad (3.16)$$

The ratio of this figure to the mean value is known as the Relative Deviation (RD).

$$RD_i = V_{X_i}(Y|X_{\sim i})/E_{X_i}(Y|X_{\sim i}) \quad (3.17)$$

Another widely used measure of sensitivity is the Sensitivity Index (SI) where the percentage of change in the output is calculated when varying one parameter from its maximum value to its minimum value.

$$SI_i = \frac{Y(X'_1, \dots, \max(X_i), \dots, X'_r) - Y(X'_1, \dots, \min(X_i), \dots, X'_r)}{Y(X'_1, \dots, \max(X_i), \dots, X'_r)}, \quad (3.18)$$

where the parameter  $X_{\sim i}$  are set to the values of interest  $X'_{\sim i}$ .

Local sensitivity analysis cannot be considered as a reliable method for the evaluation of the influence of an input on the output in complex, nonlinear systems. In such systems the surface of the objective function can be highly complex and nonlinear. Since the local sensitivity analysis merely explores a fraction of the parameter space in the vicinity of a pre-selected point, it does not reflect the overall influence of an input on the output. Therefore, the use of local sensitivity techniques as a measure of the sensitivity of nonlinear systems could lead to misleading results. More robust local sensitivity techniques include derivative-based methods and relative deviation. A more detailed review of such techniques can be found in [156].

Visualisation techniques are useful tools in the analysis of the sensitivity of systems to changes. A simple and common method for this purpose is to plot the output against the input parameters one at a time, while keeping the rest of the parameters constant according to the point of interest. An extension to this technique is to plot three-dimensional graphs where two input parameters can vary at a time. These graphs can provide a good picture about the shape and surface of the function. In [74], this visualisation technique was used a post-optimisation step in order to demonstrate the robustness of optimisation.

In the context of this study, it is important to investigate the relationship between fuel consumption and IDM's model parameters. Therefore, a visualisation technique is used to demonstrate this relationship. Figure 21 illustrates the surface of the objective function,  $Y$ , which in this case is the amount of fuel consumption for a car that drives

according to the IDM car-following model. The fuel consumption is calculated using the VT-micro model that was described in subsection 2.4.1.

In terms of experimental setup, a single pair of follower-leader is considered. The leading vehicle drives according to a real trajectory, namely the trajectory of the vehicle with ID 234, in the Naples dataset 25B [158]. This dataset provides information on the velocities, spacing, and accelerations of a platoon of four sensor-equipped vehicles that drive through a number of roadways in Naples, Italy. A more details description of this dataset is postponed to chapter 4. In this local stability analysis, while two parameters are changing at a time the rest of the model parameters are fixed to their default values [26], as seen in Table 3. The values for the parameters  $\delta$  and  $s_1$  are set to 4 and 0 respectively. This is consistent with the recommendations made in [74, 73].

Table 3. IDM default model parameters

Parameters	Default Values
$a$ [ $m/s^2$ ]	0.73
$b$ [ $m/s^2$ ]	1.67
$V_d$ [ $m/s$ ]	33.3
$s_0$ [ $m$ ]	2
$T$ [ $s$ ]	1.6

The result of this local sensitivity analysis is demonstrated in Figure 21. From this figure, one can conclude that in the vicinity of IDM's default values, the parameters  $T$  and  $s_0$ , which represent headway and jam spacing, have the highest level of influence on fuel consumption and the rest of the model parameters have only marginal impacts.

The figure that depicts fuel consumption as a function of acceleration and headway reveals an interesting result. There is a range of values for the parameter  $a$ , between  $[0.5 \ 1.5] \frac{m}{s^2}$ , where it has a significant impact on fuel consumption. However, this

impact diminishes for larger values of  $a$ . The same phenomenon could be observed for the parameter  $v_d$  which represents the desired speed. This can be a good indicator of the complexity of the optimisation surface which renders a merely local sensitivity analysis unreliable.

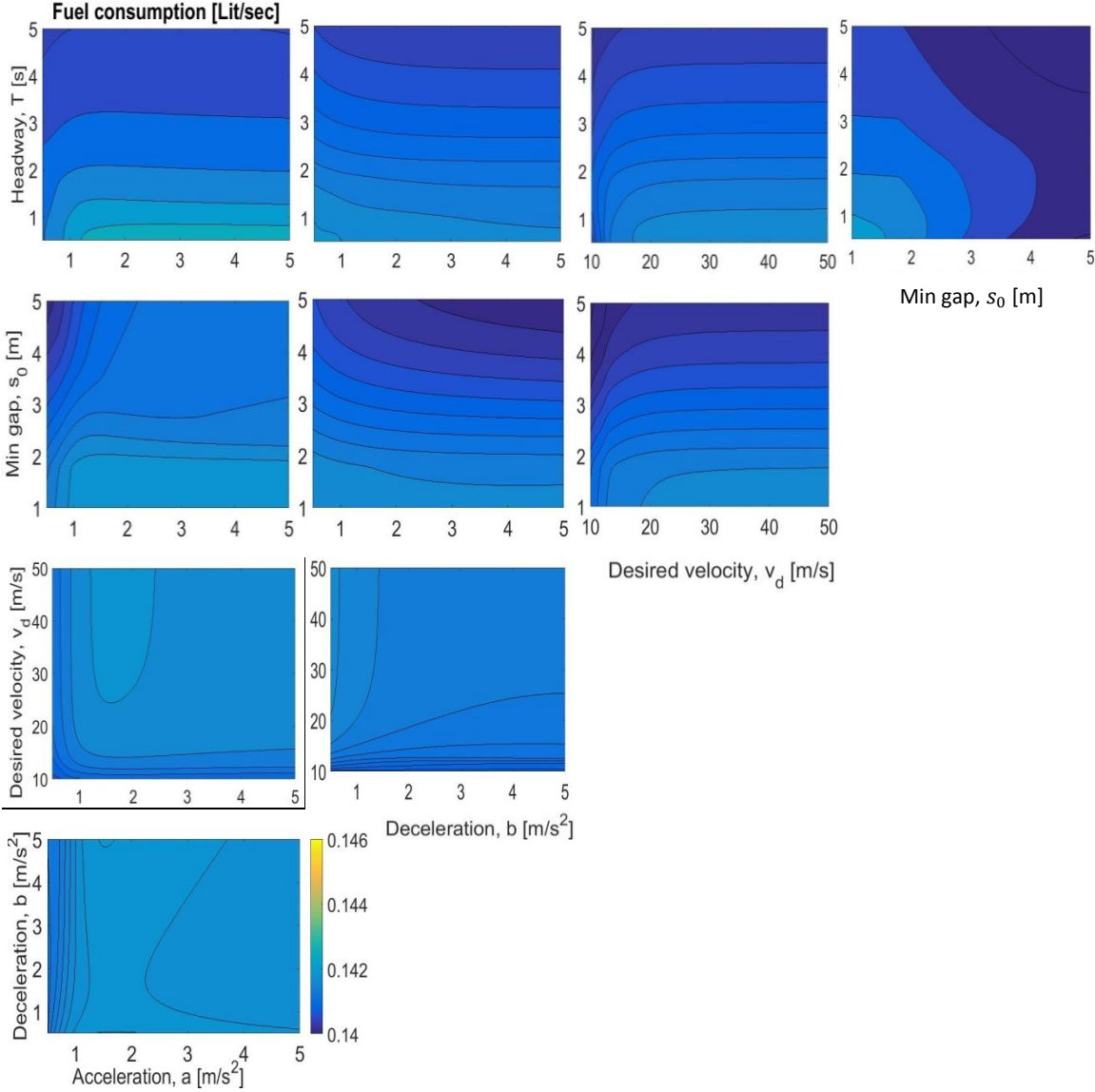


Figure 21. 2D visualisation of the local sensitivity of fuel consumption to different model parameters of the IDM car-following model. The results are derived from simulations where the subject vehicle is driving according to the IDM car-following model. The trajectory of the leading vehicle is obtained from the Naples dataset 25B, particularly vehicle with ID 234.

### 3.2.2 Global sensitivity analysis

Local sensitivity analysis evaluates changes in the output of a system when one parameter varies while the rest of model parameters are kept constant. Additionally, the magnitudes of changes are assessed around a single point in the space of model parameters. As a result of this, the method cannot adequately capture variations of the output along all the dimensions and it does not allow comprehensive exploration of the whole space of parameters. Therefore, the application of local sensitivity analysis in nonlinear systems could lead to misleading results. Global sensitivity analysis is a more reliable measure of the sensitivity of nonlinear systems. What follows provides a brief overview of this concept.

A useful technique in the visualisation of sensitivity, in the global sense, is the use of scatter plots. Scatter plots illustrates the distribution of different values of the output  $Y$  for different values of  $X_{\sim i}$  along an axis representing the values of  $X_i$ . Figure 22 illustrates scatter plots for the scenario described in subsection 3.2.1. In these plots the function  $Y$  is the amount of fuel consumption in the scenario where a vehicle that is driving according to the IDM car-following model is following another vehicle. The trajectory of the leading vehicle is obtained from the Naples dataset 25B and is related to the vehicle with ID 234.

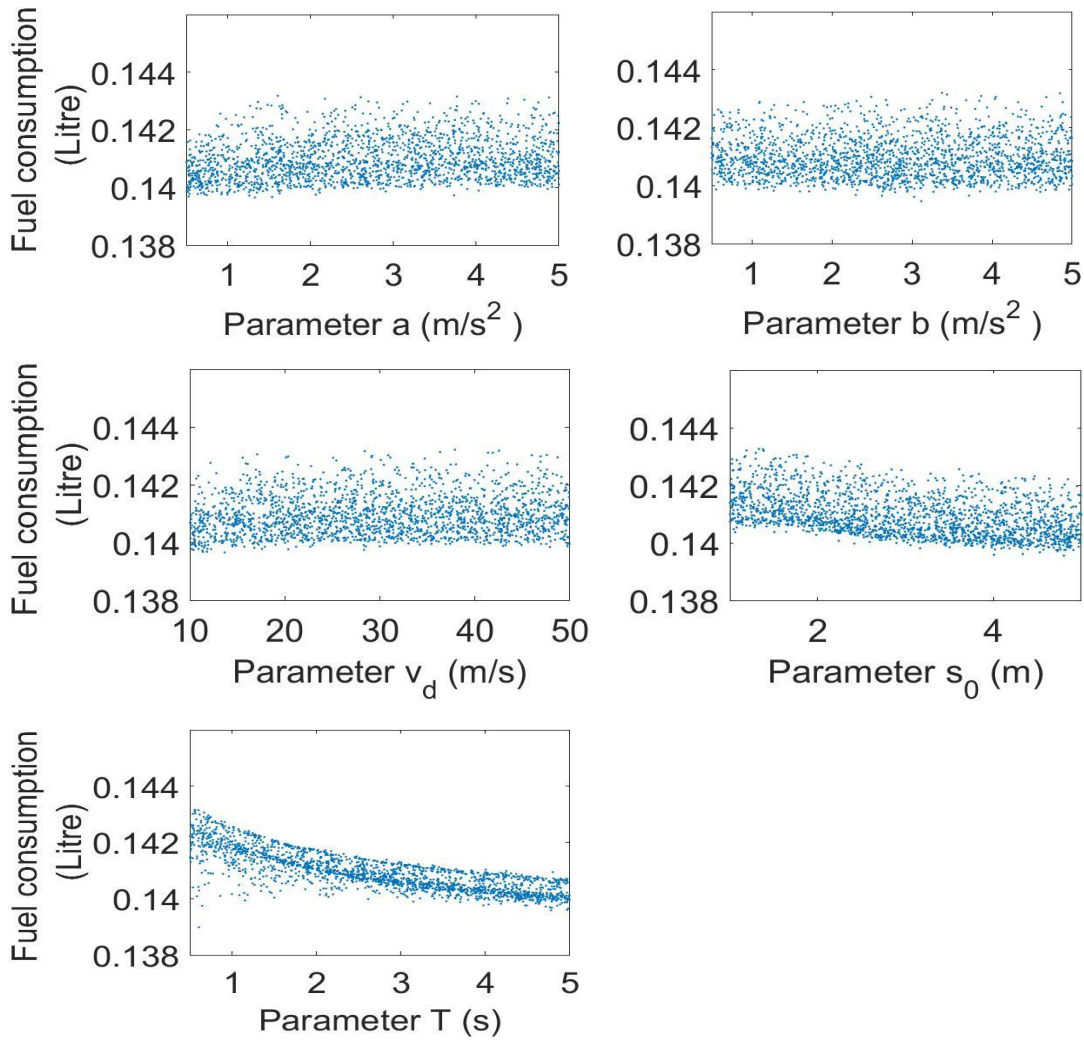


Figure 22. Scatter plots representing the fuel consumption of a vehicle that is driving according to the IDM car-following model. The trajectory of the lead vehicle is obtained from the Naples dataset 25B, particularly, vehicle with ID 234.

The parameter boundaries used for this analysis and throughout this section are reported in Table 4.

Table 4. Lower and upper boundaries used.

Parameters	LB	UB
$a$	0.5	5
$b$	0.5	5
$V_d$	10	50
$s_0$	0.5	5
$T$	0.5	5

It can be clearly seen that this analysis sets the parameter T as the most influential parameter as no significant pattern of increase or decrease in fuel consumption can be seen when other model parameters vary.

A measure to represent the existence of shape or pattern in Figure 22 can be formulated based on conditional variance;

$$S_i \propto V_{X_i}(E_{X \sim i}(Y|X_i)), \quad (3.19)$$

where the expectation operator is calculated over the  $r - 1$  dimensions of the space of model parameters while the parameter  $X_i$  is kept constant and the variance operator is calculated over all the possible values of  $X_i$ . The conditional variance,  $V_{X_i}(E_{X \sim i}(Y|X_i))$ , is known as the first-order effect of  $X_i$  on  $Y$ . Large values of  $V_{X_i}(E_{X \sim i}(Y|X_i))$  imply that changes in the value of the corresponding parameter,  $X_i$ , result in significant changes on the expectation  $E_{X \sim i}(Y|X_i)$  and therefore, this parameter has high influence on the output. Using the well-known formula

$$E_{X_i}(V_{X \sim i}(Y|X_i)) + V_{X_i}(E_{X \sim i}(Y|X_i)) = V(Y), \quad (3.20)$$

one can normalise the first-order effect to derive a sensitivity measure known as the first-order sensitivity index of  $X_i$  on  $Y$  [157],

$$S_i = \frac{V_{X_i}(E_{X \sim i}(Y|X_i))}{V(Y)}. \quad (3.21)$$

In linear models, this measure would produce a reliable means to assess the impact of,  $X_i$ , on the output. However, in nonlinear models one also needs to take into account the interactions between different factors or higher-order effects of a factor on the output. Equation (3.22) applies to linear models.

$$V(Y) = \sum_{i=1}^r V_{X_i}(E_{X \sim i}(Y|X_i)) \quad (3.22)$$

In these models the contribution of each factor to the overall variance can be a representative measure of its influence. For a nonlinear model, however, this is not

necessarily the case and the same first-order sensitivity indices can lead to misleading results; an example of this can be found in [157, pp. 25-30]. In general, the summation  $\sum_{i=1}^r S_i$  is not necessarily equal to one for nonlinear models.

The so-called ANOVA-HDMR decomposition (ANalysis Of VAriance with High Dimensional Model Representation) can be applied to nonlinear systems.

$$V(Y) = \sum_i V_i + \sum_i \sum_{j>i} V_{ij} + \dots + V_{123\dots r} , \quad (3.23)$$

where

- $V_i = V_{X_i}(E_{X_{\sim i}}(Y|X_i))$ ,
- $V_{ij} = V_{X_{i,j}}(E_{X_{\sim i,j}}(Y|X_{i,j})) - V_i - V_j$ , and
- $V_{ijk} = V_{X_{i,j,k}}(E_{X_{\sim i,j,k}}(Y|X_{i,j,k})) - V_i - V_j - V_k - V_{ij} - V_{jk} - V_{ik}$  .

By dividing both sides of Equation (3.23) by  $V(Y)$ , Equation (3.24) is obtained.

$$1 = \sum_i S_i + \sum_i \sum_{j>i} S_{ij} + \dots + S_{123\dots r} \quad (3.24)$$

Equation (3.24) provides a good framework to evaluate the composition of the variance of  $Y$  in terms of first-order and higher-order effects of individual parameters. In particular, by subtracting all the first-order and higher-order terms except for the parameter of interest,  $X_i$ , from the total variance, one could assess the effects of the factor  $X_i$  on the output. This measure is an indicator of the overall impact of any given factor on the output of nonlinear systems and is referred to as the total sensitivity index.

$$S_{T_i} = 1 - \frac{V_{X_{\sim i}}(E_{X_i}(Y|X_{\sim i}))}{V(Y)} = \quad (3.25)$$

$$1 - (\sum_n S_n + \sum_n \sum_{m>n} S_{nm} + \dots + S_{123\dots(i-1)(i+1)\dots r}) \quad \text{where } n, m \neq i$$

Using Equation (3.20) and (3.25),  $S_{T_i}$  can be written as,

$$S_{T_i} = \frac{E_{X \sim i}(V_{X_i}(Y|X \sim i))}{V(Y)}. \quad (3.26)$$

### 3.2.2.1 Variance estimators

The next step in performing sensitivity analysis is to find appropriate variance estimators. This topic has been the subject of numerous works in statistics. A comprehensive review of different estimators is beyond the scope of this work, but more details on this subject can be found in [159] and references therein. What follows describes an estimator that has been applied to the subject of car-following models [76].

Firstly, two matrices  $\mathbf{A}$  and  $\mathbf{B}$  both of dimensions  $N \times r$  need to be randomly selected from the space of parameters, where  $r$  is the number of model parameters and  $N$  is the number of simulations.

$$\mathbf{A} = \begin{bmatrix} a_{11} & \cdots & a_{1r} \\ \vdots & \ddots & \vdots \\ a_{N1} & \cdots & a_{Nr} \end{bmatrix}, \quad \mathbf{B} = \begin{bmatrix} b_{11} & \cdots & b_{1r} \\ \vdots & \ddots & \vdots \\ b_{N1} & \cdots & b_{Nr} \end{bmatrix} \quad (3.27)$$

Each row of matrices  $\mathbf{A}$  and  $\mathbf{B}$  constitute a complete set of model parameters and can be used in a simulation. Therefore,  $2N$  simulations are needed to find the corresponding output values for the rows of  $\mathbf{A}$  and  $\mathbf{B}$ . These simulations map the space of parameters to a single output denoted by  $f(\cdot)$ . For instance, since the matrix  $\mathbf{A}$  has  $N$  rows, i.e.  $N$  sets of parameters, a vector of  $N$  outputs could be associated with this matrix;

$$f(\mathbf{A}) = \begin{bmatrix} f(A)_1 \\ f(A)_2 \\ \vdots \\ f(A)_N \end{bmatrix}, \quad (3.28)$$

where the indices denote the corresponding row of the matrix  $\mathbf{A}$ .

A number of additional matrices, specifically  $r$  matrices, are formed from matrices  $\mathbf{A}$  and  $\mathbf{B}$  by swapping one column of  $\mathbf{B}$  with  $\mathbf{A}$  at a time;

$$\mathbf{A}_B^i = \begin{bmatrix} a_{11} & \cdots & b_{1i} & \cdots & a_{1r} \\ \vdots & \ddots & \vdots & \ddots & \vdots \\ a_{N1} & \cdots & b_{Ni} & \cdots & a_{Nr} \end{bmatrix} \quad i \in \{1, 2, \dots, r\}, \quad (3.29)$$

All the elements of  $\mathbf{A}_B^i$  remain the same as  $\mathbf{A}$ , except for the  $i$ -th column that is replaced with  $i$ -th column of  $\mathbf{B}$ . Subsequently, the estimators given by equations (3.30) and (3.31) can be used.

$$\bar{V}_{X_i}(E_{X_i}(Y|X_i)) = \frac{1}{N} \sum_{j=1}^N f(\mathbf{B})_j \left( f(\mathbf{A}_B^{(i)})_j - f(\mathbf{A})_j \right) \quad (3.30)$$

$$\bar{E}_{X_i}(V_{X_i}(Y|X_i)) = \frac{1}{2N} \sum_{j=1}^N \left( f(\mathbf{A})_j - f(\mathbf{A}_B^{(i)})_j \right) \quad (3.31)$$

The bar symbol is used to emphasise that the values on right-hand side of the equations are estimations of variance and expectation.

Finally, the variance of the output,  $V(Y)$ , is calculated using the column vectors  $f(\mathbf{A})$  and  $f(\mathbf{B})$  according to:

$$V(Y) = \frac{1}{2N} \sum_{j=1}^{2N} \left( f \left( \begin{bmatrix} \mathbf{A} \\ \mathbf{B} \end{bmatrix} \right)_j \right)^2 - \left( \frac{1}{2N} \sum_{j=1}^{2N} f \left( \begin{bmatrix} \mathbf{A} \\ \mathbf{B} \end{bmatrix} \right)_j \right)^2, \quad (3.32)$$

where  $\begin{bmatrix} \mathbf{A} \\ \mathbf{B} \end{bmatrix}$  is the matrix resulting from vertical concatenation of the two matrices  $\mathbf{A}$  and  $\mathbf{B}$ .

An important question in this context is the number of samples required,  $N$ , for the sensitivity indices to be reliable. Plotting graphs of the sensitivity indices against the number of samples is a convenient way to ensure the stability of these indices [76].

This subsection is concluded by applying the global sensitivity analysis to the scenario that has been used throughout section 3.2. In this scenario, a pair of vehicles is considered where the follower is driving according to the IDM and the leader is driving according to the trajectory of vehicle with ID 234 in the NGSIM Naples dataset 25B. The result is illustrated in Figure 23 and summarised in Table 5.

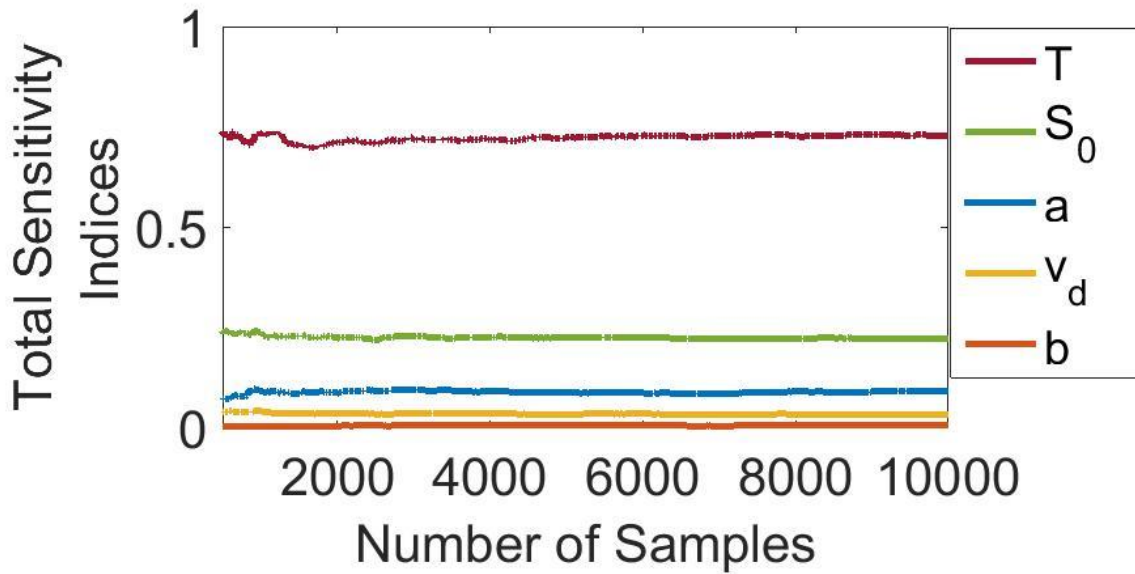


Figure 23. Total sensitivity indices for the effects of the IDM model parameters on fuel consumption in a simulation scenario where the vehicle with ID 234 from the Naples dataset 25B is the leading vehicle.

Table 5. Lower and upper boundaries used and total sensitivity indices.

Parameters	LB	UB	$S_T$
$a \left[ \frac{m}{s^2} \right]$	0.5	5	9%
$b \left[ \frac{m}{s^2} \right]$	0.5	5	0%
$V_d \left[ \frac{m}{s} \right]$	10	50	3%
$s_0 [m]$	1	5	22%
$T [s]$	0.5	0.5	73%

Based on this analysis it is clear that the parameter  $T$  has the highest impact on fuel consumption. The parameter  $s_0$  comes second in terms of its influence, however unlike what was suggested by the local sensitivity analysis, this parameter has much less influence on fuel consumption compared to parameter  $T$ . This is also consistent with the implications of Figure 22.

More details on the subject of sensitivity analysis and its application to car-following models can be found in [76, 159, 160].

### 3.2.3 Summary

Section 3.1 was concluded with the choice of the IDM car-following model for the present study. The objective of this section was to identify the parameters of this model that have the highest impact on fuel consumption. For this purpose, sensitivity analysis was discussed as an important step in any optimisation process. This analysis can be used to identify the parameters with the highest relevance to the objective function, by doing so it can; 1) simplify the optimisation by eliminating the parameters with negligible impacts on the objective function, and 2) leave a certain degree of freedom to fine-tune other model parameters according to other requirements.

Two distinct approaches to sensitivity analysis were discussed, namely local sensitivity analysis and global sensitivity analysis. The former could be used as an indicator of the sensitivity of the output function to changes in the value of model parameters around a single point. The latter delivers a much better understanding of the overall impact of each parameter on the output.

Both local and global sensitivity analyses were applied to the IDM car-following model in order to find the parameters with the highest influence on fuel consumption. Both methods pointed to the importance of the parameter  $T$ , representing the headway, for fuel consumption. This parameter was followed by parameters  $s_0$  and  $a$  that represent jam spacing and maximum acceleration respectively.

It is important to bear in mind that the experimental setup and the driving scenario that was used also affect the results of sensitivity analysis. The driving scenario was related to a single pair of follower-leader. The trajectory of the leader was selected from the Naples dataset 25B in which a variety of driving conditions are experienced. Therefore, this dataset provides the sufficient diversity that is required for the conclusions to be relevant to urban driving in a more general sense. However, the investigated scenario focuses on a single pair of vehicles and considers the fuel consumption of the follower in relation to the trajectory of the leader. This limits the extent to which the conclusions could be generalised to other operational scenarios where, for instance, the objective is to optimise fuel consumption for the whole

network and not only for individual vehicles. This topic will be further explored in chapter 4.

### **3.3 A new approach to the comparison of car-following models**

The IDM car-following was highlighted as a strong candidate for the present study on the basis of its merits, such as simplicity, availability of studies on different aspects of it, and implementation in an ACC. The objective of this section is to provide a more detailed account of the differences between the IDM model and another widely known car-following model that was also considered for this study, namely the GHR car-following model. Both models were described in chapter 2.

In chapter 2, it was discussed that the car-following models and the application of them in micro-simulations is of great importance in a broad range of fields from roadway design to conducting various investigations related to intelligent transport systems. Nonetheless, on the one hand these models are far from ideal and incautious use of them might cause misleading results in certain applications. On the other hand, in spite of fundamental differences in the mathematical structures of different car-following models, many studies have failed to give a reliable account of the strengths and weaknesses of different car-following models in modelling driving behaviour. Such studies typically rely on the calibration of different car-following models and compare them on the basis of the cumulative errors that they produce. But, it is often found that different car-following models have only somewhat marginal differences in terms of cumulative errors [72, 74, 161, 162].

The use of cumulative errors alone does not give an accurate assessment of the fundamental differences of the car-following models. Moreover, important questions such as the source of error and deficiencies of car-following models in accounting for certain driving behaviour remain unexposed in cumulative errors. Hence, a more meaningful framework for the analysis and evaluation of different car-following models is necessary. In this section a method based on parameter tracking and

unscented particle filtering is proposed in order to enable a more accurate assessment of the fundamental differences of car-following models and their deficiencies in accounting for driving behaviour. The method is then applied to the IDM and Gazis-Herman-Rothery (GHR) models and the results are compared. In order to add more depth to this analysis, two of IDM extensions, the Extended IDM (EIDM) and IDM with Variance-Driven Time headways (VDT), are also included in this study.

It is worth mentioning that car-following behaviour may be seen as random realisations of a stochastic process and this means there is an intrinsic limit to the extent to which car-following behaviour can be modelled using deterministic models.

The rest of this section is organised as follows. Subsection 3.3.1 provides a brief description of the four car-following models that were selected for this study. The calibration of car-following models is discussed in subsection 3.3.2. Subsection 3.3.3 gives an overview of Particle Filtering (PF) and its application for dynamic parameter tracking. This subsection is concluded by demonstrating the successful application of PF to the problem of tracking IDM model parameters. Prior to the application of the method for the comparison of the models, a sensitivity analysis is conducted to identify the parameters with the highest influence on the driving scenario used, the results are described in subsection 3.3.4. The comparison of the car-following models using the proposed method is carried out in subsection 3.3.5. Finally, concluding notes and potential future directions are discussed in subsection 3.3.6.

### 3.3.1 Car-following models

The GHR model is one of the most studied car-following models. Multiple modifications of this model along with studies on its calibration were discussed in chapter 2. This model is given by:

$$a_n(t) = \alpha \frac{V_n(t)^\beta}{\Delta X_n(t - \tau_n)^\gamma} \Delta V_n^{front}(t - \tau_n).$$

The model parameters and variable were previously defined in chapter 2, p.p. 28.

The IDM is another car-following model that was selected for this study. This model and its merits were discussed in chapters 2 and 3. Unlike many other car-following models, there is no explicit time delay in the IDM car-following model. Interestingly, in [73] it was shown that the introduction of an additional explicit time delay in the IDM does not improve the fit to real trajectory data. This is due in part to the “anticipative intelligent braking” which is incorporated in the IDM. In [26], it was argued that drivers compensate for their reaction time by their anticipation skills which are gained from the experience. For convenience, the equation defining this model is repeated here:

$$a_{IDM} = a \left[ 1 - \left( \frac{v}{v_{des}} \right)^\delta - \left( \frac{S^*(v, \Delta v)}{s} \right)^2 \right], \quad (3.33)$$

$$S^*(v, \Delta v) = s_0 + s_1 \sqrt{\frac{v}{v_{des}}} + T v + \frac{v \Delta v}{2\sqrt{ab}}.$$

Several modifications to the IDM have also been proposed. The Human Driver Model (HDM) extension to IDM [146] incorporates some human driving attributes into the model, namely the reaction time, imperfect estimation capabilities, and temporal and spatial anticipation. The IDM with Memory (IDMM) [163] is another modification to this model that accounts for slow adaptation of drivers to the traffic condition. In [164], the unrealistic behaviour of IDM in cut-in situations is addressed and the Enhanced IDM (EIDM) was proposed. Among different modifications of the IDM, the model that incorporates Variance-Driven adaptation of the Time headway (VDT), IDM-VDT, [165] is of particular interest as it adds an additional mechanism to the behavioural capabilities of IDM in order to account for the observed change of behaviour in congested and free traffic regimes. The change of driving behaviour in different traffic conditions is known as adaptive driving behaviour and is addressed by a number of studies [166, 167, 168]. In the IDM-VDT, this is modelled by including

additional information about local variations of speed among neighbouring vehicles in the time parameter that represents headway,  $T$ .

The EIDM and IDM-VDT models are selected for the present study. The former is given by,

$$a_{EIDM} = \begin{cases} a_{IDM} & a_{IDM} > a_{CAH} \\ (1-c)a_{IDM} + c \left[ a_{CAH} + b \tanh\left(\frac{a_{IDM} - a_{CAH}}{b}\right) \right] & otherwise \end{cases} \quad (3.34)$$

where the additional parameter  $c$  can be interpreted as a coolness factor. For  $c = 0$  the model reverts to the IDM, while for  $c = 1$  the sensitivity with respect to changes of the spacing vanishes in driving conditions where the spacing is small and velocity difference is equal to zero [164]. Here, the value of  $c = 0.99$  which was recommended in [164] is used. The variable  $a_{CAH}$  is a Collision Avoidance Heuristic that represents the maximum acceleration that does not result in crashes. This value is given by,

$$a_{CAH}(s, v, v_l, \tilde{a}_l) = \begin{cases} \frac{v^2 \tilde{a}_l}{v_l^2 - 2s \tilde{a}_l} & v_l(v - v_l) \leq -2s \tilde{a}_l \\ \tilde{a}_l - \frac{(v - v_l)^2 \Theta(v - v_l)}{2s} & otherwise \end{cases} \quad (3.35)$$

where  $\tilde{a}_l = \min(a, a_l)$  and  $\Theta(\cdot)$  is the step function.

The IDM-VDT model modifies the parameter  $T$  of the IDM according to,

$$T = \alpha T_0 = [\min(1 + \gamma V_n, \alpha_T^{max})] T_0, \quad (3.36)$$

$$V_n = \frac{\sqrt{\theta_n}}{\bar{v}_n}, \quad \bar{v}_n = \frac{1}{n} \sum_{i=1}^{n-1} v_{\alpha-i}, \quad \theta_n = \frac{1}{n-1} \sum_{i=1}^{n-1} (v_{\alpha-i} - \bar{v}_n)^2,$$

where  $\gamma$  is the sensitivity of the time headway to increasing velocity variations,  $\alpha_T^{max}$  denotes the maximum multiplication factor for the time headway found for traffic

flows of maximum unsteadiness,  $V_n$  is the variation coefficient for a platoon of  $n$  vehicles,  $\bar{v}_n$  is the local average velocity, and  $\theta_n$  is the local variance in velocities.

### 3.3.2 Calibration of car-following models

The main purpose of car-following models is to reproduce driving behaviour observed in real traffic. The calibration plays a critical role in this process. The car-following models attempt to describe the underlying driving dynamics through a number of explanatory variables, typically own velocity, relative velocity to preceding vehicle, and spacing between vehicles, and a mathematical structure relating these variables to acceleration or velocity. However, as there is a significant difference in the driving behaviour observed in different traffic conditions, one needs to adjust a given car-following model to the scenario of interest by means of calibration. These calibrated models can then be assessed based on the accuracy of predictions made by them for a separate dataset.

Interestingly, it is known that in spite of the considerable differences in the structures of different car-following models, they produce somewhat similar cumulative errors. For example, in [72] it was reported that the differences in validation errors across different car-following models are marginal. Moreover, it was found that one car-following model may best describe the trajectory of a certain driver when a certain set of trajectories is used, while another car-following model could best fit the trajectory of the same driver when a different set of data is used.

The two aforementioned observations may suggest that no car-following model is preferable over another since 1) the error produced by them is somewhat similar and 2) each of them describe a certain driving style more accurately. However, validation error or fitting quality alone cannot be a good indicator of the accuracy of car-following models. In [72], it was reported that a complex model may be more vulnerable to over-fitting compared to a simpler model. In [74], important criteria such as robustness, sensitivity to changes in the model parameters, model completeness,

and parameter orthogonality were put forward for benchmarking different car-following models. Comprehensive reviews on different aspects of car-following models and their calibration can be found in [74, 169].

Some of the studies that deal with microscopic calibration of the IDM model are [63, 72, 74, 73]. Some of these results are summarised in Table 6:

Table 6. Calibration results for the IDM car-following model using trajectory data

Source	$a \left[\frac{m}{s^2}\right]$	$b \left[\frac{m}{s^2}\right]$	$v_d \left[\frac{m}{s}\right]$	$s_0[m]$	$s_1[m]$	$T[s]$	$\delta$
Hoogendoorn (2010)* [63]	1.30	0.54	28.33	6.93		0.94	
Punzo (2007) [72]	2.57	1.69	28.36	0.74	0.56	0.69	2.84
Kesting (2009) [73]	0.76	1.58	16.1	1.68		1.30	
Treiber (2013) [74]	1.39	0.65	16.1	1.53		1.20	

\*This study provides multiple estimates for the parameters. The one used in table is selected as it was derived based on empirical data.

In [73], different estimates are given with great variations compared to one another. The reason for this variation could be related to the use of a single vehicle trajectory for deriving each of the estimates and unlike [72] and [63], neither a data-fusion method for calibration nor a diverse dataset was used in order to ensure the robustness of calibration. This gives rise to the possibility of over-fitting and less reliable results for cross validation.

It should be noted that the estimates provided in the table above vary in the use of methodology, dataset, driving scenarios, and the set of parameters that were calibrated. In [72] all seven model parameters are calibrated, while in [63, 73] five model parameters are calibrated and the remaining two parameters are set to zero. In [63], a data fusion technique based on maximum likelihood is used in order to estimate a single set of model parameters that best reproduce the flow of traffic as seen in the real data, while in [72] different sets of model parameters are obtained for individual vehicles.

Two of the important factors in calibration that are somewhat overlooked are; 1) accounting for the correlations between the model parameters and 2) recognising that not all datasets are suitable for the calibration of all the model parameters. A dataset may be lacking any information on a certain driving attribute, for example desired speed in free-flow. Such a dataset must not be used for calibration of a parameter that denotes desired speed [74, 170].

In the next subsection the dynamic system identification is introduced as a powerful method for the analysis of car-following models.

### **3.3.3 Dynamic system identification using Particle Filtering**

Calibration is a form of system identification for systems with a known model. This is known as the “grey-box system identification problem”. In this type of problems a model exists, for example a mathematical model, but certain elements of the model need to be determined from the data. By the application of system identification on car-following models, one finds a set of model parameters that result in the most plausible fit; the minimum cumulative errors is often used to determine the most plausible fit. However, as pointed out in previous sections, the goodness of fit alone cannot be a representative measure of the accuracy of a model.

In order to deal with the issue raised above, the use of dynamic system identification is proposed. This approach provides an answer to the question of “how do the parameters of a given car-following model need to change in time so that the modelled behaviour matches the real data?” The answer to this question could shed light on many different properties of car-following models, including the question of “what constitutes a good model?” A good car-following model should not only achieve a good fit to real data, but also does not need many changes to cope with different driving scenarios.

Model coefficients are meant to be constants, therefore dynamic system identification allows us to identify the shortcomings of car-following models by observing the

changes in the model parameters that are necessary in order to obtain an accurate match with the real data. In this study, the method of sequential Monte-Carlo filter or Particle Filter (PF) has been used for this purpose due to its merits in dealing with nonlinear non-Gaussian systems with complex dynamics [171, 172, 173].

The PF is a family of methods where a set of samples are used to approximate the posterior distribution in an online fashion and based on the Bayesian recursion. Initially, candidate estimates of the parameters are extracted from a prior distribution. These samples, or the so-called particles, are fed into the model and produce prediction values. The predictions are compared to the observed values in order to calculate weighted samples of the posterior, or the so-called importance weights. Subsequently, particles are drawn from the posterior, in order to produce an unweighted estimate of the posterior. This sequence is repeated in every time step, upon the reception of new data, in order to produce a more accurate estimate.

This method has been previously applied to car-following models in order to jointly estimate the traffic state and model parameters [168]. Therein, dynamic parameter estimation was used in order to track changes in the model parameters of two delayed car-following models, namely the GHR and Helly models. Additionally, a discussion of the impact of filter configuration on the parameter estimates was given. While this paper was among the sources of inspiration to the present study, the present work diverges from [168] in methodology and objectives, in the following ways:

- 1) The objective of [168] was stated to generalise dynamic parameter estimation to include reaction time in delayed car-following models. Moreover, application of this method to empirical data is served as evidence of dynamic driving behaviour, i.e. changes of the driving attributes in real driving conditions. The present study, however, employs dynamic parameter estimation as a technique for the comparison of car-following models. Inspired by the field of “Quantitative Model-Based Fault Detection and System Diagnosis” [174, 175, 176], the author intends to link dynamic model estimates to the robustness of models. In the field of fault detection and system

diagnosis, changes in the model parameters are linked to the occurrence of faults. While, due to limited modelling capabilities, avoiding false detection of faults is a big challenge, a good and robust model generally is expected to be more immune to the false detection of faults that result from drastic changes in the model parameters that do not correspond to an actual change in the system. Herein, the comparison of car-following models is carried out according to this concept.

2) Simultaneous tracking of multiple model parameters is problematic for three particular reasons:

a) The correlation of model parameters means that errors in the estimation of one model parameter [177] can be compensated for by additional errors in the estimation of another. This issue is reflected in dynamic estimation of multiple parameters when in successive applications of the method, different dynamic estimates are obtained. Inconsistent estimates in successive applications undermines the meaningfulness of the estimates.

b) It is not meaningful to consider all of the model parameters as variables. A model parameter that represents maximum acceleration, or comfortable deceleration, is expected to remain steady for longer periods, whereas a parameter that represents an inherently random attribute such as headway might change more rapidly.

c) It is neither useful nor correct to estimate all of the model parameters while some of them are almost irrelevant to a particular scenario. This relevance can be examined by sensitivity analysis [74, 170].

For all of the aforementioned reasons, in this study, unlike [168], the investigation is focused on the most important parameter of a car-following model in the scenario of interest.

As mentioned above, PF can be used to tackle the difficulty associated with the estimation of states or parameters in nonlinear, non-Gaussian systems. The state-space representation of such system is given by;

$$\begin{aligned} x_t &= f(x_{t-1}, v_{t-1}), \\ y_{t-1} &= h(u_{t-1}, x_{t-1}, n_{t-1}), \end{aligned} \tag{3.37}$$

where  $x_t$  is the state of the system that evolves under the nonlinear function  $f(\cdot)$ . The previous state of the system is denoted with,  $x_{t-1}$ , and  $v_{t-1}$  is an independent, identically distributed (i.i.d) random noise, that is known as the process noise. The true state of the system is almost always hidden from the observer. The objective of filtering is to deduce a good estimate of the state of the system through successive observations and measurements,  $\{y_t, t \in \mathbb{N}\}$ . These observations are dependant on the control input,  $u_t$ , the true state of the system,  $x_t$ , and an i.i.d noise,  $n_t$ , known as the measurement noise. This dependency is denoted by the function  $h(\cdot)$ .

The method of PF is based on the principles of Bayes theorem, which provides a mechanism for updating knowledge about the underlying system upon the reception of new data at each time instance. In Bayesian estimation, the quantity of interest is the probability distribution function of the state variable,  $p(x_t | y_{0:t})$ , given the sequence of observations made. This is known as the posterior.

In algorithms such as the Kalman Filter and the Extended Kalman Filter (EKF), the following two assumptions are made:

1. The system is linear or the locally linearised system (in the case of EKF) provides a good enough approximation of the system.
2. The underlying noise is Gaussian.

Under these assumptions the characteristics of the posterior, namely the mean and covariance, can be optimally derived. The term optimal in this context means that the resulting estimator leads to Minimum Mean-Square Error (MMSE). However, when the system of interest exhibits highly nonlinear behaviour and the noise is non-Gaussian,

the performance of KF and EKF deteriorates. PFs provide an alternative way to the linearisation of nonlinear systems and making assumptions about the underlying noise distribution. In these methods, a number of samples, which are referred to as particles, are propagated through the nonlinear systems using simulation techniques. The transformed samples are then used to extract the characteristics of the posterior.

An important step in this method is importance sampling where the importance weights are estimated.

$$w_t = \frac{p(y_{1:t}|x_{0:t})p(x_{0:t})}{q(x_{0:t}|y_{1:t})}, \quad (3.38)$$

where,  $w_t$  is the importance weight,  $p(y_{1:t}|x_{0:t})$  is conditional probability of observations,  $y$ , given the states,  $x$ ,  $p(x_{0:t})$  is the probability distribution of the states, and  $q(x_{0:t}|y_{1:t})$  is a known, easy-to-sample proposal distribution.

A sequential relationship for the importance weight is given by [171];

$$w_t = w_{t-1} \frac{p(y_t|x_t)p(x_t|x_{t-1})}{q(x_t|x_{0:t-1}, y_{1:t})}. \quad (3.39)$$

A popular choice of the proposal distribution,  $q$ , in order to simplify this equation is:

$$q(x_t|x_{0:t-1}, y_{1:t}) = p(x_t|x_{t-1}). \quad (3.40)$$

In PF, the estimate of the posterior is obtained from a number of randomly selected weighted samples. The great potential of this method in dealing with complex nonlinear non-Gaussian systems was pointed out by [171, 172].

Figure 24 provides a schematic representation of the PF method. At the first step of the algorithm, sampling,  $N$  random particles (samples) are drawn from a proposal distribution. These particles are then propagated through the nonlinear system and are subsequently associated with weights,  $\tilde{W}$ , according to their fitness that is estimated by Equation

(3.39). This step is known as the importance sampling. Subsequently, a resampling of particles with respect to their associated weights is carried out. As a result of this, particles with high weights are split into a number of unweighted particles and particles with low weights are eliminated. Finally, at the third step a random noise is applied to the group of particles in order to introduce local variety in the samples, this process is visualised in the fourth row of particles in Figure 24. Since this step provides an unweighted distribution of particles that mimics the prior distribution, it is referred to as the prediction step.

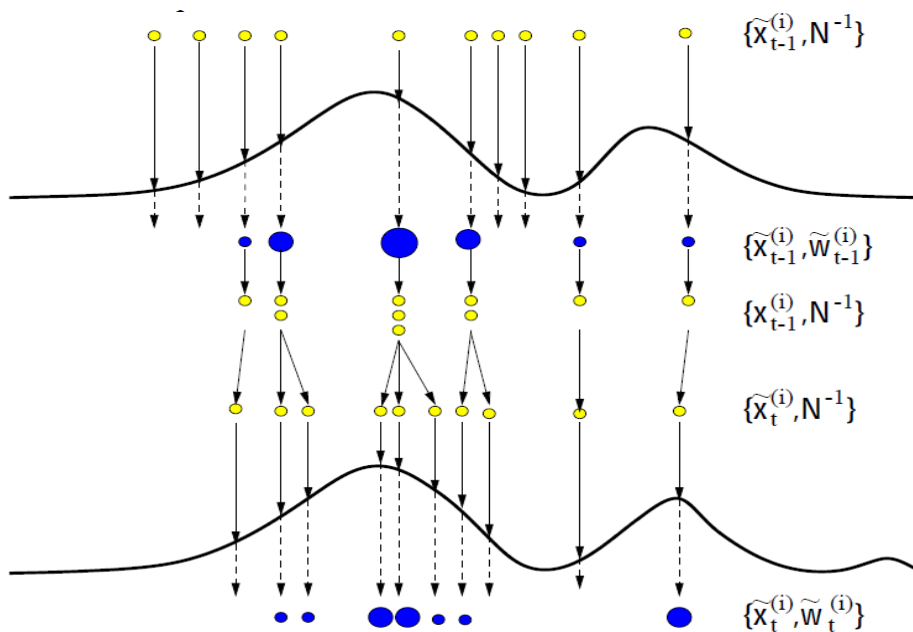


Figure 24. The visualisation of the three stages of importance sampling, resampling, and sampling (prediction) in PF, figure from [178].

More details and a pseudo-code of the method can be found in [171, 168, 172] .

In this study, the application of this method for parameter tracking is of particular interest. Given a car-following model and a time series, the estimates of model parameters can be updated at every time step. As a result, time-varying estimates of

the model parameters could be obtained. Of course, the time-varying estimates cannot be used for modelling and simulation purposes, however, they can provide a good insight into some of the very important characteristics of the model that may remain hidden in cumulative error terms.

In applications of models in simulations the parameters are constant. The use of a parameter tracking method provides information about the extent to which a model parameter should deviate from its nominal value in order to compensate for the model's deficiencies. This concept is closely related to model-based fault detection [174, 175]. If general patterns of changes are observed in the dynamic estimates, e.g. significant increase or decrease in the value of a model parameter in an identifiable driving phase, this information could be used in order to improve the quality of modelling and simulation.

#### **3.3.4 Sensitivity analysis**

In [74] it was pointed out that parameter non-orthogonality can cause misleading results in the calibration process. Parameter non-orthogonality refers to the existence of high correlations between the parameters. In this study, a global sensitivity analysis is performed in order to minimise the impact of parameter non-orthogonality. This is achieved by the identification of the model parameter that has the highest influence on driving behaviour in the simulation scenario and subsequently using the identified parameter in the parameter tracking process.

In [170] a global sensitivity analysis was applied to the IDM in order to identify the model parameters that have the highest influence on the calibration process. Therein, the trajectories of 2037 follower-leader pairs from the NGSIM-I80 dataset [136] were used. Moreover, in addition to the IDM's six model parameters, each leader/follower pair was assigned an ID and this ID was also included in the analysis. Finally, the Root Mean Square Error (RMSE) of spacing was used as the Measure of Performance (MoP) in the calibration process. It was found that the ID of the pair has the highest influence

on the calibration with the total sensitivity index of 80%. The IDM parameters  $T$ ,  $\delta$ ,  $\alpha$ ,  $s_0$ ,  $b$  and  $V_d$  obtained total sensitivity indices of 45.27%, 22.47%, 9.41%, 1.24%, 1.15%, and 0.91% respectively.

In the present study, the same parameter boundaries as [170] are used for the three IDM-based car-following models. These values are given in Table 7.

Table 7. The lower and upper boundaries used in this study.

Parameters	LB	UB
$a \left[ \frac{m}{s^2} \right]$	0.5	4
$b \left[ \frac{m}{s^2} \right]$	0.5	2.5
$V_d \left[ \frac{m}{s} \right]$	21.7	30.7
$s_0 [m]$	0.1	3
$T [s]$	0.1	3

For the GHR car-following model, the following boundaries are used;  $\alpha = [1 \ 3]$  for the sensitivity parameter, and  $\tau_n = [0.1 \ 2]$  for the time delay. These boundaries are selected in order to include the values reported by different studies [43]. Figure 25 shows the total sensitivity indices of the IDM car-following model with respect to the calibration error where the calibration error is defined as the sum of squared errors for velocity, acceleration, and distance:

$$MoP = \sum_{i=1}^N (a_i^m - a_i^r)^2 + (v_i^m - v_i^r)^2 + (s_i^m - s_i^r)^2, \quad (3.41)$$

where  $a$  is the acceleration,  $v$  is the velocity,  $s$  is the spacing,  $N$  is the number of samples, and the superscripts  $m$  and  $r$  denote modelled and real values respectively. This figure demonstrates the total sensitivity indices in a driving scenario where the trajectory of the leader is that of the vehicle with the ID 362 from the NGSIM-I80 dataset.

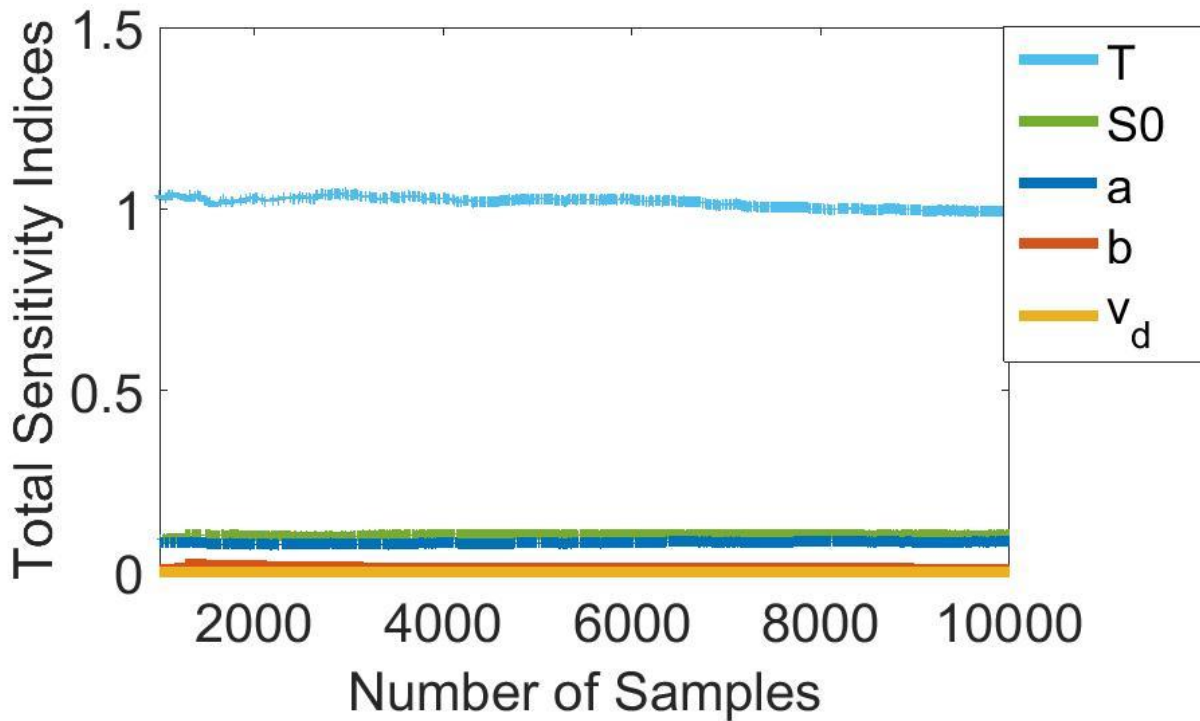


Figure 25. Total sensitivity indices of the IDM car-following model w.r.t. the calibration error in a simulation scenario where the trajectory of the lead vehicle is that of the vehicle with ID 362 from the NGSIM-I80.

In order to examine the consistency of the results, different trajectories were also used, namely the trajectories of the vehicles with ID numbers {362, 368, 378, 381, 391} and the results were cross-checked. For the three IDM-based car-following models, values consistent with the ones observed above were obtained. For the GHR car-following model, however, while in the majority of cases the parameter  $\alpha$  obtains a sensitivity index higher than parameter  $\tau_n$ , in some cases parameter  $\tau_n$  is identified as the most influential parameter. The values of the total sensitivity indices of  $\tau_n$  and  $\alpha$ , averaged for the five aforementioned trajectories, are 0.69 and 0.85 respectively. Unlike the sensitivity indices for the IDM which clearly highlight the parameter  $T$  as the most influential parameter on the calibration error, the sensitivity indices of the GHR model are not conclusive enough as to which one of the model parameters has the highest influence, therefore, for simplicity the parameter  $\alpha$  is considered in this study.

Along with the sensitivity analysis, the choice of the model parameters  $T$  for the IDM

and  $\alpha$  for the GHR could also be justified by their physical interpretations and by the scenario under investigation. For instance, the parameter representing reaction time in the GHR,  $\tau_n$ , may not be expected to have high frequency, intense changes in a short, car-following scenario whereas for the sensitivity parameter such changes could be expected and would convey more information about the deficiencies of the model. These criteria may be seen as additional requirement for such system identification studies [74].

The sensitivity indices obtained in this study are consistent with the ones reported in [170] except for one marginal difference. In the set of trajectories investigated in this study, the parameter  $s_0$  has a higher influence compared to the parameter  $a$ , whereas in [170] the total sensitivity index of the parameter  $a$  is greater than that of  $s_0$ . This minor difference might have arisen from the fact that in this study the sensitivity analysis was conducted on a much smaller number of trajectories compared to [170]. Additionally, in this study all of the investigated vehicles remain within a platoon for the whole period of observation, while the occurrence of lane-changes, which is quite common in the NGSIM-I80 dataset, could be the source of the difference observed.

Table 8. The comparison of the total sensitivity indices obtained in this study with the ones reported in [170].

IDM parameter	Trajectory 362	Trajectory 368	Trajectory 378	Trajectory 381	Trajectory 391	Results in [170]
$a$	9%	10%	5%	2%	2%	9%
$b$	1%	2%	1%	0%	1%	1%
$v_d$	0%	0%	0%	0%	0%	1%
$s_0$	10%	11%	5%	2%	6%	1%
$T$	95%	95%	99%	95%	97%	45%

### 3.3.5 Results

Prior to the application of the method to the comparison of the car-following models, PF is applied to a set of simulated data in order to demonstrate the potentials and shortcomings of PF in tracking model parameters.

The simulated data are obtained from the following scenario; a leader-follower pair was considered. The data, i.e. velocity and position time series, related to a specific vehicle from the NGSIM I-80 dataset, namely the vehicle with ID 368, were associated with the leading vehicle. The following vehicle was simulated using the IDM with parameters that changed at certain points in time. Particle filtering is then applied to the simulated dataset in order to generate dynamic estimates of the parameter  $T$ . The objective is to assess the extent to which the parameters and the times of change could be detected using PF. Figure 26 illustrates the data used.

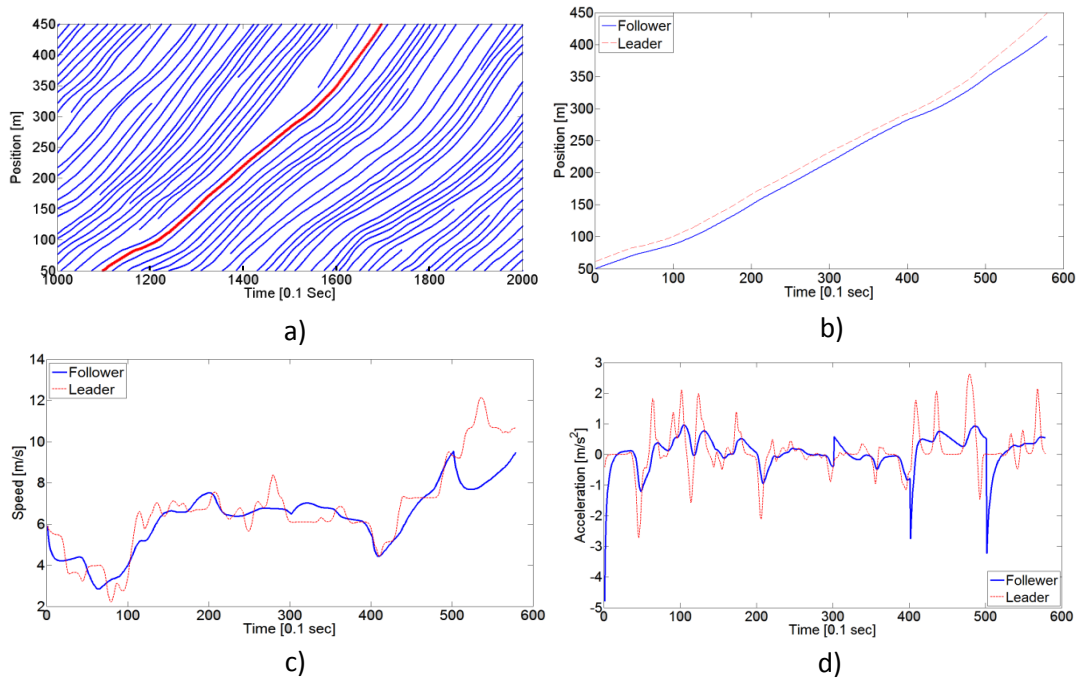


Figure 26. a) Trajectory of the lead vehicle selected from the NGSIM I-80 dataset, Lane 2 b,c,d) trajectories, velocities, and accelerations of the lead vehicle and the modelled follower in dashed red line and blue solid line respectively.

The parameter profiles used in the simulation are as follows. The values reported in [63] were used up to the time = 30 s , i.e.

$$a = 1.43 \frac{\text{m}}{\text{s}^2}, b = 0.78 \frac{\text{m}}{\text{s}^2}, v_d = 32.9 \frac{\text{m}}{\text{s}}, \delta = 4, s_0 = 2 \text{ m}, s_1 = 0 \text{ m}, \text{ and } T = 1.17 \text{ s}.$$

At  $t = 30$  s, the parameter  $a, b, v_d, T$  were changed to the following values,

$$a = 1 \frac{\text{m}}{\text{s}^2}, b = 1.5 \frac{\text{m}}{\text{s}^2}, v_d = 60 \frac{\text{m}}{\text{s}}, T = 0.5 \text{ s},$$

in order to include the case of having erroneous estimates of some of the model parameters while one of the parameters is being tracked. The value of the parameter,  $T$ , was changed again to  $T = 1$  s and  $T = 3$  s at times  $t = 40$  s and  $t = 50$  s, respectively.

The artificially generated dataset is then used to track the parameter  $T$  of IDM. While the value of the parameter  $T$  is being dynamically estimated, the rest of the model parameters are assumed to have fixed values similar to those used in the simulation, during the first time interval,  $t = 1 - 30$ s. Figure 27 shows the result of the application of the particle filtering to the simulated dataset.

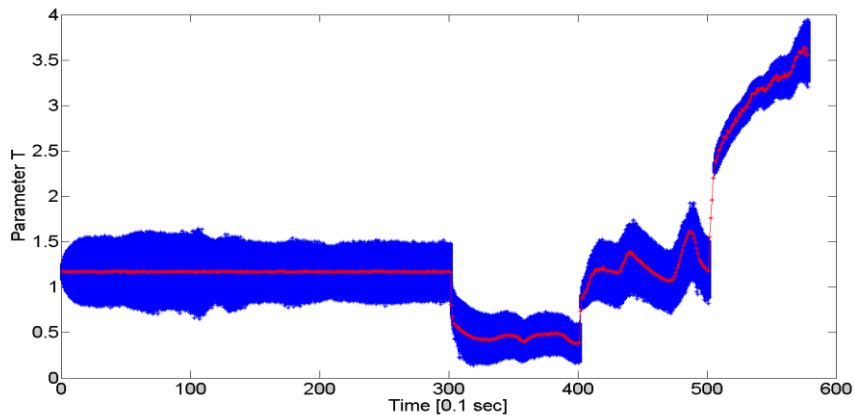


Figure 27. The result of the estimation of the parameter  $T$ . The blue shadow denotes the distribution of particles at each time instance while the red curve is the selected particle.

It can be seen that until  $t = 30$  s, the estimates of the parameter  $T$  (demonstrated by the red line) are almost error-free and stable. Within this interval,  $t = [1 \ 30]$  s, the estimates are very close to 1.17 which is, indeed, the value used in the generation of the simulated dataset. It is worth mentioning that within this interval, the correct values of the other model parameters were used in the estimation process. Therefore, it can be concluded that when:

a) the correct assumption is made about the underlying model in the estimation process (since the IDM was used in the generation of the dataset and in the estimation process) and,

b) one parameter is being tracked while the values of the other model parameters are correctly identified,

then PF can successfully detect and track the correct value of a parameter. Moreover, the PF has successfully identified the occurrence of changes in the value of the parameter  $T$  at the times  $t = 30$  s,  $t = 40$  s, and  $t = 50$  s. At these times, the value of the parameter  $T$  was changed to 0.5, 1, and 3 respectively in the simulation process. The PF has correctly identified these times and they are easily noticeable as “jumps” in the parameter estimates at  $t = 30$  s,  $t = 40$  s, and  $t = 50$  s (Figure 27).

However, after  $t = 30$  s, the estimates of the parameter  $T$ , unlike before, are unstable and fluctuate around a certain value. This is due to the fact that in the simulation stage after  $t = 30$  s some other model parameters, namely  $a$ ,  $b$ , and  $v_d$ , were also changed. Therefore, the fixed values of the parameters  $a$ ,  $b$ , and  $v_d$  that are used in the estimation are no longer correct. As a result, the effect of assigning incorrect values to these parameters in the estimation is compensated for by overestimations and underestimations of the parameter  $T$ . Nevertheless, interestingly the estimates still seem to fluctuate around the correct value of the parameter  $T$ .

Using the dynamic estimates of the parameter  $T$ , while keeping the rest of the model parameters constant and equal to their initial values throughout the simulation, leads to an almost perfect reproduction of the spacing ( $R^2 = 0.995$ ), velocity ( $R^2 = 0.993$ ) and acceleration ( $R^2 = 0.91$ ) in spite of the fact that the values of the parameters  $a$ ,  $b$ , and  $v_d$  do not match the actual ones after  $t = 30$ s. This is shown in Figure 28.

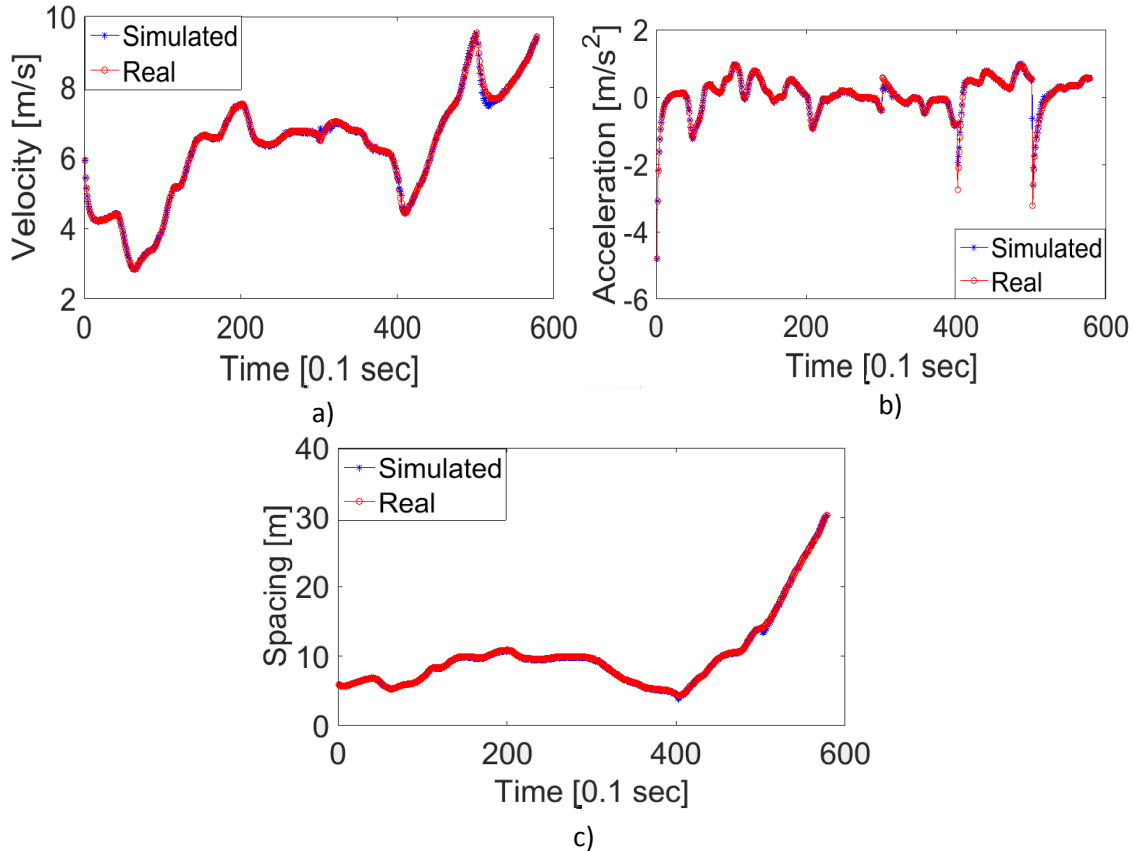


Figure 28. The comparison of the actual data with the simulated data when the dynamic estimates of the parameter  $T$ , given by particle filtering, is used.

It should be noted that in the investigated application of PF for parameter tracking, the IDM car-following model was used to generate the data related to the follower and the same car-following model was used in the parameter tracking process. In the application to real data, this is the equivalent of having a perfect knowledge of the model underlying the behaviour of drivers. Although this is obviously not the case, the findings of [169] suggest that the characteristics of the follower's behaviour can be recovered even when the model used to generate data and the model that is fit to the data are different.

So far, it was demonstrated that the PF can successfully identify changes in driving related attributes. This topic is investigated further in the appendix where after the application of PF and identification of the points where abrupt changes take place, i.e.

the “jump” points, a calibration is carried out in order to estimate the exact value of the parameter  $T$  within each interval between the jump points. It is shown that when this calibration is carried out, the actual value of the parameter  $T$  in different intervals can be almost exactly recovered. This method is then applied to real data in order to evaluate whether patterns of changes in driving attributes could be detected in different driving conditions.

In this section, however, a different application is considered. As mentioned before, the objective is to apply dynamic system identification in order to assess the goodness of a model. In this subsection, some of the model parameters were fixed and one of them was tracked. It was demonstrated that using erroneous estimates for the fixed model parameters after  $t = 30s$ , leads to fluctuations in the values of the tracked parameter. In a similar way, a model that does not sufficiently describe the underlying dynamics of driving behaviour is expected to cause intense fluctuations in the values of the tracked parameter. These fluctuations happen in order to compensate the shortcomings of a model. In this section, this effect is used in order to assess and compare different models. If the method is applied to two different models and one of the models produce much more unstable estimates, this could be an indicator of an inferior modelling goodness.

Here, PF is applied to the four car-following models that were described in subsection 3.3.1, The IDM, IDM-VDT, EIDM, and the GHR models. The inclusion of the two modifications of the IDM provide a good insight into the question of “how does each additional mechanism that is integrated within the IDM to produce the corresponding modified car-following model affect the accuracy of modelling?” The GHR model is included to provide variety in the mathematical structure of the subject car-following models, the model suggested by Ozaki [61] is used in this study. Subsequently, the analysis of the fluctuations and pattern of changes in the model parameters will provide insights into the fundamental differences of the four car-following models.

For the driving scenario certain trajectories from the real NGSIM I-80 dataset are used. In order to exclude lane-changing from the factors that influence the capability of a model to generate accurate acceleration behaviour, the trajectories of five vehicles are chosen that remain within a platoon for the whole period of observation, namely vehicles with IDs {362, 368, 378, 381, 391}.

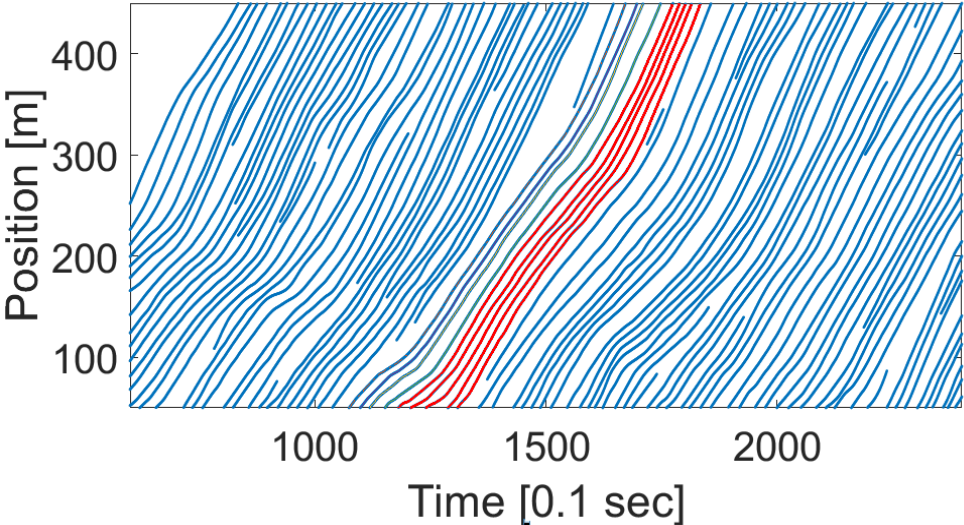


Figure 29. The trajectories of the five vehicles selected for comparison.

The parameter tracking method that was described earlier is then applied to each of the car-following models for a given trajectory. Figure 30 illustrates the simulated data using dynamic parameter estimates against the real ones for the IDM car-following model. The data depicted in this figure is also indicative of the traffic condition in which the platoon of vehicles is driving in. It can be seen that in spite of the short period of observation the data includes a variety of speeds and gaps.

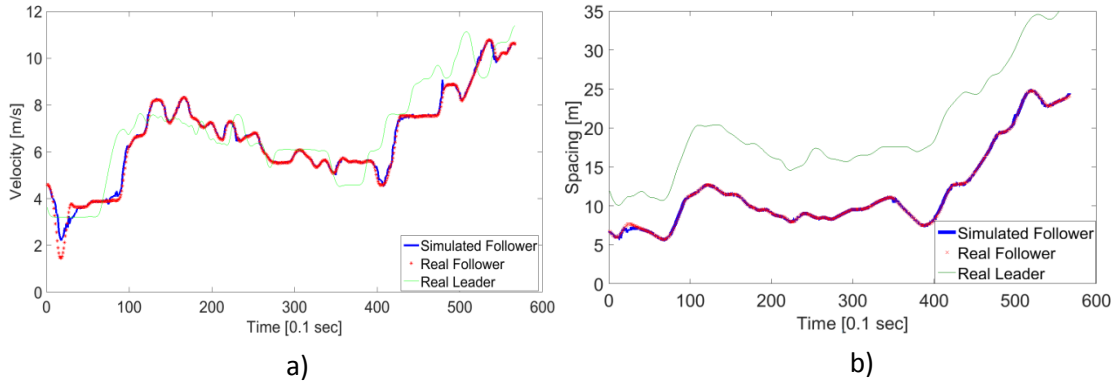


Figure 30. The comparison of real trajectories with the simulated ones for the vehicle ID 362 when the dynamic estimates of the parameter  $T$ , produced by PF, is used for the IDM car-following model.

Similar to the application of the method to the simulated data, an almost perfect match between the real data and the ones obtained using dynamic parameter estimates can be observed and this points to the accuracy of the estimation.

Figure 31 shows the dynamic estimates of the parameter  $T$  for the three IDM variants and the parameter  $c$  for the GHR model when the trajectory of the vehicle with ID 362 is used.

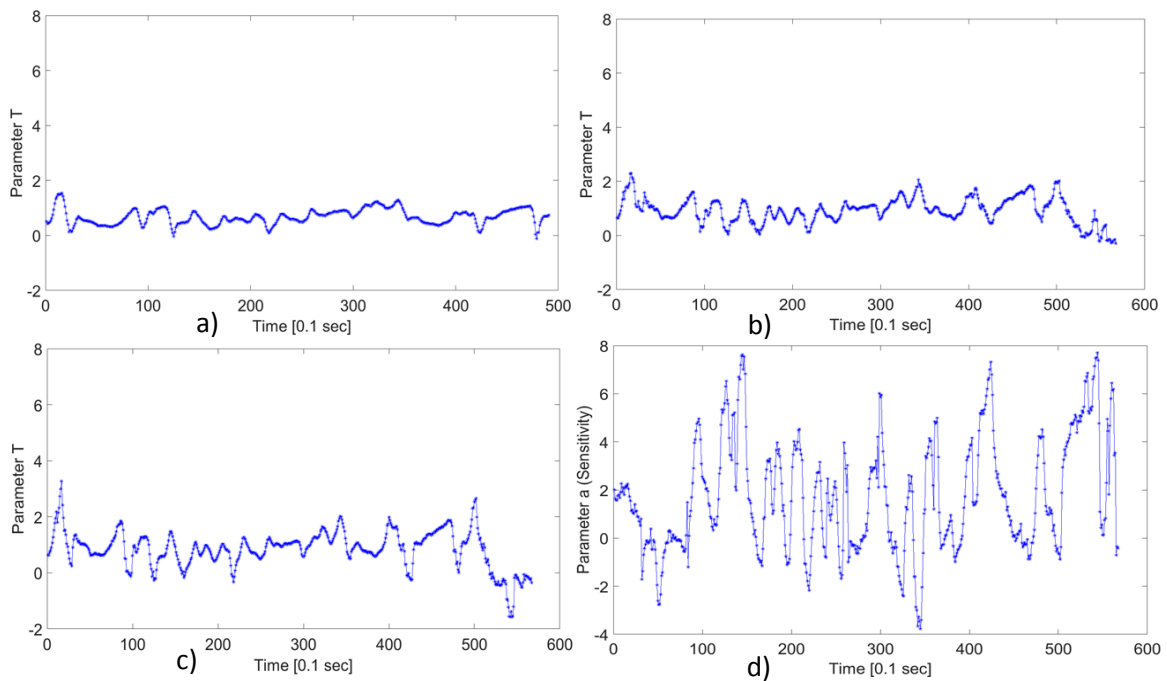


Figure 31. Dynamic parameter estimates for the for the vehicle ID 362 and the car-following models: a) IDM-VDT b) EIDM c) IDM d) GHR-Ozaki

According to the proposed criteria, the IDM-VDT outperforms the other models as only minor fluctuations around a nominal value can be seen in the dynamic estimates of the parameter  $T$  for this model compared to the other car-following models.

In the dynamic estimates for the IDM and EIDM car-following models, changes in the average value of  $T$  can also be observed. This observation is confirmed by the application of the method to the trajectories of some of the other vehicles in the same platoon and applying a moving average filter to highlight the trend.

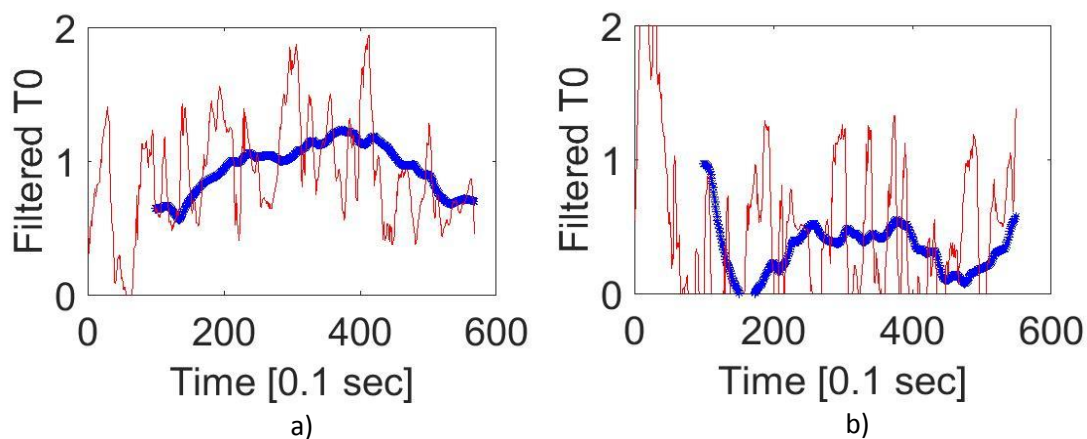


Figure 32. The application of a simple moving average filter, with the averaging time widow of **10 s**, to the dynamic estimates of the parameter  $T$  for the IDM and a) vehicle with ID 368 b) vehicle with ID 378.

Although the same increase is not observed in all other investigated trajectories, it can be seen in a significant number of them. The rise and drop in the average value of the estimates seem to be highly correlated with the changes of speed and/or spacing. This could, therefore, point to a deficiency in the car-following models in accounting for a behavioural aspect of driving.

In order to investigate this further, the same method was applied to a longer time series; that is the NGSIM Naples dataset 25B which provides data on the spacing and velocities of a number of follower-leader pairs for about five minutes. The results are demonstrated in Figure 33.

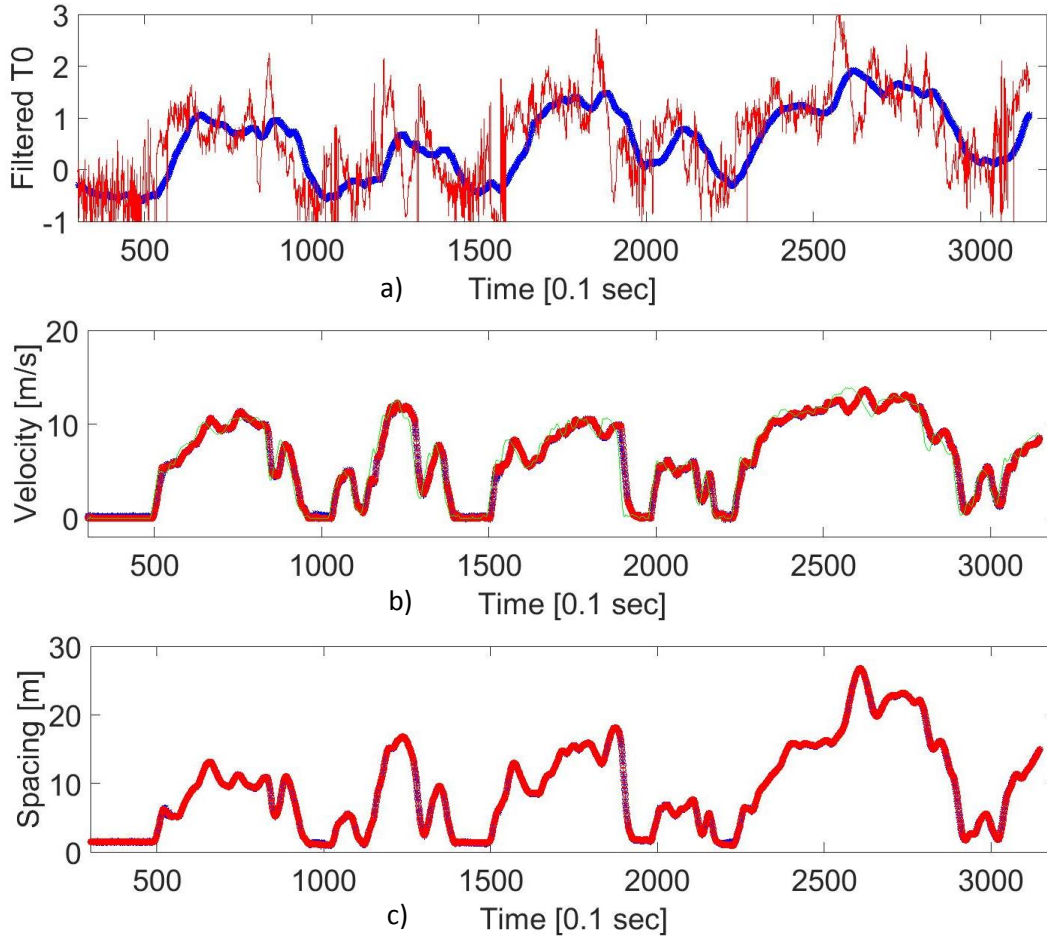


Figure 33. The comparison of the trends of the parameter  $T$  with the velocities and spacing for the IDM car-following model and NGSIM Naples dataset 25B.

The existence of a correlation between the three time series can be clearly observed in Figure 33. This points to a shortcoming in the IDM as its mathematical structure does not incorporate an observed driving behaviour, therefore this deficiency is compensated by the rises and drops in the dynamic estimates of the parameter  $T$ . The key advantage of the proposed method for the comparison of car-following models is that it captures such aspects of modelling.

The changes in the sensitivity parameter of the GHR model that occur with high magnitudes and a high frequency are an indicator of its poor performance compared to the other investigated car-following models. Since the GHR's mathematical structure is incapable of reproducing detailed driving behaviour as observed in real

trajectories, frequent jumps, with high magnitudes, in the dynamic parameter estimates take place in order to provide a good fit to the real trajectories.

In order to better visualise the differences of the four investigated car-following models, the histograms of their corresponding parameter estimates are demonstrated in Figure 34.

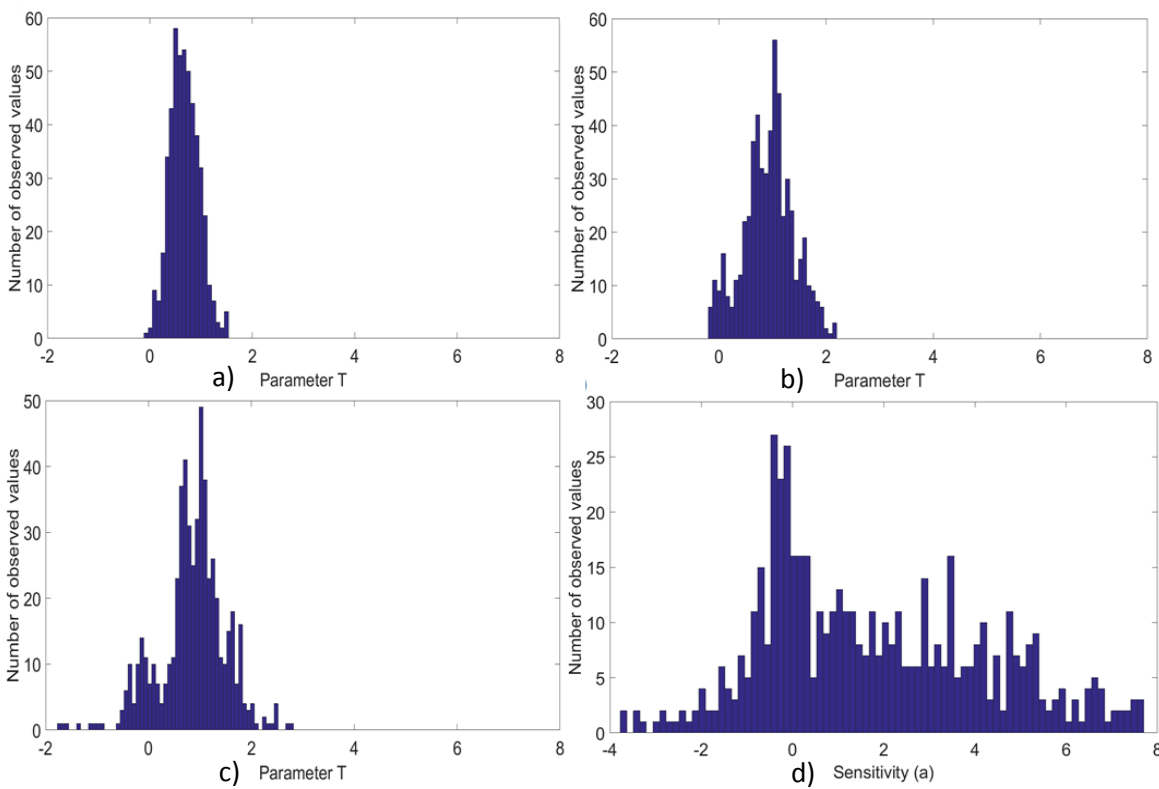


Figure 34. Histograms of the values of the tracked parameter for the vehicle ID 362 and car-following models a)IDM-VDT b)EIDM c)IDM d)GHR.

In these histograms a sharp normal distribution is advantageous over a broad and skewed distribution with multiple peaks.

Table 9 summarises the results of the application of the proposed method to the investigated trajectories and models.

Table 9. The means and standard deviations of the dynamic parameter estimates

Car-following model	Vehicle ID	Mean	Standard deviation	SSR
IDM-VDT	362	0.68	0.28	2.79
	368	0.81	0.31	3.63
	378	0.24	0.46	3.43
	381	0.45	0.44	2.51
	391	0.72	0.39	4.05
EIDM	362	0.92	0.47	3.13
	368	0.95	0.39	2.68
	378	0.43	0.48	3.17
	381	0.76	0.53	2.06
	391	1.11	0.50	5.96
IDM	362	0.85	0.66	3.13
	368	0.89	0.45	2.76
	378	0.41	0.59	2.75
	381	0.75	0.77	2.07
	391	1.06	0.54	5.92
GHR	362	1.69	1.46	3.87
	368	0.21	0.96	2.37
	378	0.78	1.28	1.96
	381	0.37	0.90	1.74
	391	0.59	1.24	4.63

	Best
	Worst

It can be seen that while the traditional Sum of Squared Residuals (SSR), as the criterion of comparison, is completely inconclusive as to which car-following model performs better, the proposed method consistently points to the dominance of the IDM-VDT. This is due to the fact that while in some cases the least SSR is achieved by the GHR car-following model, the magnitudes of changes in the dynamic parameter estimates of this model still remain higher than rest of the models.

### 3.3.6 Conclusion and future work

Numerous studies that conduct a comparison of car-following models overlook the provision of a systematic way to pinpoint the shortcomings and fundamental differences of different models in terms of the accuracy of the behaviour reproduced. This may be due to the reduction of the criteria of comparison to the single measure of the cumulative error, which, while being very informative itself, results in important

behavioural differences among different car-following models being omitted.

As a contribution of this research, the use of a new method for the comparison of car-following models based on parameter tracking has been proposed. The use of the proposed method enables a more comprehensive analysis of the fundamental deficiencies of car-following models in reproducing real driving behaviour.

In order to demonstrate the application of the method, a comparison of four car-following models was carried out, namely the IDM, the EIDM, the IDM-VDT and the GHR models. The results show that the IDM-VDT outperformed the other models with a narrow, normal-shaped distribution of parameter values. This means that the introduction of a parameter in this model that considers the local variations of speeds in the neighbouring traffic, indeed contributes to the a more accurate modelling of car-following behaviour. The EIDM comes second after the IDM-VDT. Although the EIDM has a much more complex model structure compared to the IDM, its performance is only marginally better than the IDM. The author's initial investigations confirm that the EIDM copes much better with lane-changes; which is indeed one of the stated purposes behind this modification of the IDM. Finally, the GHR model was shown to be significantly inferior in performance despite its structural complexity that arises from explicitly including a time delay in the model as well as its dual regime, and despite the fact that for certain trajectories it produces the least SSR among the four investigated car-following models.

Such a conclusive comparison of the car-following models, to the best of the authors' knowledge, was never carried out before since most of the comparison studies are based on cumulative errors, which as shown in this study and other studies cited in this work, fail to provide definitive results.

The main contribution of section 3.3 is proposing a method that overcomes the shortcomings of the traditional cumulative error for the analysis of driving behaviour and car-following models. The merits of the proposed method were illustrated using a

set of five different trajectories and it was shown that where the traditional comparison criterion, the Sum of Squared Residuals (SSR), falls short on providing any conclusive evidence for the comparison of car-following models, the proposed method provides a consistent measure of performance.

More interesting applications are envisaged for this method, as it may also be used as a valuable tool for the investigation of the behavioural aspects of driving that a car-following model fails to capture. For instance, a car-following model may lack the mathematical structure to cope with the changes observed in driving behaviour as a result of encountering different traffic conditions. This could be identifiable using the proposed method by looking for systematic changes and common patterns in the parameter estimates during particular driving conditions. The application of the method to a five-minute long dataset clearly demonstrated its potentials for this purpose. The application of this method to large datasets where a variety of driving conditions are explored could be an interesting direction of research.

An important question to be addressed in this context is finding a way to deal with the fact that car-following behaviour may be seen as random realisations of a stochastic process. This gives rise to inherent difficulties in modelling a stochastic process through a deterministic model. Distinguishing between the effect of this randomness on the dynamic parameter values and the fundamental deficiencies of a car-following model to produce realistic behaviour is another subject that could be explored further.

The method that was presented relies on tracking a single model parameter. The comparison made between the three modifications of the IDM is particularly meaningful as 1) the parameter  $T$  was identified as the most influential parameter and 2) this parameter corresponds to the same physical attribute in the three IDM-based models. Even though the intense variations in the value of the parameter  $c$  are an indicator of the GHR's structural shortcomings, the two aforementioned conditions do not hold in the comparison between the parameter  $T$  from the IDM and  $\alpha$  from the GHR. The generalisation of the method in order to simultaneously track a number of

parameters and the normalisation of the variances of the parameters, perhaps with respect to their physical interpretation, sensitivity, or simply the number of parameters, could be an interesting subject for further investigation.

#### **4. Energy Efficient Driving**

Fully automated vehicles are expected to have a significant share of the road network traffic in the near future [179]. Several commercial vehicles with full range adaptive cruise control systems or semi-autonomous functionalities are already available in the market. The potential of these systems to address the challenges of the ground motorised transport network was highlighted in chapter 1.

In chapter 2, some of the methodologies related to the automation of driving and ensuring energy efficiency were explored, their advantages and disadvantages were discussed, and it was seen that the extensive computational requirements of a system-optimal driving strategy often leads to the formulation of fuel efficiency as a user-optimal problem by researchers. In the system-optimal approach the fuel efficiency of the network is considered whereas in the user-optimal approach individual vehicles seek to minimise their fuel consumption without necessarily prioritising network-wide reductions in fuel consumption. Numerous studies in this area either target driving conditions where there are no additional complexities caused by the interactions between vehicles, or

make simplistic assumptions about the dynamics of driving behaviour and its relationship with fuel consumption in order to formulate a feasibly solvable optimisation problem. These systems consequently adopt highly conservative driving strategies. The collective impacts of such strategies can lead to the deterioration of traffic flow and increased energy consumption in the network.

In chapter 2, it was argued that the use of car-following models as the basis of control could resolve some of the issues related to computational cost. Moreover, the availability of an extensive body of research on the properties of car-following models facilitates the analysis of their collective impacts and stability features. In chapters 2 and 3 the IDM car-following model was presented as a suitable candidate for the present study and using a sensitivity analysis the most influential parameters of this model on fuel consumption were determined.

In this study, the objective is to limit the search space for optimal strategies to the parameter space of the IDM. This framework enables performing much more comprehensive optimisations and conducting more extensive tests on the collective impacts of fuel-economy driving strategies. The results demonstrated in this chapter show that the formulation of the optimisation in a short-sighted way, where merely individual vehicles are considered and no attention is paid to the collective impacts of a “fuel-economy” driving strategy, can lead to a significant increase in the fuel consumption of the whole network while delivering marginal benefits for the individual vehicles that adopt such driving styles. By doing so, this study establishes an important relationship between traffic flow and fuel consumption on the network level. It is, therefore, concluded that a network-wide reduction of fuel consumption cannot be achieved without correctly addressing the implications of fuel-efficient driving strategies on the flow of traffic in the network. The proposed method is presented in the next section.

## **4.1 Methodology**

### **4.1.1 Optimisation framework**

Given a sufficient number of model parameters in a car-following model, a variety of driving strategies could be modelled by adjusting the values of parameters. One set of model parameters can produce a sporty driving style with intense accelerations and braking while another set of model parameters can produce a conservative driving style that is less sensitive to the lead vehicle's braking by maintaining sufficiently large gaps. In other words, a car-following model with  $\mathbb{N}$  model parameters provides a  $\mathcal{R}^{\mathbb{N}}$  space where each point in the space may be regarded as a distinctive driving strategy. Therefore, one could search the space of model parameters for a set that minimises an objective function of interest. In this light, the calibration studies could be seen as an attempt to find the driving strategy in the space of model parameters of a given car-following model that best describe a particular trajectory or speed profile. This is done by the minimisation of the Euclidean distance between the modelled driving behaviour and the real one.

It is important to bear in mind that the space of strategies that is represented by the space of model parameters for a given car-following model is only a subspace of all the possible driving strategies. Constraining the search space to the one provided by a car-following model has advantages and disadvantages. On the one hand, this approach has the advantage of limiting the search space to one that could satisfy important criteria such as safety and stability while producing acceptable driving behaviour. Moreover, while in DP based algorithms the choice of actions requires evaluating the sequence of actions/states in future time steps which grow exponentially as the length of the time horizon increases, in car-following models, actions (acceleration decisions) are only dependant on the present value of the explanatory variables such as spacing, velocity, and relative velocity to the leader; therefore leading to a significant reduction in computational effort. On the other hand, the car-following models have shortcomings, for instance, a single set of model parameters cannot always produce realistic driving behaviour. Similarly, one cannot expect a single set of model parameters to provide a fuel-efficient driving strategy in all driving condition. Nevertheless, similar to calibration studies, one can obtain model parameters that can deliver fuel efficiency in particular driving conditions.

In this chapter two new and distinctive approaches in achieving fuel efficiency are investigated:

1. The optimisation of the fuel consumption of a platoon of vehicles by imposing microscopic constraints on headways in order to ensure an efficient traffic flow.
2. The optimisation of the average fuel consumption in a roadway by imposing a macroscopic constraint on the traffic throughput.

Due to the highly nonlinear formulation of the problem, simulation based optimisation is carried out to investigate the two approaches.

#### 4.1.2 Microscopically formulated optimisation

Firstly, the problem of a single pair of vehicles in the car-following regime is considered. The objective is to find the optimal parameters for which fuel efficiency is achieved. For this purpose, the problem is formulated as follows. Given a particular trajectory,  $T_l$ , the objective is to find the set of model parameters,  $\theta$ , for the IDM car-following model that result in the minimum fuel consumption for the following vehicle.

$$J^*(T_l) = \min_{\arg \theta \in \Theta} F(\theta|T_l), \quad (4.1)$$

where,  $F$  is the fuel consumption of the following vehicle calculated by the VT-micro model [119] and  $J^*$  represents the minimum possible value of fuel consumption for the subject vehicle to follow the trajectory of the leader,  $T_l$ . This value could be close to zero if the subject vehicle simply comes to a standstill therefore it is important to incorporate the requirements of traffic flow into the optimisation. In order to obtain efficiency in traffic flow, a wide range of constraints were considered based on different criteria suggested in the literature [180, 181, 115]. The following constraints produced good results and are used in this study.

$$\max\{\overline{T_h}\} < \delta_1, \quad std(T_h) < \delta_2, \quad (4.2)$$

where  $T_h$  is the time series of headways for the following vehicle,  $\overline{T_h}$  is the mean value of this time series,  $\delta_1$  and  $\delta_2$  are constants.

This type of problem formulation is similar to the works related to the car-following regime of driving that were addressed in the literature review section. In this approach, the objective is to minimise fuel consumption for the following vehicle while considering the requirements of an adequate tracking capability or traffic flow in order to ensure that a sluggish driving style is not produced.

The results obtained using this approach were observed to be highly sensitive to the initial conditions and the trajectory of the lead vehicle. Therefore, the optimisation framework was modified to include a platoon of vehicles that follow the trajectory of the lead vehicle.

$$J^*(T_l) = \min_{\arg \theta \in \Theta} \sum_{i=1}^n F_i(\theta | T_l), \quad (4.3)$$

subject to

$$\overline{T_h^1}, \overline{T_h^2}, \dots, \overline{T_h^n} < \delta_1,$$

$$std(T_h^1), std(T_h^2), \dots, std(T_h^n) < \delta_2,$$

where  $n$  is the number of vehicles in the platoon. Additionally, since the trajectory data used in this study have short time intervals, a number of trajectories from the same dataset and a similar driving condition were combined so the optimal set of parameters found is more robust to variations in the lead vehicle's driving style.

$$J^*(T_{l_{1,2,\dots,n}}) = \min_{\arg \theta \in \Theta} \sum_{i=1}^n F_i(\theta | T_{l_1}, T_{l_2}, \dots, T_{l_m}) \quad (4.4)$$

This optimisation formulation is depicted in Figure 35.

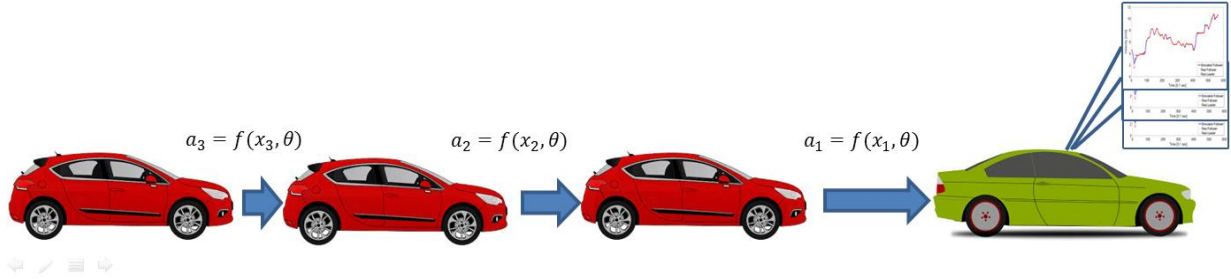


Figure 35. Schematic representation of the microscopic optimisation scenario.

### 4.1.3 Macroscopically formulated optimisation

The microscopically formulated optimisation problem that was presented in subsection 4.1.2, depicts the type of user-optimal driving solutions that were discussed in chapter 2. In chapter 2 it was mentioned that this approach could result in conservative driving styles, and therefore, the deterioration of traffic flow and increased fuel consumption for the network. Therefore, a second optimisation problem was formulated in order to broaden the horizon of the microscopic optimisation problem, to include the impacts of interactions between vehicles in a broader sense, and to produce a system-optimal solution. In this approach, the flow-related constraint could be simply reduced to a loose constraint on the traffic throughput, as opposed to the headway-based constraints that were previously used.

The optimisation problem is modified in the following way. Given a particular trajectory,  $T_l$ , for a stretch of a roadway of particular length,  $L$ , for the simulation time  $t$  seconds, and given the inflow rate at the beginning of the roadway,  $\lambda$ , the objective is to find the model parameters,  $\theta$ , for the IDM car-following model that result in the minimisation of the average fuel consumption for all of the vehicles that travel through the roadway.

$$J^*(T_l, \lambda) = \min_{\arg \theta \in \Theta} E[F(\theta|L, T_l, \lambda, t)], \quad (4.5)$$

subject to,

$$Throughput > \alpha \cdot \lambda \cdot t,$$

where the operator  $E[.]$  denotes the expected value,  $F(.)$  is the fuel consumption of a vehicle that enters the scenario and is calculated by the VT-micro model, and  $\alpha$  is a coefficient that sets a minimum threshold for the acceptable throughput as a percentage of the expected number of vehicles that enter the scenario,  $\lambda.t$ . The intervals at which vehicles enter the simulation scenario is modelled with the exponential distribution function with the average of  $\mu = 1/\lambda$ . Finally,  $J^*$  is the minimum expected fuel consumption for vehicles that drive through the simulated roadway and is dependent on the trajectory of the first vehicle that enters the scenario,  $T_l$ , and the average inflow of vehicles.

This is a stochastic optimisation problem which is quite difficult to solve, however using simulation-based optimisation an upper bound can be obtained for the optimal value.

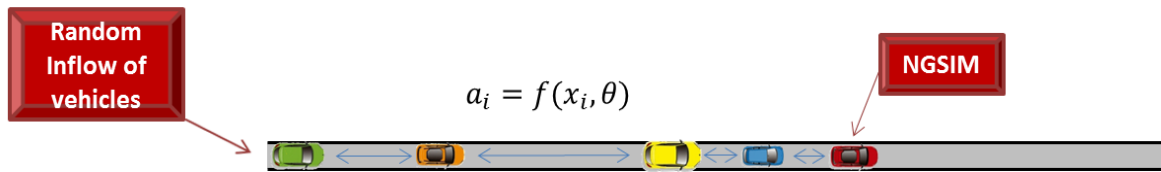


Figure 36. Schematic representation of the macroscopic optimisation scenario.

The simulations are developed in MatLab and in the following way:

1. The first vehicle that enters the roadway drives according to a real trajectory. This trajectory is obtained from one of the datasets used in this study.
2. At every time step firstly it is evaluated if there is a new arrival at the upstream end of the roadway. The arrivals are modelled using an exponential function with the average of  $\mu$ .
3. In the case of a new arrival, the vehicle will be assigned a random velocity obtained from a truncated normal distribution. The distribution has the mean of  $v_{n-1}$ , which is the velocity of its preceding vehicle, and the standard deviation of  $1 \frac{m}{s}$ . The tails of the distribution are truncated at  $v_{n-1} - 3 \frac{m}{s}$  and  $v_{n-1} + 3 \frac{m}{s}$ . If the vehicle will not produce a deceleration greater than  $-1 \frac{m}{s}$  according to IDM, it

will enter the road section, otherwise it will wait in queue until this condition is satisfied.

4. The accelerations of all vehicles in the road are calculated based on IDM with the candidate set of model parameters  $\theta$ .
5. The velocities and positions of the vehicles are updated based on the one-dimensional equations of motion and the calculated accelerations. These velocities and positions will be used in the next time step to calculate the new accelerations.
6. It is checked if any of the vehicles have reached the end of the roadway section.
7. This process is repeated every 0.1 seconds until the simulation end time is reached.

#### **4.1.4 Sensitivity Analysis**

In order to further reduce the complexity of the optimisation, the global sensitivity analysis that was described in section 3.3 is applied to identify the parameters that have the highest impact on fuel consumption. In this analysis, the microscopically formulated simulation scenario is considered where the trajectories of the vehicles with IDs 362 , 368 , 378, and 381 from the NGSIM-I80 dataset are used as the trajectories of the lead vehicle and the number of following vehicles in the platoon is assumed to be  $n = 4$ . The total sensitivity indices are demonstrated in Table 10. The lower and upper bound values in this table are also used for the selected parameters in the optimisation process, namely,  $T$ ,  $a$  and  $b$ .

Table 10. Total sensitivity indices for the effects of the IDM model parameters on fuel consumption in the microscopically formulated simulation scenario.

Parameters	LB	UB	$S_T$
$a$	0.5	5	13%
$b$	0.5	5	2%
$V_d$	20	33	0%
$s_0$	0.5	5	6%
$T$	0.5	2	78%

It can be seen that the parameter  $T$  has the highest impact on fuel consumption followed by parameters  $a$ ,  $s_0$ , and  $b$ . The parameter  $v_d$  has a negligible impact on fuel consumption and is, therefore, set to its default value of  $33.3\text{ m/s}$  throughout this study. The parameter  $s_0$  has a higher impact on fuel consumption compared to the parameter  $b$ . This parameter,  $s_0$ , along with the parameter  $T$ , define the spacing preferences between the vehicles in the car-following regime and the two parameters are correlated [177]. Since the parameter  $T$  is included in the optimisation process, the parameter  $s_0$  is set to its default value of 2 meters.

#### 4.1.5 Fuel consumption

In the present study, a fuel consumption model has been developed based on the VT-micro fuel consumption model. The VT-micro was specifically developed for the investigation of fuel consumption at the operational level of driving. However, its exponential structure and the inclusion of 32 terms added a high computation overhead to the optimisation. The new model is a simplified form of VT-micro. Various polynomial model structures were examined with the objective of reducing the computation time without compromising the accuracy. A suitable model structure was identified that produced a good fit over the whole envelope of accelerations and velocities. The new model delivers accurate predictions of fuel consumption for the tested drive cycle,

namely the US Motor Vehicle Emissions Federal Test Procedure (FTP) [182], as well as the whole envelope of accelerations and velocities compared to the VT-micro predicted values ( $R^2 = 0.94$  and  $R^2 = 0.9988$  respectively). This is illustrated in Figure 37.

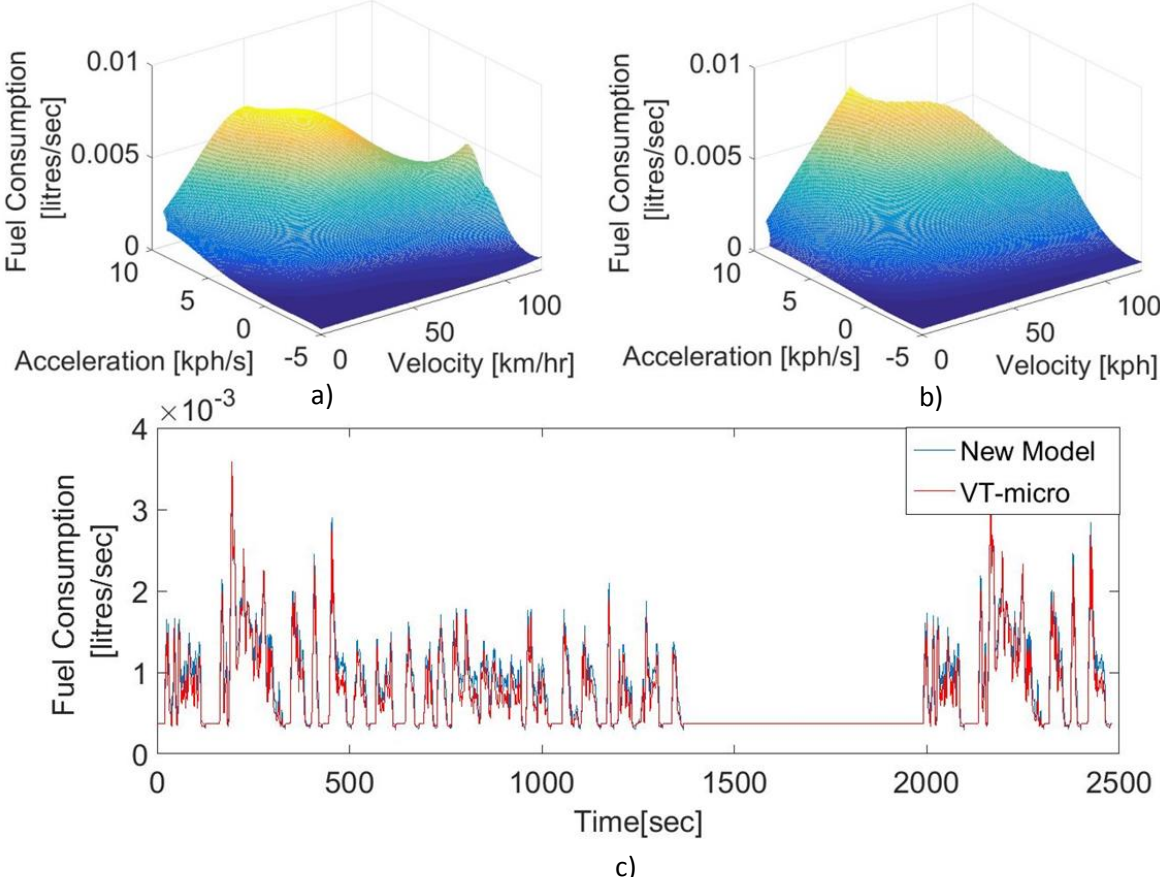


Figure 37. The comparison of fuel consumption prediction between VT-micro and the new model. a, b) Fuel consumption for the whole envelope of velocities and accelerations using VT-micro and the new model respectively. c) Instantaneous fuel consumptions for the FTP drive cycle.

The new model significantly reduces the computation overhead required for the estimation of fuel consumption. It reduces the dual-regime structure of the original VT-micro model, for positive and negative accelerations, to one. Moreover, in the new model the VT-micro's exponential function is accurately estimated with a simple polynomial. Finally, the 32 terms in the original model are reduced to only seven terms in the new model.

## 4.2 Dataset

Two datasets are used in this study. The NGSIM-I80 [136] dataset provides trajectory data from a 500-meter long stretch of a six-lane motorway. Figure 38, demonstrates the spatio-temporal velocity of the traffic.

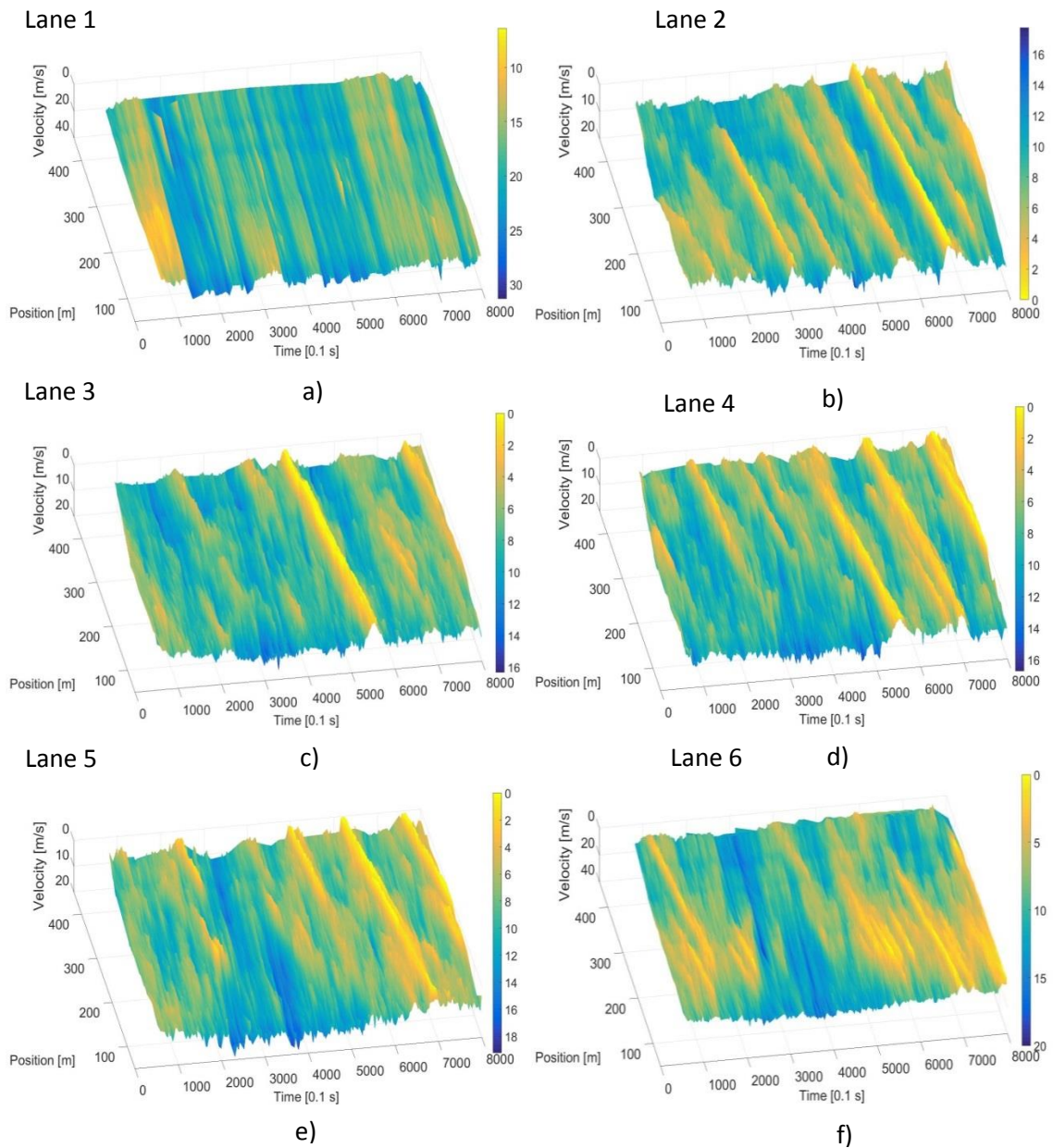


Figure 38. The spatio-temporal velocity of the traffic in lanes 1-6 in the NGSIM-I80 dataset.

It can be seen that while lane two remains quite congested and numerous stop waves can be identified that travel in the downstream direction at the well-known speed of  $-14 \frac{km}{h}$ , the traffic flow in lane one is almost free of shockwaves. Therefore, the focus is placed on two sets of trajectories in different lanes. The first set is drawn from lane one and pertains to a platoon of four vehicles, namely vehicles with IDs 441, 452, 453, and 467, that drive with high speeds, i.e. about  $90 \frac{km}{h}$ , and are not interrupted with any shockwaves. Set two on the other hand is extracted from lane 2 and represents a congested motorway section. This set of trajectories is obtained from vehicles with IDs 362, 368, 378, 381. Herein, the first set of vehicles is referred to as trajectories 441-467 and the second set of vehicles is referred to as 362-381.

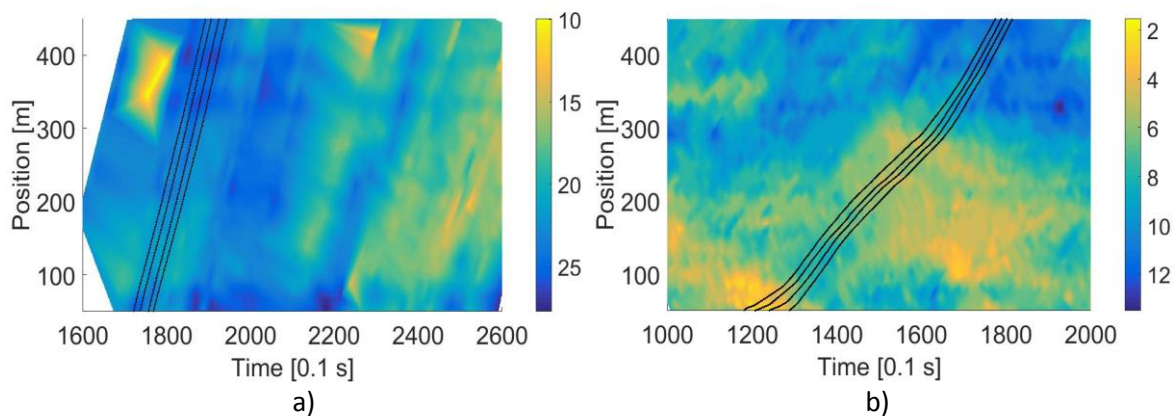


Figure 39. Trajectories of a) the platoon of vehicles with IDs 441, 452, 453, and 467 and b) the platoon of vehicles with IDs 362 , 368 , 378, 381.

The use of this dataset provides the opportunity to examine the impact of diverse driving conditions on the optimisation process. Moreover, once the optimal parameters are obtained it is possible to compare the results with the real scenario in terms of the collective impacts on fuel consumption and traffic flow. In order to exclude the influence of lane-changes and traffic conditions in the neighbouring lanes from the calculation of fuel consumption, only vehicles that remain within the same lane for the whole period of observation are considered; this is demonstrated in Figure 40. In this figure, the vehicles that follow the trajectory of the vehicle with ID 391 and remain within the same lane for

the whole period of observation are identified; consequently, the average fuel consumption for these vehicles could be calculated.

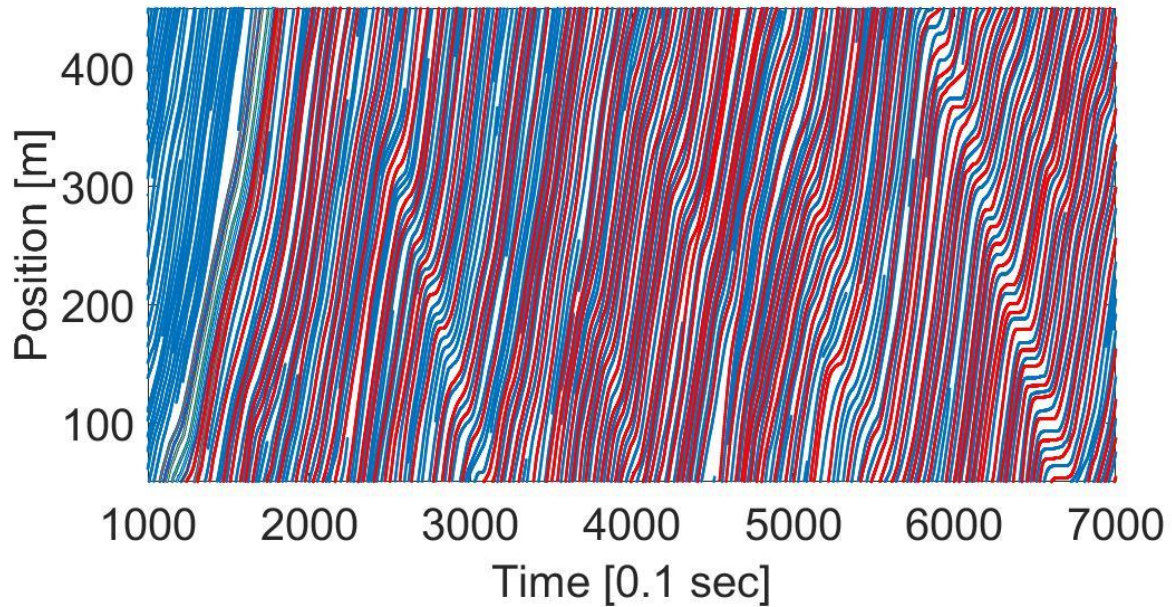
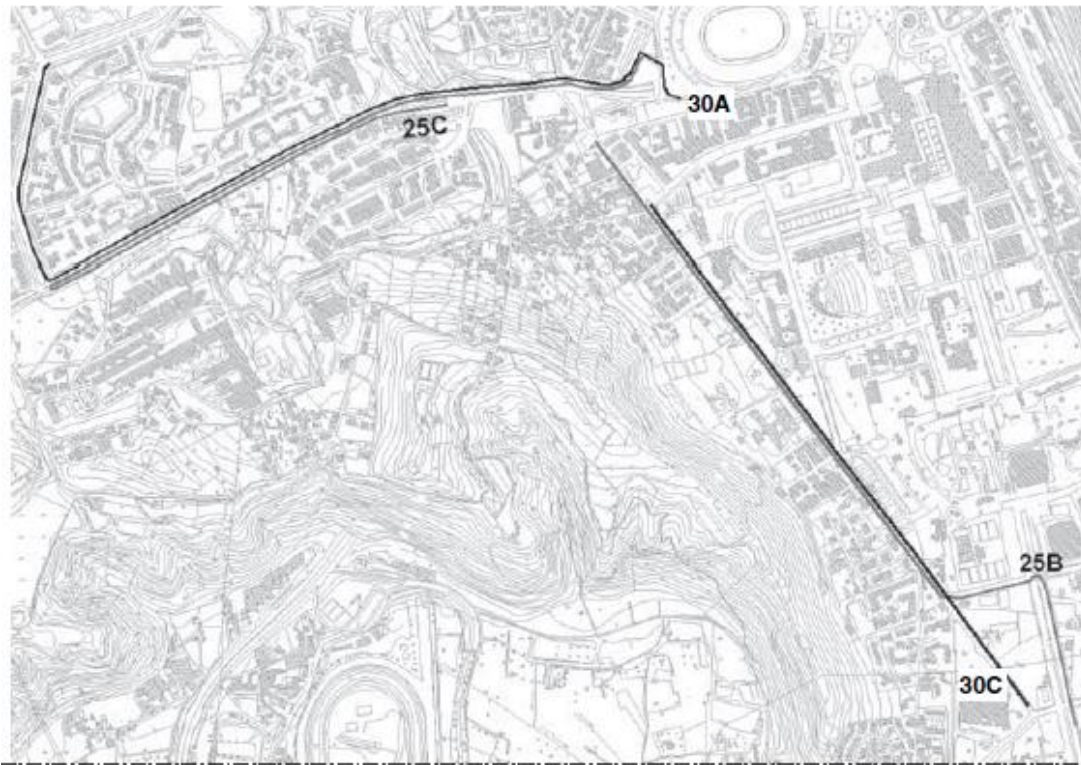
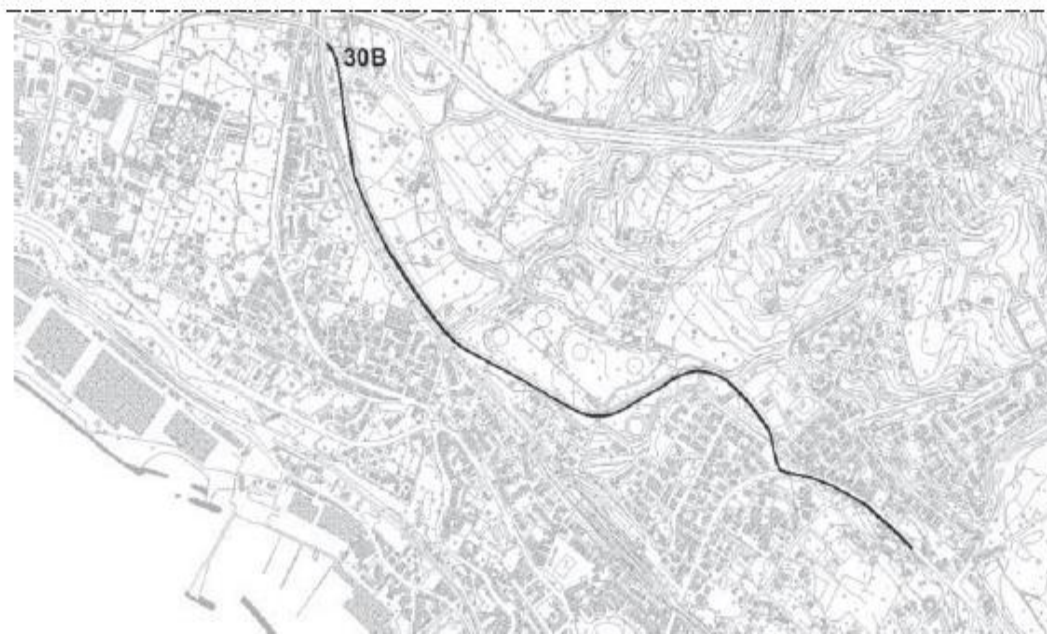


Figure 40. Vehicles that remain within the lane for the whole period of observation are denoted with red.

Another dataset that is used in the present study is the NGSIM Naples dataset. This dataset is obtained by instrumenting four vehicles and measuring their velocities and gaps while they drive through three different routes. It consists of five different sets of data. Three of the five sets, report spacing and velocity values for the platoon of vehicles while driving in three different roadways. The remaining two sets of data report measurements obtained from two previously examined routes on different dates. While this dataset does not provide any information about the surrounding traffic conditions for the subject platoon, it provides sufficient diversity in the driving conditions. Moreover, the dataset provides a better insight into the car-following behaviour compared to the NGSIM-I80 dataset due to its longer period and the absence of lane changes. Each set of data is about five minutes long. Figure 41, demonstrates the routes where the sets of data are obtained for the Naples dataset. More information on this can be found in [158].



(a)



(b)

Figure 41. Data collection sites for the Naples dataset (figure from [158]).

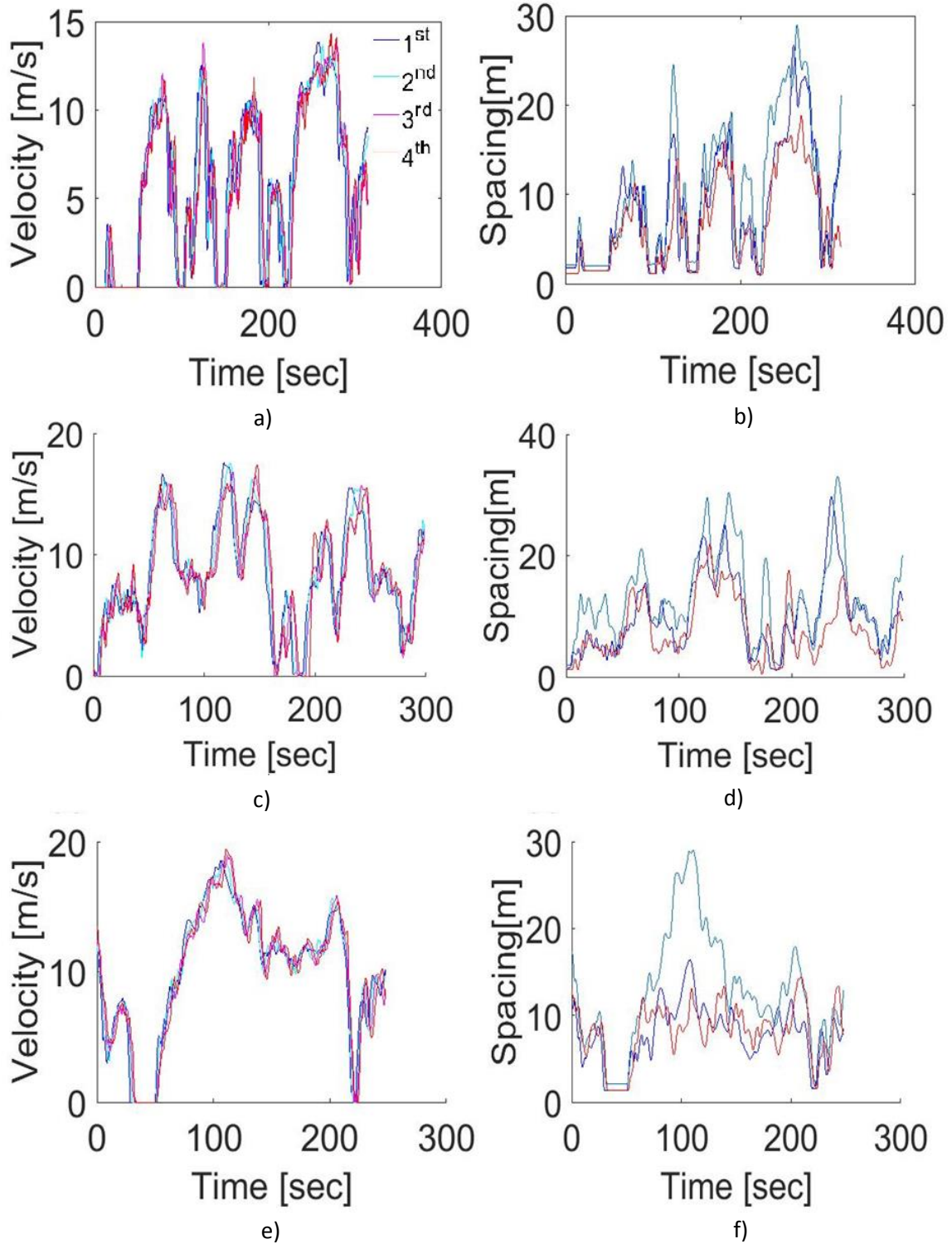


Figure 42. Velocity and spacing measures of the first to fourth vehicles in the platoon in three Naples dataset, a,b) 25B, c,d)25C, and e,f) 30B.

## 4.3 Results

### 4.3.1 Microscopically formulated optimisation

In this section the results relating to the microscopically formulated optimisation problem denoted by Equation (4.4) are reported. In order to ensure that the results are as robust as possible and deliver fuel efficiency in a wide range of driving conditions, all the trajectories available within the five Naples datasets are used as the trajectory of the lead vehicle in the optimisation. Also, the number of vehicles in the platoon is set to 4, and parameters  $\delta_1$  and  $\delta_2$  are set to 3 and 0.5 seconds respectively.

The setting of the values of  $\delta_1$  and  $\delta_2$  is a result of a thorough investigation conducted in order to examine the mean and standard deviation of the headways in different driving conditions and for different drivers within the Naples dataset. The mean and standard deviation of headways averaged over the five Naples datasets and all drivers are 1.1 s and 0.4 s respectively. These values are highest for the third driver in all five datasets and reach the values of 1.7 s and 0.5 s respectively in dataset 25B. Additionally, numerous combinations of  $\delta_1$  and  $\delta_2$  have been tested and it has been confirmed that  $\delta_1 = 3$  s and  $\delta_2 = 0.5$  s produce a conservative, yet acceptable driving behaviour.

Due to the highly nonlinear nature of the problem, the optimisation is carried out using a genetic algorithm [183]. The applications of this method to solving highly nonlinear optimisation problems related to the calibration of car-following models and finding optimal driving strategies was discussed in chapter 2. Two conditions were used as the stop criteria 1) reaching the maximum number of generations of 150, and 2) insignificant changes in the optimal value found in 50 successive generations. The optimal parameters obtained for trajectories 441-467,  $T_l = 441, 452, 453, 467$ , and a platoon of three vehicles,  $n = 3$ , following the lead trajectory is given in Table 11.

The results for trajectories 362-381 are similar to those for trajectories 441-476 and are summarised in Table 14 at the end of this section.

Table 11. The optimal parameters obtained for a platoon of three vehicles when the trajectory set 441-467 is used for the lead vehicle.

$a[m/s^2]$	0.5
$b[m/s^2]$	5
$T[s]$	2

The optimal set of model parameters results in a significant 48% improvement in the fuel consumption of the three following vehicles compared to the real trajectory, 0.0412 litres in the simulated scenario and 0.0788 litres in the real case. Moreover, a 23.7% reduction in fuel consumption is achieved with the optimal parameters compared to the case where the IDM's default set of model parameters are used, fuel consumptions of 0.0412 litres and 0.0540 litres respectively.

It is worth mentioning that due to the high level of sensitivity of fuel consumption to the parameter  $T$ , that represents the desired headway, a significant proportion of this saving, 41%, is caused by the increase in  $T$ . In order to estimate the share of  $T$  from the overall saving, the default values of the parameters  $a$  and  $b$  with the optimal value of  $T$  were used and it was observed that the fuel consumption was reduced to 0.0487 litres. The calculation below reveals the share of parameter  $T$  in the saving obtained by using the optimal parameters compared to the default values.

$$\text{Share of } T \text{ in the saving} = \frac{F(a_d, b_d, T_d) - F(a_d, b_d, T_{opt})}{F(a_d, b_d, T_d) - F(a_{opt}, b_{opt}, T_{opt})} \quad (4.6)$$

Figure 43 demonstrate the driving behaviour produced by the optimal set of model parameters.

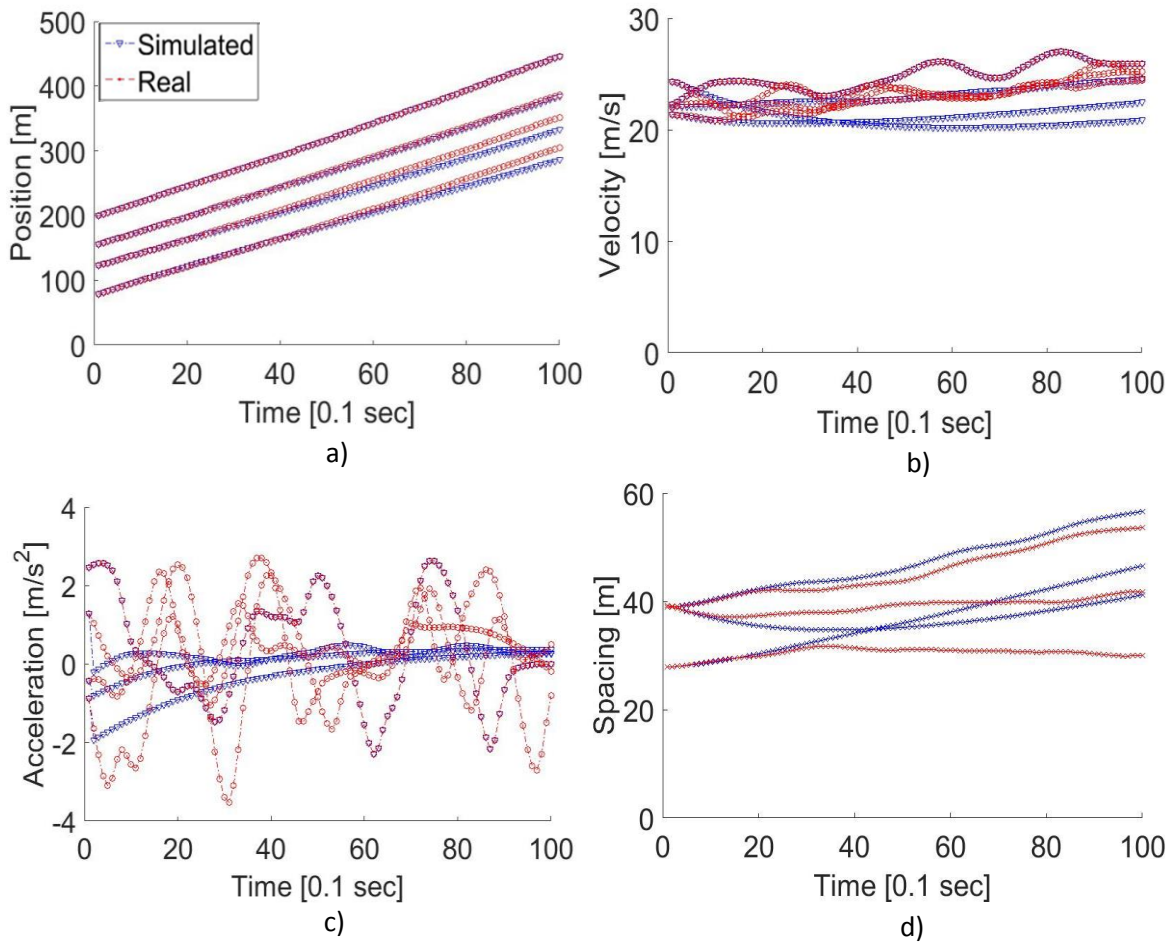


Figure 43. a) position, b) velocity, c) acceleration and d) spacing values produces using the optimal parameters compared to the real ones for the vehicles with IDs 441-467.

It can be seen that the high value of the parameter  $T$  has resulted in a more conservative driving style which is likely to have negative impacts on traffic flow in high densities. Negative impacts on traffic flow are likely to cause shockwaves and stop waves which could in return result in higher fuel consumptions for the traffic. Therefore, the collective impact of adopting such a driving strategy is investigated in a simulation where the trajectory of the lead vehicle is that of the vehicle 441 and the average inflow is set to be equal to that of lane one between times 170 [s] to 470 [s], that is  $22.2 \frac{veh}{min}$ . Figure 44 compares the spatio-temporal velocities in the real scenario with the simulated one.

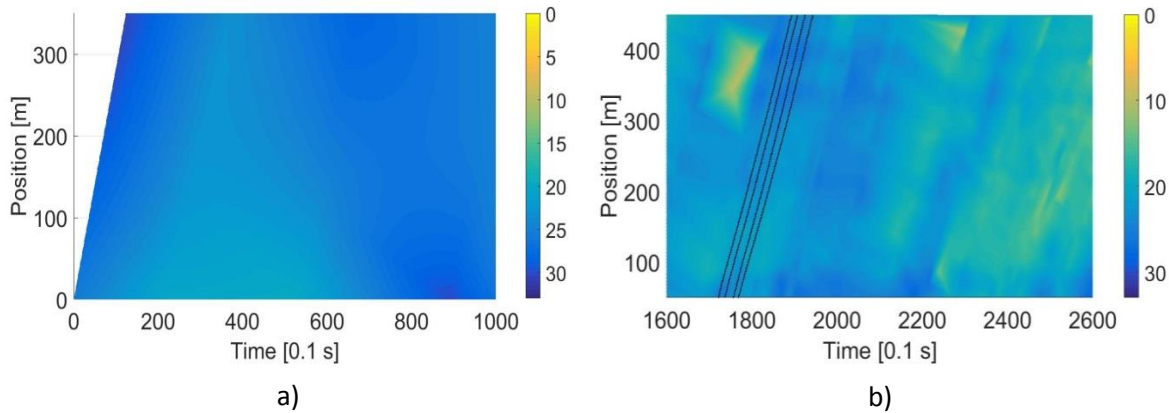


Figure 44. Comparison of the spatiotemporal velocities of the modelled scenario with the real data. The trajectory of the lead vehicle is  $T_l = 441$ .

It can be seen that the simulated scenario shows improvement over the real one in terms of the smoothness of traffic flow. It should be noted that homogenous driving in the simulated scenario and the lack of lane-changing could be one of the main contributory factors to this improvement. However, the analysis of the fuel consumption in both scenarios reveals an interesting result. The amount of fuel consumption for the first 40 vehicles following the vehicle 441 in the real scenario is 1.05 litres (average of 0.02625 for each vehicle) while for the simulated dataset this is equal to 0.99 litres (average of 0.0248 litres for each vehicle in 100 simulations). This means that despite the significant saving that is obtained for the immediate followers, the collective fuel consumption has only improved by an average of 6%. This value is obtained for a penetration rate of 100% automated vehicles and by excluding lane-changing manoeuvres. Increasing the number of following vehicles for which the average fuel consumption is calculated from 40 to 900 results in a drastic increase of 41% in the average fuel consumption (average of 0.0371 litres per vehicle in the simulation scenario compared to 0.02625 litres per vehicle in the real data). It can be concluded that such microscopic optimisations remain oblivious to the collective impacts of a driving strategy on a grand scale. To address this issue two approaches were investigated;

1. Increasing the number of vehicles in platoon,  $n$ , in the microscopically formulated optimisation problem.

2. Performing large scale optimisation scenarios where instead of microscopic constraints on headways, constraints on the actual traffic throughput are put in place. This is done in subsection 4.3.2.

Prior to performing the optimisation with the setup that was described above, the microscopic optimisation was carried out on a single follower-leader pair, Equation (4.1). The results obtained using this formulation were highly inconsistent, that is to say the optimal values obtained a) varied significantly when the trajectory of the lead vehicle in the optimisation scenario changed, and b) the optimal values obtained sometimes led to highly string unstable traffic flows. In order to address these issues, the number of follower vehicles in the optimisation scenario was extended to a platoon of 3 vehicles. This resulted in an improvement in terms of obtaining robust and consistent optimal parameters for different lead trajectories. This modification also led to a better string stability. The stability was improved due to the fact that the inclusion of a platoon of vehicles in the scenario incorporates the platoon dynamics and stability features in the optimisation framework. Nevertheless, as shown above, this framework delivers marginal savings for the immediate followers while significantly increasing the overall fuel cost in the link. This is due to the negative impacts that such a conservative driving style imposes on the traffic flow. While immediate followers benefit from fuel savings, the capacity drop that is caused by large headways leads to congestions and traffic breakdowns which in return increase the total fuel consumption.

In order to address this issue, the optimisation scenario was further extended to include a greater number of vehicles in the platoon, namely 10, 20, and 40 following vehicles. However, these modifications did not change the value of the optimal parameters and were, therefore, unable to resolve the issue of increased overall fuel consumption in the link.

The microscopic simulation-based optimisation as described above has its potential shortcomings:

1. While the optimal values obtained produce savings for the immediate followers, up to 40 following vehicles, they may lead to increased total fuel consumption in the network. Figure 45 depicts the collective impacts of this driving style on traffic flow. It can be seen that in the case of  $T_l = 441$ , after about 15 minutes a traffic breakdown takes place that leads to a decrease in the average velocities. This causes a significant drop in the traffic throughput and the formation of large queues in the upstream direction of the section. In the case of  $T_l = 362$ , since the trajectory of the leading vehicle was selected from a congested section of the roadway and it was subject to a number of slowdowns, the breakdown occurs early on.

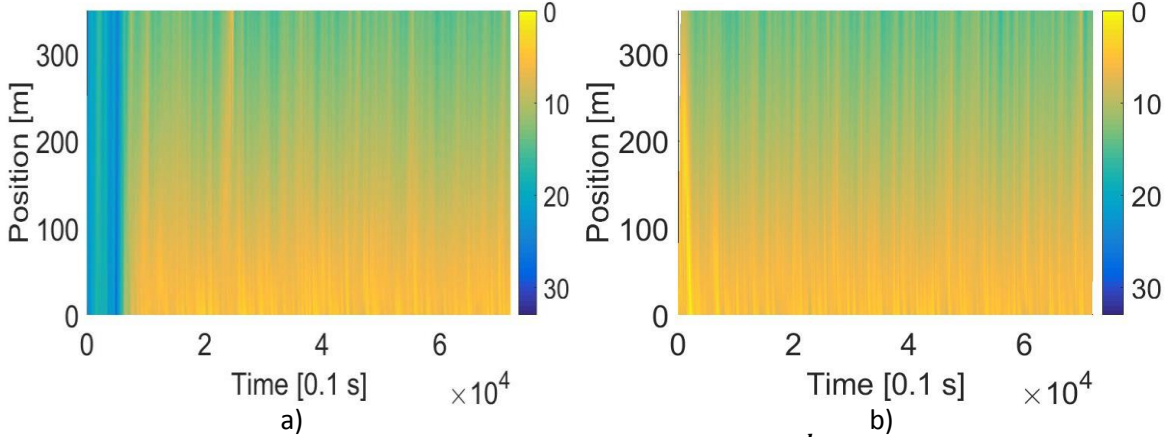


Figure 45. Two-hour-long simulation with the inflow of  $1333 \frac{veh}{hr}$  and with the microscopic optimal parameters. a)  $T_l=441$  b)  $T_l=362$ .

2. This type of optimisation based on only a single pair of vehicles is highly sensitive to initial conditions in the optimisation scenario. For instance, changes in the initial velocities of the immediate following vehicles or their positions could reduce the amount of fuel savings obtained and the optimal parameters. Increasing the number of following vehicles to values more than one addresses this issue to some extent, however as seen above, it still cannot correctly capture the broader impacts of the driving strategies on the traffic flow and the total fuel consumption.
3. The results that were reported in this section bring into question the plausibility of headway-based constraints in ensuring an efficient traffic flow.

However, it can be seen from the results obtained in this section that a user-optimal fuel efficient driving strategy for motorways can be characterised by high headway values combined with low acceleration parameter values and high deceleration parameter values. These parameters have the combined effect of maintaining large spacing between the vehicles in order to afford less sensitivity to minor brakes/accelerations of the lead vehicle. Such a strategy, therefore, produces much smoother acceleration behaviour. In terms of stability, low values of the parameter  $a$  and high values of the parameter  $b$  lead to more instability, however, this is compensated for by the increased values of the parameter  $T$ .

It is clear that for large values of  $T$ , roadway capacity is reduced. This may have a negligible impact on traffic flow when the inflow of vehicles is low and congested traffic states are not formed. This was shown in section 2.1.1, Figure 1, where it was shown that an increased parameter  $T$  does not change the shape of the left branch of the fundamental diagram for the IDM car-following model. However, as seen above, such microscopic optimisation setups cannot capture the broader impacts of a driving strategy on the traffic flow and, therefore, the driving strategies obtained using such narrowly framed optimisation frameworks can lead to the reduction of the traffic capacity and traffic breakdowns, which in return increase the cost of trip in terms of fuel consumption for other vehicles.

In what follows, the formulation of the optimisation framework is modified in order to factor in the macroscopic impacts of the driving strategies on traffic flow. The results are then compared with what was obtained in this subsection.

#### **4.3.2 Macroscopically formulated optimisation**

The objective of this section is to address the shortcomings of the microscopic optimisation raised above. For this purpose, it is necessary to broaden the horizon of the optimisation scenario in order to:

1. Directly impose macroscopic constraints on the traffic flow, as opposed to the microscopic, headway-based constraints that were used in subsection 4.3.1.
2. Capture the fuel efficiency aspects of the driving strategies in a broader sense than just a pair or a platoon of vehicles.
3. Reduce the sensitivity of the optimal parameters to the initial conditions such as initial gaps between vehicles and initial velocities.

For this purpose, the optimisation framework described in subsection 4.1.3 was performed. The following parameters were used in the simulation setup.

Table 12. Optimisation parameters for the macroscopically formulated optimisation.

$L [m]$	2000-2500
$t [min]$	10-60
$\lambda = 1/\mu \left[ \frac{veh}{h} \right]$	different values are used
$T_l$	Datasets 25B, 25C, 30A, 30B, 30C NGSIM I80 dataset
$\alpha$	70%

Similar to the user optimal approach, the optimisation is carried out using a genetic algorithm. Running the optimisation takes between one to three days on a High-Performance Computing (HPC) cluster. Each cluster node consists of two 2.5Ghz Intel Xeon E5-2670v2 processors, with 40 processors dedicated to the task.

The NGSIM Naples dataset is used for the macroscopic optimisation. The results are then validated using the NGSIM-I80 dataset. Additionally, the impact of different inflow rates is investigated by changing the value of  $\lambda$ . Table 13 demonstrates the optimal parameters obtained in each case.

Table 13. The macroscopic optimal parameters obtained for different trajectory sets from the NGSIM Naples dataset and different inflow rates when  $t = 60 \text{ min}$ .

Inflow rate $\left[\frac{vehc}{hr}\right]$	Dataset used in the optimisation				
	25B	25C	30A	30B	30C
1080	[5, 0.5, 0.5]	[5, 0.5, 0.5]	[5, 0.5, 0.5]	[5, 0.5, 0.5]	[5, 0.5, 0.5]
1296	[5, 0.5, 0.5]	[5, 0.5, 0.5]	[5, 0.5, 0.5]	[5, 0.5, 0.5]	[5, 0.5, 0.5]
1548	[5, 0.5, 0.5]	[5, 0.5, 0.5]	[5, 0.5, 0.5]	[5, 0.5, 0.5]	[5, 0.5, 0.5]
1872	[5, 0.6, 0.5]	[5, 0.5, 0.5]	[5, 0.5, 0.5]	[5, 0.7, 0.5]	[5,0.6,0.5]
2232	[5, 0.5, 0.5]	[5, 0.6, 0.5]	[5,0.6,0.5]	[5, 0.5, 0.5]	[5, 0.7, 0.5]
2664	[5,1,0.5]	[5,0.8,0.5]	[5,0.7,0.5]	[5,0.8,0.5]	[5, 0.9, 0.5]

A few things are worth noting from the results reported in table above:

1. The optimal parameters obtained are highly consistent for different driving conditions, produced by different trajectories sets, and different inflow rates.
2. The results obtained here completely contradict the microscopic optimal parameters reported in subsection 4.3.1 and also the fuel-economy driving strategies seen in the literature.

While the lower bound value was previously found to be optimal for parameter  $a$ , here the upper bound value is found to be optimal. Similarly, in the microscopically formulated problem the upper bound values were found to be optimal for the parameters  $b$  and  $T$ , whereas here the lower bound values are found to be optimal.

The combination of the parameters obtained here promotes a highly agile driving style with small headway values. This is somewhat counterintuitive as a fuel-economy driving style is usually characterised by keeping a large distance to the lead vehicle so that the following vehicles have enough time to smoothly respond to changes in the velocity of the leader. A smooth response means avoiding intense accelerations and decelerations which is perceived to be beneficial to fuel consumption. Interestingly though, the macroscopic optimal values produce an acceleration performance that would be much more intense compared to the microscopic optimal values under similar circumstances.

The key to understanding the contradiction between the microscopic optimal values and the macroscopic optimal values lies in the collective characteristics produced by each set. Small headways ensure increased capacity of traffic flow. Moreover, a large value for the acceleration parameter,  $a$ , together with a small value for the deceleration parameter,  $b$ , compensate for the instability that arises from the low value of  $T$ . This combination of parameters means that the maximum capacity of the roadway is utilised in order to avoid congested traffic states that lead to increased fuel consumptions. Figure 46 demonstrates the spatio-temporal velocity diagram when the macroscopic parameters are used.

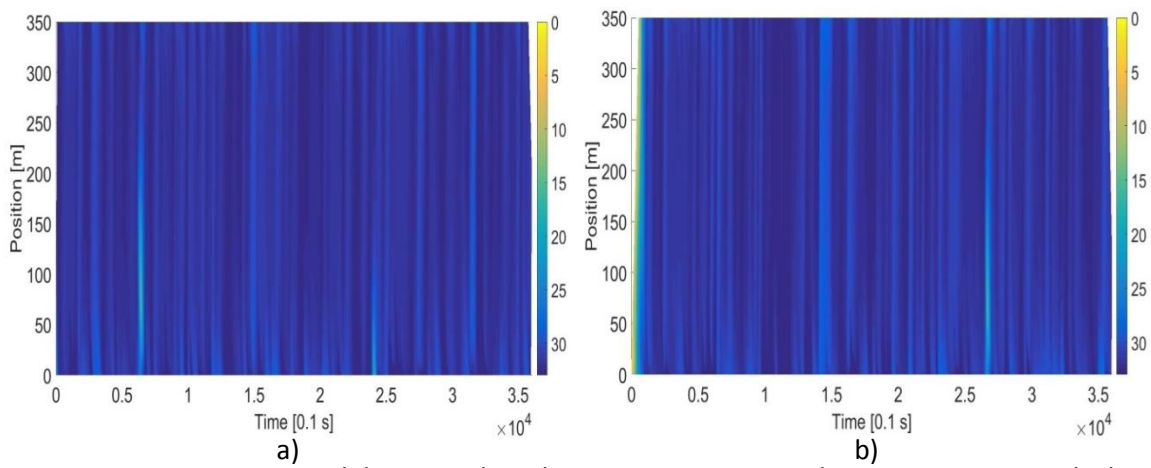


Figure 46. Spatio-temporal diagram when the macroscopic optimal parameters are used. The inflow rate is  $1333 \frac{veh}{h}$ , and the trajectories of the lead vehicle are a)  $T_l = 441$  b)  $T_l = 362$ .

It can be seen that unlike what was previously observed in the simulations with the microscopic optimal parameters in Figure 45, the traffic flow remains stable and there are no traffic breakdowns. The use of the new optimal parameters results in an average traffic throughput of about  $1333 \frac{veh}{h}$  and an average fuel consumption of about  $6.4 \frac{litre}{veh.100 km}$  for an inflow rate of  $1333 \frac{veh}{h}$ . These values are obtained in an hour-long simulation and are averaged over 100 independent simulations.

A comprehensive comparison of the results obtained so far for different model parameters and with normalised values is presented in Table 14.

Table 14. Results obtained for the microscopic and macroscopic optimisation frameworks.

Parameters' values And results	Micro		Macro t=10 min		Macro t=1 hour		Real	
Dataset used, $T_l$	441	362	441	362	441	362	441	362
$a[m/s^2]$	0.5	0.5	0.6	0.6	5	5	NA	NA
$b[m/s^2]$	5	5	4.7	4.5	0.5	0.5	NA	NA
$T[s]$	2	2	2	2	0.5	0.5	NA	NA
AFC [ $\frac{lit}{vehc.100km}$ ] <sup>1</sup>	10.5	13.5	10.1	13.7	6.4	6.5	6.74	10
TTh [ $veh/hr$ ] <sup>1</sup>	972	932	1069	855	1333	1333	1333	NA <sup>2</sup>

<sup>1</sup>AFC=Average Fuel Consumption, TTh= Traffic Throughput

<sup>2</sup> Not possible to estimate due to the large number of lane-changes

The top row of the table shows the type of optimisation carried out. The second row of this table depicts the set of trajectories used in the optimisation. The number 441 in the second row denotes that the four trajectories pertaining to vehicles with IDs 441, 452, 453, and 467 are used in the microscopically formulated optimisation (user-optimal approach). Similarly, 362 represents vehicles with IDs 362, 368, 378, and 381.

In the macroscopically formulated optimisation (system-optimal approach) only one trajectory is used, i.e. the trajectory of the first vehicle that enters the simulated roadway. The number on the second row represents this trajectory for the macroscopically formulated problem. Simulation results are obtained in a similar way and require only one trajectory (the trajectory of the first vehicle that enters the scenario) which is presented in the second row.

Rows number three to five show the optimal values of the parameters obtained for the specified optimisation and trajectories. Finally, the fourth and fifth rows show the average value of fuel consumption and traffic throughput obtained in the simulations. The simulations are similar to the one described in section 4.1.3 and are also used in the simulation-based optimisation for the system-optimal problem.

The results reported pertain to one-hour-long simulations and are averaged over 100 simulation runs. The real fuel consumption values are the average of fuel consumptions for 100 vehicles that follow the vehicle with the specified ID and remain in the same lane for the whole period of observation.

It is worth noting that the optimal parameters obtained when the simulation time in the macroscopic optimisation is 10 minutes,  $t = 10 \text{ mins}$ , are similar to the ones obtained in the microscopic optimisation. The reason for this observation is that the microscopic optimal set of parameters result in decreased fuel consumptions for the immediate followers. However, as seen in Figure 45, this set of parameters result in traffic breakdowns which in return lead to increased fuel consumptions. Therefore, only when the simulation time in the macroscopic optimisation is extended to one hour,  $t = 1 \text{ hr}$ , are such long term impacts captured and a different set of model parameters is obtained.

### **4.3.3 Impacts on traffic flow**

In order to investigate the capacity utilisation in each case, similar simulations are conducted where the trajectory of the lead vehicle is that of the leader in the NGSIM Naples 30C dataset. This dataset provides a longer period of observation for individual vehicles and, as a result, a longer stretch of the roadway can be simulated with the use of this trajectory. Additionally, multiple stops take place in this dataset and this gives rise to shockwaves. It is of interest to evaluate the impacts of such shockwaves on the traffic flow when the different optimal parameters are used.

Figure 47 shows the spatio-temporal velocity obtained when the microscopic and macroscopic sets of optimal parameters are used and for different inflow rates.

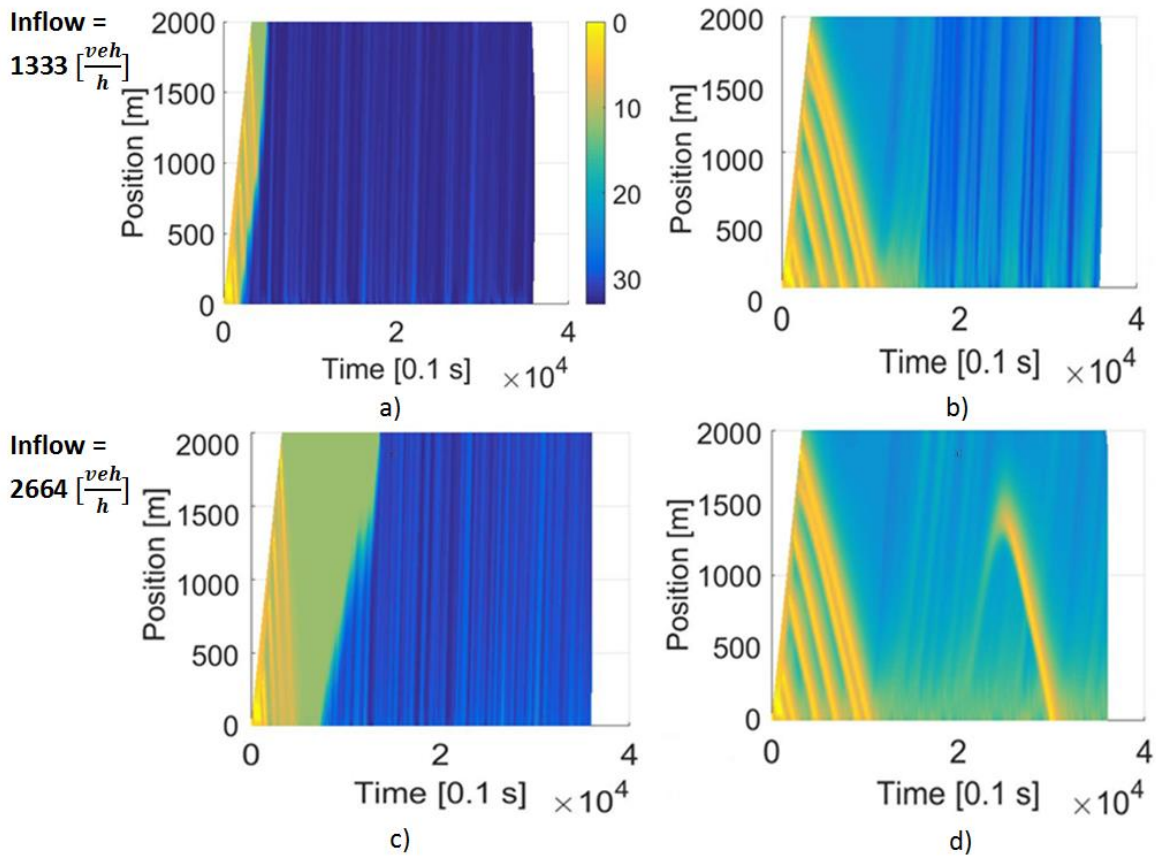


Figure 47. The comparison of the simulation results for different sets of model parameters when the trajectory of the lead vehicle from Naples 30C dataset is used. Macroscopic optimal parameters are used for diagrams on the left-hand-side and microscopic optimal parameters are used for diagrams on the right-hand-side.

From

Figure 47, it is clear that the macroscopic optimal parameters result in a much more efficient traffic flow and the shockwaves are more effectively contained. Table 15 summarises the measurements related to the average fuel consumption and traffic throughput. The values are averaged over 100 simulation runs.

Table 15. The comparison of the traffic throughput and average fuel consumptions when the micro and macro optimal parameters are used.

Inflow rate $\left[\frac{veh}{h}\right]$	Macro-optimal		Micro-optimal	
	Fuel $\left[\frac{lit}{100km}\right]$	Throughput $\left[\frac{veh}{h}\right]$	Fuel $\left[\frac{lit}{100km}\right]$	Throughput $\left[\frac{veh}{h}\right]$
1333	6.4	1333	9.5	1000

2664	7.8	2664	9.5	1000
------	-----	------	-----	------

In the case of micro-optimal parameters, since the maximum capacity has already

Figure 48 demonstrates the flow-density diagram for each of the four figures above. These results are obtained by placing three virtual detectors at positions 500 m, 1 km and 1.5 km in the roadway and measuring the flow,  $Q_i$ , average velocity,  $\bar{V}_i$ , and density,  $\rho_i$ , for different time intervals,  $i$ , according to,

$$Q_i = \frac{N_i}{T}, \quad \bar{V}_i = \frac{1}{N_i} \sum_{j=1}^{N_i} v_j, \quad \rho_i = \frac{\bar{V}_i}{Q_i}, \quad (4.7)$$

where  $T$  is the time interval equal to 1 minute,  $N_i$  is the vehicle count at time interval  $i$ , and  $v_j$  is the velocity of vehicle  $j$  that crosses the detector during interval  $i$ .

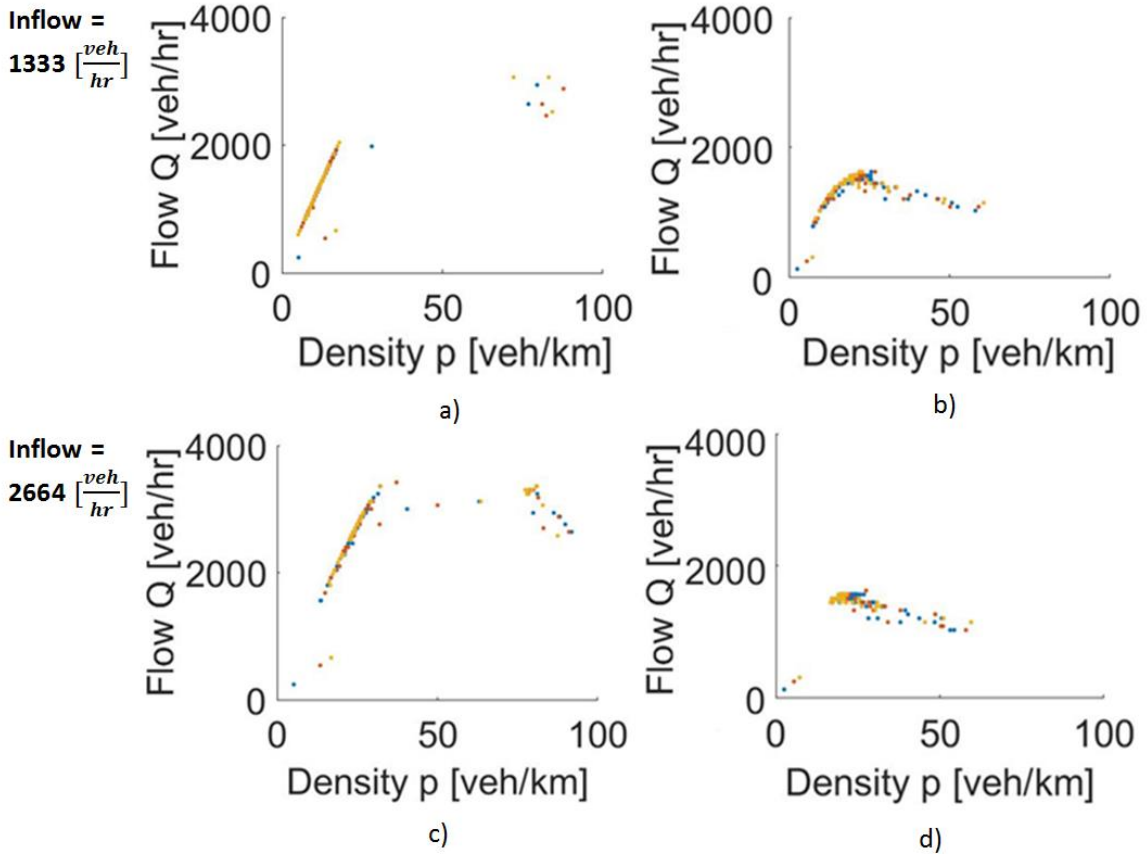


Figure 48. Comparison of flow-density diagrams for the micro and macro optimal parameters. Macroscopic optimal parameters are used for the diagrams on the left-hand-side and microscopic optimal parameters are used for the graphs on the right-hand-side.

It can be clearly seen that both the maximum capacity and the traffic flow are improved when the macroscopic optimal parameters are used.

#### 4.3.4 Stability features

In order to analyse the stability features of the micro and macro optimal parameters, a ring road analysis is carried out as described in subsection 3.1.2.

For this purpose, a ring road is simulated with 600 vehicles. All the vehicles drive according to the IDM with the model parameters that are under investigation. After allowing a sufficient time for the system to reach its equilibrium point, an instantaneous disturbance of magnitude  $-3 \frac{\text{m}}{\text{s}}$  is imposed on the velocity of one of the vehicles. This appears as a spike in the velocity of the subject vehicle in Figure 49.

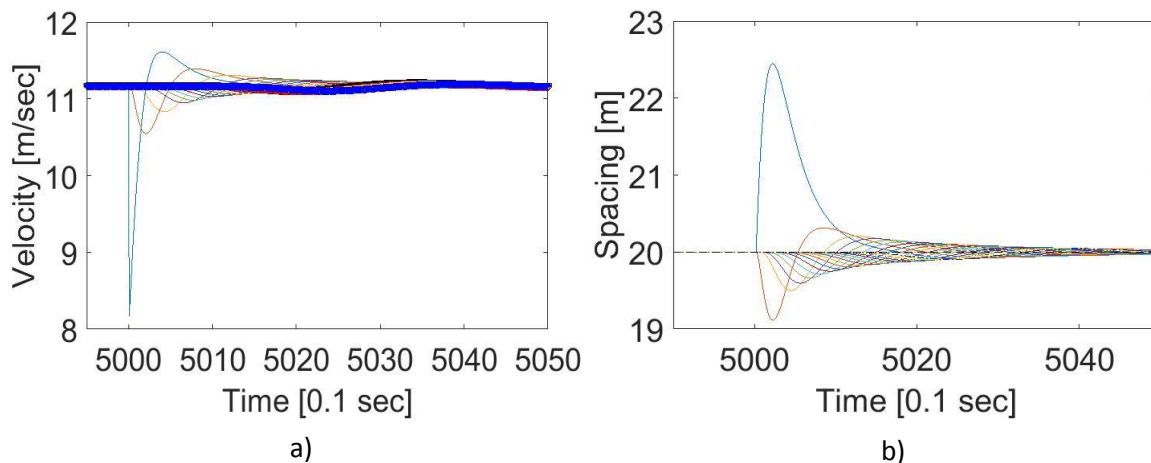


Figure 49. Response to a disturbance for the default set of model parameters when the circumference of the road is 500 meters.

The objective here is to evaluate the density at which the system becomes string unstable. Therefore, the length of the road is reduced in subsequent runs and the critical density at which the system becomes unstable is reported. The length of all the vehicles in the scenario is set to 5 meters.

The default set of model parameters remains stable regardless of the density. By reducing the length of the road below a certain threshold vehicles simply remain stationary. In other words, the equilibrium velocity of zero is obtained. Similar results can be observed for the micro optimal parameters. However, the macroscopic optimal parameters become string unstable at the density of  $133 \frac{veh}{km}$ . An interesting result though is seen by observing the equilibrium velocity at which traffic breakdown takes place. A density of  $60 \frac{veh}{km}$ , equivalent to equilibrium spacing of  $11.7 m$ , leads to an equilibrium velocity of  $17.3 \frac{km}{h}$  for the microscopic optimal parameters,  $20.6 \frac{km}{h}$  for the default set of model parameters, and  $65.9 \frac{km}{h}$  for the macroscopic optimal set of model parameters. This means that more than three times the flow could be achieved using the macroscopic optimal parameters. This is due to the increased capacity that is obtained when the parameter  $T$  is decreased.

It is also interesting to compare the stability features when the parameter  $T$  is set to a certain value. In Figure 50, the microscopic and macroscopic optimal values of  $a$  and  $b$  are once used with  $T = 0.5$  sec and once with  $T = 5$  sec. This figure demonstrates the relationship between the values of the parameters  $a, b, T$  and stability. A combination of low values of  $a$  and  $T$  clearly destabilises the system, Figure 50b [24]. High values of  $T$  increase the stability of the traffic flow while reducing the capacity, and consequently the average velocity and flow rate, Figure 50c,d. Therefore, the maximum utilisation of the capacity is achieved when a combination of high values of  $a$  and low values of  $T$  is used.

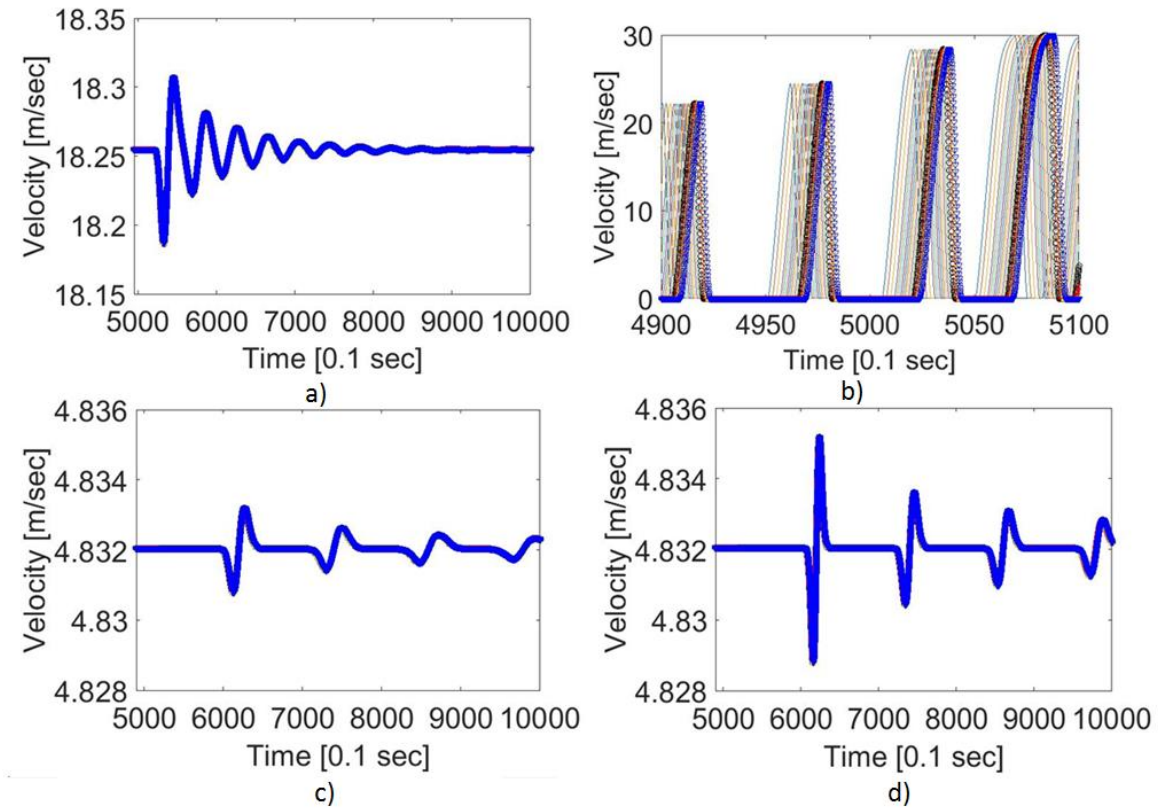


Figure 50. Fluctuations in velocities of the platoon when road length is equal to 10 km, 600 vehicles are used along with following parameters a)  $a = 5$ ,  $b = 0.5$ ,  $T = 0.5$  b)  $a = 0.5$ ,  $b = 5$ ,  $T = 0.5$  c)  $a = 0.5$ ,  $b = 5$ ,  $T = 2$  d)  $a = 5$ ,  $b = 0.5$ ,  $T = 2$ . The velocities of the first 20 vehicles are shown here.

#### 4.4 Conclusion and summary

In this study, two new frameworks for conducting optimisation with respect to fuel consumption were presented. These frameworks build on the extensive literature available on car-following models and limit the search space of optimisation to a subspace of possible driving strategies that is modelled by a particular car-following model. Depending on the car-following model, this subspace could represent a search space where important criteria of driving such as stability, safety, comfort and drivers' acceptability are satisfied. This approach provides the opportunity to perform large-scale, scenario-based optimisations, and test the impacts of the optimal strategies on the

collective features of traffic flow through extensive simulation-based tests. Performing such complex optimisation tasks and large-scale validation scenarios is made possible due to the reasonable required computational effort of the proposed framework. While fuel consumption was the primary focus of the present study, other objectives can also be investigated within this framework.

The microscopically formulated optimisation with respect to fuel consumption corresponded to the body of research that seeks to find optimal control models for the car-following regime of driving while focusing on the dynamics of driving of a single pair of vehicles. In this line of research, techniques based on the optimal control theory are typically used, such as receding horizon and dynamic programming. However, due to the complexity of the problem, the requirements of an efficient traffic flow as well as the relationship between speed/acceleration and fuel consumption are often simplified. Moreover, most of these approaches are highly computationally demanding and, therefore, the collective features of such control strategies in terms of traffic flow and stability cannot be easily investigated by means of large-scale simulations. Due to the aforementioned limitation, the effectiveness of control models is often demonstrated through simple, small-scale scenarios which do not address the collective features. For instance, these studies typically rely on the investigation of the response of the equipped vehicle when it follows a leader for validation purposes. While these approaches could produce efficient, user-optimal control models that indeed deliver significant fuel savings for individual vehicles, they could have negative impacts on the network and increase the cost of trips in terms of both fuel consumption and trip time.

The proposed approach, however, allows extensive, large-scale testing due to its computational simplicity. The optimal parameters found using the proposed approach produce a control model that is consistent with other user-optimal control methods in the literature, in the sense that the optimal parameters yield a driving behaviour that ensures a sufficient spacing between vehicles, consequently it could afford to be less

sensitive to minor accelerations/decelerations of the lead vehicle and, therefore, produces a smoother acceleration behaviour.

The collective impacts of this strategy were investigated through one-hour long simulations. It was observed that the conservative driving style produced by the microscopic optimal parameters leads to significant savings of up to 48% for the immediate followers. However, such strategy also leads to a drastic deterioration of the traffic capacity. Consequently, traffic breakdowns were observed that lead to a reverse impact on the fuel consumption of the other vehicles in the network, namely the average fuel consumption in the system could increase by about 56% as observed in the simulations. In other words, conservative, user-optimal, fuel-economy driving strategies could lead to intense traffic congestions, thereby increasing the fuel cost of trip through links.

In this chapter it was seen that the relationship between fuel consumption and traffic flow is a complex one and overlooking the collective impacts of a fuel-economy driving strategy by adopting a framework that does not appropriately take such collective impacts into account can lead to negative consequences. In order to address this, another optimisation framework was proposed which is based on large scale simulations. Such optimisation framework was made possible by limiting the search space for optimal strategies to the parameter space of a car-following model, namely the IDM car-following model.

It was shown that a fuel economy driving strategy that takes the long-term, collective fuel consumption for the whole link into account varies significantly from the one that only considers a pair of vehicles or even a large number of immediate followers. In particular, the latter, user-optimal approach, encourages a more sluggish driving style with large gaps between the vehicles while the former, system optimal approach, produces a more responsive driving behaviour. The system-optimal driving strategy was validated by evaluating the average fuel consumption in the network when the vehicles in the NGSIM-I80 dataset are replaced with equipped vehicles that drive according to the system-

optimal driving strategy. It was demonstrated that the system-optimal driving strategy produces a more stable and efficient traffic flow, and as a result, delivered savings of about 6% in a free flow condition and up to 36% in a congested condition.

The application of the proposed optimisation framework on different car-following models and for different objectives could be an interesting direction for future work.

## **5. Validation in an urban network**

In chapter 4 the proposed control algorithm was validated by the simulation of a single-lane roadway and comparison of the fuel consumption in the simulated scenario with the NGSIM-I80 dataset, even though the two systems were not completely equivalent. In particular, the stretch of motorway in the NGSIM-I80 dataset consists of six lanes and lane changes frequently occur, while lane changing was clearly absent in the simulated scenario. Additionally, the validation scenario demonstrated the potential of the proposed method in motorway driving, but its impacts on urban driving remained untested. It is, therefore, interesting to examine the impacts of the proposed control method in an urban network. For this purpose, the PTV VISSIM micro-simulation software is used. The use of this software allows the simulation of more comprehensive and realistic scenarios.

## 5.1 Simulation setup

The simulation scenario consists of a large network depicting Milton Keynes city centre which was developed by Transport Systems Catapult. The signalised junctions are calibrated according to the real values. Such a calibrated network with a wide range of driving conditions provides a good opportunity to evaluate the effectiveness of the driving strategy in an urban scenario. Figure 51, depicts the network layout.

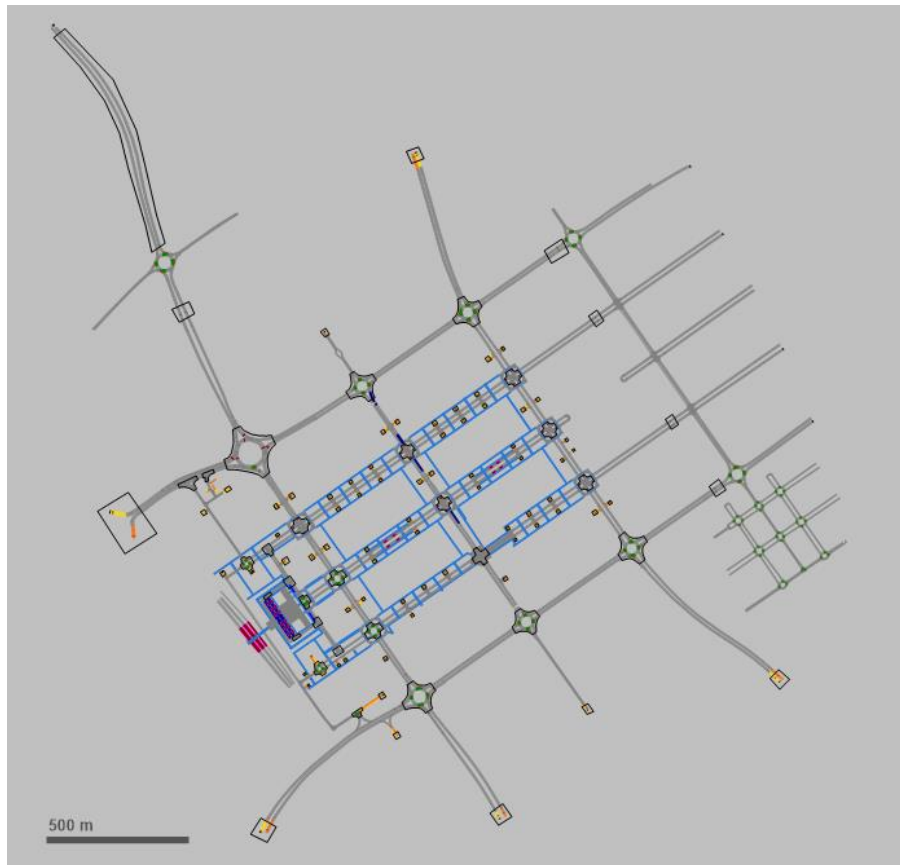


Figure 51. Milton Keynes city centre.

VISSIM's External Driver Model add-on gives users access to the driving attributes that are necessary to define new car-following models. A program was developed in C++ in order to bypass VISSIM's default car-following model and implement the proposed driving strategy.

The lane changing manoeuvres and the movement of the vehicles around junctions are handled by VISSIM's default models. The author acknowledges that this might lead to incompatibilities as VISSIM's default models are not fine-tuned to the proposed driving strategy, however, the investigation of suitable tactical and strategic decision making processes for the proposed control model is beyond the scope of the present work. In fact, one of the problems encountered in the simulations related to such incompatibilities. In particular, the shorter gaps and increased velocities that resulted from the proposed driving strategy led to issues with regard to performing lane changing manoeuvres. In order to address this issue the parameter representing jam distance was increased to the value of 5, i.e.  $s_0 = 5 \text{ m}$ . It is expected that this modification would reduce the benefits of the proposed control strategy, particularly in low velocities, however, this was necessary in order to cope with the aforementioned problem with respect to lane changing manoeuvres.

Since the interactions between the equipped vehicles and pedestrians, cyclists and other vehicle types such as heavy goods vehicles are outside the scope of the present study, the simulated traffic is fully composed of cars.

Each simulation run has a period of one hour. The inflow of vehicles from the 17 vehicle input locations are increased in 5 minute intervals until they reach their maximum values halfway through the simulation. Vehicle inflows are then consecutively decreased until they reach the value of 0 at time,  $t = 3300$  or  $3600 \text{ sec}$ . Figure 52 depicts the inflow rates from six of the vehicle input locations.

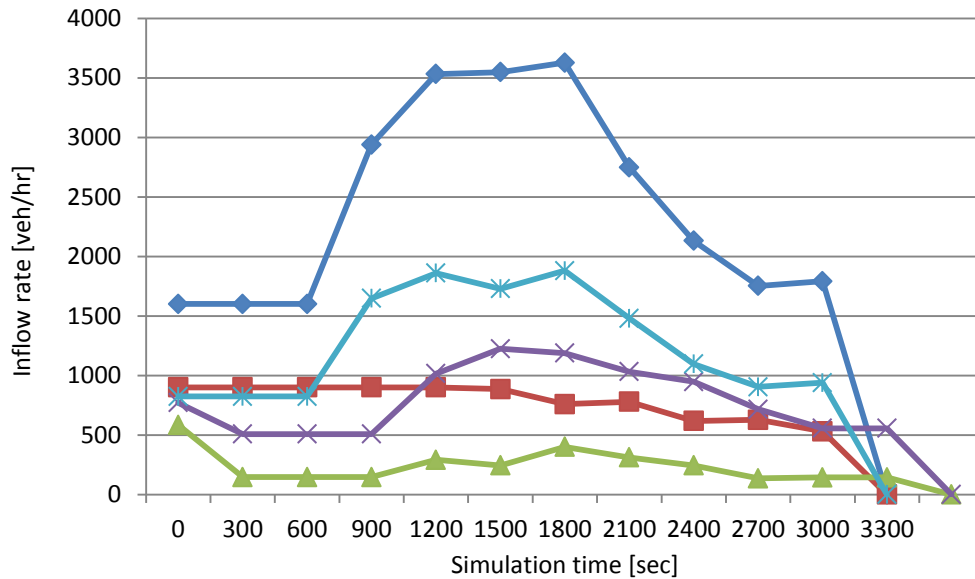


Figure 52. A representative sample of the inflow levels from 6 input section.

The use of VISSIM’s default car-following model provides the base case against which the efficiency of the proposed strategy is investigated. As mentioned in subsection 2.1.3, the software uses the Wiedeman model for the car-following regime.

## 5.2 Simulation results

The results reported in this subsection are averaged over 10 independent simulations. The initial 300 seconds was considered as the warm-up period and values related to the remaining time intervals are reported. Two sets of performance results are reported in this section;

1. The performance results related to the whole Milton Keynes city centre network.
2. The performance results related to a 1.6 km stretch of a two-lane roadway, namely Grafton Street.



Figure 53. Grafton Street.

While frequent lane-changes and multiple junctions are expected to reduce the benefits of the proposed driving strategy in the network, these phenomena are less present in Grafton Street.

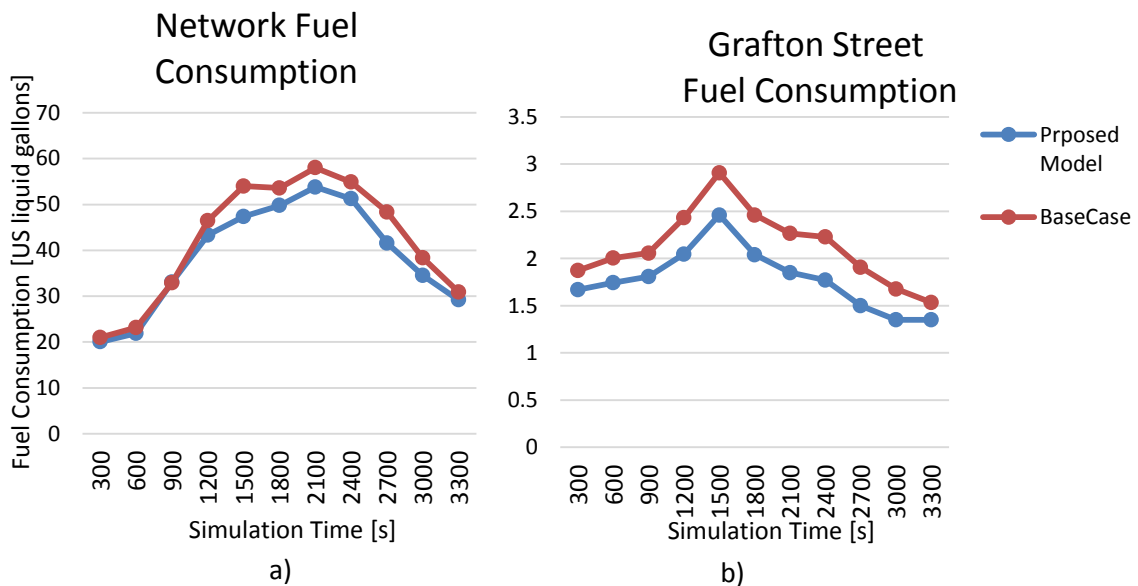


Figure 54. Average fuel consumption in a) the whole network b) Grafton Street.

From Figure 54 it can be seen that the proposed driving strategy leads to significant savings in fuel consumption, particularly savings of 7.95% and 16.18% are obtained for the network and Grafton Street respectively. This also produces proportional reductions

in emissions, namely Nitrogen Oxides (NOx), Carbon Monoxide (CO), and Volatile Organic Compounds (VOCs).

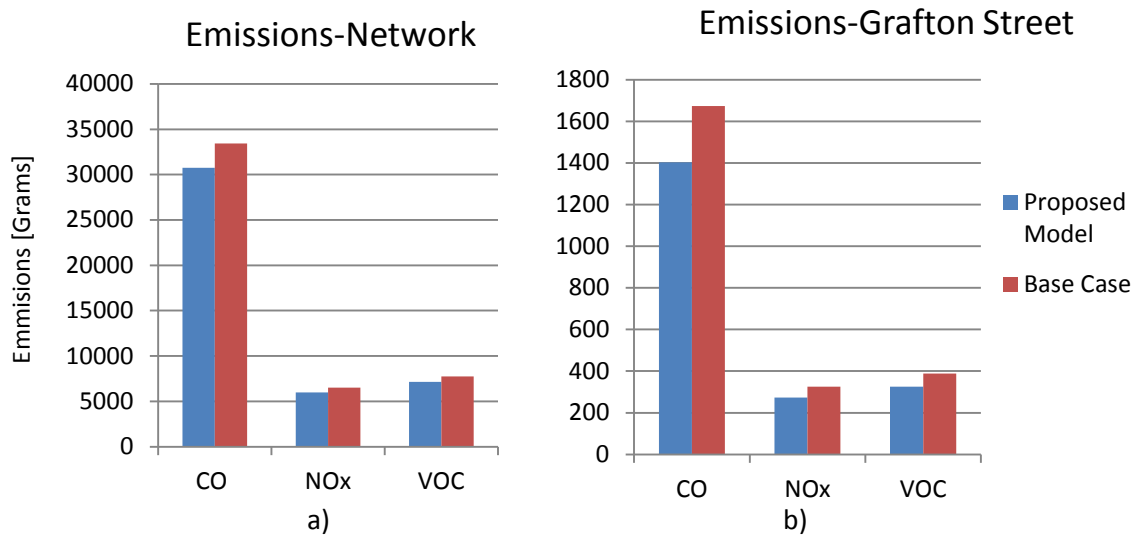


Figure 55. Total Emissions in the network and Grafton Street.

As discussed in chapter 4, the proposed model achieves fuel savings by establishing a more efficient traffic flow. This can be demonstrated by considering network performance measurements such as average velocities, travel times and delays. For the calculation of the total delay, in addition to the times spent behind traffic signals or in traffic jams, VISSIM also considers the difference between the desired speed and the actual speed using equation below,

$$Delay = Time\ step\ length - \frac{Distance\ travelled\ during\ time\ step}{Desired\ speed} \quad (5.1)$$

Figure 56 demonstrates the network performance measurements when the system-optimal driving strategy is used and in the base case.

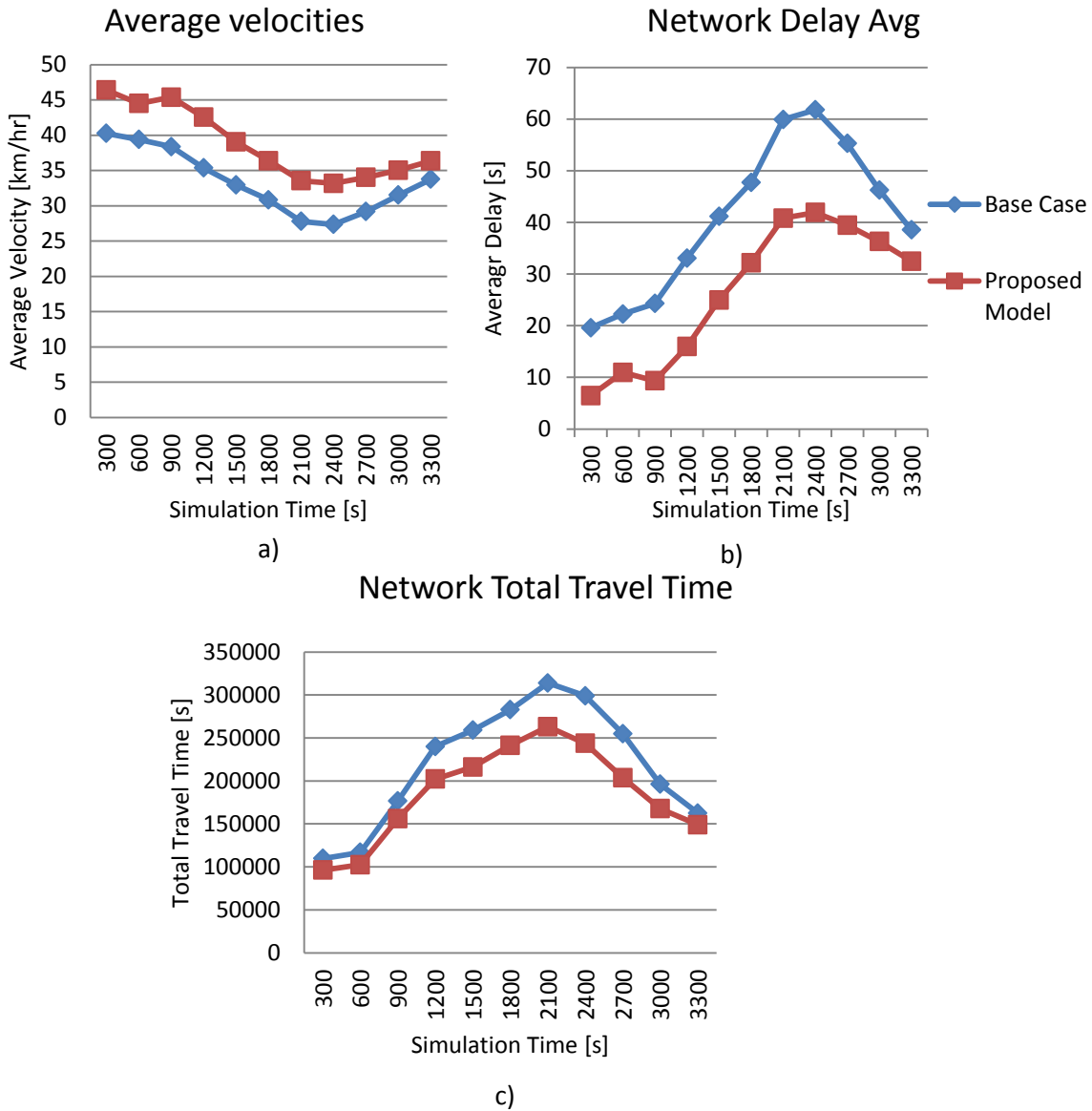


Figure 56. The comparison of the network performance measurements between the proposed driving strategy and base case.

All the measurements illustrate clear improvements when the proposed system-optimal driving strategy that was found in chapter 4 is used compared to the reference case, in particular the total network travel time and the network total delay are improved by 15% and 38% respectively.

### 5.3 Conclusion

In chapter 4, the proposed driving strategy was validated by replacing the stream of vehicles that follow a certain vehicle in the NGSIM-I80 dataset with modelled vehicles that drive according to the proposed driving strategy. This validation approach has a number of advantages and disadvantages. On the one hand, the use of real trajectory data clearly provides a reliable reference point for the evaluation traffic flow-related characteristic as well as fuel consumption and the NGSIM-I80 dataset is particularly suitable for this purpose. On the other hand, the short period of the dataset and the existence of frequent lane changes in the base case, while lane-changing was not modelled in the simulated scenario, were some of the limitations of the validation method in chapter 4. Moreover, the NGSIM-I80 dataset pertains to motorway driving and the impacts of the proposed driving strategy in urban areas remained untested in chapter 4.

In order to provide a comprehensive evaluation of the impacts of the proposed driving strategy in an urban network validation was carried out using the PTV VISSIM simulation software. A calibrated urban network, namely Milton Keynes city centre, was used for this purpose. The results reported were related to a) the whole network and b) a 1.6 km stretch of a two-lane local street where the traffic was less interrupted by traffic signals and junctions, namely Grafton Street. It was shown the proposed driving strategy offers remarkable savings both in terms of traffic flow-related performance measures and fuel consumption. As expected, due to the additional factors considered in the simulation, such as lane changes and numerous junctions, the saving was less than values reported in chapter 4. In particular, the savings of 8% and 16% were achieved for the whole network and the Grafton Street respectively.

One aspect that needs further investigation and could potentially increase the benefits of the proposed driving strategy could be the use of lane-changing and traffic signal control models that fit better with the changes in the driving behaviour that are brought about by the proposed model.

## **6. Conclusion and Future work**

### **6.1 Summary of work**

In chapter 1 it was pointed out that recent technological advances in the automation of driving could be leveraged in order to significantly improve different aspects of the ground motorised transport network. In chapter 2, some of the important aspects of traffic modelling were explored and a literature review on different methodologies relating to the efficient control of vehicles was carried out. It was discussed that the reliance on computationally expensive optimisation frameworks leads to problem formulations that may not effectively incorporate the requirements of an efficient network. Therefore, the user-optimal driving strategies that are developed in this way could have negative impacts on the transport network. The chapter was concluded by highlighting the potential of car-following models to fill the gap in the existing

methodologies and be used as the basis of control. The key advantages of car-following models are computational simplicity and the availability of an extensive body of research on microscopic and macroscopic aspects of these models.

In chapter 3, a comprehensive literature review was carried out in order to identify different requirements for an efficient control model. Additionally, sensitivity analysis was described as an important step in optimisation processes. The application of global sensitivity analysis determined which IDM model parameters have the most influence on fuel consumption. The chapter was concluded by demonstrating the merits of the IDM car-following model compared to another well-known model, the GHR model. The comparison was done using a new method that builds on the available literature on dynamic system identification and process diagnosis and fault detection.

In chapter 4, a new optimisation framework was presented. The new method is based on searching the parameter space of the selected car-following model in order to find the driving strategy that minimises fuel consumption. An estimation of the fuel consumption was carried out using a modified version of the VT-micro model that provides accurate estimates of fuel consumption with much less computational requirements.

Using the proposed framework, firstly an optimisation problem was formulated that represented the type of user-optimal control models that could widely be found in the literature. In this approach, the focus is placed on the dynamics of a single pair of vehicles. The application of the optimisation produces a driving strategy that is consistent with the findings of similar studies, in the sense that the optimal control model produces large gaps and a smooth acceleration performance, and as a result, reduces fuel consumption for the following vehicles.

Due to the reasonable required computational effort of the proposed control model, it is possible to investigate the application of the driving strategy in large-scale simulations for testing purposes. A number of simulations were carried out and it was demonstrated that the user-optimal fuel economy results in a drastic capacity drop as demonstrated in

section 4.3 and, consequently, deterioration of the traffic flow. As a result of the reduced capacity, traffic breakdowns and congestions take place more easily and this leads to increased fuel consumptions for the whole network.

In order to address the shortcomings of the user-optimal driving strategy a second optimisation problem was formulated which minimised the average fuel consumption within the link over a one-hour simulation. Interestingly, the optimal driving strategy that was found using this approach produces a highly agile driving style with short gaps between the vehicles. Although this is somewhat counterintuitive, the increase in the traffic capacity that is results from the system-optimal driving style avoids or postpones traffic breakdowns and by doing so reduces the overall fuel consumption within the network. The validation of the system-optimal driving strategy was carried out using the NGSIM-I80 dataset and the micro-simulation software PTV VISSIM in chapter 5. The former demonstrated the benefits of the proposed strategy in motorways and the latter showcased how the system-optimal driving strategy could improve urban traffic and contribute to the reduction fuel consumption within the network.

## **6.2 Contributions and future work**

On the basis of the findings, the major contributions of this research, along with potential directions of future work, are outlined next.

### **6.2.1 A new method for the comparison of car-following models**

In chapter 3, it was noted that one of the challenges in the comparison of car-following models is that it is often found that different models fit different trajectories best, even when multiple trajectories from a single driver are considered. This makes the comparison of car-following models problematic as no particular car-following model can be definitely shown to be superior over others.

In order to provide a more detailed analysis of the strengths and weaknesses of car-following models, a new method of comparison was proposed based on dynamic system

identification. The new method builds on the existing research into process fault detection and diagnosis. In section 3.3 the new method was used for the comparison of car-following models. It was shown that while the conventional comparison criterion, the cumulative error, did not provide a conclusive measure of performance when different trajectories are used, the proposed method produced consistent rankings across different trajectories.

The cumulative error has a clear advantage that may explain its widespread usage, that is, regardless of the number of model parameters or their physical interpretations, the cumulative error provides a single measure of performance for a given model. This means that it is simple and straightforward. However, it has the clear deficiency that it is often not informative.

The proposed method relies on the evaluation of the necessary changes in a model parameter to produce an almost perfect match between the modelled trajectory and the real one. One of the questions that needs further investigation relates to the diversity of coefficients in different models. In particular, model coefficients in different models do not always correspond to similar physical attributes, and more than one model parameter may have a high influence on the driving behaviour in a given driving condition. This poses a challenge on the application of the proposed method since, unlike the cumulative error, for a model with  $n$  parameters it is not straight forward to provide a  $\mathbb{R}^n \rightarrow \mathbb{R}$  mapping between the parameters and the goodness of fit.

The normalisation of parameter variations with respect to their physical interpretations, their sensitivities, or the number of parameters in the model might provide the required  $\mathbb{R}^n \rightarrow \mathbb{R}$  mapping to obtain a single measure of goodness of fit for a given model. For instance, suppose there are two models  $A$  and  $B$ , one of the following strategies could help obtain a single measure of goodness of fit.

1. A common model parameter in both models, e.g. headway ( $T$ ), might refer to a measurable physical attribute. Denote this parameter in model  $A$  by  $T_A$  and in  $B$  by  $T_B$ . If

empirical studies show that such a parameter should have a certain range or an expected value, e.g.  $T = [1, 3]s$  or  $E[T] = 2s$ , then the model  $A$  may be perceived as a better model compared to  $B$  if the dynamic estimates of  $T_A$  best match the empirical observations.

2. The proposed method captures all of the structural deficiencies of a given model in producing real observations by assessing the variations in one of the model parameters (e.g. Figure 33). Suppose that  $x_A$  is a parameter from model  $A$  and  $x_B$  is a parameter from model  $B$ . Comparing variations in  $x_A$  and  $x_B$  becomes problematic if the two do not have the same sensitivity indices. One question worth investigating is; how could the variation of  $x_A$  and  $x_B$  be normalised with respect to their corresponding sensitivities?

3. In the proposed method a single model parameter was tracked to explore model deficiencies. This could be extended to simultaneous tracking of multiple model parameters. However, this would require a post-parameter-tracking step where the variations of different parameters are mapped into a single measure of performance. An additional question that would require addressing in this context is; how could two models with different numbers of parameters be compared?

### **6.2.2 A quantitative approach to behavioural analysis of drivers**

In section 3.3 it was stated that dynamic system identification could be used in order to investigate driving behaviour and highlight the shortcomings of car-following models in the representation of driving dynamics. It was argued that the model that fits real trajectories with minimal variations in its tracked parameter should be favoured, and different car-following models were compared on this basis.

Another direction of application for this method would be to focus on the patterns of changes for the tracked parameter. In subsection 3.3.5, the method was applied to track the parameter  $T$  of the IDM using the NGSIM Naples 25B dataset. In Figure 33 it was demonstrated that the pattern of changes in the parameter resembles the velocity and spacing time-series. This is an indication that the IDM model is not ideally suited to modelling a feature of driving behaviour that is present in the investigated trajectory.

There are two possible strategies which could take advantage of information. One is to establish a relationship between the patterns and the explanatory variables and to modify the model accordingly. Another strategy would be to identify the driving conditions where drastic changes take place and investigate the impacts that such driving conditions have on static parameter estimates. The latter approach was investigated in [184] (Appendix 1) and it was demonstrated that a correlation between the occurrence of abrupt changes in the parameter estimates and change of driving conditions may be established. Further research on this subject is necessary. Firstly, the method should be applied to much larger datasets where external factors such as lane-changes are not present. Secondly, more conclusive results could be obtained with the automation of pattern recognition.

### **6.2.3 Fuel efficiency: system-optimal vs. user-optimal**

The main gap that was identified in the literature relates to the computational cost of the existing optimisation methods in the analysis of fuel-economy driving strategies. The high computational cost leads to the formulations of problems that merely consider the dynamics between a follower-leader pair and overlook the impacts of driving strategies on the traffic flow.

In order to address this issue, a new optimisation framework was proposed that uses the parameter space of car-following models, the IDM in this study, as a space where different driving strategies could be represented. The main advantages of this approach are computational efficiency, and the ease of investigating important features such as stability and impacts on traffic flow for car-following models due to the extensive body of research on these topics.

Two user-optimal and system-optimal formulations of fuel efficiency were presented and it was shown that reducing the subject of fuel efficiency to individual users could lead to drastic negative impacts on the network in terms of fuel consumption and network performance measures such as trip time. In particular, a conservative driving style

produced by a user-optimal driving strategy could deliver fuel savings for the immediate followers, however, it causes a significant drop in the traffic capacity which could consequently result in severe traffic breakdowns, increased fuel consumptions, and increased trip times in high and even moderate traffic inflows.

The system-optimal driving strategy was validated, first using the NGSIM-I80 dataset, and then using the micro-simulation software PTV VISSIM. It was shown that this driving strategy can deliver significant savings in the average fuel consumption of the network while improving the traffic flow and trip times in both urban areas and motorways.

The proposed driving strategy introduces fundamental changes in vehicles' longitudinal behaviour. In particular, it produces highly agile driving behaviour and short gaps with respect to the leading vehicle. In section 5.1, it was mentioned that this gave rise to problems with regard to lane changes in VISSIM simulations. The development of a suitable lane changing model that fits well with the proposed longitudinal control model could be the subject of future research.

Another interesting direction of research is the investigation of the potential of Vehicle to Vehicle (V2V) and Vehicle to Infrastructure (V2I) communications to support the proposed system-optimal, fuel-efficient driving strategy. The role of traffic signal control in facilitating a more steady flow of vehicles around junctions and minimising unnecessary shockwaves is also worth further investigation.

Finally, a thorough analysis of the interactions between automated vehicles and human-drivers, pedestrians, cyclists, and other vehicle types such as busses and HGVs is an important step in the realisation of an efficient road traffic network.

### **6.3 Concluding remarks**

The author believes that it is sometimes necessary to take a step back and re-evaluate the way in which problems are addressed within the scientific community. The application of machine learning approaches and control models based on optimal control theory, such as model predictive control, have become more and more popular in the field of

automated vehicles. The author acknowledges the significance of the existing body of research on these subjects; such methods will most likely play an important role in future transport systems. However, over-reliance on them could restrict the scope of the solutions according to their methodological limitations.

In this study, it was shown that the computational cost of some of these methods essentially limits the scope of the problems to individual leader-follower pairs while neglecting the complex nature of traffic. The road transport network is an interconnected, complex system; the author believes that if methodological and technological advances are to be leveraged in order to revolutionise and effectively improve it, it is important to define the expectations on the network's different entities in relation to the system's efficiency.

The proposed fuel efficient driving strategy introduced in this study is clearly distinguishable from the body of literature on this subject in terms of its underlying implications and requirements and it puts forward an alternative way of considering the problem of fuel efficiency. Interestingly, in this framework fuel efficiency and traffic flow are not opposing objectives; on the contrary, they could be seen as one.

## References

- [1] "Travel in London: Report 8," 2015. [Online]. Available: <http://content.tfl.gov.uk/travel-in-london-report-8.pdf>. [Accessed 2016].
- [2] "London Travel Report 2007," 2007. [Online]. Available: <http://content.tfl.gov.uk/London-Travel-Report-2007-final.pdf>. [Accessed 2013].
- [3] "Transport statistics Great Britain 2015," 10 December 2015. [Online]. Available: <https://www.gov.uk/government/statistics/transport-statistics-great-britain-2015>. [Accessed 2016].
- [4] "Road traffic estimates: Great Britain 2014 (R)," 21 May 2015. [Online]. Available: <https://www.gov.uk/government/statistics/road-traffic-estimates-in-great-britain-2014>. [Accessed 2017].
- [5] "SAE International's new standard J3016: Taxonomy and definitions for terms related to on-Road motor vehicle automated driving systems," SAE International, 2014.
- [6] "Road safety evolution in EU," 2017. [Online]. Available: [http://ec.europa.eu/transport/road\\_safety/specialist/statistics/index\\_en.htm](http://ec.europa.eu/transport/road_safety/specialist/statistics/index_en.htm). [Accessed 2017].
- [7] "European Commission Mobility and Transport-Road Safety," [Online]. Available: [http://ec.europa.eu/transport/road\\_safety/specialist/statistics\\_en](http://ec.europa.eu/transport/road_safety/specialist/statistics_en).
- [8] "Deliverable D61.1 of highly automated vehicles for intelligent transport HAVEit," ICT for intelligent vehicles and mobility services, 2011.
- [9] "Energy consumption in the UK," Department of Energy and Climate Change, 2013.
- [10] "Consumption of energy," eurostat-european commission, Luxembourg: Office for Official Publications of the European Communities, 2016.
- [11] "State of the art on alternative fuels transport systems," 2016 July 2015. [Online]. Available:

<https://ec.europa.eu/transport/sites/transport/files/themes/urban/studies/doc/2015-07-alter-fuels-transport-syst-in-eu.pdf>.

- [12] L. Mittal, T. Baker and G. Fuller, "London air quality network summary report 2014," Environmental Research Group, King's College London, March 2016.
- [13] "Managing urban traffic congestion," Transport research centre, Organisation for Economic Co-operation and Development OECD, 2007.
- [14] "50% Rise in gridlock costs by 2030," Centre for Economics and Business Research, 14 October 2014. [Online]. Available: <https://www.cebr.com/reports/the-future-economic-and-environmental-costs-of-gridlock/>. [Accessed 2015].
- [15] M. Wiering, " Multiagent reinforcement learning for traffic light control," in *First World Congress of the Game Theory Society Games 2000*, Utrecht, Netherlands, Basque Country University and Foundation B.B.V. Bilbao, Spain, 2000.
- [16] S. El-Tantawy, B. Abdulahi and H. Abdelgawad, "Multiagent reinforcement learning for integrated network of adaptive traffic signal controllers (MARLIN-ATSC): Methodology and large-scale application on downtown Toronto," *IEEE Transactions on Intelligent Transportation Systems*, vol. 14, no. 3, pp. 1140 - 1150, 2013.
- [17] A. Sadek and N. Basha, "Self-learning intelligent agents for dynamic traffic routing on transportation networks," in *Proceedings of the Sixth International Conference on Complex Systems*, Boston, 2006.
- [18] L. Kuyer, "Multiagent reinforcement learning and coordination for urban traffic control using coordination graphs and max-plus," Master's Thesis Artificial Intelligence, Intelligent Autonomous Systems group Faculteit der Natuurwetenschappen, Wiskunde en Informatica, Universiteit van Amsterdam, 2008.
- [19] G. R. Patil, A. L. Hall and B. A. Holmén, "Environmental traffic assignment: developing emission-based models," in *Transportation Research Board 88th Annual Meeting*, Washington, D. C., 2009.

- [20] J. Monteil and et al., "Cooperative highway traffic : multi-agent modeling and robustness assessment to local perturbations," in *Australasian Transport Research Forum 2011 Proceedings*, Adelaide, 2013.
- [21] K. Tanaka and M. Sano, "Trajectory stabilization of a model car via fuzzy control," *Fuzzy Sets and Systems, Elsevier*, vol. 70, no. 2-3, p. 155–170, 1995.
- [22] D. E. Moriarty and P. Langley, "Learning cooperative lane selection strategies for highways," in *Proceedings of the fifteenth national/tenth conference on Artificial intelligence/Innovative applications of artificial intelligence*, Madison, Wisconsin, 1998.
- [23] M. Pendrith, "Distributed reinforcement learning for traffic engineering application," in *Proceedings of the 4th International Conference on Autonomous Agents*, Barcelona, Spain, 2000.
- [24] M. Treiber and A. Kesting, "Evidence of convective instability in congested traffic flow: Asystematic empirical and theoretical investigation," *Transportation Research Part B*, vol. 45, no. 9, p. 1362–1377, 2011.
- [25] M. Schönhof and D. Helbing, "Empirical features of congested traffic states and their implications for traffic modeling," *Transportation Science*, vol. 41, no. 2, pp. 135-166, 2007.
- [26] M. Treiber, A. Hennecke and D. Helbing, "Congested Traffic States in Empirical Observations and Microscopic Simulations," *Physical Review E*, vol. 62, no. 2, pp. 1805-1824, 2000.
- [27] A. Kesting, M. Treiber, M. Schonhof and D. Helbing, "Adaptive cruise control design for active congestion avoidance," *Transportation Research Part C*, vol. 16, no. 6, pp. 668-683, 2008.
- [28] B. Kerner and P. Konhauser, "Structure and parameters of clusters in traffic flow," *Physical Review E*, vol. 50, no. 1, pp. 54-83, 1994.
- [29] B. R. Kerner, *Introduction to Modern Traffic Flow Theory and Control: The Long Road to Three-Phase Traffic Theory*, Springer, 2009.

- [30] B. S. Kerner, "Experimental features of self-organization in traffic flow," *Physical Review Letters*, vol. 81, no. 17, pp. 3797-3800, 1998.
- [31] D. Helbing, A. Hennecke and M. Treiber, "Phase diagram of traffic states in the presence of inhomogeneities," *Physical Review Letters*, vol. 82, no. 21, pp. 4360-4375, 1999.
- [32] M. Treiber and A. Kesting, "Traffic States," [Online]. Available: <http://www.traffic-states.com>. [Accessed 2014].
- [33] J. & M. J. A. Treiterer, "The hysteresis phenomenon in traffic flow.," in *In Proceedings of the Sixth International Symposium on Transportation and Traffic Theory*, Sydney, 1974.
- [34] C. F. Daganzo, "A behavioral theory of multi-lane traffic flow. Part I: Long homogeneous freeway sections," *Transportation Research Part B*, vol. 36, no. 2, p. 131–158, 2002.
- [35] C. F. Daganzo, "A behavioral theory of multi-lane traffic flow. Part II: Merges and the onset of congestion," *Transportation Research Part B*, vol. 36, no. 2, p. 159–169, 2002.
- [36] D. Helbing, "Micro- and macro-simulation of freeway traffic," *Mathematical and Computer Modelling*, vol. 35, no. 5-6, p. 517–547, 2002.
- [37] R. W. Rothery, "Car following models," [Online]. Available: <http://ocw.mit.edu/courses/civil-and-environmental-engineering/1-225j-transportation-flow-systems-fall-2002/lecture-notes/carfollowinga.pdf>. [Accessed 2013].
- [38] P. G. Gipps, "A behavioural car-following model for computer simulation," *Transportation Research*, Vols. B-15B, pp. 105-111, 1981.
- [39] R. Wiedemann, "Simulation des Strassenverkehrsflusses," Schriftenreihe des Instituts für Verkehrswesen der Universität Karlsruhe, Band 8, Karlsruhe, Germany, 1974.
- [40] B. Higgs, M. M. Abbas and A. Medina, "Analysis of the Wiedemann car following model over different speeds using naturalistic data," in *Transportation Research Board 3rd International Conference on Road Safety and Simulation*, Indiana, 2011.

- [41] "User's guide for MITSIMLab and road network editor (RNE)," March 2001. [Online]. Available: <https://its.mit.edu/sites/default/files/documents/Manual.pdf>. [Accessed 2013].
- [42] W. Burghout, "MITSIMLab model description," Centre for Traffic Engineering and Simulation Department of Infrastructure and Planning Royal Institute of Technology, Stockholm, 1999.
- [43] M. Brackstone and M. McDonald, "Car-following: a historical review," *Transportation Research Part F*, vol. 2, no. 4, p. 181–196, 1999.
- [44] P. G. Gipps, "A model for the structure of lane-changing decisions," *Transportation Research B*, vol. 20, pp. 403-414, 1986.
- [45] A. Kesting, M. Treiber and D. Helbing, "General lane-changing model MOBIL for car-following models," *Transportation Research Record*, 1999, p. 86–94., 2007.
- [46] Q. Yang, "A simulation laboratory for dynamic traffic management systems," PhD thesis, Massachusetts Inst. of Tech., Cambridge, MA, 1997.
- [47] K. I. Ahmed, "Modeling drivers' acceleration and lane change behavior," PhD thesis. Massachusetts Institute of Technology, 1999.
- [48] T. Toledo, H. N. Koutsopoulos and M. E. Ben-Akiva, "Modeling integrated lane-changing behavior," *Transportation Research Record*, vol. 1857, no. 1, pp. 30-38, 2003.
- [49] H. Rakha and B. Crowther, "Comparison of Greenshields, Pipes, and Van Aerde car-Following and traffic stream models," *Transportation Research Record*, vol. 1802, pp. 248-262, 2002.
- [50] J. J. Olstam and A. Tapani , "Comparison of car-following models," Swedish National Road and Transport Research Institute, Linköping Sweden, 2004.
- [51] R. Herman, E. W. Montroll, . R. B. Potts and . R. W. Rothery, "Traffic dynamics: analysis of stability in car-following," *Operations Research*, vol. 7, pp. 86–106, 1959.
- [52] D. C. Gazis, R. Herman and R. W. Rothery, "Nonlinear follow-the-leader models of traffic

- fLow," *Operations Research*, vol. 9, no. 4, pp. 545-567, 1961.
- [53] R. E. Chandler, R. Herman and E. W. Montroll, "Traffic dynamics: Studies in car following," *Operations research*, vol. 6, pp. 165-184, 1958.
- [54] L. A. Pipes, "An operational analysis of traffic dynamics," *Journal of Applied Physics*, vol. 24, pp. 271-281, 1953.
- [55] E. Kometani and T. Sasaki, "Dynamic behaviour of traffic with a nonlinear spacing-speed relationship," in *In Proceedings of the Symposium on Theory of Traffic Flow (pp. 105-119)*, Research Laboratories, General Motors, New York, 1959.
- [56] S. Bexelius, "An extended model for car-following," *Transportation Research* 2 (1), pp. 13-21, 1968.
- [57] G. Johansson and K. Rumer, "Drivers' brake reaction times," *Human Factors*, vol. 13, pp. 23-27, February 1971.
- [58] N. Lerner, R. Huey, H. McGee and A. Sullivan, "Older driver perception-reaction time for intersection sight distance and object detection," *Report FHWA-RD-93-168, Federal Highway Administration, US-DOT, McLean, Virginia*, vol. 1, pp. 33-40, 1995.
- [59] M. F. Aycin and R. Benekohal, "A linear acceleration car-following model development and validation," *Transportation Research Board*, vol. 1644, no. Traffic Flow Theory, pp. 10-19, 1998.
- [60] W. Leutzbach, *Introduction to the Theory of Traffic Flow*, pp. 143-146., Berlin: Springer, 1988.
- [61] H. Ozaki, "Reaction and anticipation in the car-following behavior," in *Proceedings of the 12th International Symposium on the Theory of Traffic Flow and Transportation, New York*, pp. 349-366. Elsevier, 1993.
- [62] H. Subramanian, "Estimation of car-following models," Master's thesis, MIT, Department of

Civil and Environmental Engineering , Cambridge, Massachusetts, 1996.

- [63] S. Hoogendoorn and R. Hoogendoorn , "Calibration of microscopic traffic-flow models using multiple data sources," *Philosophical Transactions of the Royal Society A*, vol. 368, no. 1928, p. 4497–4517, 2010.
- [64] G. F. Newell, "Nonlinear effects in the dynamics of car following," *Operations Research*, vol. 9, no. 2, pp. 209-229, 1961.
- [65] Q. Yang and H. N. Koutsopoulos, "A microscopic traffic simulator for evaluation of dynamic traffic management systems," *Transportation Research C* , vol. 4, no. 3, pp. 113-129, 1996.
- [66] R. F. Benekohal., "Development and validation of car-following model for simulation of traffic flow and traffic wave studies at bottlenecks," PhD Dissertation, Ohio State University, Columbus Ohio, 1986.
- [67] R. F. Benekohal and J. Treiterer, "CARSIM: car-following model for simulation of traffic in normal and stop-and-go conditions," *Transportation Research Record 1194*, pp. 99-111, 1988.
- [68] *Transportation and Traffic Engineering Handbook*, 2nd ed., Washington D.C.: Institute of Transportation and Traffic Engineering, 1982.
- [69] F. Kranke, H. Poppe, M. Treiber and A. Kesting, "Driver assistance systems for the active congestion avoidance in road traffic," *VDI-Berichte zur 22. VDI/VW Gemeinschaftstagung: Integrierte Sicherheit und Fahrerassistenzsysteme`*, vol. 1960, p. 375, 2006.
- [70] F. Kranke and H. Poppe, "2008 Traffic guard—merging sensor data and C2I/C2C information for proactive congestion avoiding driver assistance systems. Traffic guard—merging sensor data and C2I/C2C information for proactive congestion avoiding driver assistance systems," in *FISITA World Automotive Congress*, Munich, Germany, September 2008.
- [71] R. E. Wilson and J. A. Ward, "Car-following models: fifty years of linear stability analysis – a mathematical perspective," *Transportation Planning and Technology*, vol. 34, no. 1, pp. 3-

18, 2011.

- [72] V. Punzo and F. Simonelli, "Analysis and comparison of microscopic traffic flow models with real traffic microscopic data," *Transportation Research Record*, vol. 1934, no. 1, pp. 53-63, 2007.
- [73] A. Kesting and M. Treiber, "Calibrating car-following models by using trajectory data: Methodological study," *Transportation Research Record*, vol. 2088, pp. 148-156, 2009.
- [74] M. Treiber and A. Kesting, "Microscopic Calibration and Validation of Car-Following Models – A Systematic Approach," in *20th International Symposium on Transportation and Traffic Theory (ISTTT 2013)*, Noordwijk, Netherlands, 2013.
- [75] V. Punzo and B. F. Ciuffo, "Sensitivity analysis of car-following models: Methodology and application," in *Transportation Research Board 90th Annual Meeting*, Washington DC USA, 2011.
- [76] B. Ciuffo, V. Punzo and M. Mon, "Global sensitivity analysis techniques to simplify the calibration of traffic simulation models. Methodology and application to the IDM car-following model," *IET Intelligent Transport Systems*, vol. 8, no. 5, p. 479 – 489, 2014.
- [77] A. Kesting and M. Treiber, "How reaction time, update time, and adaptation time influence the stability of traffic flow," *Computer-Aided Civil and Infrastructure Engineering*, vol. 23, no. 2, p. 125–137, 2008.
- [78] "chryslergroup," chrysler, [Online]. Available: <http://www.chryslergroupllc.com/innovation/Pages/default.aspx>.
- [79] P. Planing, *Innovation Acceptance: The Case of Advanced Driver-Assistance Systems*, Stuttgart, Germany: Springer Gabler, 2013.
- [80] "Mitsubishi Motors," Mitsubishi Motors, 15 December 1998. [Online]. Available: <http://www.mitsubishi-motors.com/en/corporate/pressrelease/corporate/detail429.html>.

- [81] A. e. a. Broggi, "Autonomous vehicles control in the VisLab Intercontinental Autonomous Challenge," *Annual Reviews in Control*, vol. 36, no. 1, pp. 161-171, 2012.
- [82] e. a. A. Broggi, "The VisLab intercontinental autonomous challenge: an extensive test for a platoon of intelligent vehicles," *International Journal of Vehicle Autonomous Systems, special issue for 10th Anniversary*, vol. 10, no. 3, pp. 147 - 164, 2011.
- [83] "autonomous long distance drive research vehicle s500 intelligent drive," Mercedes-Benz, 2013. [Online]. Available: <http://www5.mercedes-benz.com/en/innovation/autonomous-long-distance-drive-research-vehicle-s-500-intelligent-drive/>.
- [84] "Nissan carries out first public test of autonomous drive on expressways in Japan," Nissan Motor Corporation, 2013. [Online]. Available: [http://www.nissan-global.com/EN/NEWS/2013/\\_STORY/131125-02-e.html](http://www.nissan-global.com/EN/NEWS/2013/_STORY/131125-02-e.html). [Accessed 2013].
- [85] "The self-driving car logs more miles on new wheels," Google, August 2012. [Online]. Available: <http://googleblog.blogspot.hu/2012/08/the-self-driving-car-logs-more-miles-on.html>. [Accessed 2013].
- [86] "IEEE Spectrum," IEEE, April 2013. [Online]. Available: <http://spectrum.ieee.org/cars-that-think/transportation/self-driving/google-autonomous-cars-are-smarter-than-ever>.
- [87] "The Wall Street Journal," Oct 2016. [Online]. Available: <https://www.wsj.com/articles/googles-self-driving-car-program-odometer-reaches-2-million-miles-1475683321>. [Accessed 2017].
- [88] D. Muoio, "Business Insider UK," Jan 2017. [Online]. Available: <http://uk.businessinsider.com/self-driving-car-milestones-coming-in-2017-2017-1/#5-googles-self-driving-car-company-waymo-could-launch-a-robot-taxi-fleet-with-its-partner-fiat-chrysler-in-2017-but-that-has-yet-to-be-confirmed-5>. [Accessed 2017].
- [89] "NissanNews," Feb 2017. [Online]. Available: <http://nissannews.com/en-US/nissan/usa/channels/us-nissan-technologies-autonomous-driving/releases/nissan-conducts-on-road-autonomous-vehicle-testing-in-europe>. [Accessed 2017].

- [90] J. White, "Wired," Jan 2017. [Online]. Available: <http://www.wired.co.uk/article/bmw-intel-driverless-tech-ces-2017>.
- [91] D. Dubois, W. Ostasiewicz and H. Prade, "Fuzzy sets: History and basic notions," in *Fundamentals of Fuzzy Sets*, Springer US, 2000, pp. 21-124.
- [92] J. Lukasiewicz, "Philosophical remarks on many-valued systems of propositional logic 1930," in *Reprinted in Selected Works (Borkowski, ed.), Studies in Logic and the Foundations of Mathematics*, North-Holland, Amsterdam, 1970,, pp. 153-179.
- [93] L. A. Zadeh, "Fuzzy sets," *Information and Control, Elsevier*, vol. 8, no. 3, p. 338–353, 1965.
- [94] S. Kikuchi and P. Chakroborty, "Car-following model based on fuzzy inference system," *Transportation Research Record*, pp. 82-91, 1992.
- [95] P. Chakroborty and S. Kikuchi, "Evaluation of the General Motors based car-following models and a proposed fuzzy inference model," *Transportation Research Part C*, vol. 7, no. 4, pp. 209-235, 1999.
- [96] A. Rekersbrink, "Microscopic traffic simulation with fuzzy logic," *Strassenverkehrstechnik*, vol. 39, no. 2, pp. 68-74, 1995.
- [97] J. Wu, M. McDonald and M. Brackstone, "A fuzzy logic microscopic simulation model for interurban ATT," in *Proceedings of the 10th European Simulation Symposium and Exhibition*, Nottingham, UK, 1998.
- [98] P. Chakroborty and . S. Kikuchi, "Calibrating the membership functions of the fuzzy inference system: instantiated by car-following data," *Transportation Research Part C: Emerging Technologies*, vol. 11, no. 2, p. 91–119, 2003.
- [99] M. McDonald, J. Wu and M. Brackstone, "Development of a fuzzy logic based microscopic motorway simulation model," in *IEEE Conference on Intelligent Transportation System*, Boston, 1997.

- [100] M. Sugeno and K. Murakami, "Fuzzy parking control of model car," in *The 23rd IEEE Conference on Decision and Control*, 1984.
- [101] M. Sugeno and M. Nishida, "Fuzzy control of model car," *Fuzzy Sets and Systems*, vol. 16, no. 2, p. 103–113, 1985.
- [102] W. H. Fleming and H. M. Soner, *Controlled Markov Processes and Viscosity Solutions*, Springer-Verlag, 1993.
- [103] D. Vrabie, F. L. Lewis and K. G. Vamvoudakis, "Reinforcement learning and feedback control: Using natural decision methods to design optimal adaptive controllers," *IEEE Control Systems Magazine*, pp. 76-105, 12 Nov 2012.
- [104] A. G. Barto, S. J. Bradtke and S. P. Singh, "Learning to act using real-time dynamic," *Elsevier Science, Artificial Intelligence*, vol. 72, pp. 81-138, 1995.
- [105] M. Wang, M. Treiber, W. Daamen, S. P. Hoogendoorn and B. van Arem, "Modelling supported driving as an optimal control cycle: Framework and model characteristics," *Procedia-Social and Behavioral Sciences*, vol. 80, pp. 491-511, 2013.
- [106] J. S. Tyler, "The characteristics of model-following systems as synthesized by optimal control," *IEEE Transactions on Automatic Control*, vol. 9, no. 4, pp. 485 - 498, 1964.
- [107] D. Zhao and et al., "Full-range adaptive cruise control based on supervised adaptive dynamic programming," *Neurocomputing: Advances in Neural Network Research and Applications*, vol. 125, p. 57–67.
- [108] J. Laumonier, C. Desjardins and B. Chaib-draa, "Cooperative adaptive cruise control: A reinforcement learning approach," *IEEE Transactions on Intelligent Transportation Systems*, vol. 12, no. 4, pp. 1248 - 1260, 2011.
- [109] J. C. Medina and R. F. Benekohal, "Q-learning and approximate dynamic programming for traffic control: A case study for an oversaturated network," in *Transportation Research Board 91st Annual Meeting*, Washington DC, 2012.

- [110] Y. Sasaki, N. S. Flann and P. W. Box, "Multi-Agent Evolutionary Game Dynamics and Reinforcement Learning Applied to Online Optimization of Traffic Policy," Utah State University, 2005. [Online]. Available: <http://digital.cs.usu.edu/~flann/multiagent.pdf>. [Accessed 2013].
- [111] T. L. Thorpe and C. Andersson, "Traffic light control using sarsa with three state representations," IBM corporation, 1996.
- [112] B. Abdulhai and L. Kattan, "Reinforcement learning: Introduction to theory and potential for transport applications," *Canadian Journal of Civil Engineering*, vol. 30, no. 6, pp. 981-991, 2003.
- [113] R. Sukthankar, S. Baluja and J. Hancock, "Evolving an intelligent vehicle for tactical reasoning in traffic," in *IEEE International Conference on Robotics and Automation Proceedings Vol. 4*, Albuquerque, 1997.
- [114] P. Papadimitratos and et al., "Vehicular communication systems: Enabling technologies, applications, and future outlook on intelligent transportation," *IEEE Communications Magazine*, vol. 47, no. 11, pp. 84 - 95, 2009.
- [115] G. Marsden, M. McDonald and M. Brackstone, "Towards an understanding of adaptive cruise control," *Transportation Research Part C: Emerging Technologies*, vol. 9, no. 1, p. 33–51, 2001.
- [116] A. El Sallab, M. Abdou, E. Perot and S. Yogamani, "Deep Reinforcement Learning framework for Autonomous Driving," *IS&T Electronic Imaging, Autonomous Vehicles and Machines AVM-023*, pp. 70-76, 2017.
- [117] X. Xiong, J. Wang, F. Zhang and K. Li, "Combining deep reinforcement learning and safety based control for autonomous driving," 2016. [Online]. Available: <https://arxiv.org/abs/1612.00147>. [Accessed 2017].
- [118] E. Al Sallab, M. Abdou, E. Perot and S. Yogamani, "End-to-end deep reinforcement learning for lane keeping assist," in *Machine Learning for Intelligent Transportation Systems*

*Workshop, NIPS, Barcelona, 2016.*

- [119] K. Ahn, "Microscopic fuel consumption and emission modeling," *Civil and Environmental Engineering*. Virginia Polytechnic Institute and State, Blacksburg, 1998.
- [120] T. Mu, J. Jiang and Y. Wang, "Heterogeneous delay embedding for travel time and energy cost prediction via regression analysis," *IEEE Transactions on Intelligent Transportation Systems*, vol. 14, no. 1, pp. 214-224, 2013.
- [121] K. Ahn, H. Rakha, A. Trani and M. V. Aerde, *Estimating vehicle fuel consumption and emissions based on instantaneous speed and acceleration levels*, *Civil and Environmental Engineering*, Virginia Polytechnic Institute and State, 1998.
- [122] G. Z. B. O. Changxu Wu, "A fuel economy optimization system with applications in vehicles with human drivers and autonomous vehicles," *Transportation Research Part D: Transport and Environment*, vol. 16, no. 7, pp. 515-524, Oct 2011.
- [123] H. Rakha and Y. Ding, "Impact of stops on vehicle fuel consumption and emissions," *Journal of Transportation Engineering*, vol. 129, no. 1, pp. 23-33, 2003.
- [124] H. Rakha and K. Kamalanathsharma, "Eco-driving at signalized intersections using V2I communication," in *14th International IEEE Conference on Intelligent Transportation Systems*, Washington, DC, USA, October 2011.
- [125] P. Themann, J. Bock and L. Eckstein, "Energy efficient adaptive cruise control utilizing V2X information," in *eCoMove 9th European Congress and Exhibition*, Dublin, Ireland, 2013.
- [126] P. Themann and L. Eckstein, "Modular approach to energy efficient driver assistance incorporating driver acceptance," in *Intelligent Vehicles Symposium*, Alcalá de Henares, Spain, June 2012.
- [127] P. Markschläger, H. G. Wahl, F. Weberbauer and M. Lederer, "Assistance system for higher fuel efficiency," *ATZ worldwide*, vol. 114, no. 11, pp. 8-13, 2012.

- [128] "Porsche Annual Report," 2012.
- [129] J. Å. ,. L. N. Erik Hellström, "Design of an efficient algorithm for fuel-optimal look-ahead control," *Control Engineering Practice, Special Issue on Automotive Control Applications, 2008 IFAC World Congress*, vol. 18, no. 11, p. 1318–1327, 2010.
- [130] J. Zhang and P. Ioannou, " Longitudinal control of heavy trucks in mixed traffic: environmental and fuel economy considerations," *IEEE Transactions on Intelligent Transportation Systems*, vol. 7, no. 1, pp. 92-104, 2006.
- [131] S. Li, K. Li, J. Wang, L. Zhang, X. Lian, H. Ukawa and D. Bai, "MPC based vehicular following control considering both fuel economy and tracking capability," in *IEEE Vehicle Power and Propulsion Conference*, Harbin, China, 2008.
- [132] C. Manzie, H. Watson and S. Halgamuge, "Fuel economy improvements for urban driving: Hybrid vs. intelligent vehicles," *Transportation Research Part C: Emerging Technologies February 2007*, vol. 15, no. 1, pp. 1-16, 2007.
- [133] S. E. Li and H. Peng, "Strategies to minimize fuel consumption of passenger cars during car-following scenarios," in *American Control Conference* , San Francisco, CA, USA, 2011.
- [134] M. Treiber, A. Kesting and C. Thiemann, "How Much Does Traffic Congestion Increase Fuel Consumption and Emissions? Applying Fuel Consumption Model to NGSIM Trajectory Data," in *Transportation Research Board 87th Annual Meeting*, Washington DC, 2008.
- [135] J. Halkias and J. Colyar, "NGSIM Interstate 80 freeway dataset," US Federal Highway Administration, FHWA-HRT-06-137, Washington, DC, USA, 2006.
- [136] M. Montanino and V. Punzo, "Reconstructed NGSIM I80-1. COST ACTION TU0903 - MULTITUDE," 2013. [Online]. Available: <http://www.multitude-project.eu/exchange/101.html>.. [Accessed 2015].
- [137] "Prioritising the safety potential of automated driving in europe," April 2016. [Online]. Available: [http://etsc.eu/wp-content/uploads/2016\\_automated\\_driving\\_briefing\\_final.pdf](http://etsc.eu/wp-content/uploads/2016_automated_driving_briefing_final.pdf).

[Accessed 2017].

- [138] . P. Ioannou and C. Chien, "Autonomous intelligent cruise control," *IEEE Transactions on Vehicular Technology*, vol. 42, no. 4, pp. 657-672, 1993.
- [139] E. N. Holland, "A generalised stability criterion for motorway traffic," *Transportation Research Part B: Methodological*, vol. 32, no. 2, p. 141–154, 1998.
- [140] W. Tan and A. Packard, "Stability region analysis using polynomial and composite polynomial Lyapunov functions and sum-of-squares programming," *IEEE Transaction on Automatic Control*, vol. 53, no. 2, pp. 565-571, 2008.
- [141] R. Genesio, M. Tartaglia and A. Vicino, "On the estimation of asymptotic stability regions: State of the art and new proposals," *IEEE Transactions on Automatic Control*, Vols. AC-30, no. 8, pp. 747-755, 1985.
- [142] C. Liebe, R. Mahnke, R. Kuhne and H. Wang, "Traffic flow perspectives from fundamental diagram to energy balance," *Transportation Research Circular E-C149: 75 Years of the Fundamental Diagram for Traffic Flow Theory*, pp. 63-72, 8 July 2008.
- [143] B. S. Kerner, "Dependence of empirical fundamental diagram on spatial-temporal traffic patterns features," 31 Aug 2003. [Online]. Available: arXiv:cond-mat/0309018 [cond-mat.stat-mech]. [Accessed 2013].
- [144] R. E. Wilson, "Mechanisms for spatio-temporal pattern formation in highway traffic models," *Philosophical Transactions of the Royal Society A*, vol. 366, no. 1872, pp. 2017-2032, 2008.
- [145] J. A. Ward and . R. E. Wilson, "Criteria for convective versus absolute string instability in car-following models," in *proceedings of the Royal Society A*, 2011.
- [146] M. Treiber, A. Kesting and D. Helbing, "Delays, Inaccuracies and Anticipation in Microscopic Traffic Models," *Physica A*, vol. 360, no. 1, pp. 71-88, 2006.

- [147] K. Yi and J. Chung, "Nonlinear brake control for vehicle CW/CA systems," *IEEE/ASME Transactions on Mechatronics*, vol. 6, no. 1, pp. 17-25, 2001.
- [148] J. Martinez and C. Canudas-De-Wit, " A safe longitudinal control for adaptive cruise control and stop-and-go scenarios," *IEEE Transactions on Control Systems Technology*, vol. 15, no. 2, pp. 246-258, 2007.
- [149] L. Luo, H. Liu, P. Li and H. Wang, "Model predictive control for adaptive cruise control with multi-objectives: comfort, fuel-economy, safety and car-following," *Journal of Zhejiang University Science A*, vol. 11, no. 3, pp. 191-201, 2010.
- [150] A. Dragan, D. Sadigh, C. Basu and S. Seshia, "Predictable and customizable autonomous driving," university of berkeley, 2016.
- [151] M. Saffarian, J. C. F. Winter and R. Happee, "Automated driving: Human-factors issues and design solutions," *Proceedings of the Human Factors and Ergonomics Society Annual Meeting*, vol. 56, no. 1, pp. 2296-2300, 2012.
- [152] M. Cunninghama and M. A. Regana, "Autonomous Vehicles: Human factors issues and future research," in *Australasian Road Safety Conference*, Gold Coast, Queensland, Australia, 2015.
- [153] H. A. Hamersma and P. Schalk Els, "Longitudinal vehicle dynamics control for improved vehicle safety," *Journal of Terramechanics* , vol. 54, p. 19–36, 2014.
- [154] T. D. Gillespie, *Fundamentals of Vehicle Dynamics*, Warrendale, PA, USA: Society of Automotive Engineers, 1992.
- [155] J. Y. Wong, *Theory of Ground Vehicles*, 4th Edition, John Wiley & Sons, 2008.
- [156] D. M. Hamby, "A review of techniques for parameter sensitivity analysis of environmental models," *Environmental Monitoring and Assessment* , vol. 32, no. 2, pp. 135-154, 1994.
- [157] A. Saltelli and et al., *Global Sensitivity Analysis: The Primer*, West Sussex: Wiley, 2008.

- [158] V. Punzo, . D. J. Formisano and V. Torrieri, "Nonstationary Kalman filter for estimation of accurate and consistent car-following data," *Transportation Research Record*, no. 1934, pp. 3-13, 2005.
- [159] A. Saltelli, P. Annoni, I. Azzini, F. Campolongo, M. Ratto and S. Taranto, "Variance based sensitivity analysis of model output. Design and estimator for the total sensitivity index," *Computer Physics Communications*, vol. 181, no. 2, p. 259–270, 2010.
- [160] J. Jacques , C. Lavergne and N. Devictor, "Sensitivity analysis in presence of model uncertainty and correlated inputs," *Reliability Engineering & System Safety*, vol. 91, no. 10-11, p. 1126–1134, 2006.
- [161] E. Brockfeld, R. D. Kühne and P. Wagner, "Calibration and validation of microscopic traffic flow models," in *83rd Annual Meeting Transportation Research Board*, Washington, D.C., 2003.
- [162] P. Ranjitkar, T. Nakatsuji and M. Asano, "Performance evaluation of microscopic traffic flow models with test track data," *Transportation Research Record*, vol. 1876, no. 1, pp. 90-100, 2004.
- [163] M. Treiber and D. Helbing, "Memory effects in microscopic traffic models and wide scattering in flow-density data," *Physical Review E*, vol. 68, no. 4, p. 046119, 2003.
- [164] A. Kesting, M. Treiber and D. Helbing, "Enhanced intelligent driver model to access the impact of driving strategies on traffic capacity," *Philosophical Transactions of the Royal Society A* 368, pp. 4585-4605, 2010.
- [165] M. Treiber, A. Kesting and D. Helbing, "Understanding widely scattered traffic flows, the capacity drop, and platoons as effects of variance-driven time gaps," *Physical Review E*, vol. 74, no. 1, p. 016123, 2006.
- [166] J. C. Munoz and C. F. Daganzo, "Moving bottlenecks: A theory grounded on experimental observation," in *Transportation and Traffic Theory in the 21st Century. Proceedings of the 15th International Symposium on Transportation and Traffic Theory*, Adelaide, Australia,

2002.

- [167] X. Ma and I. Andréasson, "Behavior measurement, analysis, and regime classification in car following," *IEEE Transactions on Intelligent Transportation Systems*, vol. 8, no. 1, pp. 144-156, 2007.
- [168] S. Hoogendoorn, S. Ossen, M. Schreuder and B. Gorte, "Unscented particle filter for delayed car-following models estimation," *Proceedings of the IEEE Intelligent Transportation Systems Conference*, pp. 1598-1603, 2006.
- [169] S. Ossen and S. Hoogendoorn, "Calibrating car-following models using microscopic trajectory data," Delft University of Technology, Delft, Netherlands, 2008.
- [170] V. Punzo, M. Montanino and B. Ciuffo, "Do we really need to calibrate all the parameters? variance-based sensitivity analysis to simplify microscopic traffic flow models," *IEEE Transactions on Intelligent Transportation Systems*, vol. 16, no. 1, pp. 184 - 193, 2015.
- [171] R. van der Merwe, A. Doucet, J. F. de Freitas and E. Wan, "The unscented particle filter, Technical Report CUED/F-INFENG/TR 380," Cambridge University Engineering Department, 2000.
- [172] M. S. Arulampalam, S. Maskell, N. Gordon and T. Clapp, "A tutorial on particle filters for online nonlinear/non-Gaussian Bayesian tracking," *IEEE Transactions on Signal Processing*, vol. 50, no. 2, pp. 174-188, 2002.
- [173] H. U. Voss, J. Timmer and J. Kurths, "Nonlinear dynamical system identification from uncertain and indirect measurements," *International Journal of Bifurcation and Chaos*, vol. 14, no. 6, pp. 1905-1932, 2004.
- [174] R. Isermann, "Process fault detection based on modeling and estimation methods-A survey," *Automatica*, vol. 20, no. 4, p. 387-404, 1984.
- [175] V. Venkatasubramanian, R. Rengas, K. Yinc and S. N. Kavurid, "A review of process fault detection and diagnosis: Part I: Quantitative model-based methods," *Computers & Chemical*

*Engineering*, vol. 27, no. 3, p. 293–311, 2003.

- [176] P. M. Frank, S. X. Ding and T. Marcu, "Model-based fault diagnosis in technical processes," *Transactions of the Institute of Measurement and Control*, vol. 20, no. 1, pp. 57-101, 2000.
- [177] K. Jiwon and H. S. Mahmassani, "Correlated parameters in driving behavior models: Car-following example and implications for traffic microsimulation," *Transportation Research Record*, no. 2249, pp. 62-77, 2011.
- [178] R. van der Merwe , A. Doucet, N. de Freitas and E. Wan, "The Unscented Particle Filter," 2000. [Online]. Available: <http://www.cs.berkeley.edu/~jfgf/papers/upfnips.ps.gz>. [Accessed 2015].
- [179] D. Begg, "A 2050 vision for London-what are the implications of driverless transport?," *Transport Times London*, London, 2014.
- [180] P. Zwaneveld and B. van Arem, "Traffic effects of automated vehicle guidance systems," Department of Traffic and Transport, Delft University, Delft, Netherlands, 1997.
- [181] J. Bierstedt and et al., "Effects of next generation vehicles on travel demand and highway capacity," Jan 2014. [Online]. Available: [http://orfe.princeton.edu/~alaink/Papers/FP\\_NextGenVehicleWhitePaper012414.pdf](http://orfe.princeton.edu/~alaink/Papers/FP_NextGenVehicleWhitePaper012414.pdf). [Accessed 2015].
- [182] United States Environmental Protection Agency, [Online]. Available: <http://www.epa.gov/otaq/sftp.htm#cycles>.
- [183] D. E. Goldberg, *Genetic Algorithms in Search, Optimization & Machine Learning*, Addison-Wesley Professional, 1989.
- [184] M. Mamouei, I. Kaparias and G. Halikias, "A quantitative approach to the behavioural analysis of drivers in highways using particle filtering," *Transportation Planning and Technology*, vol. 39, no. 1, pp. 78-96, 2016.

## **Appendix – A quantitative approach to behavioural analysis of drivers in motorways using particle filtering**

The analysis of driving behaviour is a challenging task in the transport field that has numerous applications, ranging from highway design to micro-simulation and the development of advanced driver assistance systems (ADAS). There has been evidence suggesting changes in the driving behaviour in response to changes in traffic conditions, and this is known as adaptive driving behaviour. Identifying these changes and the conditions under which they happen, and describing them in a systematic way, contributes greatly to the accuracy of micro-simulation, and more importantly to the understanding of the traffic flow, and therefore paves the way for introducing further improvements with respect to the efficiency of the transport network. In this paper adaptive driving behaviour is linked to changes in the parameters of a given car-following model. These changes are tracked using a dynamic system identification method, called particle filtering. Subsequently, the dynamic parameter estimates are further processed to identify critical points where significant changes in the system take place.

### **1. Introduction**

A look at the more than six-decade-long body of studies on micro-simulation points to the difficulty of representing the dynamics of driving under different traffic conditions and for different drivers by a single mathematical equation. There have been studies reporting that the behaviour of different drivers is best represented using different model structures (Punzo and Simonelli 2007, Ossen and Hoogendoorn 2007), which in essence means that different drivers drive according to different models. Furthermore, individual drivers also exhibit different driving patterns in different traffic conditions, a

phenomenon that has been identified by many researchers (Munoz and Daganzo 2002, Ma and Andréasson 2007, Hoogendoorn, et al. 2006). The very fact that the calibration of car-following models is highly dependent on the driving condition, as confirmed by numerous studies (such as Punzo and Simonelli (2007), Ossen and Hoogendoorn (2008) and Kesting and Treiber (2009)) is further testimony of the existence of this phenomenon.

Much research has partly addressed the issue of adaptive driving behaviour by developing multi-regime car-following models, which are able to achieve greater accuracy in the reproduction of the driving behaviour. Notable examples include the models proposed by Wiedemann (1974), Yang and Koutsopoulos (1996) and Fritzsche (1994), implemented in the VISSIM, MITSIM, and Paramics micro-simulation software tools, respectively. However, while the passive reproduction of driving behaviour is a significant improvement, important questions that remain open are whether it is possible to actively identify the conditions under which changes in driving behaviour happen, and in what way these conditions may be affecting the driving behaviour. As a matter of fact, being able to identify and represent the drivers' adaptive behaviour in micro-simulation would bring about even greater improvements in terms of modelling accuracy and would deliver a better insight into the traffic flow.

Some previous research in the direction of identifying and modelling adaptive driving behaviour exists. Notably, Ma and Andréasson (2007) used data collected from an instrumented vehicle to identify different regimes of driving and applied a fuzzy clustering method to a combination of accelerations and velocities of lead and follower vehicles, as well as to their spacing, in order to group the data into different regimes. Thiemann, Treiber and Kesting (2008) calculated probability density functions for headways from a large dataset of vehicle trajectories and identified a significant correlation between the headway and driving-behaviour-related variables, such as speed, approach speed and traffic condition. Treiber, Kesting and Helbing (2006) proposed a general adaptation method that can be integrated within a wide range of

car-following models, which essentially states that the headway in smooth traffic flow increases linearly with variations in the local traffic conditions; a measure for representing these variations was then given, and the model was calibrated empirically using data from a Dutch highway. And Hoogendoorn et al. (2006) used a method called particle filtering to calibrate two car-following models dynamically (the Gazis-Herman-Rothery (GHR) and the Helly models), which allowed the model parameters to vary at each time instance in order to minimise the estimate error, as opposed to static system identification methods requiring the whole set of time series data to be used to find the single set of parameters resulting in least error.

Building on the work of Hoogendoorn et al. (2006), the aim of the present study is to investigate the possibility of utilising particle filtering for purposes beyond the simple demonstration of variations in model parameters. Specifically, the main objective is to analyse whether a link between changes in the model parameters and external stimuli or driving conditions can be established. Deriving a conclusion in this regard will deliver two significant benefits: on one hand, such information will help gain a better insight into traffic dynamics and dynamic driving behaviour, with corresponding improvements in micro-simulation modelling; on the other hand, it will enable the assessment of the capabilities of car-following models on the basis of the robustness of their parameter estimates and of their ability in accounting for different driving phenomena. For instance, if a car-following model fails to account for a certain driving phenomenon, this deficiency will exhibit itself in the form of systematic changes in the model parameter estimates, when the phenomenon becomes present.

The rest of this paper is organised as follows: the background of the study, including an overview of previous relevant work on the topics of car-following models, calibration methods and particle filtering is given in Section 2. Section 3 presents the application of particle filtering to a simulated dataset and proposes a simple method for the discretisation of the dynamic parameter estimates, so as to facilitate the identification and analysis of dynamic driving behaviour. Section 4 then applies the

proposed method on a vehicle trajectory dataset from a real highway and discusses the results. Finally, Section 5 summarises the conclusions and identifies areas of future work.

## **2. Background**

Car-following models, and acceleration models in general, describe the behaviour of human drivers. These models, integrated in simulation software, are used to assess policy-making in various fields related to transport networks, ranging from highway design to the evaluation of advanced driver assistance systems (ADAS). However, not all of these models are developed for the same purpose, and different levels of accuracy might be required accordingly, and so different car-following models may best serve different purposes. A large number of car-following models have been developed over several decades, and comprehensive reviews of the topic are given by Brackstone and McDonald (1999) and by Ahmed (1999).

System identification is an important aspect for car-following models, as such models may describe the structure of the stimuli-response processes underlying the car-following behaviour in a mathematical form, but they need to be adjusted and tailored if they are to be applied in a specific scenario. This may be done through calibration using an appropriate dataset. In this section, the Intelligent Driving Model (IDM) car-following model, used in this work, is presented, followed by a discussion of some of the considerations related to calibration that need to be made, and by a brief description of the particle filtering method.

### **2.1 The IDM car-following model**

The IDM car-following model is selected for the present study on the basis of a number of advantages that it presents over other models. Namely, in addition to being computationally simple and relying only on a small number of parameters, each with an intuitive meaning, the IDM has also been found to perform well in terms of both macroscopic and microscopic calibration (Treiber, Hennecke and Helbing 2000, Treiber

and Kesting 2013, Punzo and Simonelli 2007). Numerous studies on different aspects of the IDM have been carried out, including calibration, stability and other microscopic and macroscopic properties, and the advantages have been confirmed (Wilson and Ward 2011, Kesting and Treiber 2009).

The IDM is given by the following general equation:

$$\dot{v} = a \left[ 1 - \left( \frac{v}{v^d} \right)^\delta - \left( \frac{s^*(v, \Delta v)}{s} \right)^2 \right], \quad (1)$$

$$s^*(v, \Delta v) = s_0 + s_1 \sqrt{\frac{v}{v^d}} + T v + \frac{v \Delta v}{2\sqrt{ab}},$$

$$\Delta v = v - v_p,$$

which calculates the value of the output variable  $\dot{v}$ , denoting the acceleration of the subject vehicle, as a function of the following input variables: the speed of the subject vehicle  $v$ ; the speed of the preceding vehicle  $v_p$ ; and the distance headway  $s$ . The model is then also dependent on a number of parameters, including: the maximum acceleration  $a$ ; the desired speed  $v^d$ ; the acceleration exponent  $\delta$ ; the jam distances in fully-stopped and in high-density traffic  $s_0$  and  $s_1$  respectively; the safe time headway  $T$ ; and the comfortable deceleration  $b$ .

## 2.2 Calibration of car-following model

Many factors must be taken into account in the calibration of a car-following model, including the choice of the dataset, the calibration method employed and the purpose for which the calibrated model is to be used. When a certain level of accuracy in the collective behaviour or traffic flow is required to reproduce the same flow-density characteristics as observed in the real data, a certain set of model parameters for a given car-following model may work best (Treiber, Hennecke and Helbing 2000). However, for the different purpose of modelling microscopic behaviour of individual

drivers, including details such as the velocity and spacing of individual vehicles, another set of model parameters may work best, which would be different from the former (Treiber and Kesting 2013). Even for the same driver, significant inconsistencies between the calibration results with different trajectory data can be found. This means that if one intends to reproduce accurate trajectories for a given driver in a specific driving condition on a specific highway (e.g. upstream of a bottleneck, taking into account the traffic flow and density, weather conditions, etc.), the data used for the calibration must match the specific scenario under investigation in terms of traffic characteristics.

Even excluding the question of intra-driver inconsistencies, this gives rise to the so called phenomenon of over-fitting, which means that the model is so accurately adapted to a given specific scenario that it loses its generality, delivering inaccurate results even for very slight variations in the driving scenario. Over-fitting means that the resulting model is rendered unreliable for making any predictions, which makes the trade-off between accuracy and robust calibration evident. Other considerations regarding calibration include the choice of error measurement (e.g. travel time, spacing, velocity, acceleration), system identification method (e.g. Maximum-Likelihood Estimation (MLE), Least Squares Estimation (LSE), nonlinear optimisation methods), and error tests (e.g., Root Mean Square error (RMSE), Root Mean Square Percentage error (RMSQe), and Theil's inequality coefficient (U)). Comprehensive reviews of some of these considerations have been carried out by Punzo and Simonelli (2007), Ossen and Hoogendoorn (2008), Treiber and Kesting (2013), and Ranjitkar, Nakatsuji and Asano (2004).

### **2.3 Particle filtering**

Sequential Monte-Carlo filtering or particle filtering (PF) can be used to tackle the difficulty associated with the estimation of states or parameters in nonlinear, non-Gaussian filtering. The state-space representation of such a system is denoted below:

$$x_t = f(x_{t-1}, v_{t-1}), \quad y_t = h(u_t, x_t, n_t) \quad (2)$$

where  $x_t$  is the state of the system that evolves under the nonlinear function  $f(\cdot)$ . The previous state of the system is denoted by  $x_{t-1}$ , and  $v_{t-1}$  is an independent and identically distributed (i.i.d) random noise, that is known as the process noise. The true state of the system is almost always hidden from the observer, however one can deduce a good estimate of it through successive observations and measurements  $\{y_t, t \in \mathbb{N}\}$ . This, in fact, is the ultimate purpose of filtering. These observations are dependant on the control input  $u_t$ , the true state of the system  $x_t$ , and an i.i.d noise  $n_t$ , known as the measurement noise. This dependency is denoted by the function  $h(\cdot)$ .

The method of PF is based on the principles of Bayes theorem, which provides a mechanism for updating knowledge about the underlying system upon receipt of new data on the observed states of the system at each time instance. In Bayesian estimation, the quantity of interest is the probability distribution function of the state variable given the sequence of observations made  $p(x_t | y_{0:t})$ , which is known as the posterior distribution.

In algorithms such as the Kalman Filter and the Extended Kalman Filter, the following two assumptions are made: the system is linear, or a locally linearised system provides a good enough approximation (in the case of EKF); and the underlying noise is Gaussian. Under these assumptions the characteristics of the posterior, namely the mean and covariance, can be optimally derived. The term optimal in this context means that the resulting estimator leads to Minimum Mean-Square Error (MMSE). However, when the system of interest exhibits highly nonlinear behaviour and the noise is non-Gaussian, the performance of KF and EKF deteriorates.

PFs provide an alternative way to linearisation and holding assumptions about the underlying noise distribution. In these methods a number of samples, that are referred to as particles, are propagated through the nonlinear system using simulation

techniques, and then these samples are used to extract the characteristics of the posterior. An important step in this method is importance sampling, where an estimate of the ratio below is calculated:

$$w_t = \frac{p(y_{1:t}|x_{0:t})p(x_{0:t})}{q(x_{0:t}|y_{1:t})}, \quad (3)$$

where  $w_t$  is the importance weight,  $p(y_{1:t}|x_{0:t})$  is the conditional probability of the observations  $y$  given the states  $x$ ;  $p(x_{0:t})$  is the probability distribution of states; and  $q(x_{0:t}|y_{1:t})$  is a known, easy-to-sample proposal distribution.

A sequential relationship for the importance weight can be drawn, as shown by van der Merwe, et al. (2000), namely:

$$w_t = w_{t-1} \frac{p(y_t|x_t)p(x_t|x_{t-1})}{q(x_t|x_{0:t-1}, y_{1:t})}, \quad (4)$$

which gives rise to the popular choice of the proposal distribution

$$q(x_t|x_{0:t-1}, y_{1:t}) = p(x_t|x_{t-1}), \quad (5)$$

which results in the simplification of equation (4).

In PF the estimate of the posterior is based on a number of randomly selected weighted samples. The great potential of this method in dealing with complex nonlinear non-Gaussian systems has been pointed out by van der Merwe et al. . (2000) and by Arulampalam et al. (2002), and a schematic representation is given in Figure 1. At the first step of the algorithm (sampling)  $N$  random particles (samples) are drawn from a proposal distribution. These particles are then propagated through the nonlinear system and are subsequently associated with weights  $\tilde{W}$  according to their fitness, i.e. equation (4). This step is known as importance sampling. Subsequently, a resampling of particles with respect to their associated weights is carried out, as a result of which particles with high weights are split into a number of unweighted particles and particles with low weights are eliminated. Finally, the introduction of a

random noise to the group of particles at the third step results in local variety in the samples. This process is visualised in the fourth row of particles in Figure 1. Since, this step provides an unweighted distribution of particles that mimic the prior distribution, it is referred to as the prediction step.

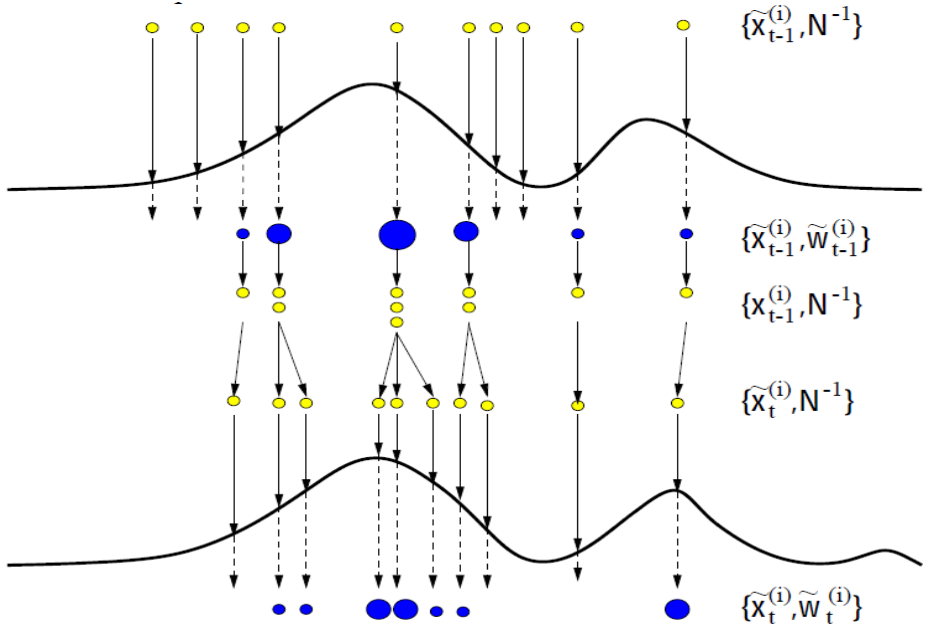


Figure 1. Illustration of the three stages of importance sampling, resampling, and prediction in PF, figure from van der Merwe et al. (2000).

In the present study, the application of PF for parameter tracking is of particular interest. Given a car-following model and a set of data, one can update the estimates of model parameters upon the receipt of new data. As a result, one will obtain time-varying estimates of the model parameters. Naturally, these time-varying estimates cannot be used for modelling and simulation purposes, but they can provide a good insight into some of the very important model characteristics that may otherwise remain hidden in cumulative error terms. In particular, in simulation-based applications the parameters are constant, and hence the use of a parameter tracking method gives information about how a model parameter should deviate from its nominal value to compensate for modelling flaws. This concept is closely related to model-based fault detection (Isermann 1984, Venkatasubramaniana, et al. 2003).

There is a possibility that in some cases general patterns in changes of the model parameters are observed (e.g. significant increase or decrease in the value of a model parameter in an identifiable driving phase), and this type of information can then be used to improve the quality of modelling and simulation.

### **3. Methodology**

In this section PF is applied to simulated data to investigate the extent to which the properties of the adaptive driving can be identified using this method. The section first introduces the simulated dataset, and then goes on to present the results of the application. The choice of the objective function for the calibration is also described, and a simple method for the discretisation of the estimates is proposed. The discretisation of the dynamic estimates is an important step in the interpretation of the raw estimates obtained initially and in the linkage of the changes in the model parameters to the traffic conditions.

#### **3.1 Simulated dataset**

In this section the application of particle filtering to simulated data is investigated to illustrate the extent to which this method can be utilised for the purpose of “meaningful” parameter tracking in car-following models. The additional constraint arising from the term “meaningful” refers to the fact that, sometimes by calibrating a number of model parameters simultaneously, an error in the estimate of one model parameter may be compensated by an error in another. This could happen due to the existence of correlation between model parameters and the fact that the information available is less than what is required for the determination of the unknowns uniquely, thus causing erroneous tracking of model parameters.

For the data simulation, the trajectories of a specific vehicle from the enhanced NGSIM I-80 dataset (Montanino and Punzo 2013) were selected. The NGSIM I-80 dataset is an open source trajectory data that has been collected from a 500-m long stretch of an interstate freeway in the San Francisco Bay area, CA (Halkias and Colyar

2006), and the enhanced dataset has been made available by the MULTITUDE project (Montanino and Punzo 2013). The selected trajectories were then used to generate trajectories for follower vehicles with the IDM model proposed by Treiber, Hennecke and Helbing (2000), and a specific parameter profile was used for this purpose. In the profile used, certain parameters were varied at certain points in time, and particle filtering was applied to the simulated trajectories to generate dynamic estimates of the model parameters. Figure 2 illustrates the trajectories used for the leader vehicle.

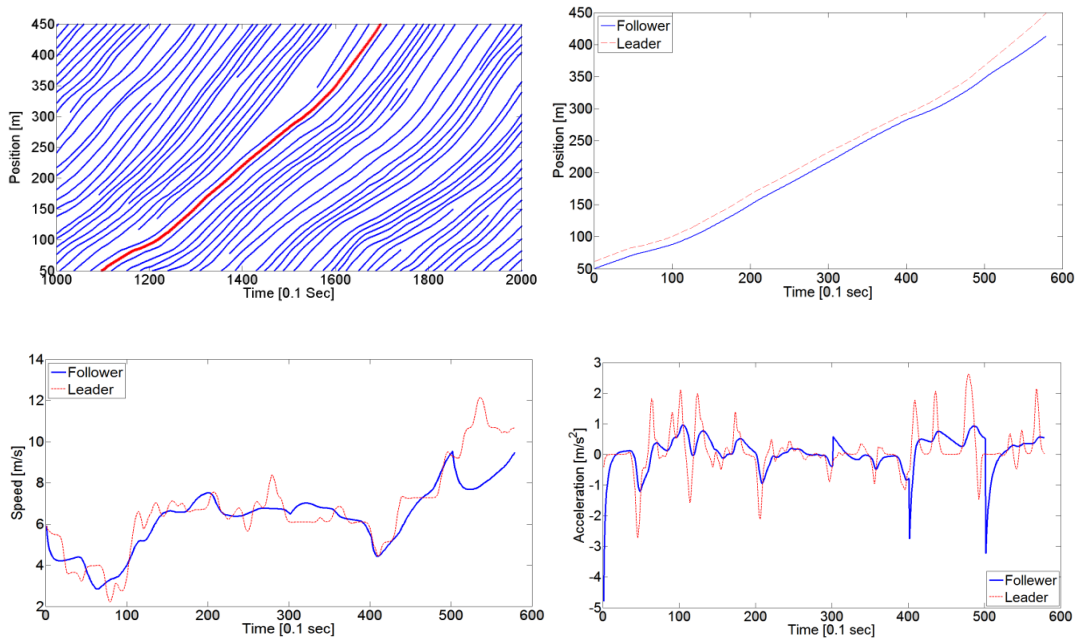


Figure 2. a) Trajectory of the lead vehicle selected from NGSIM data Lane 2 b,c,d) Position trajectories, velocities, and accelerations of the lead vehicle and synthesized follower in dashed red line and blue line respectively.

The parameter profiles used for the simulation of the trajectories shown were as follows: the default model parameters reported by Treiber, Hennecke and Helbing (2000) were used up to Time = 30 s, i.e.  $a = 0.73 \frac{m}{s^2}$ ,  $b = 1.67 \frac{m}{s^2}$ ,  $v_d = 33.3 \frac{m}{s}$ ,  $\delta = 4$ ,  $s_0 = 2 m$ ,  $s_1 = 0 m$ , and  $T = 1.6 s$ ; then, at  $t = 30 s$ , the following parameters were changed to the given values:  $b_0 = 1.5 \frac{m}{s^2}$ ,  $a_0 = 1 \frac{m}{s^2}$ ,  $v_d = 60 \frac{m}{s}$ ,  $T = 0.5 s$ . As such, the simulation includes the case of having erroneous estimates for some of the model

parameters while another one is being tracked. Additionally, the value of the parameter  $T$  changes again to the values  $T = 1$  s and  $T = 3$  s at time points  $t = 40$  s and  $t = 50$  s, respectively.

### 3.2 Sensitivity analysis

One important consideration in the model calibration is addressing the question of how the dataset used reflects the characteristics of the model parameters. This is especially of importance in models, such as IDM, where some degree of orthogonality between model parameters exists, and different model parameters are best set according to different types of data in different regimes of driving (Treiber and Kesting 2013). If this question is not addressed, misleading estimates of model parameters or unnecessary high computational complexity may result (Ciuffo, Punzo and Mon 2014).

Global sensitivity analysis is used for this purpose, and the more representative “total sensitivity indices” are used, that capture the impact of parameters across all the feasible region in the hyperspace of parameter values (Ciuffo, Punzo and Mon 2014, Saltelli, et al. 2010, Jacques , Lavergne and Devictor 2006). Figure 3 illustrates the results for total sensitivity as a function of the number of samples used for the same trajectory as above. As expected, the results for other vehicles were also found to be consistent with the ones illustrated, as well as those reported by Ciuffo, Punzo and Mon (2014). The parameter related to headway,  $T$ , has the highest impact with a total sensitivity index value of 0.788, and the parameter related to spacing in jam traffic,  $s_0$ , has the second highest impact, with a total sensitivity index value of 0.268. The rest of the indices have values very close to zero and can be seen as a horizontal line roughly coinciding with the x-axis. The upper boundary (UB) and lower boundary (LB) values for parameters are given in Table 1.

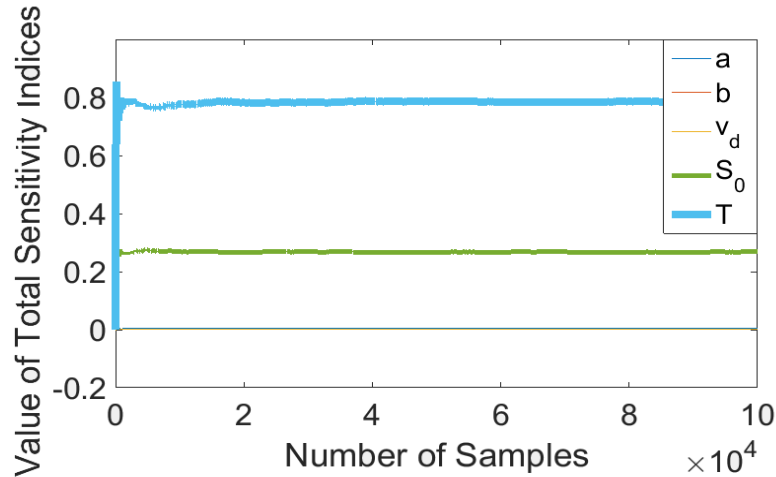


Figure 3. Total sensitivity indices for the simulation scenario.

Table 1. Lower and upper bound values of the model parameters in the global sensitivity analysis.

Parameters	LB	UB
$a$	1	3
$b$	1	3
$V_d$	20	50
$s_0$	2	10
$T$	0.5	3

As pointed out by Ciuffo, Punzo and Montanino (2014), since the assumption of parameter independence for such models is unlikely to hold, the results may be subject to bias. Nonetheless, the conclusions were also verified through a local sensitivity analysis around the calibrated parameter values, as well as through investigation of the use of different parameter values and different combinations thereof for parameter tracking. Furthermore, an additional justification to the choice of the parameter used in this study is the physical meaning of it.

### 3.3 Application of particle filtering to simulated data

Figure 4 shows the results of the application of particle filtering to the simulated dataset. For this purpose, all of the model parameters are set to their default values, except for parameter  $T$ , which is to be estimated dynamically.

As was seen, a reason for focusing on T in parameter tracking is that it was found that no other parameter was capable of tracking the changes in driving behaviour for multiple trajectories when selected alone. Also, variations in this model parameter remain low compared to other model parameters. Furthermore, one of the advantages of IDM is that the parameters have intuitive meanings, and if one parameter is to be selected among others representing comfortable deceleration, maximum acceleration, desired velocity, etc., the choice of parameter T, representing headway, is most sensible. This parameter was also used in Treiber, Hennecke and Helbing (2000) to generate variations in traffic conditions, and hence driving behaviour, and by doing so the empirical data related to the formation of traffic jams were successfully simulated.

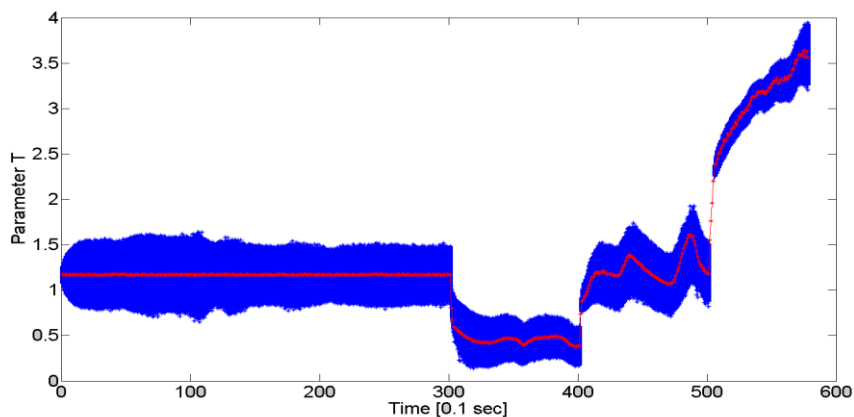


Figure 4. The result for estimation of the parameter T. The blue shadow denotes the distribution of particles at each time instance while the red curve is the selected particle.

It can be seen that up to time  $t = 30$  s, the estimation of parameter T is almost error-free and stable. Also, the subsequent changes at the times  $t = 30$  s,  $t = 40$  s, and  $t = 50$  s can be identified from Figure 4 by “jumps” in the values of the parameter at these times, compared to the smooth curves in the intervals between the changes. The estimations of parameter T at times after  $t = 30$  s, unlike before, are unstable and fluctuate around a certain value. This is due to the fact that beyond time  $t = 30$  s, other model parameters were changed to values other than the ones used in the

estimation process. As a result, the effect of this false estimation needs to be compensated by overestimations and underestimations of parameter T.

Using the parameter estimation given by the application of particle filtering (Figure 4), an almost perfect estimation of the spacing ( $R^2 = 0.995$ ), velocity ( $R^2 = 0.993$ ) and acceleration ( $R^2 = 0.91$ ) can be derived, despite the errors in the other model parameters from  $t = 30$  s onwards). This is shown in Figure 5.

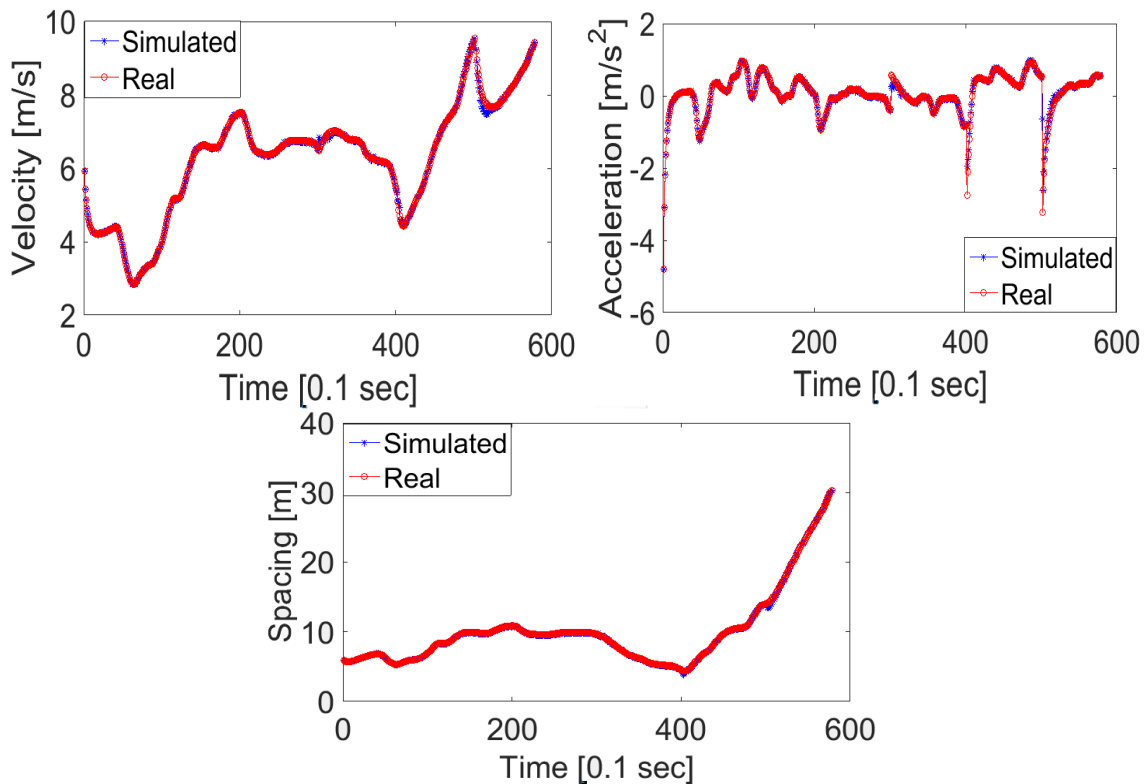


Figure 5. The comparison of real trajectories with simulated trajectories when the dynamic estimation of the parameter T, given by particle filtering, is used.

It should be noted that the IDM car-following model was used to generate trajectories for the follower vehicles, and the same car-following model was used in the calibration process. In the application to real data, this is the equivalent of assuming knowledge of the model underlying the behaviour of human drivers. Although this is obviously not the case, the findings of Ossen and Hoogendoorn (2008) may justify use of such simulated data. Therein, it was found that the characteristics of

the followers' behaviour can be recovered by calibrating a car-following model to the data, even when the real model is different to the model used for calibration.

### **3.4 Objective function**

The objective function defines a measure of error that is intended to be minimised. For this purpose, one needs to choose among measures of performance (MOPs), such as spacing, speed, and acceleration, in addition to an appropriate error test (functional form of the defined error), such as root mean square error (RMSE) and root mean square percentage error (RMSPe), as outlined in numerous studies in the literature (Punzo and Simonelli 2007, Ossen and Hoogendoorn 2008, Treiber and Kesting 2013, Ranjitkar, Nakatsuji and Asano 2004).

In Punzo and Simonelli (2007) the inter-vehicle spacing was suggested as the most reliable MOP. In this work, however, it was found that the best result is obtained when a combination of errors on spacing, velocity, and acceleration was used in the objective function instead of a single variable. This is due to the use of the information available on all variables, which avoids outliers and non-smooth modelled data in any of the three measures individually. In Ossen and Hoogendoorn (2008), in addition to the different variables for calibration, the use of a combination of speed and spacing in the objective function was investigated. Therein, despite the fact that the use of a combinatory objective function including both the spacing and the velocity was found to be dependent on the specific model used, it was concluded that when such prior information about the model is lacking, the use of an objective function including both speed and spacing could be advantageous. Here, a uniformly weighted sum of squared errors of all three variables was used, which is an extension to the suggestion made by Ossen and Hoogendoorn (2008). The accuracy of the acceleration trajectories in the NGSIM data is somewhat questionable, as pointed out by Thiemann, Treiber and Kesting (2008), but excluding the acceleration error between the predicted values and the real values from the objective function results in randomly fluctuating estimates of acceleration with unrealistically large values of jerk. This can be avoided by including

the acceleration error in the objective function with a low weight to suppress the significant influence of these inaccurate data on the estimation process. Figure 6 illustrates the simulated acceleration trajectory when the acceleration error is excluded from the objective function. Although in this case a slight improvement in the simulated velocity and spacing trajectories is obtained, this improvement comes at the cost of the acceleration, as can be seen from the figure.

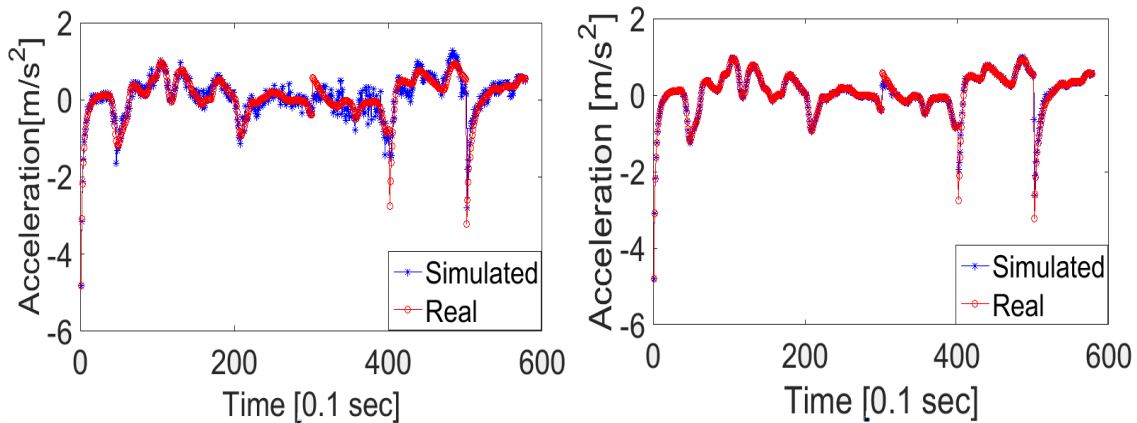


Figure 6. Comparison of the simulated accelerations with the real values when the acceleration error is: a) excluded from the objective function; b) included in the objective function.

### 3.5 Interpreting dynamic parameter estimations

As was shown in Figure 4, although the “jumps” in the values of the model parameters are visually identifiable, the resulting estimates are much harder to interpret when the method is applied to real data. This makes the identification of the points where sudden changes in the model parameters take place difficult, which is due to two reasons: 1) the actual underlying model is not known in advance; and 2) the changes are much smaller but more frequent. As one would expect from human drivers, they do not drive in a crisp and deterministic fashion, and neither do they immediately change their underlying driving attributes as soon as they reach a different traffic condition; instead a smooth and gradual change in driving behaviour is to be expected from them.

Hence, a way to identify significant changes and to filter out the smooth fluctuations from the dynamic model parameter estimate is required. A simple approach is adopted here for this purpose, whereby the points where maximum changes in the subsequent values of the parameter under estimation are identified. These points are referred to as “breaking points”. Following that, the model parameter under investigation is separately calibrated for each interval between the breaking points.

The detection of breaking points is governed by two conditions, both of which must hold for a breaking point to exist:

- 1) The change in the value of model parameter is greater than a certain value, set to be 0.5 *sec* for parameter  $T$  here.
- 2) The distance between each two breaking points is greater than a certain value. This condition is imposed to avoid frequent changes of the parameter in a short interval, and its implementation may also be justified by the fact that frequent and sudden changes in driving behaviour and driving parameters in a short time interval are highly unlikely among human drivers. The value of 5 seconds (50 time steps for the NGSIM dataset) is used here.

The application of the proposed discretisation method to the result illustrated in Figure 4 leads to the correct identification of the jumps. Subsequently, parameter  $T$  is recalibrated in separate time intervals: [0, 300], [300, 400], [400, 500], and [500, 600]. Figure 7 shows the promising results obtained using this method.

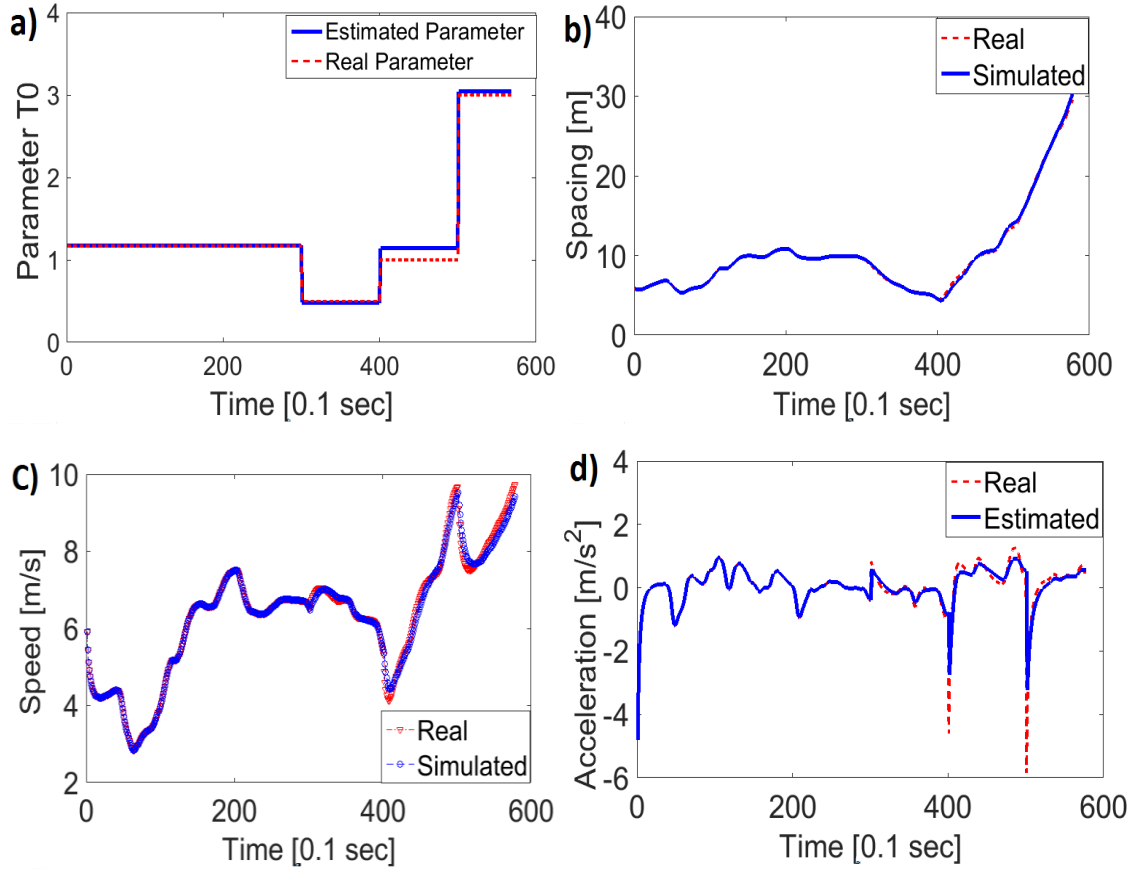


Figure 7. Comparison of the simulated trajectories when averaging between the breaking points is applied with real results for: a) the estimation of parameter T; b) spacing; c) speed; d) acceleration.

It can be seen that not only the points where the parameter is changed are identified correctly, but also that the values of the parameter within corresponding intervals are estimated with very high accuracy. Hence, the acceleration, velocity, and spacing trajectories are generated with significantly better accuracy than any conventional calibration method.

#### 4. Results

In the previous section it was shown that using the particle filtering along with the proposed discretisation method, the changes in the model parameters can be identified and consequently the changes in the driving behaviour can be captured. In

this section, this method is applied to the NGSIM trajectory dataset to investigate the question of the identification of the adaptive driving behaviour.

#### 4.1 Application to the NGSIM dataset

The functionality of the proposed method was illustrated using simulated data. In this section the proposed method is applied to a platoon of nine vehicles driving in the second lane to investigate the following two issues: 1) whether the assumption of systematic changes in driving attributes can be validated; and 2) whether these changes can be identified using car-following models, such as the IDM, and a dynamic system identification method, such as particle filtering. The procedure is as follows:

1. The five model parameters  $\{a, b, v_d, s_0, T\}$  are calibrated using a genetic algorithm to minimise the sum of squared errors across all the three variables, namely, spacing, speed, and acceleration (Equation 6).

$$U = \sum_{i=1}^n \left( (s_i^{obs} - s_i^{model})^2 + (v_i^{obs} - v_i^{model})^2 + (a_i^{obs} - a_i^{model})^2 \right) \quad (6)$$

where: the abbreviations “obs” and “model” denote the observed value and the modelled value respectively;  $n$  is the number of sample points; and  $s$ ,  $v$ , and  $a$  denote the spacing, velocity, and acceleration respectively. The objective function above is the sum of the squared Euclidean distances between the three-dimensional observed states and the modelled states.

2. At the second step, the parameters  $\{a, b, v_d, s_0\}$  are fixed to their calibrated values, while parameter  $T$  is being tracked given the lead vehicle’s trajectory and the real trajectory of the follower vehicle. The calibrated values for all the vehicles in the platoon are reported in Table 2.

3. The dynamic estimates of parameter  $T$  in several runs are then analysed using the method described in Section 3.5 to identify the breaking points.
4. Once the breaking points are identified, parameter  $T$  is then calibrated once more for each time interval between the breaking points.

Table 2. The calibrated values of the parameters

Parameters	V348	V343	V354	V362	V368	V378	V381	V391
$a$	1.598	0.886	1.620	1.688	2.681	0.815	0.824	1.087
$b$	5.000	0.602	5.000	5.000	0.500	1.509	0.500	5.000
$V_d$	11.412	33.298	12.903	10.000	33.300	33.298	33.299	15.929
$s_0$	1.000	2.529	5.000	3.319	4.843	4.848	3.164	1.000
$T$	1.094	0.400	1.952	0.903	0.881	0.400	0.695	1.146

All the vehicles observed remain in the platoon for the whole duration of the experiment, which means that the dynamics are undisturbed by any lane changing attempts. Figure 8 illustrates the application of the proposed method to one of the vehicles, and the top-left graph illustrates the discretised parameter estimate.

It should be noted that when applied to the dynamic parameter estimates for real trajectories, the proposed discretisation method yields breaking points that are less robust compared to the investigated case of simulated data. In other words, the breaking points are not always uniquely identified, and while some are detected with a high level of certainty, others may only be detected in a small percentage of cases. Herein, only the points that were detected in more than 50% of cases were selected.

The discretised parameter profile is subsequently used to simulate the driving behaviour for the follower vehicle. The comparison of the simulated states (spacing, speed, and acceleration) with the real states points to the accuracy of the simulated behaviour. The reason why the acceleration estimates are less solid than the spacing

and speed estimates is due to the low weight of the acceleration variable in the objective function, as explained earlier.

An interesting finding of this work that can be identified from Figure 8, is the correlation between the estimate of parameter  $T$ , and speed. This will be explained further in the following section.

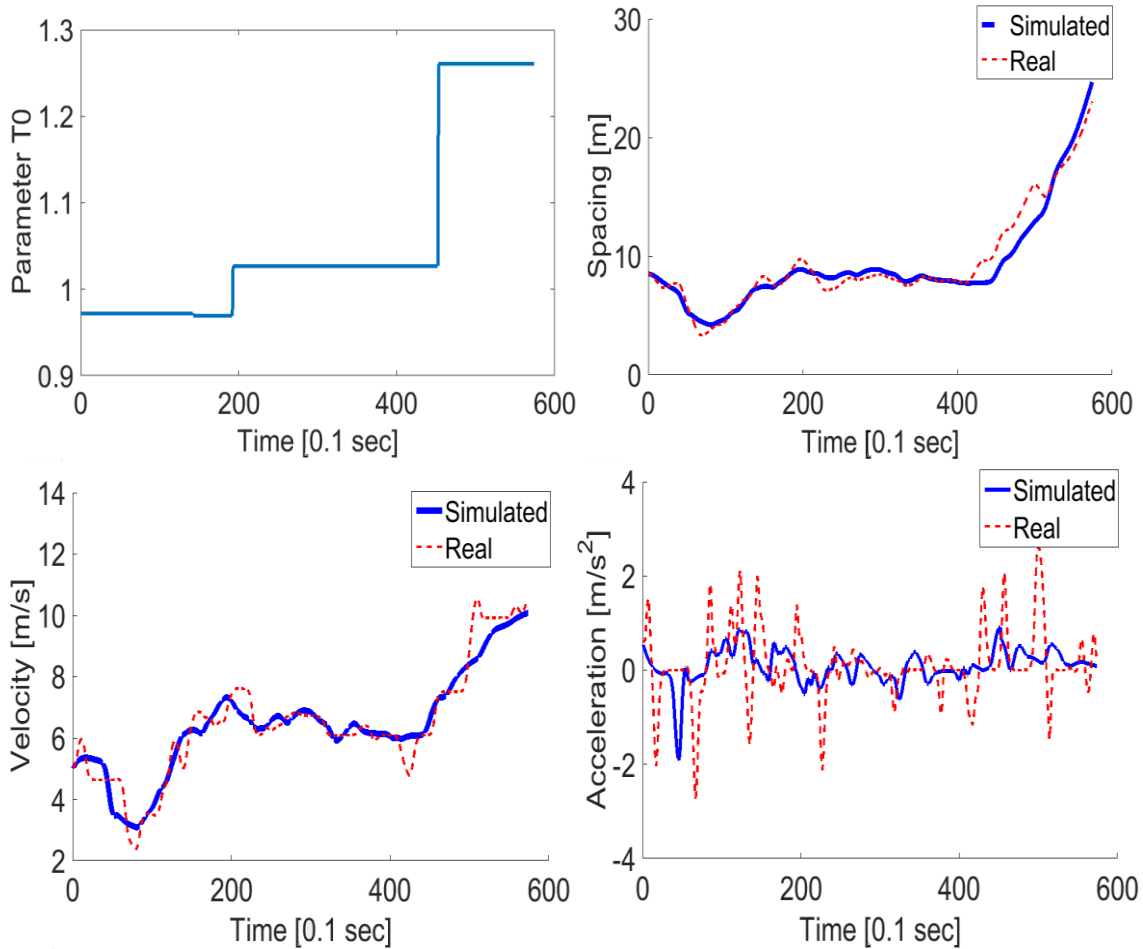


Figure 8. Trajectories resulting from application of the proposed method to vehicle no. 348 of the NGSIM data.

## 4.2 Analysis of the parameter estimates

Figure 9 illustrates the resulting parameter estimates for the vehicles, based on which highly accurate estimates of the spacing and velocity trajectories can be obtained.

Table 2 summarises the errors in the estimation of velocity and spacing.

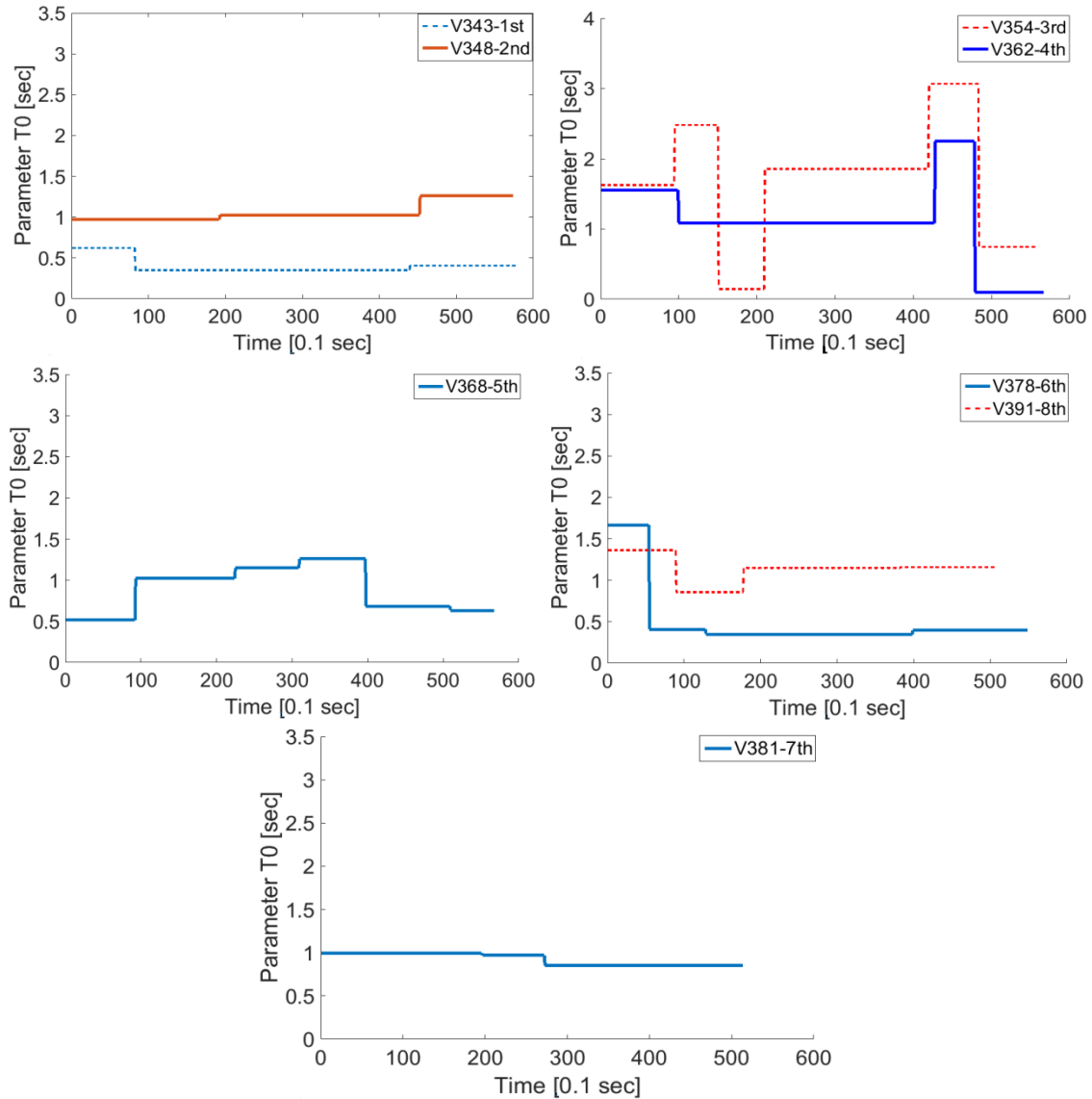


Figure 9. Parameter estimates for the eight vehicles following vehicle no. 329 in the NGSIM data. The position of each vehicle inside the platoon is specified in front of the vehicle ID no.

Table 3. Measures regarding quality of fit for each of the vehicles in the platoon

	V348	V343	V354	V362	V368	V378	V381	V391
Average absolute error for spacing	0.7366	0.8333	1.8907	1.0251	0.5108	0.7039	0.8268	1.7798
Average absolute error for speed	0.3885	0.5072	0.6117	0.5066	0.4249	0.5032	0.4805	0.6909

One of the interesting findings is that in the majority of investigated trajectories, a noticeable relationship between the average speed and estimate of parameter  $T$  can be observed. In particular, from the parameter estimates related to vehicles with IDs 348, 354, 362, and to a lesser extent 343, 378, 391, it can be seen that with the increases in the average speed, the estimate of parameter  $T$  increases, and that sudden drops in the average speed results in drops of parameter  $T$ . The detection of common patterns is an encouraging result, as it points to a driving phenomenon that the car-following model fails to account for.

However, interestingly, two other patterns can be observed within the estimates for this platoon: 1) the inverse relation with the average speed, as in the case of vehicle no. 368; and 2) irrelevant or no changes in the estimated parameter with respect to average speed, which is the case for vehicle no. 381. Similar patterns are observed in many other examined vehicles, and can be most likely be attributed to differences in driving styles, intentions (such as preparation for performing a lane change), or maybe a more complicated relation between the average speed and spacing, which could describe the changes in the model parameter better. Moreover interestingly, in a statistically significant number of cases, the breaking points are detected at a point in time where there has been a change in the driving conditions. For instance, considering the velocity profile of the vehicle no. 348 (Figure 8), it can be seen that the two breaking points identified correspond to points where: 1) there is a transition from driving through a shockwave into more homogeneous congested traffic, at about  $t = 20$  s; and 2) there is a transition from homogenous congested

traffic to a less congested state where the vehicle starts accelerating at about  $t = 43$  s.

It should be acknowledged here that, indeed, the random nature of driving may be amplified at low speeds and under stop-and-go conditions, and therefore decisive conclusions can only be made when sufficiently large numbers of suitable data are analysed. A suitable dataset for this purpose would be one consisting of trajectories with long observation times, where large enough numbers of drivers can be tracked through different driving conditions. The implementation of the proposed framework on such a dataset would enable the analysis and interpretation of the jumps in the parameter values in a broader perspective, and would allow the modification of the method and its parameters for better performance. The further investigation of these topics and the application of the method to more trajectories will shed more light on some of these issues.

## **5. Conclusion and future work**

In this paper, particle filtering was utilised to examine the dynamic behaviour of drivers in different traffic conditions. In order to interpret the estimates given by the particle filtering process, a simple discretisation method was used, and promising results from its application to simulated and real data were obtained. This helped isolate minor fluctuations, which could be due to the fuzzy and stochastic nature of human driving, or minor errors in the modelling of car-following behaviour, and to convert the raw estimates given by the particle filtering process to an interpretable form.

The application of this method to real data delivered interesting results. Specifically, for a large number of cases, an interesting relationship between average speed and the parameter under investigation was observed. This frequent pattern may point to a common driving behaviour that may not be addressed by the mathematical structure of the model under investigation. Moreover, two additional patterns were,

interestingly, observed: 1) an inverse relation with the average speed; and 2) no relation with average speed. Additionally, in a significant number of cases the points that were detected as breaking points seemed to be the ones where, indeed, a change in the driving condition took place. Therefore, the employed framework was found to have great potential in investigating the properties of traffic flow, as well as in examining the robustness and performance of car-following models.

In future work, the application of suitable clustering methods, such as consolidated fuzzy clustering (Ma and Andréasson 2007) will be considered for grouping the estimation results. Moreover, due to the stochastic nature of particle filtering, the values of the breaking points identified are subject to changes in consecutive runs. The uncertainty arising from this issue could be tackled by calculating confidence intervals for these values. Finally, in order to draw reliable conclusions about how driving behaviour may change with reference to car-following models, an analysis of larger groups of trajectory data needs to be carried out.

## References

- Ahmed, K. I. 1999. *"Modeling drivers' acceleration and lane changing behavior"* PhD diss. Massachusetts Institute of Technology/
- Arulampalam, M. S., S. Maskell, N. Gordon , and T. Clapp. 2002. "A tutorial on particle filters for online nonlinear/non-Gaussian Bayesian tracking." *IEEE Transactions on Signal Processing* 50, no. 2: 174-188.
- Brackstone, M., and M. McDonald. 1999. "Car-following: a historical review." *Transportation Research Part F: Traffic Psychology and Behaviour* 2, no. 4: 181–196.
- Ciuffo, B., V. Punzo, and M. Mon. 2014. "Global sensitivity analysis techniques to simplify the calibration of traffic simulation models. Methodology and application to the IDM car-following model." *IET Intelligent Transport Systems* 8, no. 5: 479 – 489.
- Fritzsche, H.T. 1994. "A model for traffic simulation." *Traffic Engineering and Control*: 317–321.

Halkias, John, and James Colyar. 2006. *NGSIM Interstate 80 Freeway Dataset*. Washington, DC, USA: US Federal Highway Administration, FHWA-HRT-06-137.

Hoogendoorn, S., S. Ossen, M. Schreuder , and B. Gorte. 2006. "Unscented Particle Filter for Delayed Car-Following Models Estimation." *Proceedings of the IEEE ITSC 2006 IEEE Intelligent Transportation Systems Conference*. Toronto, Canada.

Isermann, R. 1984. "Process Fault Detection Based on Modeling and Estimation Methods-A Survey." *Automatica* 20, no. 4: 387–404.

Jacques , J., C. Lavergne, and N. Devictor. 2006. "Sensitivity analysis in presence of model uncertainty and correlated inputs." *Reliability Engineering & System Safety* 91, no. 10-11: 1126–1134.

Kesting, A., and M. Treiber. 2009. "Calibrating Car-Following Models by Using Trajectory Data: Methodological Study." *Transportation Research Record: Journal of the Transportation Research Board* 2088: 148-156.

Ma, Xiaoliang , and I. Andréasson. 2007. "Behavior Measurement, Analysis, and Regime Classification in Car Following." *IEEE TRANSACTIONS ON INTELLIGENT TRANSPORTATION SYSTEMS* 8, no. 1: 144-156.

Montanino , M., and V. Punzo. 2013. "Making NGSIM Data Usable For Studies On Traffic Flow Theory." *Transportation Research Record*: 99-111.

Montanino, M., and V. Punzo. 2013. *Reconstructed NGSIM I80-1. COST ACTION TU0903 - MULTITUDE*. <http://www.multitude-project.eu/exchange/101.html>.

Munoz, J. C., and C. F. Daganzo. 2002. "MOVING BOTTLENECKS: A THEORY GROUNDED ON EXPERIMENTAL OBSERVATION." *Transportation and Traffic Theory in the 21st Century. Proceedings of the 15th International Symposium on Transportation and Traffic Theory*. Adelaide, Australia. 441-461.

Ossen , S., and S. Hoogendoorn. 2008. *Calibrating car-following models using microscopic trajectory data*. Delft, Netherlands: Delft University of Technology.

Ossen, S., and S. P. Hoogendoorn. 2007. "Car-following behavior analysis from microscopic trajectory data." *Transportation Research Record: Journal of the Transportation Research Board* Volume 1934 / 2005 Traffic Flow Theory 2005: 13-21.

Punzo, V., and F. Simonelli. 2007. "Analysis and comparison of microscopic traffic flow models with real traffic microscopic data." *Transportation Research Record: Journal of the Transportation Research Board* 1934, no. 1: 53-63.

Ranjitkar, P., T. Nakatsuji, and M. Asano. 2004. "Performance Evaluation of Microscopic Traffic Flow Models with Test Track Data." *Transportation Research Record: Journal of the Transportation Research Board* 1876 , no. 1: 90-100.

Saltelli, A., P. Annoni, I. Azzini, F. Campolongo, M. Ratto, and S. Taranto. 2010. "Variance based sensitivity analysis of model output. Design and estimator for the total sensitivity index." *Computer Physics Communications* 181, no. 2: 259–270.

Thiemann, C., M. Treiber , and A. Kesting. 2008. "Estimating Acceleration and Lane-Changing Dynamics Based on NGSIM Trajectory Data." *Transportation Research Record: Journal of the Transportation Research Board* 2088: 90-101.

Treiber, M., A. Hennecke, and D. Helbing. 2000. "Congested traffic states in empirical observations and microscopic simulations." *Physical Review E* 62, no. 2 : 1805–1824.

Treiber, M., A. Kesting, and D. Helbing. 2006. "Understanding widely scattered traffic flows, the capacity drop, and platoons as effects of variance-driven time gaps." *Phys. Rev. E* 74, no. 1: 016123.

Treiber, M., and A. Kesting. 2013. "Microscopic Calibration and Validation of Car-Following Models – A Systematic Approach." *20th International Symposium on Transportation and Traffic Theory (ISTTT 2013)*. Noordwijk, Netherlands, 922–939.

van der Merwe, R., A. Doucet , J . F. de Freitas, and E. Wan. 2000. *The unscented particle filter*, *Technical Report CUED/F-INFENG/TR 380*, . Cambridge University Engineering Department.

Venkatasubramaniana, V., R. Rengas, K. Yinc, and S. N. Kavurid. 2003. "A review of process fault detection and diagnosis: Part I: Quantitative model-based methods." *Computers & Chemical Engineering* 27, no. 3: 293–311.

Wiedemann, R. 1974. *Simulation des Strassenverkehrsflusses*. Karlsruhe, Germany: Schriftenreihe des Instituts für Verkehrswesen der Universität Karlsruhe, Band 8.

Wilson, R. E., and J. A. Ward. 2011. "Car-following models: fifty years of linear stability analysis – a mathematical perspective." *Transportation Planning and Technology* 34, no. 1: 3-18.

Yang, Q., and H. N. Koutsopoulos. 1996. "A microscopic traffic simulator for evaluation of dynamic traffic management systems." *Transportation Research C* 4(3), 4, no. 3 : 113-129.